In-vitro assessment of modified resin adhesive-tooth interfaces

Almahdy, Ahmed

Awarding institution:
King's College London

IN-VITRO ASSESSMENT OF MODIFIED RESIN ADHESIVE-TOOTH INTERFACES

Ahmed Essam Ahmed Almahdy

A thesis submitted for the degree of

Doctor of Philosophy

King's College London

2013

Abstract

Objectives:

This research aimed to characterize the interfacial characteristics of modified dental resin-based adhesive systems bonded to sound and carious dental tissue. The modification included the incorporation of matrix metalloproteinase (MMP) inhibitors within the primers of these adhesives.

Materials and methods:

Two MMP inhibitors (BB94 and GM6001) were added to three adhesive primers, Optibond FL "OB" (Kerr, USA), Prime&Bond NT "PB" (Dentsply, USA) and G-Bond "GB" (GC, UK) and bonded to sound dentine. The inhibitory effect of the modified adhesive on recombinant MMPs and on sound dentine MMPs was assessed using FRET-based measurement of MMP activity and substrate zymography, respectively. Micro-tensile bond strength and micro-permeability were used to evaluate the modified adhesives' physical properties. Micro-Raman spectroscopy analysis was validated on carious dentine and it was used to evaluate the interface between the modified OB primer and caries-affected dentine. The inhibitory effect of the modified adhesive on caries-affected dentine was studied using in-situ zymography.

Results:

The fluorometric assay and zymography showed that modified adhesives had high affinity toward both synthetic FRET-peptides and dentine powder substrates, respectively.

The immediate micro-tensile bond strength was enhanced for OB (48.0 MPa ± 20.3 SD for BB94 and 42.0 MPa ± 18.7 SD for GM6001) and GB (34.8 MPa ± 19.2 SD for BB94 and 41.7 MPa ± 17.6 SD for GM6001). However, no changes were detected between the control and the inhibitor groups following 3-month storage. Additionally, the micro-permeability of PB and GB showed less dye seepage, to the "hybrid layer" and to the "adhesive", respectively.

The caries-infected dentine was defined significantly by the KHN (< 20.6), AF (> 14.4 A.U.) and by the relative contribution of the mineral (< 36.4%), Porphyrin fluorescence (> 25.3%) and Infected dentine signal (> 0.3%) Raman clusters. The caries-affected

dentine-adhesive interface exhibited more hydrophobic resin (32.8% ± 3.9 SD) that maintained over four-week aging.

Conclusions:

The addition of MMP inhibitors to contemporary dental adhesive systems resulted in modified adhesives that had an enhanced dentine-adhesive interface with inhibited MMP activity. Such properties enhance the clinical performance of adhesive systems.

Table of Contents

Figure Legends

Table Legends

List of abbreviations

10-MDP: 10-methacryloyloxydecyl dihydrogenphosphate.

4-MET: 4-methacryloyloxyethyl trimellitic acid.

ADAMs: a disintegrin and metalloproteinase-like.

ADAMTS: a disintegrin and metalloproteinase with thrombospondin motifs.

AF: autofluorescence.

BHT: butylhydroxytoluene.

Bis-GMA: bisphenol-A glycidyl methacrylate.

BMPs: Bone morphogenetic proteins.

BPDM: biphenyl dimethacrylate.

CFOME: confocal fibre-optic micro-endoscope.

CLSM: confocal laser scanning microscopy.

CQ: camphorquinone.

DGP: Dentine Glycoprotein.

DMP-1: dentine matrix protein 1.

DPP: Dentine Phosphoproteins.

DSP: Dentine SialoProtein.

DSPP: dentine sialophosphoprotein.

FGF2: fibroblast growth factor 2.

FISH: fluorescent in-situ hybridisation.

GDMA: glycerol dimethacrylate.

GPDM: glycerol phosphate dimethacrylate.

HEMA: hydroxyethyl methacrylate.

ILGF: Insulin-Like Growth Factor.

KHN: Knoop hardness number.

MMEP: mono-2-methacryloyloxyethyl phthalate.

MMPs: matrix metalloproteinases.

NIR: near-infrared.

NPG-GMA: N-phenylglycine and glycidyl-methacrylate.

ODMAB: 2-(ethylhexyl)-4-(dimethylamino)benzoate (co-initiator).

PCR: polymerase chain reaction.

PDGF: Platelet-derived growth factor.

PENTA: dipentaerythritol pentacrylate monophosphate.

Phenyl-P: 2-(methacryloyloxyethyl)phenyl hydrogenphosphate.

QLF: quantitative laser-induced fluorescence.

SIBLINGs: small integrin-binding ligand N-linked glycoproteins

SLRPS: small leucine-rich proteoglycans.

TEGDMA: triethylene glycol dimethacrylate.

TGF: Transforming growth factor.

UDMA: urethane dimethacrylate.

UV: ultraviolet.

Acknowledgements

In the name of Allah most gracious most merciful, to whom is all the praises and thanks for the grants I have been blessed within my life.

The completion of this PhD degree would not have been possible without the interest and support of all members of the Dental Biomaterials Science Department, Dental Institute, King's College London. I would like to express grateful thanks and appreciation to all those involved.

My deepest thanks to:

Professor Avijit Banerjee, my first supervisor, for his encouragement, inspiration and constant support, without which this dissertation would not be possible. I am grateful to him for being always available for help and advice throughout my PhD studies. I could not have imagined having a better advisor and mentor for my PhD studies.

Professor Timothy Watson, my second supervisor, for providing his continuous scientific advice and moral support throughout this project.

Dr. Frederic Festy, for offering his precious time and expertise and for his remarkable help in the use and analysis of the micro-Raman spectroscopy.

Professor Andrea Streit, my postgraduate coordinator, for her advice and continuous evaluation of my progression during my studies.

Dr. Garrit Koller and **Dr. Salvatore Sauro**, Research Associates, for their help and support during the designing of the experiments.

Mr Peter Pilecki for continuous assistance in the lab and for proof reading my thesis.

Dr. Martyn Sherriff, for his invaluable advice on statistics.

I wish to express my deep appreciation and gratitude to my employer, **Department of Pediatric Dentistry and Orthodontics, College of Dentistry, King Saud University, Riyadh, Saudi Arabia** and to the **Royal Embassy of Saudi Arabia, Cultural Bureau in London** for their generous financial grant and continuous support throughout my study.

Last but not least, I would like to express my sincere thanks to my parents, for their tremendous encouragement, understanding and patience that supported me throughout the

last six years; I will be always indebted to them. I owe my deepest gratitude to my dear wife, Hadeel, for her limitless support and encouragement, who shared with me all the difficult and pleasant times to finish my studying years. Many deepest thanks to my family and friends for their great support and wishes.

I dedicate this work to my lovely son and daughter

Essam and Jude

Introduction

The mechanical, physical, and functional properties of dentine bonding agents have been improved as a result of numerous investigations into the chemical balance between their hydrophilic and hydrophobic functional components. The degradation of the adhesive-dentine interface, including the disorganization of collagen fibrils and loss of resin from inter-fibrillar spaces, is a limitation both chemically and clinically of these systems.

Host-derived matrix metalloproteinases (MMPs), found both in saliva and in etched dentine, have been shown to be involved in the degradation of the unprotected collagen fibrils within the hybrid layer. These proteases are secreted by odontoblasts during dentinogenesis and remain inactive within the dentine extracellular matrix. The acidic environment, resulting from adhesive systems or the biological carious process, activates different dentine MMPs. Various matrix metalloproteinases inhibitors had been used previously to prevent collagen fibril degradation in the dentine extracellular matrix.

In this study two types of MMP inhibitors were added to contemporary dental adhesive systems. The effects of such an addition on both the MMP inhibitor ability and on the adhesive properties were examined when the modified adhesive bonded to sound and carious dentine.

The first chapter of this thesis is dedicated to a review of the literature. It is divided into four main topics: dentine structure, dental caries, matrix metalloproteinases (MMPs) and dentine bonding agents. In Chapter 2, the effect of modified adhesives, bonded to sound dentine, on the MMPs activity was investigated and discussed. The micro-tensile bond strength and the micro-permeability of the modified adhesive were assessed in Chapter 3. A novel micro-Raman spectroscopy technique was validated, prior to its use, by scanning carious teeth in Chapter 4. The last experimental chapter, Chapter 5, evaluated the effect of bonding the modified adhesive to caries-affected dentine on its MMP activity and on the chemical content of caries-affected dentine-adhesive interfaces.

Aims

The aim of this project was to evaluate the effect of incorporating MMP inhibitors to contemporary dental adhesive systems on both the MMP activity and on the adhesives' physical properties when the resulting modified dental adhesive systems were bonded to both sound and carious dentine tissues. The ultimate aim was to produce a dental adhesive system that had improved properties by the prevention of dentine collagen matrix degradation.

Objectives

The objectives of this project and the experimental methods used are summarised in Figure i-1. These objectives involve:

1. The evaluation of the effects of modified dental adhesives on MMPs found in sound dentine using:
    a. FRET-based measurement of MMP activity
    b. Substrate zymography
2. The physical properties of modified adhesives assessment using:
    a. Micro-tensile bond strength testing and failure mode assessment
    b. Micro-permeability assessment
3. Chemical analysis of carious dentine using:
    a. Micro-Raman spectroscopy
    b. Microhardness
    c. Autofluorescence detection
4. The effect of modified adhesives on caries-affected dentine which included analysis using:
    a. In-situ zymography
    b. Micro-Raman spectroscopy

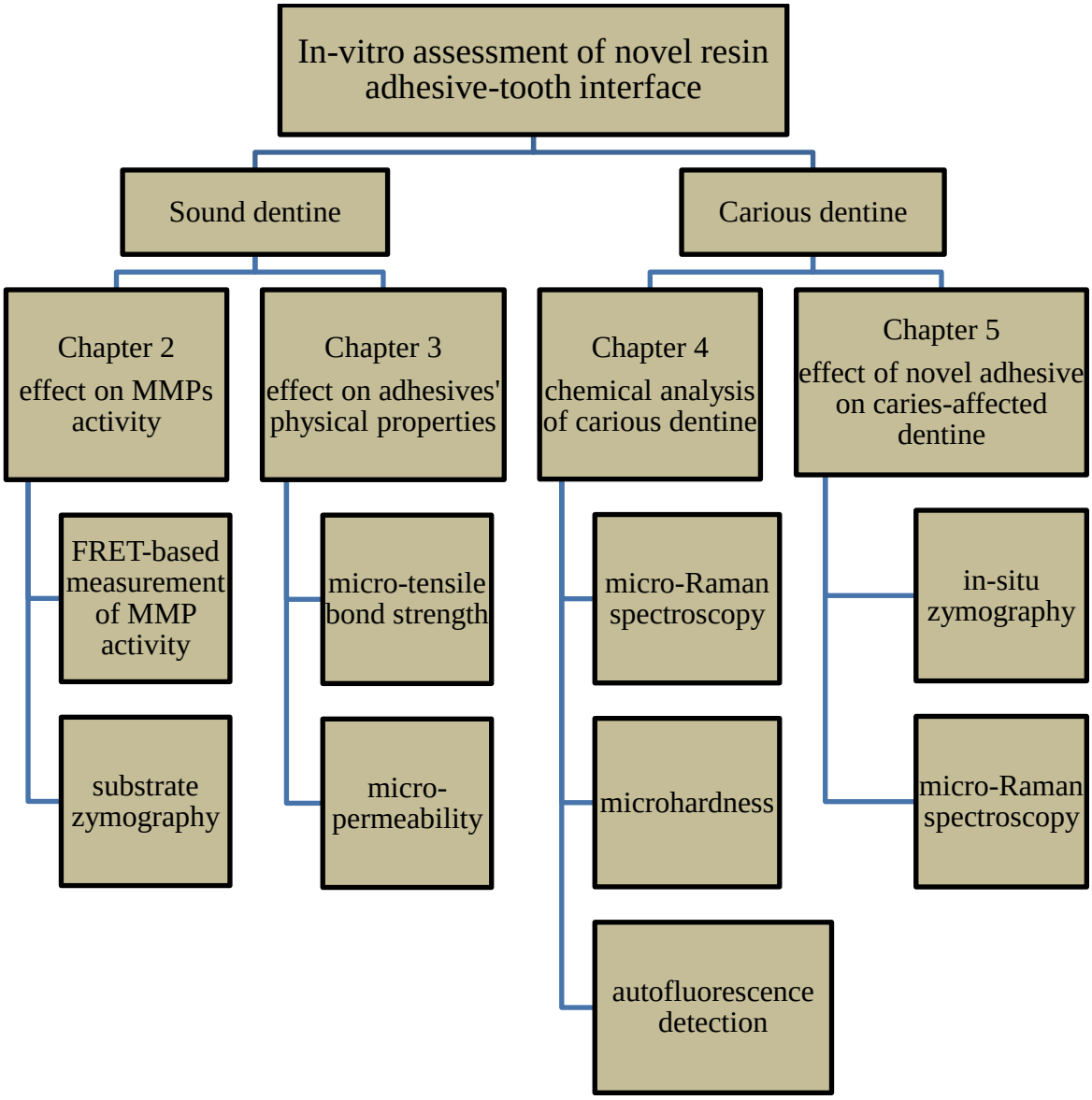

Figure i-1 Flowchart of the experiments accomplished in this study.

Chapter 1 Literature review

1.1 Dentine structure

1.1.1 Introduction

Dentine is the thick mineralised structure that forms the major component of dental hard tissues. It is covered by the highly mineralised and protective enamel in the crown and by cementum in the root. As for connective tissues in general, the constituents of the extracellular space primarily give the tissue its functional characteristics. Dentine is considered as a modified connective tissue that is derived from the ectomesenchymal cells, the odontoblasts, found in the dental papilla (Linde and Goldberg, 1993; Patel, 2001). The extracellular matrix of dentine is modified by incorporating the mineral phase, thus making it possible for the tissue to fulfil the physical functional requirements that are enamel support, to withstand the stress of occlusal forces, and pulpal protection (Pashley, 1991). When compared to bone, the extracellular matrix of dentine has an absence of significant extracellular matrix turnover although they have a similar matrix composition. This suggests that dentine is a much less dynamically active tissue when compared to bone (Smith et al., 2012).

On a weight basis, dentine is composed of approximately 70% in the form of mineral phase, 20% is organic material and the remaining portion water. On a volume basis, which perhaps provides a more relevant picture, the mineral and the organic phases account for about 50 and 30%, respectively (Linde and Goldberg, 1993; Marshall et al., 1997). This difference is due to the difference in the specific gravity of these components. The organic matrix is formed initially by odontoblasts and then mineralises during dentinogenesis. Gradual mineralisation continues with age (Goldberg, 2011).

1.1.2 Mineral content

The dentine mineral phase consists of hydroxyapatite $Ca_{10}(PO_4)_6(OH)_2$ crystals. These crystals are needle-shaped with a thickness of approximately 5 nm and a length of 20 nm (Mjör, 1984). The initiation of mineralisation is explained by three different mechanisms (Posner and Tannenbaum, 1984):

- The elevation of the local calcium- phosphate supersaturation level that causes spontaneous precipitation

- The presence of extracellular matrix vesicles, containing phosphoproteins and glycoproteins, which create nucleation sites for initial mineralisation
- The deactivation of bone mineral inhibitors, such as proteoglycans, that allows the precipitation of hydroxyapatite

During dentinogenesis, the foci of mineralisation grow into spherical structures called calcospherites, which fuse with neighbouring spheres (Jones and Boyde, 1984). The failure of this fusion creates poorly mineralised areas within the dentine called interglobular dentine which are found in conditions including X-linked hypophosphatemic rickets (Seow, 2003) and severe fluorosis (Nikiforuk and Fraser, 1979). Additionally, dentine mineralisation occurs in an incremental linear pattern that can be considered to reflect the rhythmicity in formation and disturbances in mineralisation. Mineral formation within the non-mineralised precursor tissue, predentine, occurs at a rate that varies between 4 to 20 μm per day, so creating these incremental lines (Linde and Goldberg, 1993).

1.1.3 Organic material

The organic extracellular dentine matrix contains collagens in the form of Type I fibres predominantly (90% by weight) and a minimal amount of type III and V. In addition, it contains a number of other proteins and proteoglycans, collectively referred to as the non-collagenous proteins (NCPs). The organic content found in dentine extracellular matrix is summarised in Table 1-1.

Table 1-1 Organic composition of dentine extracellular matrix. SIBLINGs: small integrin-binding ligand N-linked glycoproteins; DSPP: dentine sialophosphoprotein; DSP: Dentine SialoProtein; DGP: Dentine Glycoprotein; DPP: Dentine Phosphoproteins; DMP-1: dentine matrix protein 1; SLRPS: small leucine-rich proteoglycans; MMPs: matrix metalloproteinases; ADAMs: a disintegrin and metalloproteinase-like; ADAMTS: a disintegrin and metalloproteinase with thrombospondin motifs; FGF2: fibroblast growth factor 2; TGF: Transforming growth factor; BMPs: Bone morphogenetic proteins; ILGF: Insulin-Like Growth Factor; PDGF: Platelet-derived growth factor.

Organic material	Proteins family	Proteins	Function
Collagens		Type I collagen	structural macromolecules which act as scaffolds for mineralisation
		Type III collagen	
		Type V collagen	
Non-collagenous proteins	SIBLINGs	DSPP: DSP, DGP, DPP	promote the hydroxyapatite crystal nucleation
		DMP-1	regulates the mineralisation
	proteoglycans	SLRPS	essential for collagen fibril formation
		large aggregate: versican	
	γ-Carboxyglutamate containing proteins	osteocalcin	regulates the hydroxyapatite crystals growth
		matrix Gla protein	inhibits dentine mineralisation
	other acidic non-collagenous proteins	osteopontin	inhibits hydroxyapatite crystal formation and growth
		osteonectin	binds hydroxyapatite to collagen-coated surfaces
Enzymes	alkaline phosphatase	Tissue-nonspecific alkaline phosphatase	provides inorganic phosphate for mineralisation
	MMPs	collagenases, gelatinases, stromelysin-1, enamelysine	extracellular matrix degradation
	other extracellular metalloproteinases	ADAMs	proteolysis of cell surface molecules
		ADAMTS	degradation of proteoglycans

Other matrix content	proteolipids	Phosphatidylcholine, phosphatidylethanolamine, sphingomyelin, diphosphatidyl-glycerol	have essential role in dentinogenesis process
	blood serum proteins	Albumin, Alpha$_2$-HS glycoprotein, Fetuin	
	polyamines	Spermine, spermidine, putresceine	
	growth factors	FGF2, TGF beta1, BMPs, ILGF I & II, PDGF	
	Calcium-binding proteins	calmodulin, calbindin, annexines, nucleobindin	

1.1.3.1 Collagens

All collagen types found within the dentine extracellular matrix are fibrillar structural macromolecules which include in their structure one or more domains that have a characteristic triple helical conformation that is characterized by the intertwining of three helical polypeptides forming "coiled coil" structure (Van Der Rest and Garrone, 1991) (Figure 1-1a). Additionally, each helical chain contains non-triple helical regions at both the NH_2-terminal and COOH-terminal ends (Butler, 1984) (Figure 1-1b). The triple helical domains have sizes ranging from 33 to over 1000 amino acids per chain (Van Der Rest and Garrone, 1990). The type I collagen protein unit is composed of two identical α1 chains and one distinct α2 chain intertwined to form a 280 nm molecule (Goldberg et al., 2011) (Figure 1-1a and b). In contrast, Type III collagen has three α1 chains that are uniquely disulphide-bonded at the COOH-terminal end (Butler, 1984). The Type V molecules are arranged such that their triple helical domain lies within the interior of type I collagen with the NH_2-terminal domain extending perpendicular to the long axis (Linsenmayer et al., 1993).

The collagen molecules are self-aligned and crosslinked to produce a characteristic staggered arrangement (Figure 1-1c). These arrangements, observed in the form of periodic banding patterns using electron microscopy (Petruska and Hodge, 1964), represent areas of gaps and overlaps in the alignment of the molecules on the axial surface. Each gap and overlap is repeated constantly every 690 Å axial length that is known as the D-periodic unit in collagen structure (Petruska and Hodge, 1964; Van Der Rest and Garrone, 1991) (Figure 1-1d). In every D-periodic unit, five molecules in cross-section represent the overlap and only four molecules represent the gap (Orgel et al., 2006). Using atomic force microscopy, the periodic banding is found in the form of

elevated and depressed zones. The elevated bands width was 24 nm and the difference between the top of the elevated zone and the bottom of the depressed zone was 16 nm (Revenko et al., 1994).

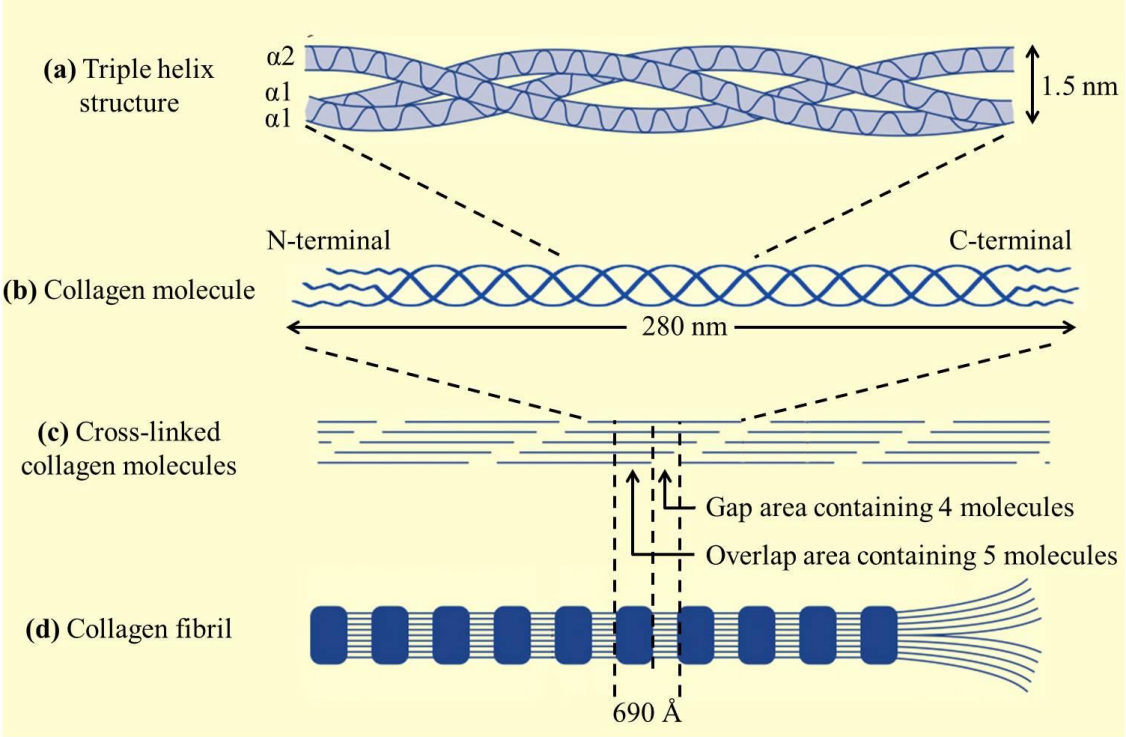

Figure 1-1 Type 1 collagen structure (modified from Cawston (1998)) (a) triple helix which is formed of two α1 chains and one α2 chain. (b) the 280 nm collagen molecule containing the non-triple helical regions at both the NH_2-terminal and COOH-terminal ends. (c) the staggered collagen molecules packed and cross-linked. (d) collagen fibril showing the periodic banding patterns and the D-periodic unit representing one gap and one overlap (690 Å axial length).

Prior to mineralisation, dense collagen fibrils are exocytosed by odontoblasts in the predentine. These fibrils provide the structural scaffolding necessary for mineralisation to occur (Linde and Goldberg, 1993; Milan et al., 2005). The synthesis of collagen fibrils is influenced by the presence of small leucine-rich proteoglycans (SLRPS) (Embery et al., 2001).

1.1.3.2 Non-collagenous proteins (NCP)

In general, the non-collagenous proteins (NCPs) are found in the dentine extracellular matrix and represent the remaining organic content. They include the small integrin-binding ligand N-linked glycoproteins (SIBLINGs), proteoglycans (PGs), γ-

carboxyglutamate containing proteins, enzymes and some other acidic non-collagenous proteins (Table 1-1). The NCPs are associated strongly with the mineral phase and they are extractable only after demineralisation (Linde et al., 1980). It is thought that these acidic, highly hydrated proteins cover the collagen fibrils to varying extents to initiate and promote mineralisation (Qin et al., 2004).

Small integrin-binding ligand N-linked glycoproteins (SIBLINGs)

SIBLINGs are a family of glycophosphoproteins comprising dentine sialophosphoprotein (DSPP) and dentine matrix protein 1 (DMP-1) (Bellahcene et al., 2008).

The Dentine SialoPhosphoProtein (DSPP) is expressed primarily in dentine with minimal amounts found in bone. It is cleaved immediately after secretion into three different molecules:

- Dentine SialoProtein (DSP) from the N-terminal region of DSPP (Macdougall et al., 1997; Qin et al., 2001)
- Dentine Glycoprotein (DGP) from the region of the DSPP protein between the DSP and DPP, found only in porcine dentine extract (Yamakoshi et al., 2005)
- Dentine Phosphoproteins (DPP) or phosphophoryn from the C-terminal region of DSPP

DSP and DPP are expressed exclusively by odontoblasts and found in dentine (Butler and Ritchie, 1995). Both proteins account for as much as 5–8% and 50% by weight, respectively, of NCPs (Patel, 2001). DPP is a highly acidic phosphoserine-rich (45-50% by volume) protein with a high content of aspartic acid (35% by volume) (Munksgaard et al., 1977). DPP has a strong affinity for Ca^{2+} and promotes the nucleation and modulation of hydroxyapatite crystal formation (Qin et al., 2001). Additionally, it binds to collagen and induces intra-fibrillar mineralisation (Milan et al., 2006). Depending on its concentration, DPP has a dual role in the mineralisation process. Low levels of DPP (0.010-l μg/ml) induce hydroxyapatite formation while high levels (100 μg/ml) inhibit the mineralisation process (Boskey et al., 1990; Butler, 1995; Begue-Kirn et al., 1998).

DSP has a high carbohydrate (30% by weight) and sialic acid (10% by weight) content (Butler et al., 1992). The precise role of DSP in the formation of dentine matrix is still unknown. However, D'souza et al. (1995) found that DSP is a specific biochemical marker of functional odontoblasts that is synthesized and secreted exclusively by them.

Recently, it was suggested that DSP is a contributor to mineralisation regulation, influencing apatite formation and growth (Boskey et al., 2000; Suzuki et al., 2009).

Mutations in the signal peptide of the DSPP gene have been shown to cause several dentine disorders such as dentinogenesis imperfecta and dentine dysplasia (Mcknight et al., 2008).

Another prominent member of SIBLINGs found in dentine extracellular matrix is dentine matrix protein 1 (DMP-1). DMP-1 is a serine-rich protein that has an overall composition between that of bone phosphoproteins and dentine phosphophoryn (Butler, 1995). Qin et al. (2007) suggested that DMP-1 has a participant role in regulating the mineralisation due to the presence of acidic domains in its structure. It was also suggested that DMP-1 is essential for odontoblast differentiation and for dentine tubule morphology (Lu et al., 2007).

Proteoglycans (PGs)

Proteoglycans (PGs) are large, complex macromolecules consisting of glycosaminoglycan (GAG) side chains, comprising repeating disaccharides units, covalently linked to a core protein (Goldberg and Takagi, 1993). PGs are found in the matrices of mineralising as well as non-mineralising tissues. The presence of sulphate and uronic acid carboxyl groups in the GAG chains, together with the high proportion of carbohydrate relative to protein, results in the highly acidic character of PGs (Linde, 1984). Seven types of GAG have been described: hyaluronan, dermatan sulphate, chondroitin-4-sulphate, chondroitin-6-sulphate, keratin sulphate, heparan sulphate and heparin (Embery et al., 2001). Chondroitin-4-sulphate and chondroitin-6-sulphate are the main GAG side chains identified in dentine (Clark et al., 1965). According to Hjerpe et al. (1983), the former accounts for about 81% of the GAG chains in human dentine, whereas the latter constitutes approximately 14%. The difference between the two types is in the location of the sulphate group on the galactosamine (Linde and Goldberg, 1993). Small amounts of hyaluronic acid, dermatan sulphate and a non-sulphated galactosaminoglycan were also demonstrated within dentine (Jones and Leaver, 1974).

Extracellular matrix PGs are subdivided, according to their molecular size and state of aggregation, into aggregating proteoglycans, such as aggrecan, versican, brevican and neurocan, and small leucine-rich proteoglycans (SLRPS). Large PGs, mainly versican which contains chondroitin-4-sulphate and chondroitin-6-sulphate isomers, and a smaller

sized PG are composed exclusively in the predentine (Waddington et al., 2003). In dentine, only small-sized PGs, composed exclusively of chondroitin-4-sulphate, are found (Rahemtulla et al., 1984; Goldberg and Takagi, 1993).

PGs in predentine are located between and on collagen fibres and show rapid turnover. These PGs are essential for fibril formation and promotion of the linear addition and aggregation of collagen molecules to form the initial dimers and trimers for fibrillogenesis (Milan et al., 2005). In dentine, PGs appear as needle-like structures and are located along individual fibres or groups of mineralising collagen fibres. Dentine PGs are stable and are associated with the collagen periodic banding pattern (Goldberg and Takagi, 1993; Hall et al., 1999).

Hall et al. (1999) proposed that predentine macromolecules are degraded or partially removed during dentinogenesis by stromelysin-1 (matrix metalloproteinase-3) to enable a second pool of PGs to be released near the predentine mineralisation front. This second pool of PGs, predominantly chondroitin sulphate in nature, has an increased affinity for hydroxyapatite and, with dentine phosphoproteins (DPP), are involved in the initiation, stabilization, and control of hydroxyapatite crystal growth (Waddington et al., 2003; Milan et al., 2005).

γ-Carboxyglutamate containing proteins (Gla)

γ-carboxyglutamate is an unusual amino acid that is identified in proteins participating in the blood coagulation cascade. It is also found in mineralised tissues proteins with unrelated structure to the blood coagulation factors (Linde and Goldberg, 1993). Two major groups of Gla-containing proteins are present in bone and dentine, osteocalcin (or bone Gla-protein) and the matrix Gla protein (MGP) (Linde and Goldberg, 1993; Butler, 1995). The former is synthesized mainly in mineralised tissues while soft tissues synthesize the latter (Goldberg et al., 2011).

Osteocalcin (OCN) is one of the most abundant proteins of bone matrix, from which it was originally isolated (Butler and Ritchie, 1995). It is also synthesized and secreted by odontoblasts (Camarda et al., 1987) and found in the dentine extracellular matrix (Linde et al., 1982). OCN is formed from glutamic acid residues by a post-translational modification reaction, which is vitamin K-dependent, and has a high Ca^{2+} binding affinity (Linde and Goldberg, 1993). In developing bone and dentine, OCN acts as a regulator for

the growth of hydroxyapatite crystals by inhibiting tissue transglutaminase activity rather than inhibiting the mineralisation (Romberg et al., 1986; Goldberg et al., 2011).

Matrix Gla protein (MGP) is an essential regulator for mineralisation in both blood vessels and mineralised tissues. The absence of such protein results in extensive hypomineralisation in dentine and alveolar bone (Kaipatur et al., 2008). Extensive mineralisation of the extracellular matrix in arteries and premature mineralisation of cartilage have been observed when MGP is knocked out (Luo et al., 1997). Thus MGP is important as an inhibitor of dentine mineralisation (Goldberg et al., 2011).

Other acidic non-collagenous proteins

Other proteins are also present within the dentine extracellular matrix and not included in the previous families. The main ones found in dentine include osteopontin and osteonectin.

Osteopontin (OPN) is expressed in dentine and has an inhibitory effect on hydroxyapatite formation and mineral crystal growth (Boskey et al., 2002). It was initially discovered as a phosphoprotein secreted by transformed, malignant epithelial cells (Senger et al., 1979). OPN has diverse functions that include (1) cell attachment and cell signalling via its arginine-glycine-aspartic acid (RGD) sequence; (2) regulation of the formation and remodelling of mineralised tissues, (3) interaction with Ca^{2+} in a way that influences OPN protein conformation and may be important in Ca^{2+} mediated or Ca^{2+} dependent processes, (4) inhibition of the growing apatite crystal lattices in bone and dentine and (5) cell migration (Butler and Ritchie, 1995).

The Secreted Protein, Acidic and Rich in Cysteine (SPARC), also known as osteonectin (Goldberg et al., 2011), binds both to hydroxyapatite crystals and to type I collagen. Termine et al. (1981) suggested that this protein can mediate the binding of hydroxyapatite to collagen-coated surfaces which initiates active mineralisation in normal skeletal tissue. The structure of the SPARC molecule, extracted from dentine, is composed of three functional domains: an acidic Ca^{2+}-binding domain that binds to hydroxyapatite, a follistatin-like domain and kazal motifs with intra-molecular disulphide bridges and an extracellular calcium-binding domain (Chun et al., 2006).

1.1.3.3 Enzymes

Different enzymes have been identified within the dentine extracellular matrix such as alkaline phosphatase and metalloproteinases. These metalloproteinases include matrix metalloproteinases (MMPs), ADAMs (a disintegrin and metalloproteinase-like, or adamalysin) and ADAMTS (a disintegrin and metalloproteinase with thrombospondin motifs) (Goldberg et al., 2011).

Tissue-non-specific alkaline phosphatase, one of the four human alkaline phosphatases, is expressed by both osteoblasts and odontoblasts. This enzyme hydrolyses pyrophosphate, at pH 8-10 (Granstrom and Linde, 1976), to provide inorganic phosphate to promote mineralisation (Orimo, 2010). This reduces also the pyrophosphate level which is an inhibitor for hydroxyapatite formation (Linde and Goldberg, 1993).

Certain members of the MMP family are embedded within the dentine structure including collagenases, gelatinases, stromelysin 1 and enamelysin (Chaussain-Miller et al., 2006). These enzymes target the components of the extracellular matrix during dentinogenesis and influence the dental tissue formation and mineralisation (Fanchon et al., 2004). Tissue inhibitors of matrix metalloproteinases (TIMPs) are also present within the extracellular matrix to control and regulate the activity of MMPs (Embery et al., 2001). A detailed review about MMPs and their functions will be discussed later in Section 1.3.

ADAMs and ADAMTS are groups of enzymes that participate in the degradation and reorganization of extracellular matrix alongside MMPs. ADAMs have been associated with cellular adhesion processes and with the proteolytic processing of cell surface molecules (Overall and Lopez-Otin, 2002). ADAMTS, a counterpart for ADAMs that have a thrombospondin-1-like domain, is a family of extracellular proteases that is involved in the degradation of proteoglycans (Porter et al., 2005). It was found that dental tissue cells secrete different types of ADAMTS during root development (Sone et al., 2005).

The MMP role in extracellular matrix degradation continues into mature tissues, whereas the role of ADAMTS is limited to the tissue formation stages only (Tang, 2001).

1.1.3.4 Other matrix content

Dentine structure also contains other components that are important during dentinogenesis. These include certain proteolipids, proteins taking origin from blood

serum, polyamines and different growth factors (see Table 1-1) (Linde and Goldberg, 1993; Goldberg et al., 2011). Calcium-binding proteins are also found. These proteins are implicated in Ca^{2+} transport through the odontoblast and the sequestration of Ca^{2+} ions during mineralisation (Linde and Goldberg, 1993; Somogyi et al., 2004).

1.2 Dental caries

1.2.1 Introduction

Dental caries is considered a multi-factorial lifestyle-related disease process involving the plaque biofilm which can be controlled by a combination of strategies addressing its aetiological factors (Pitts and Wefel, 2009). The caries process starts at the enamel surface when the bacteria within the oral biofilm ferment dietary carbohydrates and produce organic acids as by-products. To create the cariogenic environment that causes demineralisation of the enamel surface, other factors are important including the time, increased density of the developing biofilm, microbiological shifts within the complex biofilm, the pH drop below the critical value (pH 5.5) (Dawes, 2003) and the oxygen tension (Marquis, 1995). Additionally, the caries process can be disturbed by saliva's ability to buffer acid, exposure to fluoride, a reduced frequency of dietary carbohydrates consumption and by the physical removal of the oral biofilm (Selwitz et al., 2007).

The sum of these factors results in pH fluctuations at/near the enamel surface. These fluctuations may cause demineralisation of the enamel surface when the pH is dropping or remineralisation when the pH is increasing (Manji et al., 1991). The incipient lesion begins to form when demineralisation occurs more frequently than remineralisation, resulting in overall mineral loss (Kidd and Fejerskov, 2004). In general, the caries process is an initially reversible chronic condition that progresses slowly and can be arrested by disturbing the plaque biofilm. To understand the histological changes within the carious dentine tissues it is important to understand the progress of the carious lesion from the enamel through to the pulp over time.

1.2.2 Enamel lesion

At the initial stage of lesion formation, changes within the enamel surface can not be detected clinically even after one week of an undisturbed biofilm formation (Holmen et al., 1985a). However, at the ultrastructural level, the intercrystalline spaces are enlarged due to the partial dissolution of hydroxyapatite crystal peripheries (Holmen et al., 1985b).

After two weeks with an undisturbed biofilm, the enamel lesion is visible clinically when the enamel surface is dried. It appears as a smooth, frosty white/opaque and non-cavitated lesion which is known as a white spot lesion (Gustafson, 1957). The white spot lesions are areas of subsurface demineralisation that are covered by a virtually intact surface zone

of enamel with a thickness of approximately 10 to 30 μm (Dawes, 2003; Selwitz et al., 2007). Microscopically, a distinct enlargement of the intercrystalline spaces with complete dissolution of individual hydroxyapatite crystals is seen at this stage (Holmen et al., 1985b).

After three and four weeks, the white spot lesions will appear even on wet enamel surfaces. They appear as a chalky, rough and microcavitated surface (Arends and Christoffersen, 1986). An increased loss of the hydroxyapatite crystals with the appearance of a more uniform subsurface dissolution area is seen microscopically (Holmen et al., 1985a; Kidd and Fejerskov, 2004). At this stage and before the lesion reaches the enamel-dentine junction (EDJ), enamel caries can be classified, depending on the lesion porosity and mineral loss, into four different zones. These zones appear from enamel surface towards the sound enamel tissue as following (1) the surface zone, (2) the body of the lesion, (3) the dark zone and (4) the translucent zone (Darling, 1961). Robinson et al. (2000) review had discussed the chemical differences between these zones (Table 1-2). The surface zone is less susceptible to acid attack as it contains high concentration of fluoride that modify the hydroxyapatite structure into fluorapatite $Ca_{10}(PO_4)_6F_2$ (Weatherell et al., 1974; Arends and Christoffersen, 1986; Ten Cate and Featherstone, 1991). This decreases the demineralisation on the surface and promote tissue repair (Ten Cate, 1999).

Table 1-2 The enamel caries lesion zones and the changes in the mineral crystal morphology and the resulted porosity of each zone according to Robinson et al. (2000).

Enamel caries zone	**Mineral crystal morphology changes**	**Porosity**	**Comments**
Surface zone	enlargement of intercrystalline spaces	1-2%	relatively intact surface similar to sound enamel
Body of the lesion	dissolution of hydroxyapatite crystals	25-50%	pores are enlarged until cavitation occurs
Dark zone	5-10% mineral loss	large and small pores	small pores are generated from the occlusion of larger spaces
Translucent zone	dissolution of hydroxyapatite crystals boundaries (1-2% mineral loss)	small number of relatively large pores	the advancing front of the enamel caries lesion

1.2.3 Dentine carious lesion

The dentine-pulp complex is considered a vital tissue that has specific defence reactions to external stimuli. Enamel demineralisation and the increased surface porosity encourage the pulp-dentine organ to respond before the advancing front of the enamel extends to the EDJ. Its first defence reaction is tubular occlusion, in which deposition of mineral along and within the dentine tubules results in their gradual obliteration (Fejerskov and Kidd, 2008). Other important defence reactions are the formation of tertiary dentine, which starts before bacterial invasion of dentine, and pulpal inflammation (Kidd and Fejerskov, 2004; Banerjee and Watson, 2011). The dentine lesion starts as a brownish discolouration immediately subjacent to the EDJ. The lateral extent of this lesion at the EDJ corresponds with the extent of the enamel lesion at the tooth surface, which in turn is dependent on the extent of the overlying plaque biofilm (Bjørndal and Thylstrup, 1995; Bjørndal et al., 1999). At this stage, the lesion can be arrested by regular disturbance of the biofilm as long as the enamel surface zone is intact.

Once the enamel lesion cavitates, the plaque biofilm will be able to accumulate on the exposed dentine surface and produce acids that demineralise the dentine mineral content at a relatively higher pH value of 6.0 (Van Houte, 1994; Vanuspong et al., 2002). This is followed by the degradation of the extracellular organic matrix which is a prerequisite for cavity formation (Van Strijp et al., 2003). The matrix degradation has traditionally been thought to be caused by bacterial proteolytic enzymes only (Steinman, 1960; Dacosta and Gibbons, 1968). Recent studies have suggested that the proteolytic enzymes may be derived from oral bacteria, yeasts or from the dentine structure itself (Dung et al., 1995; Van Strijp et al., 2003). The spread of the dentine lesion will undermine the overlying enamel, with a related grey shadow, and make it brittle and breakable (Ismail, 1997; Selwitz et al., 2007).

Dentine structure deterioration and the opposing reparative defence reaction, by the pulp-dentine organ, create histological changes to the original structure from the EDJ through to the pulp. These changes are classified into different interrelated layers that cannot be separated biologically. The main two layers of the carious dentine lesion are the outer caries-infected and inner caries-affected dentine (Fusayama and Terachima, 1972; Fusayama, 1979; Yamada et al., 1983).

1.2.3.1 Caries-infected dentine

Caries-infected dentine is the superficial outer layer of the caries lesion (Figure 1-2). It appears clinically as a dark brown, soft, wet and mushy layer (Fusayama et al., 1966; Kidd et al., 1996; Kleter, 1998; Banerjee, 1999). Biofilm bacterial invasion and accumulation in this layer results in significant levels of demineralisation and in the destruction of extracellular matrix. Thus, it is considered as a necrotic and non-reparable area.

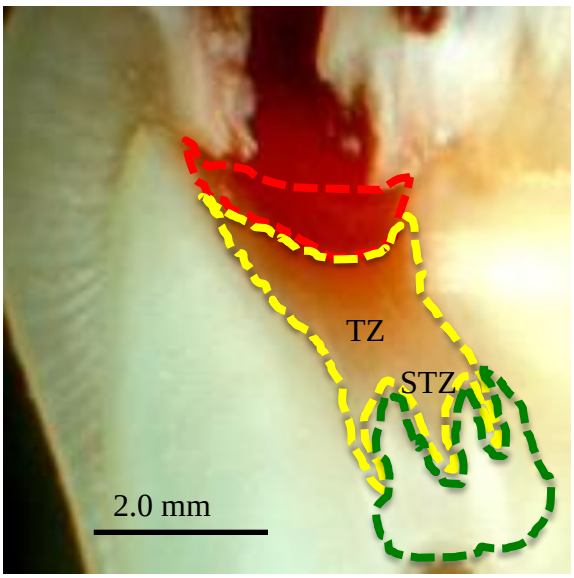

Figure 1-2 A clinical microphotograph of carious tooth section showing the different dentine caries layers. The red dotted line represents the caries-infected dentine, which has a dark brown colour. The yellow dotted line is the caries-affected dentine, which has a paler brown colour and contains the transparent (TZ) and the subtransparent (STZ) zones (Fusayama, 1979; Yamada et al., 1983; Marshall et al., 2001). The green dotted line represents the sound dentine tissue.

1.2.3.2 Caries-affected dentine

Caries-affected dentine is the inner layer of carious dentine that is described clinically as a paler brown, harder, sticky and scratchy dentine (Banerjee, 1999). The caries-affected dentine represents the advancing front of the lesion. It can be subdivided histologically into three zones: the discoloured or turbid zone, the transparent zone and the subtransparent zone (Fusayama, 1979; Yamada et al., 1983; Marshall et al., 1997; Marshall et al., 2001) (Figure 1-2).

The discoloured zone is characterized by the presence of bacteria at a lesser extent, partial demineralisation and by the lesser damage to the collagen matrix when compared to the

infected dentine (Kuboki et al., 1977). Acidic environment, within this zone, results in a demineralisation followed by the activation of different proteases, mainly MMPs, which cause the defibrillation of the unprotected collagen fibrils (Kleter et al., 1998; Carrilho et al., 2009). These make the discoloured zone, and the caries-affected dentine in general, repairable by the pulp-dentine complex as the exposed collagen matrix acts as a scaffold for mineral crystal re-precipitation.

The transparent, or sclerotic, zone is formed as a result of mineral apposition within the dentine tubules to isolate the caries lesion and prevent further penetration of substances toward the pulp (Marshall et al., 2001). It appears translucent histologically when examined under transmitted light due to the reduction in light scattering as a result of the structural homogeneity (Bernick et al., 1954). Mineral apposition within the tubules occurs in the form of plate-like acid-resistant β-octocalciumphosphate (whitlockite) crystals (Lester and Boyde, 1968; Fejerskov and Kidd, 2008). These crystals have a weaker crystalline structure, compared to hydroxyapatite, which results in relatively softer tissue than the sound dentine (Ogawa et al., 1983; Banerjee et al., 1999; Marshall et al., 2001). The process is driven by the relative increase in the pH at the advancing front (Daculsi et al., 1987) and by the presence of vital odontoblasts (Yamada et al., 1983). In a rapidly progressing lesion, the odontoblast processes are destroyed without having produced tubular occlusion (Kidd, 2004). Additionally, the lack of correlation between the caries-infected and the translucent dentine volumes indicates that such intratubular mineral apposition is limited to a certain extent (Arnold et al., 2003).

The subtransparent area represents the transitional area between the transparent zone and the normal dentine. Gradual return of the tubular structure and the formation of very fine intratubular crystals are seen in this zone (Marshall et al., 2001).

1.2.4 Differentiation between caries-infected and caries-affected dentine

In minimally invasive operative caries management, complete excavation of the caries-infected layer is recommended whilst retaining the relatively harder caries-affected dentine to which an adhesive restoration may be sealed (Marshall et al., 1997; Banerjee and Watson, 2011). Several clinical and laboratory methods have been used in attempts to delineate caries-infected dentine. Clinical methods include visual inspection, relative tissue hardness and the use of caries detector dyes. Laboratory methods include bacterial analysis and microhardness measurement. Autofluorescent (AF) detection is used both clinically and in the laboratory research to define the caries-infected and caries-affected

dentine. Table 1-3 is summarising the methods and devices used to differentiate between caries- infected, caries-affected and sound dentine.

1.2.4.1 Visual inspection

The aetiology of the colour changes within the caries lesion is not clear but it is indicated that the Maillard reaction contributes to lesion discolouration. This biochemical reaction occurs between proteins and small aldehyde molecules produced by bacteria in an anaerobic, moist and acidic biological environment found in dentine lesions (Kleter, 1998). As described before, caries-infected dentine has a darker brownish discolouration when compared to the caries-affected dentine generally. This is because of the relatively longer exposure of the outer layer to the Maillard reaction and to the oxidation as the environment shifts from anaerobic to aerobic in open cavities.

The differentiation between the caries-infected and an affected tissue based on the histological appearance is subjective and depends on operator expertise. The reliability on this technique alone is questionable as the bacterial and histological changes are not consistently colour dependent (Banerjee et al., 2010b). In rapidly advancing lesions, for instance, the caries-infected dentine has a paler brownish colour that could be misdiagnosed clinically. The arrested caries lesion has a black/dark brown colour although it has a limited bacterial count (Kidd et al., 1996; Iwami et al., 2011). Other diagnostic techniques should be used in addition to visual inspection for proper differentiation.

Table 1-3 Methods and devices used to differentiate between caries-infected, caries-affected and sound dentine and their reporting studies. AF: autofluorescence; UV: ultraviolet; QLF: quantitative laser-induced fluorescence; CLSM: confocal laser scanning microscopy; CFOME: confocal fibre-optic micro-endoscope; NIR: near-infrared; PCR: polymerase chain reaction; FISH: fluorescent in-situ hybridisation; KHN: Knoop hardness number.

Technique	Physical principles	Methods and devices	Type	Infected dentine	Affected dentine	Sound dentine	Comments	References
Clinical	Visual inspection	Colour changes	subjective	dark brown	paler brown	yellow/white	relay on the operator skills	(Fusayama et al., 1966), (Kidd et al., 1996), (Banerjee, 1999)
	Relative tissue hardness	Consistency and moisture	subjective	soft and wet	sticky and scratchy	hard and scratchy	different criteria had been reported	(Kidd et al., 1993a), (Banerjee et al., 2010b)
	Dye penetration	Caries detector dyes	subjective	dark red colour	pale red colour	pink/white colour	stain the organic matrix without any caries tissue specificity	(Fusayama and Terachima, 1972)
Both clinical and laboratory	AF reduction	UV illumination	objective	loss of AF signal with no difference between infected and affected tissues		AF signal	Basic clinical method	(Angmar-Mansson and Ten Bosch, 1987)
		QLF	objective	loss of AF signal with no difference between infected and affected tissues		AF signal	mathematical quantification of AF changes	(De Josselin De Jong et al., 1995)
	Blue-green AF	CLSM	objective	relative increase in the AF signal	relative decrease in the AF signal	no AF signal detected	enhance the weak caries AF signal	(Banerjee, 1999), (Shigetani et al., 2003), (Banerjee et al., 2010b)
		CFOME	objective				modified CLSM for clinical usage	(Banerjee et al., 2010a)
	Red-NIR AF	DIAGNOdent™	objective	DIAGNOdent™ values > 30		DIAGNOdent™ values < 30	Clinical devise for caries AF detection	(Lussi et al., 2004), (Hibst et al., 2001)
		Fluorescence spectroscopy	objective	AF signal detected		no AF signal	Initial method used to detect caries AF	(König et al., 1993)

Technique	Physical principles	Methods and devices	Type	Infected dentine	Affected dentine	Sound dentine	Comments	References
Laboratory	Bacterial analysis	Culturing method	objective	infected has more pathogens than affected dentine		no pathogens are detected	specific known pathogens are cultured from the tissues	(Loesche and Syed, 1973), (Hoshino, 1985)
		PCR	objective	infected has more species than affected dentine		no species are detected	wide range of species are detected depending on the analysis of DNA sequence	(Munson et al., 2004), (Iwami et al., 2007), (Iwami et al., 2011)
		FISH	objective	significant decrease in the species from the infected dentine through towards the sound dentine			detect rRNA sequences by a fluorescently labelled probe	(Banerjee et al., 2002), (Al-Ahmad et al., 2007)
	Microhardness	Knoop diamond indenter	objective	KHN < 25	KHN from 25-40	KHN > 40	unaffected by sample variability	(Ogawa et al., 1983), (Banerjee et al., 1999), (Banerjee et al., 2010a)

1.2.4.2 Relative tissue hardness

To detect infected carious tissue, a relative tissue hardness assessment, or the tactile sensation, is used clinically using a rounded dental explorer. This technique is usually associated with the visual inspection and they are well established and universally taught for caries diagnosis. Despite the fact that these techniques show some clinical validity, they are affected widely by operator subjectivity. A review by Bader et al. (2001) found that the visual and relative hardness methods provide low sensitivity (39–59%) and high specificity (> 95%) in detecting lesions. This indicates how difficult it is to differentiate between the caries-infected and caries-affected dentine when the initial diagnosis of nearly half of the carious lesions could be missed using these techniques. Additionally, different clinical criteria have been used for caries lesion assessment (Ismail, 2004) which make the techniques rely more on operator skill and expertise.

Kidd et al. (1993a) proposed certain clinical criteria for the differentiation between caries-infected and caries-affected dentine depending on the lesion consistency and moisture. Soft texture is determined when the probe readily enters the tissue; medium texture is when the probe enters tissue only if pressed firmly and hard consistency when the discoloured tissue is as hard as the surrounding sound tissue. Lesion wetness is determined by moisture oozing from the lesion following its penetration by the dental probe. The study found that the soft wet tissue showed significant increase in the bacterial count, which represent the caries-infected dentine. Banerjee et al. (2010b) indicated that the sound dentine is hard and scratchy to a sharp dental explorer, caries-infected dentine has a soft, ‘‘mushy’’ consistency and caries-affected dentine falls in between.

1.2.4.3 Caries detector dyes

Several studies had attempted to differentiate between the two carious dentine layers using various protein dyes. Fusayama and Terachima (1972) explained the use of 0.5% basic fuchsin-propylene glycol solution to stain the outer caries-infected layer and differentiate it from the inner caries-affected dentine. Varieties of dyes are available now and have been marketed as dentine caries detection agents to enhance complete removal of caries-infected dentine. These dyes stain the organic matrix of less well-mineralised dentine without any caries detection specificity. This can give a false positive result by staining the uninfected areas, which contain a high proportion of organic matrix if near the pulp chamber or at the EDJ (Mccomb, 2005). A microbiological study on the dye-stained and the dye-unstained EDJ areas, considered clinically sound, showed low

numbers of bacteria with no difference in the levels of infection between them (Kidd et al., 1993b). The complete excavation of all dye-stained dentine results in the excessive removal of sound tooth structure (Ansari et al., 1999). False negative results are also seen in slightly demineralised dentine that is not porous enough to hold the stain (Pugach et al., 2009).

1.2.4.4 Fluorescence detection

Fluorescence occurs as a result of the interaction between photons illuminating the object and the molecules in this object. The photon energy is absorbed by the object molecule and then released at a lower energy level of longer wavelength and different colour.

Dental hard tissues exhibit natural fluorescence without the addition of other luminescent substances that is referred to as the autofluorescence (AF). Early studies had found that enamel and dentine exhibit bluish-white fluorescence and an intense blue fluorescence respectively when the tissues are excited with an ultraviolet wavelength (Benedict, 1928). It was also found that this fluorescence signal is related to the organic components found in these tissues, which explains why dentine fluoresces much more intensely than the enamel (Hartles and Leaver, 1953).

In the caries lesion, the nature of the tissues AF is changed as a result of the structural changes. Under UV illumination, these changes are noticed as a dark spot against the healthy tissue autofluorescence background (Angmar-Mansson and Ten Bosch, 1987). It was thought that the dark spots represent areas where autofluorescence is lost as a result of organic components destruction during the carious process (Armstrong, 1963). However, it was found that the caries-infected dentine has its own characteristic AF signal that is weaker, with a slower fluorescence decay (Mcconnell et al., 2007), than the sound structure (König et al., 1999; Borisova et al., 2006).

Two different types of AF signal were detected in caries dentine lesions. The nature or type of AF is dependent on the excitation wavelength employed (Ribeiro Figueiredo et al., 2005). Illumination with blue light (488 nm) produces green AF (distinguished through 515–590 nm band pass detection filters). This type of AF is attributed to the breakdown of structural proteins (Van Der Veen and Ten Bosch, 1996; Banerjee and Boyde, 1998; Mcconnell et al., 2007). Red excitation (655 nm) generates near-infrared (NIR) fluorescence that is detected with a long pass filter (transmission > 680 nm). The Red-NIR AF was the first caries AF to be described (König et al., 1993). Protoporphyrin

IX produced by bacterial decomposition and other oral bacterial metabolites are responsible for generating this type of AF (König et al., 1993; König and Schneckenburger, 1994; Hibst et al., 2001; Lussi et al., 2004; Stookey, 2005; Lennon et al., 2006).

Depending on the AF changes of the caries lesion, different devices have been used clinically and in laboratory investigations to delineate the outer caries-infected and the inner caries-affected dentine layers. These devices can be divided into devices that measure the AF reduction, blue-green AF devices and red-NIR AF devices.

AF reduction measurement

Quantitative laser-induced fluorescence (QLF) was used to detect the caries lesion based upon the decrease of the fluorescence luminosity (De Josselin De Jong et al., 1995). It has been used in both the clinical (Al-Khateeb et al., 1998) and the laboratory investigations (Van Der Veen and Ten Bosch, 1996) for detecting and monitoring the progress or regress of the caries lesion (Stookey, 2005; Twetman et al., 2012). Blue light is used to illuminate the tissues and the AF is detected using a green band pass filter (Stookey, 2005). The device can be also modified so that the green and the red fluorescence signals are detected to determine the lesion activity (Pretty, 2006). The use of this technique to differentiate between the caries-infected and the caries-affected dentine is not satisfactory, as the software needs to be calibrated for the two types of tissues before using it (Pretty, 2006) and so is reliant on operator subjectivity. For this reason it shows a very low specificity (11%) and high sensitivity (95.8%) in detecting caries lesions, which is similar to the visual inspection (Stookey, 2005; Zandoná et al., 2010).

Blue-green AF devices

Confocal laser-scanning microscopy (CLSM) had been used to detect the blue-green AF signal in laboratory investigations (Banerjee, 1999; Shigetani et al., 2003; Banerjee et al., 2010b). Confocal microscopy, in general, has the ability to control the depth of field and eliminate the background information away from the focal plane when compared to conventional wide-field optical microscopy. The basic key to the confocal approach is the use of an aperture in the conjugate focal plane of an objective lens in both the illuminating and imaging pathways of a microscope (Watson et al., 2008). The area surrounding the aperture rejects stray photons returning from areas that are not in the focal plane of the lens. Thus, the sound dentine overwhelming AF signal is eliminated and the relatively weaker blue-green caries AF signal is enhanced (Banerjee, 1999).

The use of CLSM in the detection of such an AF signal has been proposed as an alternative microscopic marker to highlight the caries-infected dentine objectively. It was found that the blue-green AF is highly correlated with the mineral distribution (Banerjee and Boyde, 1998), the bacterial count (Banerjee et al., 2002) and the tissue microhardness (Banerjee et al., 1999). The technique has been also developed to include a 600 μm field-width, plane-ended fibre optic probe that allows the intake of AF signal from different points across the caries lesion (Banerjee et al., 2010a). The confocal fibre-optic micro-endoscope (CFOME) has a potential to be used directly on patients during treatment. Blue-green AF detection had been already used to evaluate the efficiency and the effectiveness of caries-infected dentine excavation methods *in vitro* (Banerjee et al., 2000b) and as an objective evaluation for the remaining caries-affected dentine substrate prior to adhesive restoration application (Banerjee et al., 2010b).

Red-NIR AF devices

Early work on caries lesion AF detection was based on the detection of the NIR signal using fluorescence spectroscopy (König et al., 1993; König and Schneckenburger, 1994). Based on the same technique, a clinical device that is used to detect caries lesions has been marketed under the trade name DIAGNOdent™ (Karlsson, 2010). The system provides a quantitative measurement of the caries AF intensity (Lussi et al., 2004). It has a scale ranged from 0 to 99 in units related to a calibration standard of a known and stable fluorescence source (Hibst et al., 2001). An association between the system readings and the caries lesion progression, to provide cut-off values, has been investigated (Lussi et al., 2001; Huth et al., 2008). It was found that the borderline reading for the caries-infected tissue that requires excavation is set at a value of 30 (Lussi et al., 2004). Many laboratory and clinical studies had reported the applications of this apparatus in detecting the initial caries lesion. Although a recent systematic review found that the device sensitivity (75%) was higher than its specificity (55%) (Twetman et al., 2012), wide variations in the device sensitivity (19% to 100%) and specificity (52% to 100%) were found (Karlsson, 2010). In one study the visual inspection performed better than red-NIR device (Braga et al., 2009). In addition, the evidence of its use to differentiate between the caries-infected and caries-affected dentine is not clear. As the lesion depth increases into dentine, a wide range of readings with greater variation is found (Huth et al., 2008). This was explained by the possible interference of the fluorescence signal by pulpal tissues (Lussi et al., 2000) or by the diffusion of the porphyrins through the relatively wider dentine tubules (Alleman and Magne, 2012). Yonemoto et al. (2006) had reported that the endpoint for caries-infected

dentine excavation could be set at 11–20 DIAGNOdent™ values. This result should be considered carefully as the caries-infected zone was highlighted using caries detector dyes in this study, which have no specifity for caries detection as mentioned earlier.

Other factors such as plaque, stains and other fluorescence materials also affect the DIAGNOdent™ values and they give more false-positive readings in caries detection, which is another drawback of the system (Shigetani et al., 2003; Lussi et al., 2004; Mendes et al., 2004; Pretty, 2006).

1.2.4.5 Bacterial analysis

As described previously, the outer caries-infected dentine layer, which is exposed to the oral environment, contains large quantity of biofilm bacteria that invade and accumulate in this layer (Ogawa et al., 1983). The inner caries-affected dentine has a relatively reduced bacterial population (Hoshino, 1985; Kidd et al., 1996; Iwami et al., 2007). Based on this, many studies had tried to differentiate between the two tissues by looking at the causative pathogens. In general, the bacterial analysis method is considered as a gold standard to which all other tissue identification techniques are compared.

Different studies relied on various culture methods to detect, distinguish and quantify the bacteria present in samples of carious dentine (Loesche and Syed, 1973; Hoshino, 1985). The technique simply involves the identification of specific known pathogens by culturing the biofilm samples *in vitro* in conditions that are optimum for the multiplication of these specific species. The main species that are cultured from dental caries are *Streptococcus mutans*, *Lactobacillus casei*, *Actinomyces* species and *Veillonella* species. Kidd et al. (1996) found that caries-affected dentine had significantly less mutans streptococci and lactobacilli using the conventional culturing methods when compared to the caries-infected dentine. Isolated anaerobic bacteria was also found to be in lower concentrations in the caries-affected dentine using the same method (Hoshino, 1985).

A major limitation of the cultural method is that approximately 50% of the oral microflora is unculturable leading to underestimating the total bacterial population (Wilson et al., 1997; Wade, 2002). Advances in molecular biology technology have allowed the studying of mixed bacterial communities within oral infections in their entirety, avoiding the biases of cultural techniques (Dymock et al., 1996).

The polymerase chain reaction (PCR) technique was used to detect a range of microorganisms within the dental caries lesion. It relies on the analysis of the DNA

sequences of a conserved region in the 16S ribosomal DNA of these organisms (Wade, 2002). PCR has allowed the detection of diverse microflora present in the dentine carious lesion (Munson et al., 2004) with some found in deep caries-affected dentine (Iwami et al., 2007). It was also used to relate the caries lesion colour (Iwami et al., 2008) and red-NIR AF signal (Iwami et al., 2011) to its bacterial activity. In all these studies, the caries-infected dentine peripheries were determined by the presence of active bacterial species. This was clear in Iwami et al. (2007) study where it was concluded that the objectivity of caries removal using the caries detector dye is low as bacterial DNA can be still found the dye-free tissues. In general, PCR technique is sensitive enough to amplify any ribosomal DNA within the sample. It requires certain precaution to prevent cross-contamination during samples collection or from the lab environment (Scherczinger et al., 1999).

A more accurate method of microbiological analysis had been proposed to explore bacteria present in carious dentine. It involves the use of fluorescent in-situ hybridisation (FISH) to detect nucleic acid sequences by a fluorescently labelled oligonucleotide probe that hybridizes specifically to its complementary target sequence within the intact cell (Moter and Gobel, 2000). The most widely used nucleic acid target for bacterial cell detection is the 16S rRNA molecule (Wade, 2002). Banerjee et al. (2002) used the technique to quantify the total number of bacteria within the caries-infected, caries-affected and sound dentine. Despite the limited number of sample used in this study, oral microflora was still found in the advancing front of the dentine lesion. Such finding highlights the importance of detecting the necrotic caries-infected dentine tissue through the analysis of structural changes rather than looking for the whole bacterial population. FISH was also used to analyse the dynamical changes of bacterial constituents within the oral biofilm over a one-week period (Al-Ahmad et al., 2007). In general, the FISH technique has a complicated preparation process due to the fact that probes are tailored for the identification of specific DNA sequences (Trask, 1991). The technique is more useful for the identification and studying the behaviour of un-cultured species rather than the differentiation between the caries-infected and caries-affected dentine.

1.2.4.6 Microhardness measurement

Microhardness measurement retains direct clinical translational value to operators using the relative tissue hardness to delineate excavation margins (Banerjee et al., 2010a). It has been used as a reference for dentine's inherent physical properties, as it is not affected by the variability of samples (Bresciani et al., 2010; Kirsten et al., 2010). Using an Ultra-

Micro-Indentation System (UMIS), it was found that the hardness of carious dentine is associated with relative mineral content (Angker et al., 2004; Sakoolnamarka et al., 2005). However, microhardness measurement of dental tissue is considered as a destructive test where only one single indentation can be made in each measurement site. Additionally, sample positioning and its moisture condition can affect the hardness value.

The Knoop diamond indenter has been used in in-vitro studies to determine the hardness of different carious layers and to detect the changes in the consistency of the dental hard tissues after being subjected to different types of treatments (Banerjee, 1999; Bedini et al., 2010; Bresciani et al., 2010; Kirsten et al., 2010). It was found that the caries-infected dentine has a Knoop hardness number (KHN) less than 25, caries-affected dentine KHN ranged from 25 to 40 and the sound dentine has KHN above 40 (Ogawa et al., 1983; Banerjee et al., 1999; Banerjee et al., 2010a).

1.3 Matrix metalloproteinases (MMPs)

1.3.1 Introduction

Matrix metalloproteinases (MMPs), also known as matrixins, are a multigene family within the metalloproteinase class of calcium-dependent zinc-containing endopeptidases capable of degrading all extracellular matrix (ECM) and basement membrane components including different collagens in both native and denatured forms (Sulkala et al., 2001; Sorsa et al., 2004; Hannas et al., 2007; Perdigão, 2010).

The first MMP (collagenase or MMP-1) was identified by Gross and Lapiere (1962) as a collagenolytic factor that acts on native collagen at neutral pH and physiologic temperature. Before MMP-1 detection, it was thought that collagen is removed in two stages. Firstly, that the collagen structure is altered by low pH, elevated temperatures or denaturing substances. Secondly, that the altered protein is degraded by nonspecific lysosomal cathepsins (Ehrmann and Gey, 1956; Woessner, 1962; Reynolds, 1970). In general, cathepsins are acidic enzymes that are enclosed within subcellular granules, termed lysosomes, and released into digestive vacuoles within the cytoplasm following the rupture of the lysosome membranes (Gianetto and Duve, 1955; Woessner, 1962; Duve, 1975; Bainton, 1981). Unlike MMPs, cathepsins function optimally in an acidic environment and they are inactivated by neutral pH (Turk et al., 1999). In addition, the phagocytic collagen degradation, by lysosomal cathepsins, is prevalent particularly in areas of rapid collagen turnover such as the periodontal ligament (Melcher and Chan, 1981; Birkedal-Hansen et al., 1993).

The MMP family is involved in certain physiological processes including development, tissue remodelling and angiogenesis (Birkedal-Hansen et al., 1993; Vu and Werb, 2000). MMPs also play a key role in the regulation of cellular communication, molecular shedding and immune functions by processing bioactive molecules, including cell surface receptors, cytokines, hormones, defensins, adhesion molecules and growth factors (Sorsa et al., 2004; Bourboulia and Stetler-Stevenson, 2010). MMPs are found during wound healing and in pathological states such as atheroma, arthritis, cancer, ischaemic cerebrovascular disease and tissue ulceration (Watanabe and Ikeda, 2004; Zsolt and Krasimir, 2011; Martins et al., 2012).

To date, 24 different MMPs have been cloned genetically, of which 23 are found in humans and 26 well characterized members have been reported. MMPs share extensive

sequence homology, but differ in terms of substrate specificity and transcriptional regulation (Chaussain-Miller et al., 2006; Hannas et al., 2007). A review by Iyer et al. (2012) reported the common features that are shared among MMP family members (Table 1-4).

Table 1-4 Requirements for an enzyme to be classified as an MMP family member (Iyer et al., 2012).

1	Proteolysis of at least one ECM component
2	Catalysis dependent on zinc at the active site
3	Activation by proteinases or organomercurials
4	Inhibited by EDTA (ethylenediaminetetraacetic acid), 1,10-phenanthroline and one of the TIMPs
5	cDNA has sequence homology to MMP-1

The structure of MMPs consists of a signal peptide sequence prodomain, an aminoterminal catalytic domain, a hinge region and a hemopexin domain (Figure 1-3a). The main functional part of the MMP is the aminoterminal catalytic domain as it contains a highly conserved Zn binding site (Figure 1-3b) (Birkedal-Hansen, 1995). Six recognition and binding subsides; S3, S2, S1, S1′, S2′, and S3′ are also found around the catalytic zinc and they correspond to the minimum length of the hydrolysable peptide substrates (Figure 1-3c) (Dorman et al., 2010).

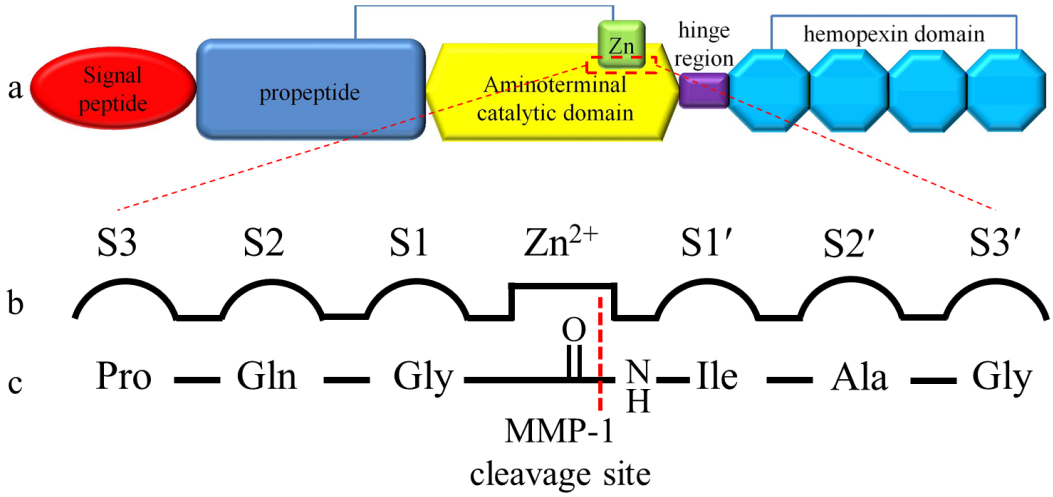

Figure 1-3 The domain structure for MMP-1 as an example for all MMPs. (a) the main four parts for an inactive MMP-1. A conserved Cys residue in the propeptide coordinates the zinc ion. Enzyme activation results from a combined cleavage within the propeptide and between the propeptide and the catalytic domain (Page-Mccaw et al., 2007); (b) the Zinc binding site on the catalytic domain of an active enzyme and the 6 surrounding subsides (S); (c) a sequence in the collagen α chain, where the MMP-1 cleavage site is located, that matches the catalytic domain subsides.

MMPs are classified into six main groups based on their substrate specificity, sequence similarity and domain organization (Visse and Nagase, 2003; Chaussain-Miller et al., 2006). The main functions of each of these groups are summarised in Table 1-5.

Table 1-5 Classification of MMPs based on their substrate specificity, sequence similarity and domain organization.

MMPs group	MMPs	Main functions
Collagenases	MMP-1, MMP-8, MMP-13, MMP-18	interstitial collagens cleavage
Gelatinases	MMP-2, MMP-9	denatured collagens (gelatins) degradation and they are important for osteogenesis
Stromelysins	MMP-3, MMP-10, MMP-11	extracellular matrix digestion and proMMPs activation
Matrilysins	MMP-7, MMP-26	process cell surface molecules such as pro–α-defensin, Fas-ligand, pro–tumour necrosis factor (TNF)-α and E-cadherin
Membrane-type MMPs (MT-MMPs)	MMP-14, MMP-15, MMP-16, MMP-17, MMP-24, MMP-25	Pro-MMP-2 activation, extracellular matrix digestion and have an important role in angiogenesis.
Other MMPs	MMP-12, MMP-19, MMP- 20, MMP-21, MMP-22, MMP-23, MMP-27, MMP-28	MMP-12: expressed during macrophages migration MMP-19: a T-cell–derived autoantigen MMP-20 (Enamelysin): amelogenin digestion MMP-28: tissue haemostasis and wound repair

1.3.2 MMP activity regulation

MMP functional activity is regulated by four mechanisms: by positive and negative transcriptional control of MMP genes, by activation from the latent state, by differences in substrate specificity and, finally, modulation by serum inhibitors or tissue inhibitors of metalloproteinases (TIMPs) (Hannas et al., 2007). The transcriptional control of MMP genes usually results in low basal levels of these enzymes in normal physiology with a tight control of cell specific expression. As a result, MMPs are often co-expressed or co-repressed in response to multiple stimuli, including inflammatory cytokines, growth factors, glucocorticoids or retinoids (Yan and Boyd, 2007; Fanjul-Fernández et al., 2010). During this process, signalling proteins are involved in the activation of transcription factors by phosphorylation. These signalling proteins include the nuclear factor kappa B (NF-κB), the mitogen activated protein kinases (MAPK), the signal transducers and activators of transcription (STAT) and the Smad family of proteins. Interestingly, MMPs that are co-regulated in their expression under certain conditions share several

transcription-binding sites in their promoter sequences, whilst functionally related MMPs differ greatly in the composition of the cis-elements present in their respective promoter regions (Fanjul-Fernández et al., 2010).

1.3.3 Host derived MMPs in the oral environment

MMPs are synthesized and secreted by connective tissues cells, such as fibroblasts, osteoblasts and odontoblasts, into the extracellular matrix to create the cellular environment required during the development, morphogenesis and remodelling of tissues that occurs throughout life. MMPs are also secreted by a variety of pro-inflammatory cells including macrophages, neutrophils, and lymphocytes (Verma and Hansch, 2007).

In the oral environment, MMPs have been identified in saliva, gingival crevicular fluid, enamel, dentine and pulp. It has been postulated that the MMPs present in the dentine matrix or in saliva may be responsible for the dentine matrix degradation in dentine caries lesions (Tjaderhane et al., 1998; Van Strijp et al., 2003; Hannas et al., 2007).

1.3.3.1 MMPs in saliva

Both collagenases and gelatinases have been detected in whole saliva (Makela et al., 1994; Uitto et al., 2003), originating either from gingival crevicular fluid (GCF) or salivary gland secretions. Under physiological conditions, MMP concentrations are strictly controlled by specific and non-specific inhibitors such as α_2-macroglobulin (Birkedal-Hansen, 1993). MMPs in saliva and GCF have a destructive role in the inflammatory process as well as the modification of host response. Therefore, levels of MMPs in GCF cannot be interpreted as indicating tissue degradation alone, but protective and destructive as a whole (Uitto et al., 2003; Van Strijp et al., 2003; Chaussain-Miller et al., 2006).

In the presence of carious lesions in the oral environment, the MMPs found in the soft, necrotic caries-infected dentine (MMP-1, MMP-2, MMP-8 and MMP-9) are also present in saliva (Tjaderhane et al., 1998; Van Strijp et al., 2003). These salivary MMPs degrade the exposed dentine organic matrix and their inhibition reduces the gelatinolytic activity and retards caries progression (Sulkala et al., 2001).

1.3.3.2 MMPs in enamel and dentine

MMPs have been implicated in tissue remodelling and regulation of cell-matrix interactions during enamel and dentine morphogenesis (Fanchon et al., 2004; Hannas et

al., 2007). Dentine MMPs may be involved in various physiological processes occurring in dentine, such as maturation and the formation and mineralisation of intra- and intertubular dentine during dentinogenesis as well as dentine caries progression (Van Strijp et al., 2003; Sulkala et al., 2007). Although MMPs may be involved in enamel and dentine formation, their fate after mineralisation is not clear. Upon mineralisation, they may be trapped in the mineralised phase, bound to collagen or hydroxyapatite crystals (Martin-De Las Heras et al., 2000).

The collagenases (MMP-1 and MMP-8), gelatinases (MMP-2 and MMP-9), stromelysin-1 (MMP-3), MMP-2 activator (MT1-MMP) and enamelysin (MMP-20) have all been identified in either odontoblasts or within the predentine/dentine compartment (Tjaderhane et al., 1998; Palosaari et al., 2000; Palosaari et al., 2002; Van Strijp et al., 2003; Chaussain-Miller et al., 2006; Sulkala et al., 2007; Zheng et al., 2011). MMPs found in predentine contribute to organic matrix reorganization before mineralisation. The main MMPs found in dentine are summarised in Table 1-6.

Enamelysin (MMP-20) is known to be almost exclusively expressed by odontoblasts. It has unique structural and enzymatic properties, being capable of degrading amelogenin and has been attributed an important role during early stages of enamel development. Amelogenin is considered as the major structural component protein of the enamel matrix. MMP-20 is also expressed by mature human odontoblasts, which secrete it into the dentinal fluid. Being produced during primary dentinogenesis, MMP-20 is incorporated into dentine and may be released during the progression of dental caries (Sulkala et al., 2002).

MMP-2, along with its activator membrane type-1 matrix metalloproteinase (MT1-MMP or MMP-14), is expressed in differentiating and secretory ameloblasts and odontoblasts, having an important role in remodelling and degradation of the basement membrane during human tooth morphogenesis (Heikinheimo and Salo, 1995).

The more highly proteolytic stromelysins (MMP-3) are found in secretory ameloblasts and odontoblasts, and in the forming enamel, predentine, and where mineralisation is initiated. In predentine, MMP-3 is probably involved in proteoglycan turnover by controlling and activating proMMPs as described earlier in Section 1.1.3.2 (Hall et al., 1999; Hannas et al., 2007).

Table 1-6 Domain structures, substrates and studies reporting the functions of main MMPs found in dentine: Fn, fibronectin domain; I, type I transmembrane domain; Cp, cytoplasmic domain.

MMP	Structure	Substrate	Reported studies
MMP-1 (Collagenase-1)	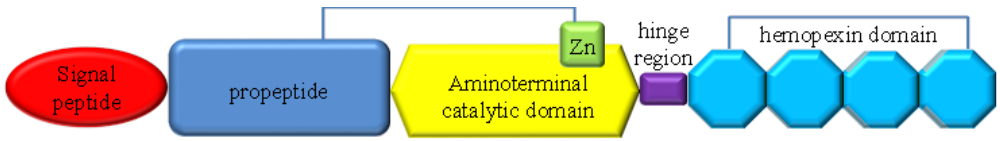	collagens (I, II, III, VII, VIII, X, XI) and gelatin	(Van Strijp et al., 2003; Zheng et al., 2011)
MMP-3 (Stromelysin-1)		collagens (III, IV, V, VII, IX, X, XI), elastin and gelatin	(Hall et al., 1999)
MMP-8 (Collagenase-2)		collagens (I, II, III, V, VII, VIII, X) and gelatin	(Palosaari et al., 2000; Sulkala et al., 2007)
MMP-20 (Enamelysin)		Amelogenin	(Sulkala et al., 2002)
MMP-2 (Gelatinase A)	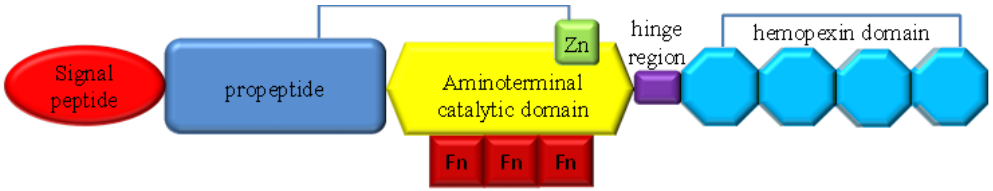	collagens (I, III, IV, V, VII, X, XI, XIV), gelatin and elastin	(Heikinheimo and Salo, 1995; Tjaderhane et al., 1998; Van Strijp et al., 2003)
MMP-9 (Gelatinase B)		collagens (IV, V, VII, X, XI, XIV) and gelatin	(Heikinheimo and Salo, 1995; Tjaderhane et al., 1998; Van Strijp et al., 2003)
MMP-14 (MT1-MMP)	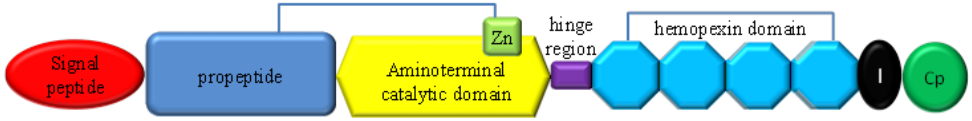	collagens (I, II, III) and gelatin	(Palosaari et al., 2002)

Sulkala et al. (2007) found that MMP-8 is the major collagenolytic enzyme in human dentine. They concluded that MMP-8 was found mostly in the unbound protein fraction while most of the gelatinolytic activity was observed in organic matrix and released only after demineralisation.

1.3.4 MMP activation and inhibition

Disease processes associated with matrix metalloproteinases are generally related to imbalance between their activation and inhibition resulting in either increased extracellular matrix degradation, as in rheumatoid arthritis or malignancy, or accumulation of extracellular matrix, as in fibrotic diseases. In normal physiological conditions, MMPs are precisely regulated and inhibited by natural tissue inhibitors which are the endogenous Tissue Inhibitors of Metalloproteinases (TIMPs). In seeking to regulate the MMP-TIMP balance in pathological conditions to block or reverse disease progression, either increasing the local concentration of TIMPs or MMP activity inhibition using small molecule synthetic inhibitors have been investigated. The local concentration of TIMPs is usually increased by recombinant protein administration or gene transfer. Increasing the local concentration of TIMPs in carious dentine may limit matrix destruction and promote remineralisation and, thus, represents a potential strategy for future restorative dental therapy (Baker et al., 2002; Visse and Nagase, 2003; Chaussain-Miller et al., 2006).

1.3.4.1 MMP activation

MMPs are secreted as inactive precursors and require activation to degrade the extracellular matrix components (Figure 1-3a). They can be activated *in vitro* by proteinases or by chemical agents such as thiol-modifying agents (4-aminophenylmercuric acetate, $HgCl_2$ and *N*-ethylmaleimide), oxidized glutathione, SDS, chaotropic agents and reactive oxygens. Mildly acidogenic conditions (pH 4.5 – 6.5) and heat treatment can also lead to MMP activation (Tay et al., 2006). It has also been suggested that MMPs in carious dentine, whether derived from saliva or from dentine, can be activated by bacterial proteinases and acids. Furthermore, phosphorylated proteins interact with the inhibited dentinal MMPs within the lesion and reactivate them during the demineralisation process which enhances matrix degradation. These activating agents most likely work through the disturbance of the cysteine-zinc interaction of the cysteine switch (Van Strijp et al., 2003; Visse and Nagase, 2003).

Several in-vitro studies reported that application of 35% phosphoric acid for 15 seconds during cavity etching can activate and release dentine MMPs. This method was also used to extract different MMPs from dentine samples (De Munck et al., 2009; Breschi et al., 2010a). Similarly, the relatively mild acidity of self-etch adhesive systems was found to be sufficient to activate latent MMPs in dentine powder (Tay et al., 2006). This activity was found to be increased slowly *in vitro* to near maximum levels over several months and contributed to the degradation of resin–dentine interface, due to the acidic environment created by these adhesives or by the progressive loss of inhibition by the TIMPs (Nishitani et al., 2006).

1.3.4.2 MMPs inhibition

The MMP inhibitors are divided into two types: natural tissue inhibitors and synthetic MMP inhibitors.

Natural Tissue Inhibitors

TIMPs are the major physiological regulators of MMP local activity, exhibiting variable efficacy against different MMPs, as well as different tissue expression patterns and modes of regulation (Baker et al., 2002). So far, four TIMP members (TIMP-1, TIMP-2, TIMP-3 and TIMP-4) have been described in vertebrates and their expression is regulated during development and tissue remodelling.

TIMP is a single peptide consisting of 184-194 amino acids with 12 conserved cysteines (Figure 1-4) (Williamson et al., 1990; Murphy and Nagase, 2008). The mechanism of TIMP inhibition of MMPs has been elucidated based on the crystalline structure of the 1:1 stoichiometry TIMP-MMP complexes (see Figure 1-5). The catalytic zinc atom is bidentately chelated by the N-terminal amino group and the carbonyl group of Cys1, which expels the water molecule bound to the zinc atom (Nagase et al., 2006). This crystal structure provides a foundation for the design of a new class of synthetic MMP inhibitors, based on the central two-segment docking site of TIMP-1 and the unusual zinc chelating residue Cys 1 (Gomis-Ruth et al., 1997).

Three TIMPs have been well characterized at the present time, each capable of inhibiting all tested metalloproteinases, but each showing specific binding to a particular MMP at a site distinct from the active site (Wojtowicz-Praga et al., 1997).

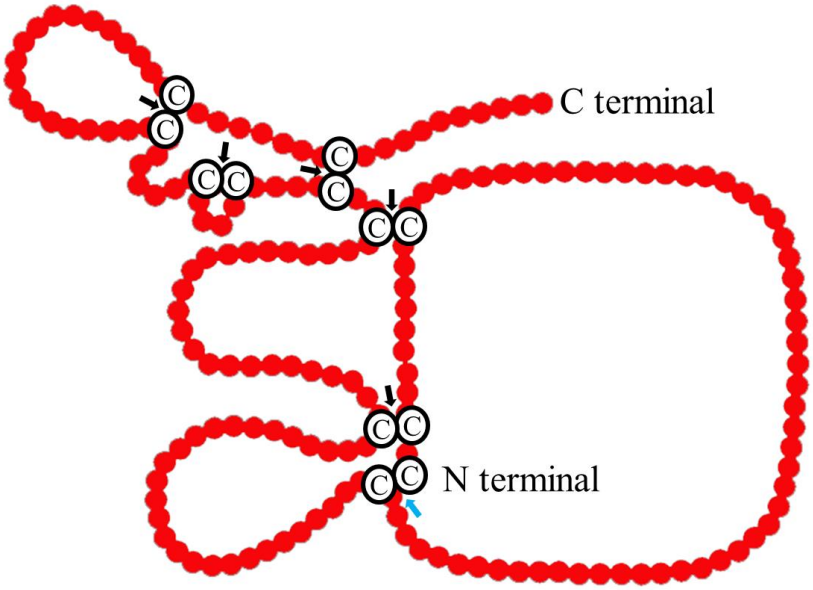

Figure 1-4 TIMP-1 molecule structure which contains 12 conserved cysteines (C) and six disulphide bonds (arrows) (modified from Birkedal-Hansen et al. (1993)). The overall shape of the TIMP molecule is ‘‘wedge-like’’ and the N-terminal four residues Cys1-Thr-Cys-Val4 and the residues Glu67-Ser-Val-Cys70 (residues are in TIMP-1) that are linked by a disulfide (blue arrow) from a contiguous ridge that slots into the active site of the MMPs.

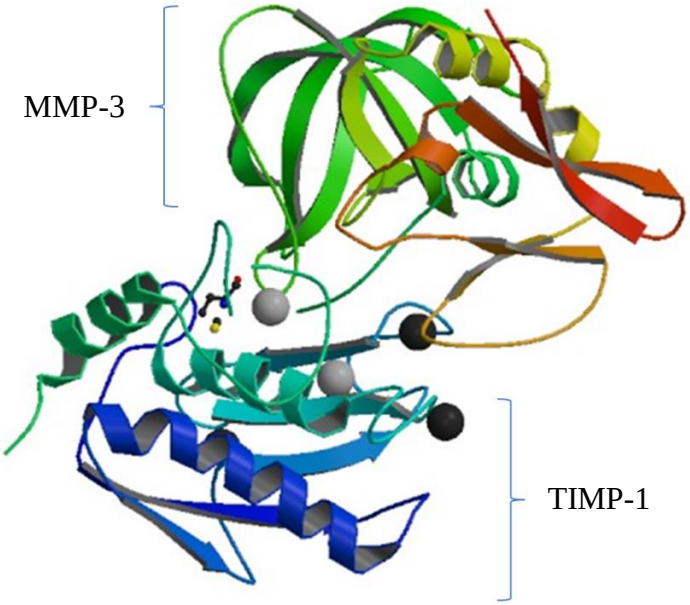

Figure 1-5 Ribbon structure of the TIMP-1 and MMP-3 complex. The image was prepared from Brookhaven Protein Data bank entry 1UEA (Orientation in Solution of MMP-3 Catalytic Domain and N-TIMP-1 from Residual Dipolar Couplings) using Pymol.

Using immunoblotting, Ishiguro et al. (1994) demonstrated the presence of TIMP-1 in pulverized dentine powder and it was found that concentrations increased consistently toward the predentine as they are synthesized and secreted by mature odontoblasts and pulp tissue. In addition, TIMP-2 and TIMP-3 mRNA was also expressed by the same cells. TIMP-2 in association with MT1-MMP mediates proMMP-2 activation, the mechanism which possibly also activates human tooth proMMP-20. TIMP-3, which is capable of binding to compartments of the extracellular matrix, may also induce cell apoptosis. The TIMPs are involved in the regulation of dentine mineralisation by controlling MMPs activities (Wojtowicz-Praga et al., 1997; Palosaari et al., 2003).

Synthetic MMP Inhibitors

Due to the role of MMPs in the progression of cancerous lesions, different attempts have been reported to try to inhibit the expression or activity of MMPs. It was suggested previously that the inhibition of MMPs activity can be achieved by an increase in the local concentration of TIMPs (Bourboulia and Stetler-Stevenson, 2010). TIMPs cannot be used as an anti-cancer therapy and are probably not suitable for pharmacologic applications due to their short half-life *in vivo* (Blavier et al., 1999). Several chemotherapeutic agents, such as antibiotics and synthetic peptides, which are able to modulate production or activity of different classes of MMPs, were developed to mimic the collagen structure (Wojtowicz-Praga et al., 1997).

The development of synthetic MMP inhibitors has relied on the peptide sequence of the target protease. For a molecule to be an effective MMP inhibitor, it requires a functional group (hydroxamic acid, formylhydroxylamine, sulfhydryl, phosphinic acid, aminocarboxylate and carboxylic acid) capable of chelating the active-site zinc ion (ZBG in Figure 1-6), at least one functional group which provides a hydrogen bond interaction with the enzyme backbone and one or more side chains (P in Figure 1-6) which undergo effective van der Waals interactions with the enzyme subsides (Whittaker et al., 1999). Based on the subsides that are occupied by the side chains, synthetic MMP inhibitors can be divided into 3 main groups; combined inhibitors (Figure 1-6b) where all the six subsides are occupied, right hand side inhibitors (Figure 1-6c) where the S1′-S3′ subsides are occupied and left hand side inhibitors (Figure 1-6d) where the S1-S3 subsides are occupied.

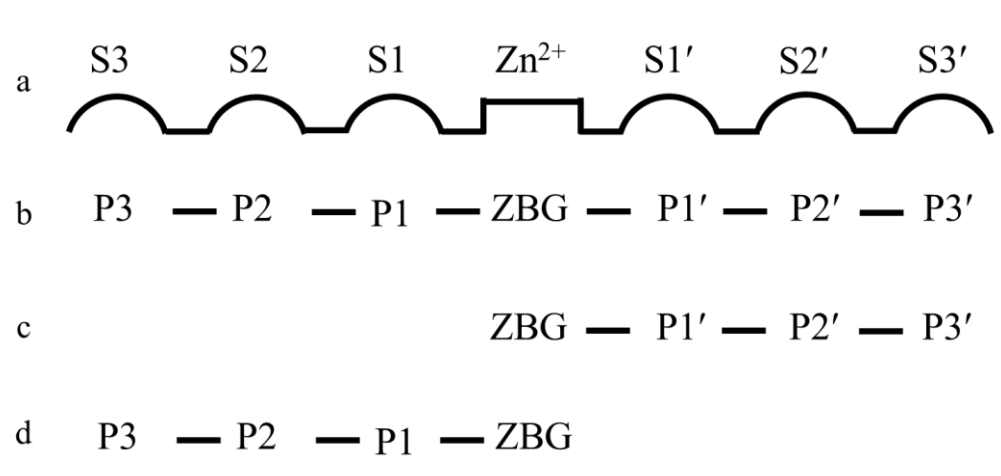

Figure 1-6 Different designs for synthetic MMP inhibitors (a) the Zinc binding site on the catalytic domain of an active enzyme and the 6 surrounding subsides (S); (b) a combined inhibitor; (c) a right hand side inhibitor; (d) a left hand side inhibitor; ZBG: Zinc binding group; P: inhibitor side chain.

The first generation of the collagen-mimicking peptides contained the collagen amino acid sequence near the collagenase cleavage site, combined with a zinc-binding hydroxamate structure inhibiting enzymatic activity specifically. Batimastat was one of the first-generation inhibitors to be studied in humans with advanced malignancies, but its usefulness has been limited by its poor water solubility, requiring intraperitoneal administration of the drug as a suspension (Whittaker et al., 1999). This led to the development of second-generation MMP inhibitors, such as Marimastat, which have the same collagen-mimicking hydroxamate structure and they are orally available (Rasmussen and Mccann, 1997; Wojtowicz-Praga et al., 1997). These drugs were developed mainly to be used in anti-cancer therapy but seem to be inappropriate for dentine caries inhibition as they are accompanied by significant side effects (Coussens et al., 2002; Overall and Lopez-Otin, 2002).

MMPs inhibition is used as an adjunctive therapy for periodontal disease. Early studies showed that tetracycline, doxycycline, minocycline and non-antimicrobial chemically modified tetracyclines (CMTs) inhibit both activity and secretion of MMPs in gingival crevicular fluid via different mechanisms (Golub et al., 1998; Golub, 2011). These include direct inhibition through Ca^{2+} and Zn^{2+} chelation, enzyme expression inhibition and inhibition of the activation of proMMP. The systemic administration of a submicrobial dose of doxycycline resulted in a significant improvement in tooth attachment as well as reduction of pocket depth and bleeding after probing. These

inhibitors are among the few MMP inhibitors that are considered to be safe and effective, particularly after oral administration (Sapadin and Fleischmajer, 2006). In addition, the local application of doxycycline in deep periodontal sites in conjunction with simplified subgingival instrumentation can be considered as a justified approach for non-surgical treatment of chronic periodontitis and can reduce overall treatment time (Wennström et al., 2001).

1.3.5 MMPs and Dental Caries

As described earlier, the carious process begins with the demineralisation of hydroxyapatite by acids produced by oral biofilm bacteria, followed by degradation of the extracellular organic matrix of dentine (Van Strijp et al., 2003). Kawasaki and Featherstone (1997), found that proteolytic enzymes, mainly collagenase, attack the organic extracellular matrix predominantly after the demineralisation stage at pH 7.0. They also found that collagenase has no effect on the extracellular matrix during the demineralisation at pH 4.3. This finding supported the idea that the bacterial proteolytic enzymes contribution to dental matrix degradation may be less important than was initially thought, as they are released only in an acidic environment. In addition, it was found that various highly active MMPs, including MMP-8, MMP-2, MMP-9 and MMP-20 are present in human dentine caries lesions (Tjaderhane et al., 1998; Sulkala et al., 2001). These findings imply that host-derived MMPs, localized both in dentine and in the saliva, may have a more important role in dentine organic matrix degradation.

It has been shown that saliva-derived TIMP-1 retains stability at low pH and therefore could remain active after pH increase and exert a potential inhibitory role on host derived MMPs in dentine caries progression. However, in active caries lesions, the level of TIMPs may be insufficient to block destruction progression (Chaussain-Miller et al., 2006).

The effects of several synthetic MMP inhibitors on dentine caries, such as CMTs, zoledronate and their combination, have been tested *in vivo* on young rats. Sulkala et al. (2001) found that most MMP inhibitors applied systemically had potential effects on the carious lesions and they found also that CMT-3 is the most potent inhibitor of dentine caries progression. Zoledronate, a third generation bisphosphonate that inhibits MMPs proteolytic activity without affecting synthesis, also showed a reduced caries progression in dentine under fissures, but the CMT-3-zoledronate combination did not potentiate the effect. It was also reported that low concentration chlorhexidine directly inhibits MMP-2,

MMP-8 and MMP-9 activities by chelation and has a broad spectrum of activity (Gendron et al., 1999).

1.4 Dentine bonding agents

1.4.1 Introduction

Adhesion is defined as the bonding or the attachment of dissimilar materials. Dentine bonding agents, or dental adhesives, are solutions of resin monomer materials designed to bond resin composite to both enamel and dentine after the monomers polymerize into polymer chains (Eick et al., 1997; Perdigão, 2007). The adhesive capacity of bonding agents is based on a twofold adhesion. First, the bond adheres to enamel and dentine by a micromechanical adhesion mechanism, and second, it binds to resin composite by co-polymerization within the oxygen inhibition layer (Van Landuyt et al., 2007).

The first attempt to develop a dentine bonding system was made by Oskar Hagger, a Swiss chemist working for the DeTrey/Amalgamated Dental Company in London and Zurich in 1949. The system contained glycerophosphoric acid dimethacrylate (GPDM) and marketed as a cavity seal liquid (Sevriton Cavity Seal) in conjunction with a chemically cured restorative resin (Sevriton) (Mclean, 1999; Söderholm, 2007). Kramer and Mclean (1952) described the formation of a 3μm-wide interaction zone between dentine and the cavity seal liquid. This interaction zone was demonstrated on the tissue surface during histological examination, which later was described as the hybrid layer.

In 1955, Buonocore's discovery of the acid-etch technique using 85% phosphoric acid led to significant improvements in the retention of acrylic resin restorations and consequently the ascension of adhesive dentistry. It was also found that the phosphate group in the GPDM-based cavity seal was responsible for the effective bonding with dentine (Buonocore et al., 1956; Kramer and Lee, 1960).

The aim of dental adhesives is to provide retention for resin composite-based restorative materials. Optimal dental adhesion should prevent leakage along restoration margins as well as withstand mechanical forces which include polymerization shrinkage stresses from the resin composite (Van Landuyt et al., 2007). An "ideal" dentine bonding agent should have certain criteria that are summarised in Table 1-7. The degradation of bond between the adhesive and different histological structures can lead to gap formation which may jeopardise the adhesive restoration longevity (Amaral et al., 2007). Clinical failure of adhesive restorations occurs more often due to inadequate sealing of cavity margins, with subsequent discolouration, rather than complete loss of retention (Van Meerbeek et al., 2003; Van Landuyt et al., 2007).

Table 1-7 Criteria for the ideal dentine bonding system as reported by Eick et al. (1997).

1	Provide immediate and permanent high bond strength to dentine similar to that to enamel
2	Biocompatible with dental tissue
3	Reduce marginal microleakage
4	Prevent recurrent caries and marginal staining
5	Be easy to use and minimally technique-sensitive
6	Compatible with a wide range of resin composites
7	Has a good shelf-life

1.4.2 Classification

Different methods have been used to classify dentine bonding agents. A common classification uses the chronological development of the chemical composition, referred to as "generations" (Table 1-8). This classification is unclear even in the literature as some reviews classify dentine bonding agents into six generations (Kugel and Ferrari, 2000; Koh et al., 2001) while others classify them into seven generations (Moszner et al., 2005; Knobloch et al., 2007; Söderholm, 2007). This is confusing when trying to understand the bonding mechanism for each bonding agent prior to its clinical application. Additionally, such nomenclature suggests that each successive generation is an improvement over prior ones, which is not true as shown clearly by bond strength data and sealing ability studies (Leloup et al., 2001; Sarr et al., 2010).

A more appropriate way to classify dentine bonding systems was introduced by Van Meerbeek et al. (2003), based on the underlying adhesion strategy and on the clinical application steps. The main two groups for dentine bonding systems are etch and rinse and self-etch adhesive systems. Etch and rinse adhesives involve a separate step of acid application (conventionally 30-40% orthophosphoric acid) and rinsing. This is followed by primer and then bond application in the three-step systems (type 1). Simplified two-step etch-and-rinse adhesives combine the primer and bond into one application (type 2). In the self-etch systems, the rinsing step is eliminated by the use of intrinsic acidic primers which dissolve the smear layer. This will be followed by the application of the bond (type 3). A single bottle self-etch adhesive system (type 4) is also available where all the components are placed in one bottle. Type 1, 2, 3 and 4 adhesive systems represent the 4^{th}, 5^{th}, 6^{th} and 7^{th} generations respectively in the previous classification (Table 1-8) (Banerjee and Watson, 2011; Green and Banerjee, 2011).

Table 1-8 The seven generations of dentine bonding agents with their chronological appearance proximal time. The main chemical composition, bonding mechanism, common features and problems, bond strength and examples of the commercial products are shown for each generation. GPDM: glycerophosphoric acid dimethacrylate; NPG-GMA: N-phenylglycine and glycidyl-methacrylate; bis-GMA: bisphenol-A glycidyl methacrylate; HEMA: hydroxyethyl methacrylate; 4-MET: 4-methacryloyloxyethyl trimellitic acid; BPDM: biphenyl dimethacrylate. a: Amalgamated Dental Company, London and Zurich; b: Kuraray Co. Ltd., Japan; c: 3M ESPE, USA; d: Kerr Corporation, USA; e: Dentsply, USA; f: GC Corporation, Japan.

Generation	**Chronological appearance**	**Chemical composition**	**Bonding mechanism**	**Common features**	**Bond strength (MPA)**	**Examples of clinical products**	**Reporting studies**
1st	before 1970	GPDM NDG-GMA	chemical bonding of NPG-GMA to calcium and cyanoacrylate to collagen	- GPDM intra-oral hydrolysis - cyanoacrylate polymerization problems	2-3	Sevriton Cavity Seal [a]	(Kramer and Mclean, 1952; Bowen, 1965)
2nd	late 1970's	-phosphate ester (bis-GMA) -polyurethanes (HEMA)	chemical bonding of phosphorous esters to calcium and isocyanates forms covalent bonds with collagen	systems contain two reactive groups	5-13	Clearfil Bond System-F [b]	(Fusayama et al., 1979; Fusayama, 1990)
3rd	mid 1980's	-acid: maleic acid -primer: 4-MET, HEMA and BPDM - bond: unfilled resin	micromechanical retention between dentine and resin	partial removal or modification of smear layer	13-18	Scotchbond 2 [c]	(Watson, 1989; Van Meerbeek et al., 1992)
4th	1991	-etchant: 15-20% phosphoric acid -hydrophilic primer -bond: unfilled resin	micromechanical interlocking achieved through complete removal of smear layer and resin tag formation	simultaneous total etch of enamel and dentine	35-64	- Scotchbond MP [c] - OptiBond FL [d]	(Sarr et al., 2010)

Generation	Chronological appearance	Chemical composition	Bonding mechanism	Common features	Bond strength (MPA)	Examples of clinical products	Reporting studies
5th	1993-1994	- Etchant: 37% phosphoric acid -adhesive: primer and bond	micromechanical interlocking achieved through complete removal of smear layer and resin tag formation	one bottle system	31-52	-Prime&Bond NT [e] - Scotch Bond 1XT[c] - XP Bond[e]	(Sarr et al., 2010)
6th	1993	self-etch primer bond	smear layer dissolve	self-etch primer bonding	31-44	- Clearfil Protect Bond [b] - Clearfil SE Bond [b]	(Watanabe and Nakabayashi, 1993; Sarr et al., 2010)
7th	1998	hydrophilic functional monomer	smear layer dissolve	single step application	11-31	- Adper Prompt L-Pop [c] - G-Bond [f] - Xeno III [e] - Clearfil S^3 Bond [b]	(Sarr et al., 2010)

1.4.3 Chemical composition

Irrespective of the application procedures, all dentine bonding systems contain similar ingredients. Nevertheless, the proportional composition differs between the different classes of bonding agents. Traditionally, bonding agents contain polymerizable acrylic resin monomers that are dissolved in an organic solvent, photoinitiators, stabilizers and sometimes filler particles (Stangel et al., 2007; Van Landuyt et al., 2007).

Monomers are considered as the key components of the dentine bonding agent which provide structural continuity and their physico-mechanical properties. The molecular backbone of monomers is divided into three distinct parts: two or more particular chemical groups attached onto a spacer (Figure 1-7). Basically, two types of monomers are recognised: cross-linkers and functional monomers.

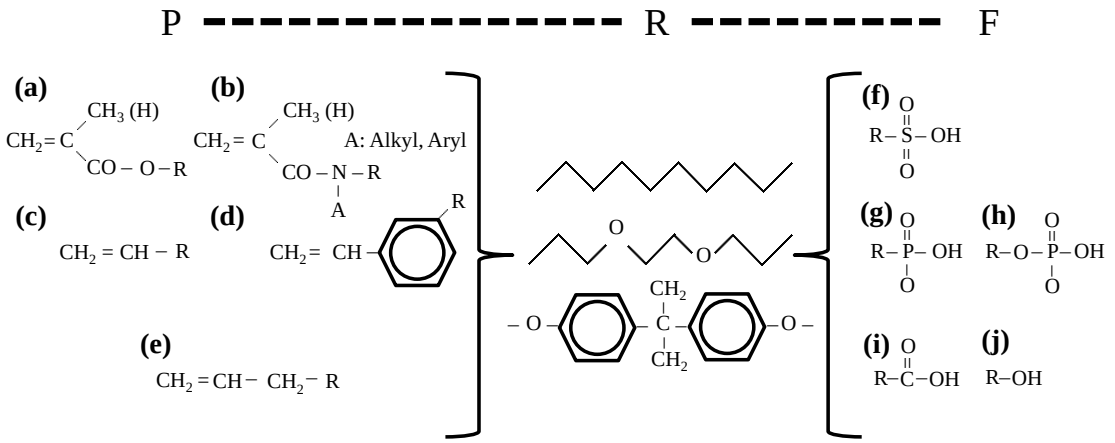

Figure 1-7 Molecular backbones of acrylic resin functional monomers which consist of three parts. The spacer R is attached to a polymerizable group P such as (a) (meth)acrylate, (b) (meth)acrylamide, (c) vinyl, (d) styryl and (e) allyl. On the other spacer part, a hydrophilic functional group F is attached. The common acidic functional groups used within dentine bonding agents, ranked based on their acidity and etching aggressiveness, are (f) sulfonic acid, (g) phosphonic acid, (h) phosphoric acid, (i) carboxylic acid and (j) alcohol.

Cross-linkers have two or more polymerizable groups (–C=C– or vinyl-groups) attached to the spacer to form cross-linked polymers and enhance the mechanical strength for bonding agents. These cross-linkers (e.g. bis-GMA, UDMA and TEGDEMA (Figure 1-8)) are hydrophobic in nature and are similar to monomers found in resin composite restorative materials. Thus a good covalent bond between the bonding and the overlying composite is assured.

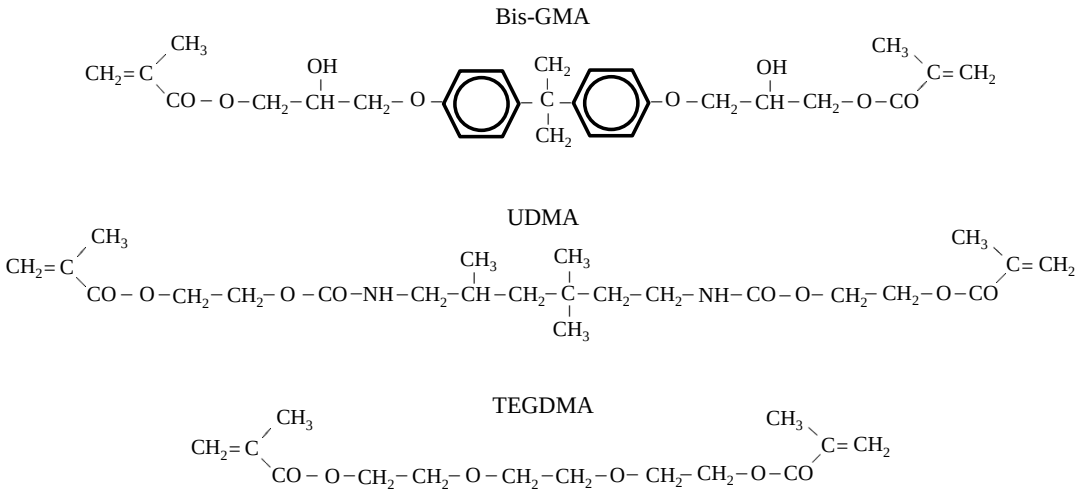

Figure 1-8 Examples of cross-linkers that are commonly used within commercial dentine bonding agents (Van Landuyt et al., 2007). Bis-GMA: bisphenol-A glycidyl methacrylate; UDMA: urethane dimethacrylate; TEGDMA: triethylene glycol dimethacrylate.

Functional monomers commonly have one polymerizable group and a hydrophilic functional group that define monomer-specific functions (Figure 1-7) (Van Landuyt et al., 2007). The main role of the functional monomers is to enhance the wetting of the dental surface by forming linear polymers upon curing. This is realised by the affinity of the hydrophilic terminations to the dentine surface and by the capability of the hydrophobic groups to co-polymerize with the cross-linkers monomers and/or the resin composite. In addition, acidic functional monomers (e.g. HEMA, 4-MET, 10-MDP and phenyl-P (Figure 1-9)) have the ability to demineralise the dental hard tissue component by releasing protons in aqueous solutions. Some monomers are also capable of releasing fluoride (such as PEM-F) (Han et al., 2006) or have antibacterial properties (MDPB) (Imazato et al., 1995).

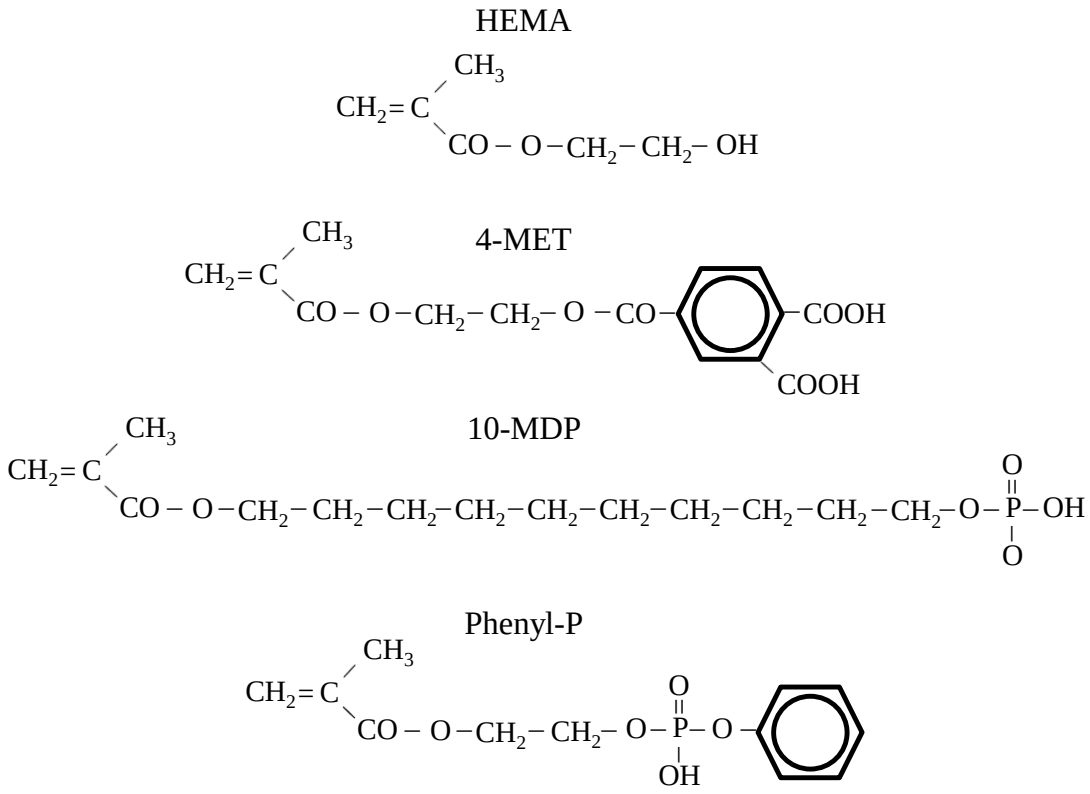

Figure 1-9 Examples of functional monomers that are commonly used within commercial dentine bonding agents (Van Landuyt et al., 2007). HEMA: hydroxyethyl methacrylate; 4-MET: 4-methacryloyloxyethyl trimellitic acid; 10-MDP: 10-methacryloyloxydecyl dihydrogenphosphate; Phenyl-P: 2-(methacryloyloxyethyl)phenyl hydrogenphosphate.

The chemical adhesion of monomers to dental hard tissue is accomplished by the formation of primary chemical bonds, such as covalent or ionic bonds, between acidic groups and inorganic components. Furthermore, additional reactive groups in the monomeric acids result in the establishment of covalent bonds between the dentine collagen fibres and the adhesive monomer (Moszner et al., 2005).

The structure of the spacer groups (R in Figure 1-7) influences the monomer properties, including the volatility, solubility, viscosity, wetting and penetration ability (Nishiyama et al., 2004; Moszner et al., 2008). Moreover, it also affects the resulting polymer's properties, such as hydrophilicity, swelling properties, flexibility or stiffness. The substitution of two carbon atoms by oxygen atoms, as found in the spacer of HEMA, 4-MET, Phenyl-P (Figure 1-9) and TEGDMA (Figure 1-8) monomers, improves the water solubility and the wetting behaviour of the corresponding monomer, whereas the 10-MDP spacer (Figure 1-9), which contains ten carbon atoms, results in a more rigid and hydrophobic monomer (Sideridou et al., 2002; Moszner et al., 2005).

In general, monomers are viscous materials and dissolved usually in different solvents to improve their diffusion ability (Stangel et al., 2007; Pashley et al., 2011b). These solvents are also capable of re-expanding the collapsed demineralised collagen network after dehydration and thus, enhance the wettability through the higher affinity for H-bond formation (Pashley et al., 2001). In self-etch systems, solvents are used as an ionizing medium for activating the acidic monomers (Van Meerbeek et al., 2011). The most common solvents used in dentine bonding agents are water, ethanol and acetone (Van Landuyt et al., 2007). Complete evaporation of these solvents is required as any remaining solvent can dilute the free monomers and increase the permeation of the adhesive layer (Hashimoto et al., 2004). This can result in the phase separation of the hydrophobic components (Tay et al., 1996).

1.4.4 Bonding mechanism to dentine

1.4.4.1 Etch and rinse adhesives

Acid etching, using 32–37% phosphoric acid (pH 0.1–0.4) removes the smear layer completely, demineralises the superficial 5–8 μm dentine surface and exposes a delicate network of collagen matrix fibrils (Hashimoto et al., 2003b). During the water-rinsing process, the entire volume of surface and subsurface inorganic phase (50%) is replaced by water which, when combined with the intrinsic water volume (20%), yields new water content of 70% by volume. This water keeps the surrounding collagen fibrils network (30% by volume) swollen. Complete drying of the demineralised surface, following the rinsing process, results in the collapse of the collagen network, limiting the penetration ability of resin monomers (Tay et al., 1996). Kanca (1992) introduced the concept of "wet-bonding" which involved the re-wetting of the collapsed collagen matrix by water prior to primer application. The wet-bonding technique resulted in better infiltration of the resin monomer and in the enhancement of the bond strength (Pashley et al., 2007).

Ideally, the new water content should be replaced completely by the resin co-monomers during the subsequent infiltration phase of resin from the primer and/or bond. The solvent evaporation removes the water and allows monomers to polymerize *in situ* and hybridise with the collagen matrix resulting in hybrid layer formation (Nakabayashi et al., 1982; Pashley et al., 2007). Such a process provides micro- and nano-mechanical interlocking between the dentine and bonding agent (Aboushelib et al., 2008; Marshall et al., 2010). Contemporary dentine bonding systems do not exhibit complete solvent evaporation and some residual solvent can be found within the hybrid layer to varying extents. In the

three-steps systems, better penetration of the hydrophilic functional monomers is achieved as less/no solvent is added. This could explain the better clinical performance for these systems when compared to the two-step systems (Peumans et al., 2005).

1.4.4.2 Self-etch adhesives

Based on their pKa values, self-etch adhesives are subdivided into strong (pH < 1), moderate (pH ≈ 1.5) and weak (pH > 2) (De Munck et al., 2005; Green and Banerjee, 2011). Strong self-etch adhesives, e.g. adhesives containing methacrylic acid, exhibit a bonding mechanism and interfacial characteristic resembling that formed by etch and rinse adhesives. Such adhesives, which are also considered as aggressive adhesives, form a hybrid layer of up to 5 μm thickness (Tay and Pashley, 2001). Mild self-etch adhesives, e.g. adhesives containing 10-MDP, dissolve the dentine surface partially leaving some inorganic structure remaining within the 0.5μm-thick hybrid layer. The acidic functional group, i.e. the phosphate group, chemically bonds to residual inorganic components and results in another bonding mechanism that supports the micro- and nano-mechanical interlocking (Yoshida et al., 2004). Moderate adhesives, e.g. those with phenyl-P functional monomer, have a penetration depth of up to 2 μm into dentine structure (Tay and Pashley, 2001). The penetration depth difference between the three types is explained by the rapidity of the buffering ability of the nearly neutral pH dentine, which results in calcium salt formation (Salz et al., 2006). This calcium salt is embedded within the hybrid layer and affects the interfacial integrity (Van Meerbeek et al., 2011).

Self-etch bonding systems require water, either from the adhesive itself or from the wet dentine, for the self-etching effect to occur (Moszner et al., 2005). They contain higher percentages of hydrophilic monomers, such as HEMA, compared to etch and rinse adhesives in order to reduce the phase separation (Van Landuyt et al., 2005). This makes the self-etch adhesives exhibit high degrees of water permeability after polymerization (Van Meerbeek et al., 2011). 'Water trees' are found within the adhesive layer of one-step systems as a result of water and pulpal fluid sorption (Breschi et al., 2008). Thus, the bond strength and the durability of such systems are reduced.

1.4.5 Dentine bonding agents' assessment

In recent years, dentine bonding systems have evolved and different chemical formulas have been introduced to the market. In order to ensure that these chemicals fulfil the dentine bonding systems' ideal criteria (Table 1-7), different methods have been used to test them. These can be classified into clinical trials and laboratory studies.

1.4.5.1 Clinical trials

Clinical trials are considered as the ultimate test for the assessment of bonding effectiveness. These studies involve mostly the use of non-carious class V lesions as a cavity that is conditioned by the bonding agents and filled by the restorative material (Peumans et al., 2005). Such lesions do not provide any form of macro-mechanical retention and the bonding agent only retains the restoration. The evaluation of the restoration's clinical presence is the only objective parameter that is used in these trials. Marginal integrity and discolouration are also used as a measure of bonding effectiveness. However, these parameters are less objective and require quantification to be used effectively (De Munck et al., 2005).

Earlier studies indicated that the smear layer-removing adhesive systems performed clinically better than smear layer-dissolving systems (Van Meerbeek et al., 1998). However, recent studies have shown that the two-step self-etch adhesive systems are retained clinically for up to 5 years with annual failure rates similar to that of etch and rinse systems (Peumans et al., 2007; Van Meerbeek et al., 2010). Inefficient clinical performance was reported for the one-step self-etch adhesives (Peumans et al., 2005).

The main concern regarding clinical trials is that they require a long duration in order to predict the exact clinical performance for any bonding system. This could mean that by the time the clinical trial ends, the investigated material is no longer available on the market as a result of its rapid development (Peumans et al., 2005; Sarr et al., 2010). In addition, other clinical variables that are unique to the oral environment can affect the adhesive performance and the specific factor behind bond failure cannot be discriminated (Van Meerbeek et al., 1998).

1.4.5.2 Laboratory studies

Distinctive laboratory methods have been developed to evaluate different dental adhesive systems to overcome the problems associated with clinical trials. Thus, the ultimate objective of a laboratory test should be to gather data in prediction of the eventual clinical outcome. According to Van Meerbeek et al. (2010), the advantages of laboratory investigations over clinical trials are:

- The speed of data gathering on a specific property
- The relative ease of the test methodology used commonly

- The ability to measure one specific parameter, while keeping all other variables constant
- The ability to compare directly the performance of a new experimental material or technique with that of the current 'gold-standard'
- The ability to test simultaneously many experimental groups within one study set-up
- The ability to use relatively unsophisticated and inexpensive test protocols and instruments

The most common reported in-vitro method for evaluating the dentine bonding agents is the bond strength assessment (De Munck et al., 2012). Interface morphology, microleakage, nanoleakage and micro-permeability are also used to assess the sealing ability of the bonding agent.

Bond strength

Different methodologies can be used in order to measure the bonding effectiveness of adhesives to tooth structure. The bond strength can be measured *in vitro*, statically using a macro- or micro-test set-up, depending upon the size of the test bond area. The macro-bond strength, with a bond area larger than 3 mm^2, can be measured in 'shear', 'tensile', or using a 'push-out' protocol (Van Meerbeek et al., 2010).

Macro-tensile bond strength testing has been traditionally used to test the bond strength of dental adhesive systems. It is accomplished by creating one test specimen per tooth which is then loaded to failure in tensile manner (Braga et al., 2010). Studies have shown that macro-tensile testing is influenced significantly by the variability in specimen geometry, loading conditions and materials properties (El Zohairy et al., 2010). In addition, more laborious and time consuming specimen preparation is involved in this test (Van Meerbeek et al., 2010).

To overcome some of these limitations, Sano et al. (1994) developed micro-tensile testing to measure the ultimate tensile strength and modulus of elasticity of mineralised and demineralised dentine. Using this method, multiple specimens can be obtained from each tooth. Each of these specimens will have a bonded test surface area of less than 2 mm^2.

Micro-tensile bond strength testing is used commonly to evaluate adhesive strength of bonding systems to the tooth substrate (Armstrong et al., 2010; De Munck et al., 2012). Both immediate and aged micro-tensile bond strengths are required in order to predict the

clinical effectiveness of adhesives (Van Meerbeek et al., 2010). The advantages of this technique include easier sample collection, measurement of higher interfacial bond strengths and more uniform loading stress distribution over a smaller bonded area. It also permits the calculation of means and variances for single teeth and permits testing of irregular surfaces. Finally, this test facilitates the use of the high-magnification imaging techniques for examining the failed bond location when compared to the macro-tensile bond strength testing (Armstrong et al., 2010; El Zohairy et al., 2010). Due to the small test area, micro-tensile bond strength tests result in more adhesive failures and fewer cohesive failures. This makes the micro-tensile bond strength testing reliable as the adhesive failure represents the "true" adhesive bond strength value while the cohesive failure can result from technical errors within the test setup (Scherrer et al., 2010).

However, the micro-tensile bond strength test has disadvantages which include the labour intensity, technical demands and dehydration and damage potential of the smaller specimens (Armstrong et al., 2010). Other important factors such as specimen–jig configuration and attachment, specimen-loading rate and alignment, do influence the final result and therefore must be standardised within the test set-up to permit meaningful data interpretation (Van Meerbeek et al., 2010).

Failure mode

The investigation of failure mode should occur in conjunction with bond strength identification. It assesses the location of the failure within each specimen. It was reported that there is no clear consensus in the literature regarding failure mode classification, nor have these modes been diagnosed based on the same analytical microscopy technologies (Scherrer et al., 2010).

The reported failure mode has been divided into three main types depending on the failure path: cohesive, adhesive and mixed failure. Cohesive failure occurs within the test material (Figure 1-10a) or tooth substrate itself (Figure 1-10b). Adhesive failures occur at the adhesive interface (Figure 1-10c) and mixed failure designates a mixture of adhesive and cohesive failure within the same fractured surface (Figure 1-10d and e) (Armstrong et al., 2010; Scherrer et al., 2010).

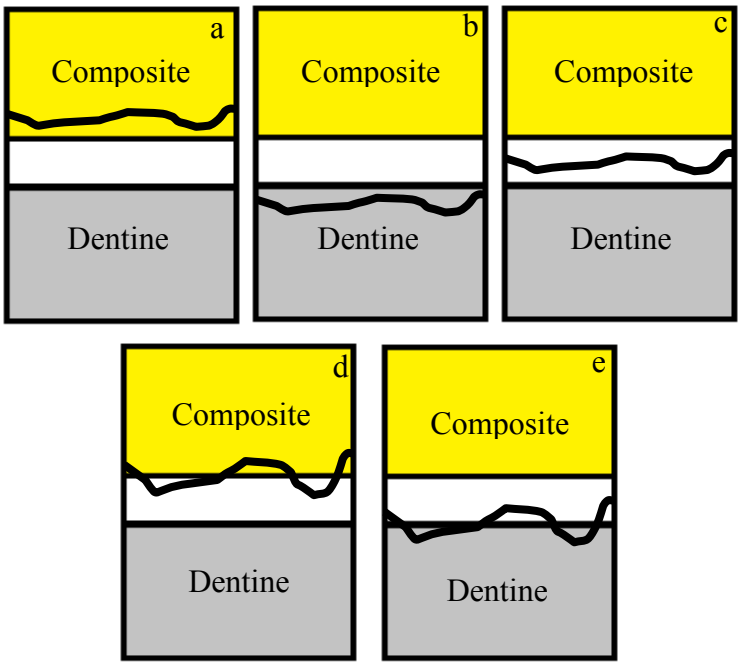

Figure 1-10 Failure modes: (a) cohesive in composite, (b) cohesive in dentine, (c) pure adhesive, (d) mixed Composite-adhesive, (e) mixed dentine–adhesive.

Appropriate magnification should be used to determine failure location and debond path (Armstrong et al., 2010). Cohesive failures within dentine or resin can be evaluated with a stereomicroscope at low magnification. Proper decision on the mode of failure for the adhesive interface or mixed failures is made using a Tandem Scanning Microscope (TSM) or a Scanning Electron Microscope (SEM) (Scherrer et al., 2010).

A meta-analytical study found that there is a strong correlation between the failure mode and the mean bond strength; the higher the bond strength, the higher the incidence of cohesive failure. Conversely, when the adhesive interface is weak, the failure occurs at this location (Leloup et al., 2001).

Cohesive failure in dentine or resin can occur with the micro-tensile bond test due to errors in the alignment of the specimen along the long axis of the testing device or from the introduction of micro-cracks during cutting or trimming of the specimens (Scherrer et al., 2010).

Interface morphology and sealing efficiency

The in-vitro evaluation of the morphology of the dentine/adhesive interface is important to help predict the durability of the adhesive material. In the clinical situation, the longevity of an adhesive restoration depends on its interfacial sealing quality. The more

hydrophilic the dental adhesive, such as the one step self-etch systems, the greater is the water sorption and plasticisation of polymers and the weaker are its mechanical properties (Dundar et al., 2011).

The interfacial morphology assessment has been studied using a variety of techniques including SEM, transmission electron microscopy (TEM), Raman spectroscopy and fluorescence confocal microscopy (Griffiths et al., 1999). The latter has the advantage of visualization of the subsurface interface with minimal sample preparation. Fluorescent labelling of the bonding system allows the study of the relation between the different components. However, the introduction of the fluorophore within these chemical systems can potentially affect the polymerization process by reducing the monomer conversion or by inhibiting the light from reaching the photoinitiators (D'alpino et al., 2006).

Different in-vitro methods have been used to test the sealing efficiency. These include microleakage studies which use organic dyes to mimic the passage of fluids between a cavity wall and the restorative material applied to it (De Munck et al., 2005). However, such a method gives a gross assessment of the quality of the interface and lacks the detection of small differences between various materials. To overcome this problem, recent studies have examined the interfaces using SEM and TEM to assess the nanoleakage through porosities in the hybrid layer (Suppa et al., 2005). Porosities may result from incomplete infiltration of the primer and resin into the demineralised dentine, and/or from shrinkage during polymerization.

Additionally, fluids can permeate from the pulp chamber to the dentine/restorative interface which affects its sealing ability. Using confocal laser scanning microscopy (CLSM), the micro-permeability of resin-bonded dentine has been demonstrated (Griffiths et al., 1999). In this technique a fluorescent dye is infiltrated from the pulp chamber into the resin-dentine interface without the need of immersing the specimens in a solution of fluorophore and with minimal specimen preparation. This method also reveals micro-porosity and pathways for water permeability in the hybrid layer (Sauro et al., 2008).

1.4.6 MMP inhibitors in dental adhesive systems

Basic properties of dental adhesive systems, such as mechanical, physical and functional properties, have been improved as a result of numerous investigations and many recent products on the market exhibit acceptable clinical performance. However, undesirable

consequences, such as recurrent caries and marginal failure/discolouration, are often found in adhesive restorations following long-term clinical use (Amaral et al., 2007).

Hashimoto et al. (2003a) showed that there are degradation patterns within the hybrid layer observed after water ageing. These degradation patterns include the disorganization of the collagen fibrils and loss of resin from interfibrillar spaces which affect the bond strength and the overall longevity of the dental adhesive. It has also been shown that small ions or molecules can diffuse into the hybrid layer in the absence of detectable interfacial gap formation. This diffusion, or nanoleakage, is observed in different dental adhesive systems including two-step etch and rinse, two-step self-etch and one-step self-etch systems, but with differing patterns. Nanoleakage could be explained by the difficulty these adhesive systems have to infiltrate the highly hydrophilic domains of the dentine extracellular matrix or due to the increase in water permeability within the photocured adhesives (Suppa et al., 2005).

As discussed earlier in Section 1.3.4.1, the acidic environment created during the adhesion process activates the host-derived MMPs found both in saliva and etched dentine. Unprotected collagen fibrils may be degraded by these MMPs (Chaussain-Miller et al., 2006; Hannas et al., 2007; Mazzoni et al., 2011), which may explain the reported gradual fall in micro-tensile bond strengths with ageing (Armstrong et al., 2004; Pashley et al., 2011a).

Studies have attempted to prevent collagen fibrillar degradation in dentine extracellular matrix by using different MMP inhibitors during the adhesion process, mainly using chlorhexidine as the preferred MMP inhibitor (Komori et al., 2009; Liu et al., 2011). Chlorhexidine electrostatically binds to exposed collagen peptides and forms a physical barrier around them (Kim et al., 2010a). Thus, collagen fibrils resist the MMP degradation through a protective action more than by a chemical inhibitory effect. Zhou et al. (2011) found minimal MMP inhibition, which was difficult to detect, when chlorhexidine was mixed with dentine powder. Pashley et al. (2004) suggested that the application of chlorhexidine disinfecting solution to acid-etched dentine prior to the use of etch and rinse adhesive systems prevented the degradation of collagen fibrils in dentine hybrid layers as well as its beneficial antimicrobial action. It was also shown that 2% chlorhexidine application after acid etching will not affect the bond strength immediately but preserves both the durability and bond strength of the hybrid layer after aging for 6 months (Carrilho et al., 2007).

Breschi et al. (2010a) found that the use of low concentration chlorhexidine, i.e. 0.2%, significantly reduces the loss of bond strength and nanoleakage, as seen in two-step etch and rinse dental adhesive system artificially aged for 2 years.

De Munck et al. (2009) reported the effects of admixing two MMP inhibitors with the primer of both etch and rinse and self-etch adhesive systems on exposed dentine powder. They used 0.05% chlorhexidine as a non-specific MMP inhibitor and MMP-2/MMP-9 specific inhibitor, SB-3CT, at a concentration of 10 μM. It was found that the "built-in" MMP inhibitors appeared effective in reducing bond degradation only for etch and rinse adhesive but not for the self-etch adhesive. This finding could be explained by the displacement of the chlorhexidine protective layer. It was found that the H-bond, formed by chlorhexidine, is easily removed by water while it is relatively resistant to displacement by ethanol or HEMA, so enhancing chlorhexidine activity (Kim et al., 2010a; Sadek et al., 2010).

All of these studies suggested that the use of chlorhexidine would inhibit MMPs over time without affecting the initial bond strength which indicates that chlorhexidine is not interfering with the polymerization process (Carrilho et al., 2007; De Munck et al., 2009; Breschi et al., 2010a).

Carvalho et al. (2009) reported the inhibition effect of different concentrations of HEMA on extracted MMP-2 *in vitro*. HEMA alone cannot be used as an MMP inhibitor in the clinical situation. The monomer is water-soluble and its effect will be diminished as soon as it contacts the oral environment. However, it was found that HEMA incorporated within the self-etch two-step adhesive systems inhibits collagen degradation through the adsorption of MMPs (Osorio et al., 2011). This suggests that HEMA may promote the activity of other MMP inhibitors.

Other MMP inhibitors such as galardin (GM6001), polyvinylphosphonic acid (PVPA), benzalkonium chloride and quaternary ammonium methacrylates have been used with dentine bonding agents to preserve the exposed collagen fibrils network.

Galardin (GM6001) is a synthetic MMP inhibitor with specific activity against MMP-1, MMP-2, MMP-3, MMP-8 and MMP-9 (Whittaker et al., 1999). It has a collagen-like backbone to facilitate binding to the active site of MMPs and chelating the zinc ion, which is located in the catalytic domain of MMPs (Figure 1-3). Galardin has been used as an experimental primer on acid-etched dentine prior to the application of an etch and rinse

adhesive (Breschi et al., 2010b). It showed no effect on immediate bond strength, while it significantly reduced the bond degradation after 12 months with an enhanced sealing ability.

Polyvinylphosphonic acid (PVPA) is a biomimetic analogue for phosphoproteins, such as DMP-1, bone sialoprotein and phosphophoryn, that had been employed in the experimental remineralisation approach through its binding ability to collagen fibrils (Tay and Pashley, 2008; Kim et al., 2010b). Tezvergil-Mutluay et al. (2010) found that PVPA possesses an inhibitory effect on the demineralised dentine MMPs. However, the effect of this inhibition on the bond's physical properties was not evaluated.

Benzalkonium chloride (BAC) was used initially as an antibacterial agent that was added to the phosphoric acid etchant to deactivate bacteria that invade the bond interface through microleakage (Vicente and Bravo, 2008). In the absence of resins, BAC is effective at inhibiting both soluble recombinant MMPs and matrix-bound dentine MMPs (Tezvergil-Mutluay et al., 2011a). The effect of BAC on the micro-tensile bond strength was not reported in the literature. However, a recent conference paper had shown that the use of etchant containing BAC resulted in the preservation of the micro-tensile bond strength and in the nanoleakage reduction after one year of aging (Santos et al., 2013).

Quaternary ammonium compounds are antibacterial agents that are used widely as disinfectants in hospitals and in the food industry (Pernak et al., 2001). The polymerizable quaternary ammonium methacrylates (QAMs), including 12-methacryloyloxydodecylpyridinium bromide (MDPB), possesses degrees of MMP inhibitory activity (Tezvergil-Mutluay et al., 2011b). QAMs are cationic (i.e., they have a positive charge) and bind electrostatically to the exposed, negatively charged collagen matrix (Markowitz and Rosenblum, 2010). Thus, they protect collagen fibrils from MMP activity in a similar way to chlorhexidine. However, QAMs have the advantage of copolymerizing with adhesive monomers. This suggests the possibility of incorporating these MMP inhibitors into adhesive systems (Liu et al., 2011). Several studies have investigated the effect of incorporating QAMs with dental adhesives, as antibacterial agents (Soeno et al., 2001; Xiao et al., 2009; Chai et al., 2011). These studies concluded that QAMs did not jeopardise the bonding ability and no enhancement in the micro-tensile bond strength was reported.

Section I Sound dentine

Chapter 2 The effect of modified adhesives on the MMPs activity.

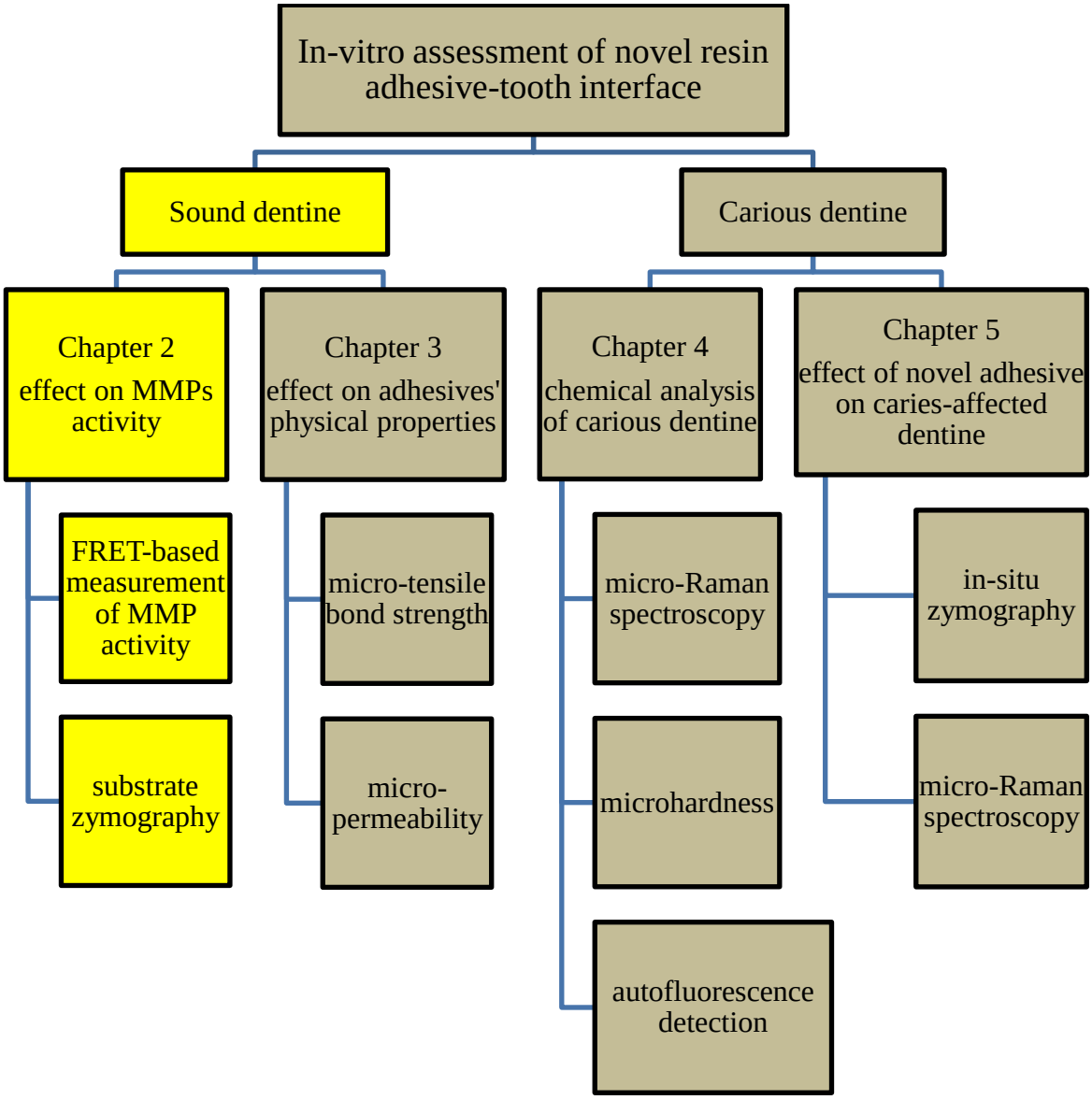

2.1 Introduction

Different MMP inhibitors have been used to prevent collagen fibrillar degradation in the dentine extracellular matrix (Section 1.4.6). These inhibitors, including chlorhexidine (Pashley et al., 2004), were applied directly and separately to acid-etched dentine prior to the placement of the dental adhesive of choice. To simplify the clinical application steps, chlorhexidine was admixed directly with the primer of dental adhesive systems (De Munck et al., 2009; Zhou et al., 2009; Zhou et al., 2011) and resulted in MMPs inhibition over time without affecting the initial bond strength. Liu et al. (2011) suggested the possibility of incorporating quaternary ammonium methacrylates (QAMs) into adhesive systems to prevent collagen matrix degradation by forming a protective layer around the fibrils (Section 1.4.6).

BB94 (batimastat) is a synthetic low molecular weight MMP inhibitor. Structurally, it comprises a peptide-like analogue of the collagen substrate that was shown to be capable of inhibiting tumour growth and metastatic spread. BB94 exhibits an effective broad-spectrum inhibitory effect against most of the major MMPs found in the oral environment (Whittaker et al., 1999) (Table 1-6). GM6001 (galardin or ilomastat) is another synthetic MMP inhibitor with specific activity against MMP-1, MMP-2, MMP-3, MMP-8 and MMP-9 (Whittaker et al., 1999). GM6001 has been used to identify the activity of the MMPs (Sulkala et al., 2007). It was also used as a reference to detect the inhibitory potential of other compounds (Nordstrom et al., 2008).

Based on their structures (Figure 2-1), BB94 and GM6001 are considered as right hand side succinyl hydroxamate inhibitors (Section 1.3.4.2 and Figure 1-6). They both have hydroxamaic acid as a zinc binding group (ZBG) which is effective against collagenase when compared to the other ZBGs (Castelhano et al., 1995). The small alkyl group (isobutyl in P1′) allows the inhibitor to occupy readily the shallow S1′ sub-site found in MMP-1. Effective van der Waals interactions occur between the side chains and the enzyme sub-sites (Whittaker et al., 1999). It is thought that both compounds work by competitive, potent, but reversible, inhibition mechanisms as they are mimicking the MMPs substrates (Rasmussen and Mccann, 1997).

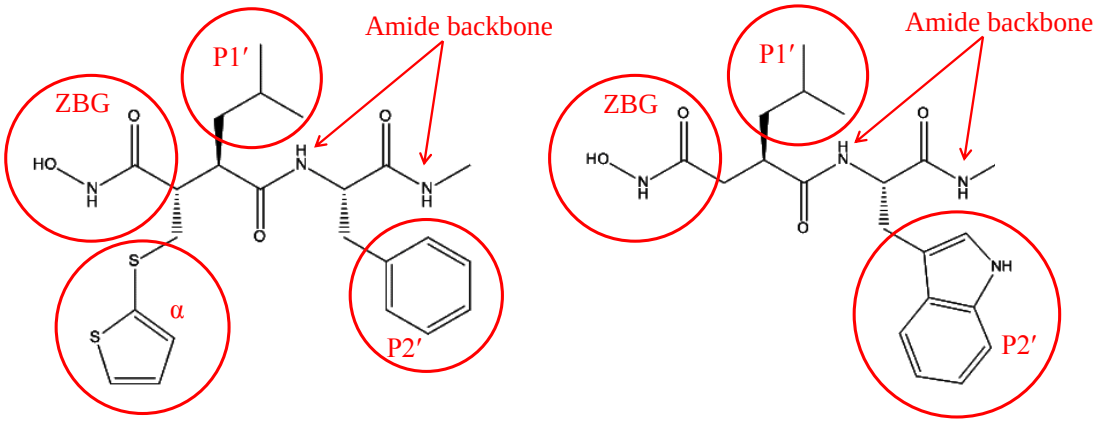

Figure 2-1 The chemical structures of two types of MMP inhibitor. Both compounds are right hand side inhibitors with hydroxamic acid as a zinc binding group (ZBG). P1′ and P2′ are side chains that occupy the S1′ and S2′ subsides in the MMP catalytic domain. BB94 has isobutyl (P1′), thienylthiomethylene (α) and phenylalanine (P2′) side chains which make it very effective against MMP-1 (Whittaker et al., 1999). GM6001 is a potent inhibitor as it contains isobutyl at P1′ and tryptophan at P2′ (Grobelny et al., 1992).

The effectiveness of any MMP inhibitor is measured by the half maximal inhibitory concentration (IC_{50}), which is the quantitative measurement of the amount of inhibitor required to inhibit the MMP activity by half. The IC_{50} of BB94 and GM6001 against different MMPs (Table 2-1) are relatively low when compared to the other inhibitors.

Table 2-1 The half maximal inhibitory concentration (IC_{50}) of BB94 and GM6001 against different MMPs as reported by Whittaker et al. (1999).

MMP	**BB94 IC_{50} (nM)**	**GM6001 IC_{50} (nM)**
MMP-1	10	0.4
MMP-2	4	0.39
MMP-3	20	26
MMP-8	10	0.18
MMP-9	1	0.57
MMP-14	3	

To detect the activity of MMPs and the effectiveness of their inhibition in biological samples, numerous techniques have been reported (Kupai et al., 2010). These techniques include fluorescence resonance energy transfer (FRET)-based measurement of MMP activity, substrate zymography, in-situ zymography and enzyme-linked immunosorbent assay (ELISA).

FRET-based measurement of MMP activity uses the short synthetic peptides that mimic the native substrate of the targeted MMP. These peptides include a fluorophore and quencher pair on opposite ends (Stack and Gray, 1989; George et al., 2003). As the peptide cleaved by MMPs, the pair separates and the fluorescence signal intensity increases (Knight et al., 1992). This method is simple and it is used widely as a screening test to identify the activity of MMPs and different inhibitors (George et al., 2003; Kupai et al., 2010).

For better detection of MMP activity, an electrophoretic technique that is based on sodium dodecyl sulphate polyacrylamide gel electrophoresis (SDS-PAGE) (described by Heussen and Dowdle (1980)) has been used. Substrate zymography involves the use of a substrate that is impregnated with the polyacrylamide gel and the MMP activity is detected based on molecular weight separation (Michaud, 1998). Both latent and active MMPs forms are identified as they have different molecular weights. Gelatine zymography has been used to detect MMP-2 and MMP-9 (Mazzoni et al., 2007), collagen zymography is used for MMP-1 and MMP-13 and casein zymography is used to detect MMP-1, MMP-7, MMP-12, and MMP-13 (Snoek-Van Beurden and Von Den Hoff, 2005). Substrate zymography is used as a qualitative technique to investigate the presence of MMPs. Quantitative assessment of enzyme activity is also achievable when the enzyme dose is controlled (Kleiner and Stetler-Stevenson, 1994; Leber and Balkwill, 1997).

In-situ zymography is a histochemical technique that is used to identify and localise the proteolytic enzymes and their activity within tissue samples (Galis et al., 1995; Mungall and Pollitt, 2001). It involves the overlaying of a fluorescently labelled specific substrate above the already activated enzyme within the tissue to be examined. Substrate-based photographic emulsion has been used to detect the MMP activity *in situ* (Galis et al., 1995).

An enzyme-linked immunosorbent assay (ELISA) is used to detect the quantity of MMPs rather than their activity. It has been used to detect the levels of MMP-9 as a potential marker for acute ischaemic stroke (Ramos-Fernandez et al., 2011).

The aim of this study was to evaluate the effect of adding MMP inhibitors to three commercial dental adhesives on the activity of recombinant MMPs (rhMMP) and on the dentine powder MMPs. FRET-based measurement of MMP activity was used for the former substrate while gelatine zymography was used for the latter.

The null hypotheses investigated in this study were that the addition of MMP inhibitors to each dental adhesive would not significantly affect substrate MMP activity of the recombinant MMP nor the dentine powder MMPs at a significance predetermined at $\alpha = 0.05$.

2.2 Materials and methods

Commercial recombinant human MMP-1 and MMP-2 were obtained (PeproTech, Rocky Hill, USA) along with quenched fluorogenic peptide substrates utilising fluorescence resonance energy transfer (FRET) and intra-molecular fluorescence energy transfer (IFET; Biozyme Inc., Apex, USA).

Caries-free human (aged 18-30 years) extracted molars were collected after patients' informed consent was obtained under a protocol reviewed and approved by the East Central London Research Ethics Committee (Reference 10/H0721/55). All extracted teeth, stored in refrigerated distilled water, were used within one week post-extraction.

2.2.1 Modified primer preparation

Two MMP inhibitors, GM6001 (Millpore Ltd., Watford, UK) and BB94 (British Biotech Ltd., Oxford, UK), were added to the primer component of three commercial adhesive systems: Optibond FL "OB" (Kerr, Orange, USA), Prime&Bond NT "PB" (Dentsply, York, USA) and G-Bond "GB" (GC, Tokyo, Japan) at a concentration of 5 μM (see Table 2-2 for chemical composition). Nine experimental groups were created including the positive control groups which comprised each adhesive without the inhibitors.

Table 2-2 The chemical composition and pH values of adhesive systems used in this study. The groups created from each adhesive system are also included. HEMA: 2-hydroxyethyl methacrylate; GPDM: glycerol phosphate dimethacrylate; MMEP: mono-2-methacryloyloxyethyl phthalate; CQ: camphorquinone; Bis-GMA: bisphenol A diglycidyl methacrylate; GDMA: glycerol dimethacrylate; BHT: butylhydroxytoluene; ODMAB: 2-(ethylhexyl)-4-(dimethylamino)benzoate (co-initiator); PENTA: dipentaerythritol pentacrylate monophosphate; TEGDMA: triethylene glycol dimethacrylate; 4-MET: 4-methacryloyloxyethyl trimellitic acid; UDMA: urethane dimethacrylate.

Adhesive	**Manufacturer**	**Composition**	**pH**	**Test groups**
Optibond FL "OB"	Kerr, Orange, USA	Etchant: 37.5% H_3PO_4 Primer: HEMA, GPDM, MMEP, water, ethanol, CQ, BHT Adhesive: Bis-GMA, HEMA, GDMA, CQ, ODMAB, filler (fumed SiO_2, barium aluminoborosilicat, Na_2SiF_6), coupling factor A174 (approximately 48wt% filled)	Primer: 1.9 Adhesive: 6.9	Control GM6001 BB94
Prime&Bond NT "PB"	Dentsply, York, USA	Etchant: H_3PO_4 Adhesive: PENTA, TEGDMA, Bis-GMA, cetylamine hydrofluoride, acetone, nanofiller (amorphous silicon dioxide 8 nm), resin R5-62-1, T-resin, D-resin, CQ	2.68	Control GM6001 BB94
G-Bond "GB"	GC, Tokyo, Japan	4-MET, phosphoric ester-monomer, UDMA, TEGDMA, acetone, water, stabilizer, silica filler, water, photo-initiator	2	Control GM6001 BB94

2.2.2 Effect on recombinant MMPs

Synthetic, internally-quenched MMP-FRET substrates, as described by Moss and Rasmussen (2007), for MMP-1 (Dabcyl-Pro-Cha-Gly-Cys(Me)His-Ala-Lys(5-FAM)-NH_2) and MMP-2 (Dabcyl-Leu-Ala-Gln-Ala-Homophenylalanine-Arg-Ser-Lys(5-FAM)-NH_2) were used to evaluate the effect of the modified adhesives on active MMPs. Plates

were coated in a N_2 anaerobic pouch with 20 µl of adhesive and blocked overnight using 2% (w/v) bovine serum albumin. Recombinant MMP-1 (rhMMP-1) and MMP-2 (rhMMP-2), activated as per manufacturer's instructions at a concentration of 500ng ml^{-1}, were pre-incubated overnight prior to transfer of supernatants to a new plate and addition of the MMP-FRET substrate solution. Reactions were carried out in black 96-well micro-titre plates (Nunc, Roskilde, Denmark) (Figure 2-2) and were incubated at 37°C for 24 hours. Fluorescence was measured at an excitation wavelength of 485 nm and at an emission wavelength of 530 nm using a FluoStar Optima Plate Reader (BMG Labtech, Germany). The increase in the fluorescence signal over time represented the presence of active rhMMP that cleaved the MMP-FRET substrates. The assays were performed in two sets of plates where the reactions from each rhMMP were carried out in a separate plate. Corresponding blanks without enzyme (rhMMP) were included to evaluate the background degradation of the fluorogenic (MMP-FRET) substrates.

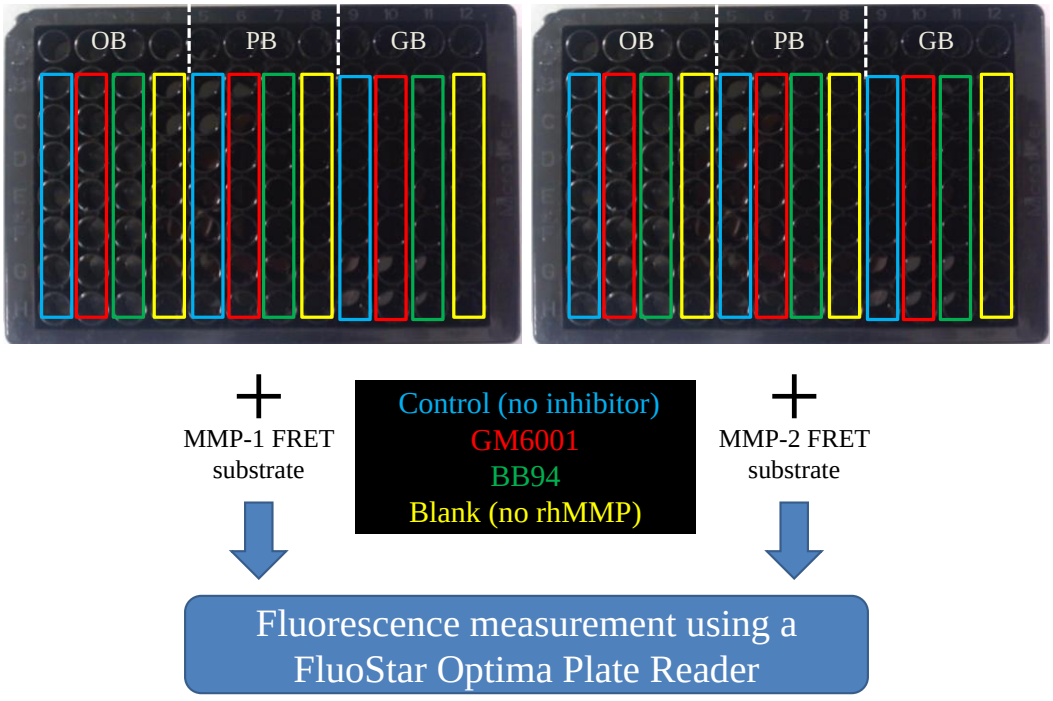

Figure 2-2 The method used to detect the effect of modified adhesives on the inhibitor activity using recombinant MMP.

2.2.3 Effect on dentine MMPs

The enamel, cementum and pulp tissue of five sound extracted human teeth were removed using a water-cooled circular saw diamond blade (Diamond wafering blade XL 12205, Benetec Ltd, London, UK) and a slow speed diamond bur to produce sound,

coronal dentine blocks. Each block was pulverized into a fine powder using 100 MPa compressive load. 100 mg of the dentine powder, containing all MMPs, were placed in 8 µm pore diameter Transwell (Corning, USA) inserts and placed in 24 adhesive-coated well plates (Figure 2-3). Zymography was performed in SDS–polyacrylamide gels containing gelatine (0.1% w/v) to assess the enzymatic effect of the modified adhesives. Dentine powder was also mixed with Laemmli sample buffer without a reducing agent (as a negative control (Figure 2-3)) and subjected to electrophoretic analysis without boiling. After incubating with 2.5% Triton X-100 in 50 mM Tris-HCl (pH 7.5), the gelatine gels were incubated for 24 hours at 37ºC in 50 mM Tris-HCl (pH 7.5), containing 150 mM NaCl, 10 mM $CaCl_2$ and 0.1% Triton X-100. The gels were stained with Coomassie Blue G250 and the disappearance of gelatine staining determined the enzymatic reaction semi-quantitatively.

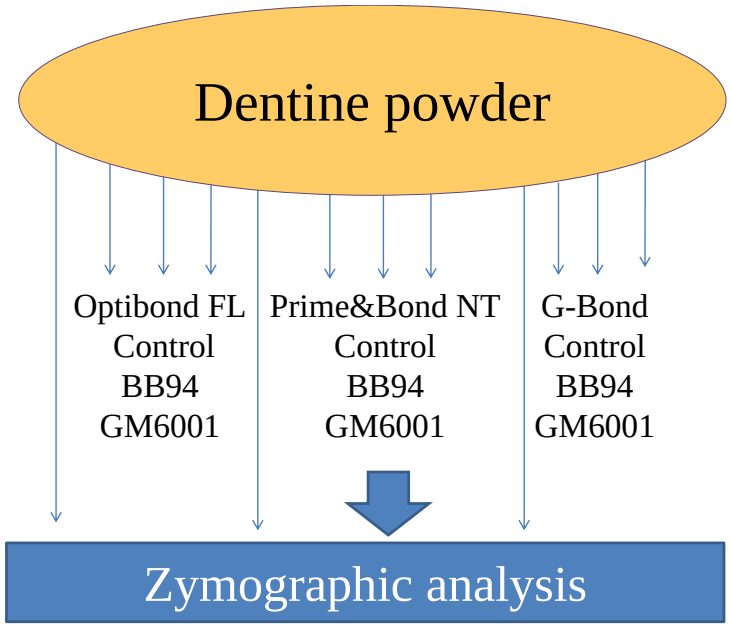

Figure 2-3 Dentine powder, containing all MMPs, was mixed with the three test groups of each adhesive system. Zymography analysis was performed on SDS–polyacrylamide gels containing gelatine. The enzymatic activity of dentine MMPs without adhesives was acquired as a negative control.

2.3 Results

2.3.1 Effect on recombinant MMPs

The three OB test groups showed high fluorescence signals initially with no changes in the signal over time for both rhMMP-1 and rhMMP-2 (Figure 2-4a and b). The other two adhesive systems (PB and GB) had a constant increase in the fluorescence with the time.

Both MMP-FRET substrates exhibited an increase in the fluorescence over time resulting from their dissolution (Figure 2-4).

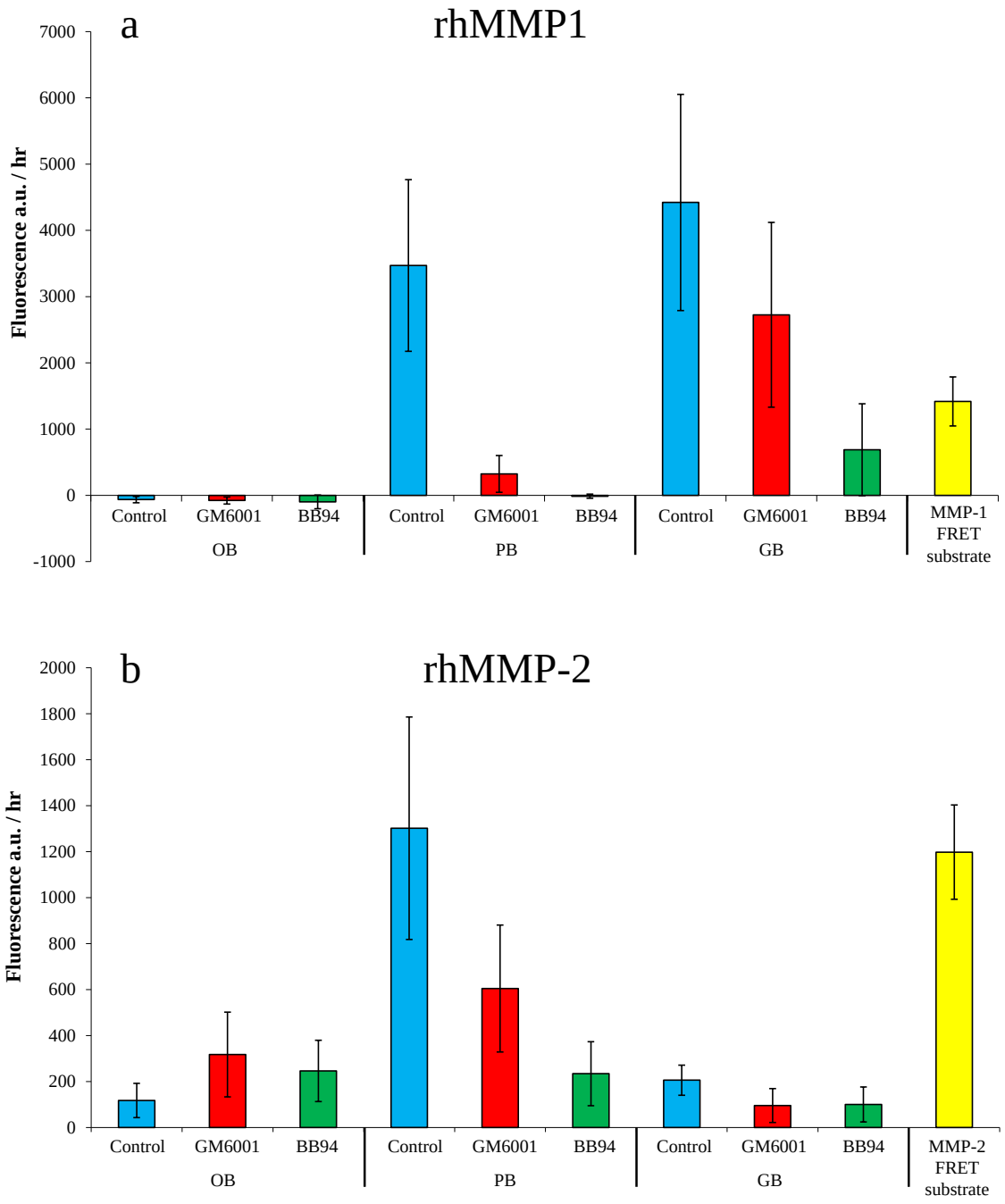

Figure 2-4 The mean fluorescence signal obtained from the cleavage of (a) MMP-1 FRET and (b) MMP-2 FRET substrates by rhMMP-1 and rhMMP-2 respectively. Minimal changes were observed when the reaction was carried out in the presence of all OB test groups. The fluorescence signal was reduced when GM6001 and BB94 were added to PB and GB adhesives. The background signal from MMP-FRET substrates was increased over time without the addition of rhMMP. The error bars represent the standard deviation.

The statistical analysis showed that adding BB94 to PB and GB resulted in significant inhibition of rhMMP-1 (Figure 2-5a) and rhMMP-2 (Figure 2-5b) activity. However, adding GM6001 to GB and PB demonstrated no significant change in the activity of rhMMP-1 and rhMMP-2 respectively.

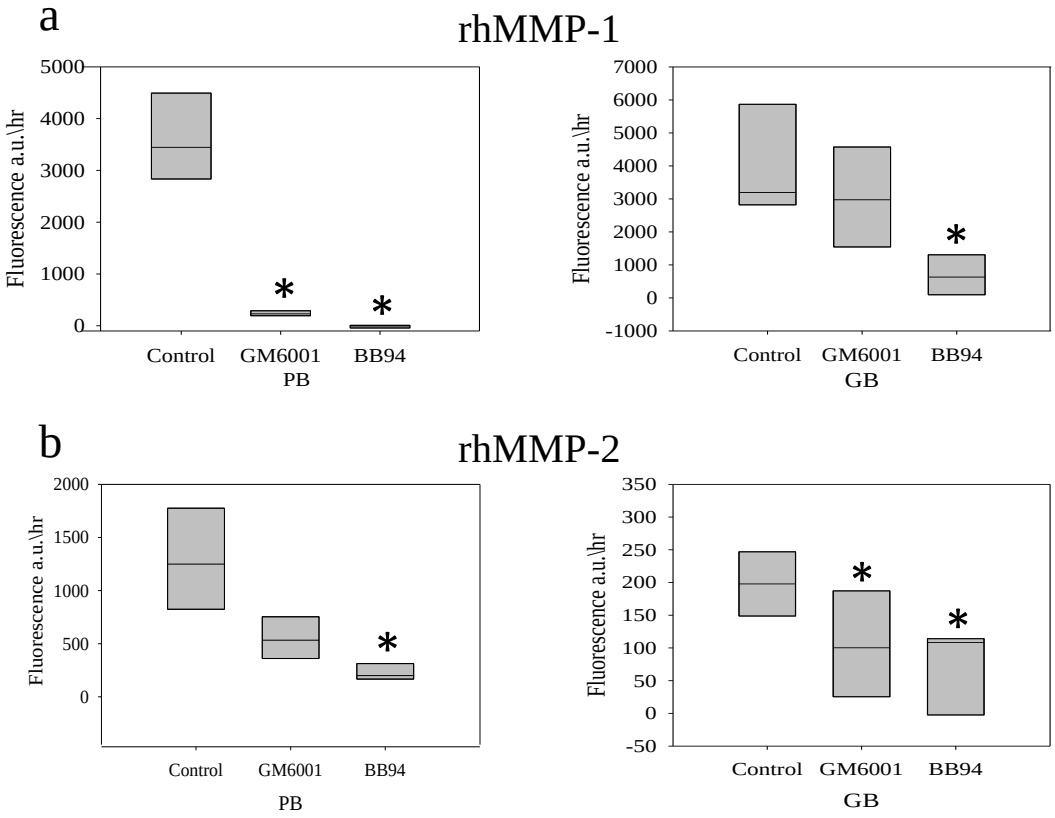

* Significant difference when compared to control

Figure 2-5 The statistical analysis results for the effect of inhibitor containing adhesives (PB and GB) on the activity of (a) rhMMP-1 and (b) rhMMP-2. The box plots represent the 75% confidence intervals for the data presented in Figure 2-4 after adjustment by removing the fluorescence background. The modified PB with both inhibitors blocked the activity of rhMMP-1 significantly while only PB with BB94 inhibited the activity of rhMMP-2. No significant difference was found in the activity of rhMMP-1 when GM6001 was added to GB. However, rhMMP-2 was significantly blocked by GB when both inhibitors were added.

2.3.2 Effect on dentine MMPs

The qualitative evaluation of the gelatine zymograms revealed the inhibition of dentine MMP-2 when both inhibitors were mixed with three adhesive systems. Figure 2-6 is showing the zymograms for OB adhesive as an example for all data. Gelatine present in the whole SDS–polyacrylamide gels was stained with Coomassie Blue G250. The

disappearance of gelatine staining, observed as highlighted areas, represents the reaction between the MMP and the gelatine substrate.

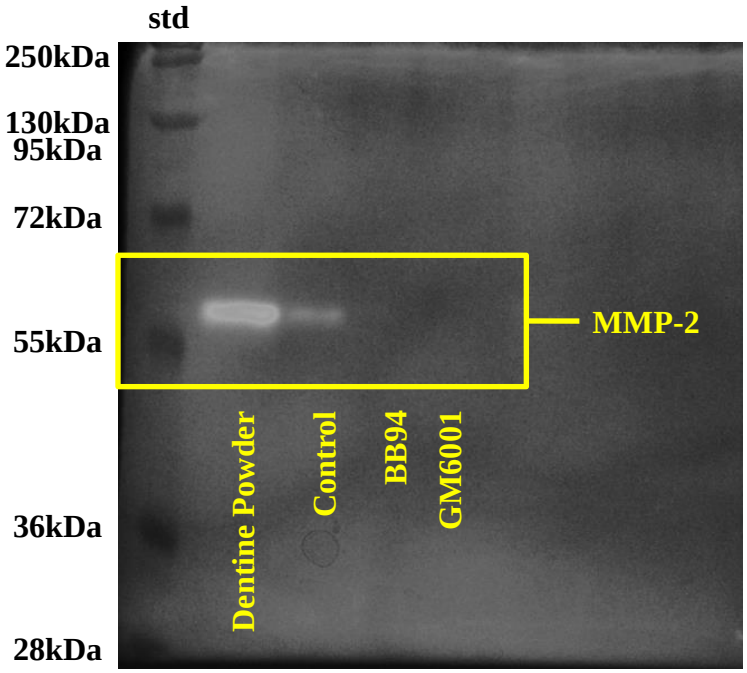

Figure 2-6 Gelatine zymogram for OB. The highlighted areas represent the protease activity consistent with MMP-2 activity with gelatine (66 kDa). No reaction was observed when adhesives containing both MMP inhibitors were mixed with dentine powder. Molecular masses, expressed in kDa, are reported in the std lane.

2.4 Discussion

The first null hypothesis was partially rejected. The inclusion of BB94 resulted in the inhibition of both rhMMPs while GM6001 inhibited rhMMP-1 when it was mixed with PB and rhMMP-2 when it was mixed with GB. The second null hypothesis was rejected as the inclusion of both MMP inhibitors within the three dental adhesives resulted in a significant inhibition of dentine powder MMPs.

The three adhesive systems (OB, PB and GB) were selected in this study to represent type 1, type 2 and type 4 adhesive systems respectively (Section 1.4.2). These systems represent contemporary adhesives with physical characteristics that are fully understood (Van Meerbeek et al., 2003; Sarr et al., 2010; Scherrer et al., 2010; Van Meerbeek et al., 2010). The only two-step, self-etch system (type 3) that fulfils such criteria is the Clearfil SE Bond (Kuraray Co. Ltd., Tokyo, Japan). The type 3 system was not included in this study as it contains 10-MDP functional monomer which possesses a degree of MMP

inhibitory activity (De Munck et al., 2009; Tezvergil-Mutluay et al., 2011b). Such a property would interfere with the aim of this study.

In current study, the two types of MMP inhibitors, BB94 and GM6001, were mixed with the adhesives' primer at a concentration of 5 µM. Although this concentration was much higher than the IC_{50} required for inhibiting the targeted MMPs for both inhibitors (Table 2-1), they were diluted in a relatively large pool of primer containing different functional and crosslinking monomers. Such admixing was thought to affect the ability of both MMP inhibitors to block the MMP activity.

Adding MMP-FRET substrates to OB adhesives resulted in the immediate bond breakdown between the dye and quencher and represented as a high initial fluorescence signal. This could be explained by the relatively high acidity of the OB primer when compared to the other adhesives (Table 2-2). Such a finding made the results obtained from OB not considerable, as both MMP-FRET substrates were not stable within the constraints of the experiments system used.

In addition, the MMP-FRET substrates revealed an increase in the fluorescence signal overtime, which highlighted another drawback of this experiment. To overcome such background fluorescence, the results from PB and GB were adjusted to reflect the MMP inhibitors functions. In general, using rhMMPs with a short peptide sequence is simulating partially the interactions between the natural substrates' sequence and MMPs (Kupai et al., 2010). FRET-based measurement of MMP activity was used in this experiment as a simple screening test before performing the more sensitive substrate zymography.

Gelatine zymography was able to detect the GM6001 and BB94 inhibitor activities when they were mixed with all adhesive systems. This was in favour with previous studies where it was shown that the use of these two inhibitors alone had an inhibitory effect against recombinant and dentine MMP-2 (Bildt et al., 2009; Breschi et al., 2010b).

Although it was used as a qualitative method to assess inhibitor activity within the dental adhesive, the zymographs revealed that the dentine powder had a more intense band than if it is mixed with the adhesives' primer (Figure 2-6). This could be explained by the presence of functional monomers, such as HEMA, that obscured partially the MMP activity. Quantification of the zymographs was achieved previously by measuring the change in the intensity of the remaining substrate within the SDS–polyacrylamide gels

(Kleiner and Stetler-Stevenson, 1994). For reliability and reproducibility, such a procedure requires standardization in the MMP substrate dose and a modification in the two-step staining/destaining technique (Leber and Balkwill, 1997).

Substrate zymography, in general, had been used to distinguish different MMPs present in sound dentine structure (Mazzoni et al., 2007; Sulkala et al., 2007). It was also used to detect the ability of different adhesive systems, including OB, PB and GB, to activate dentine MMPs (De Munck et al., 2009; De Munck et al., 2010). The inhibitory effect of HEMA (Carvalho et al., 2009) and chlorhexidine on dentine MMPs was also evaluated using substrate zymography.

As discussed earlier, limited studies had looked at the possibility of incorporating MMP inhibitors with dental adhesives. However, none of these studies had looked closely at how the inhibitory potential of MMP inhibitors could be affected following their combination with dental adhesive systems. Using FRET-based measurement of MMP activity, Zhou et al. (2011) found that chlorhexidine had a limited inhibitory effect when added the primer of Clearfil SE Bond adhesive. This inhibition was achieved only when the dentine powder was exposed to the acidic primer for limited time (20 seconds). Such a result was related to the reduced calcium-ion release that blocks the chlorhexidine activity. It could be also related to the relatively limited number of MMPs activated within the dentine powder substrate. No other techniques were used in this study to verify the findings.

In De Munck et al. (2009) study, gelatine zymography was used to evaluate the ability of dental adhesives to activate dentine MMPs. In contrast to Zhou et al. (2011), gelatine zymography showed that Clearfil SE Bond had an inhibitory effect on dentine MMP-2. Although the aim of that study was to evaluate the effect of admixing two types of inhibitors with dental adhesives, the inhibitory potential of the incorporated inhibitors was not evaluated.

In conclusion, this study showed that the modified adhesives containing both MMP inhibitors had high affinity towards both recombinant and dentine powder substrates.

Section II Sound dentine

Chapter 3 The physical properties of modified adhesives.

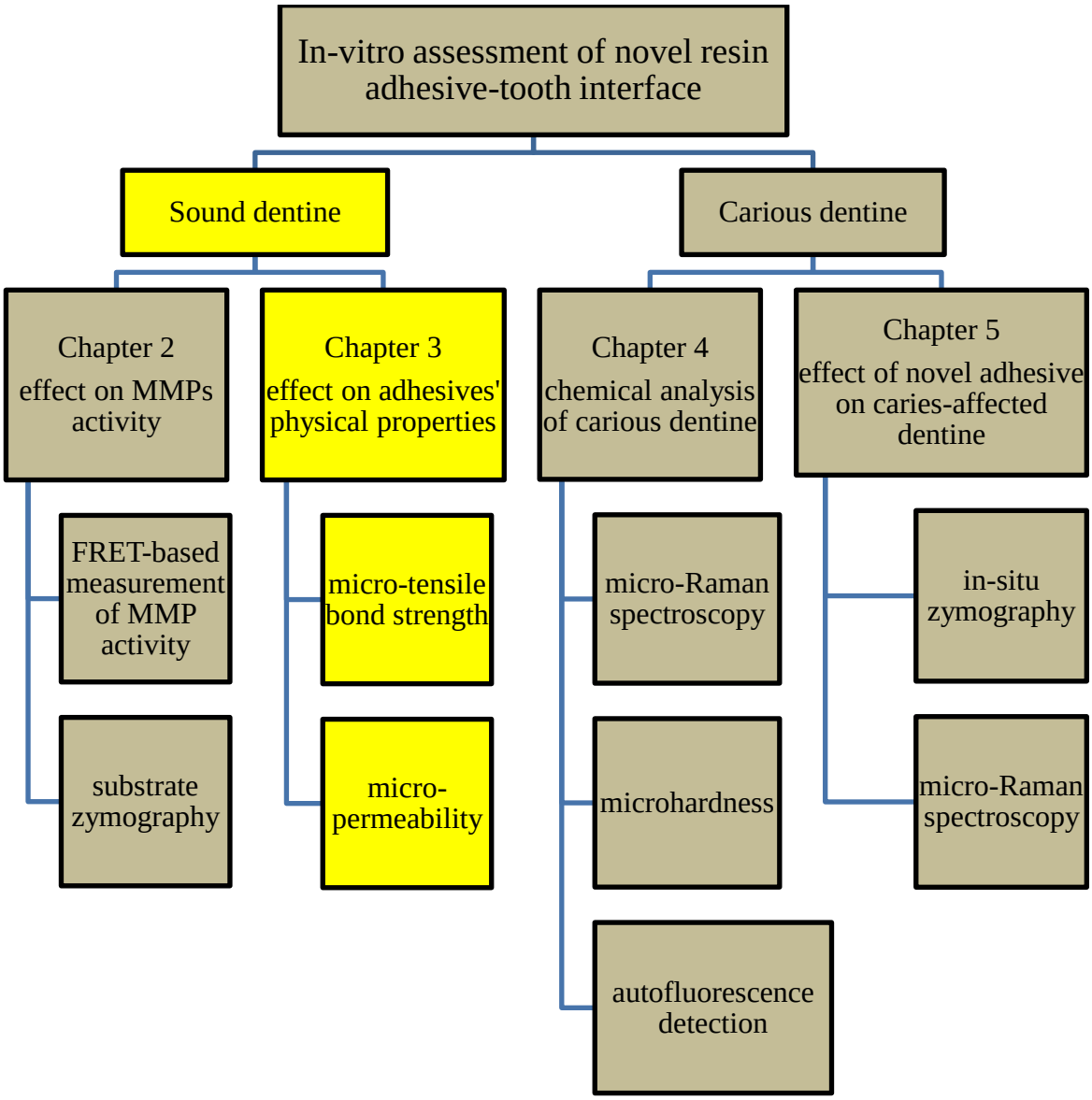

3.1 Introduction

As reported in Chapter 2, adding GM6001 and BB94 to the three adhesive systems resulted in the inhibition of recombinant MMPs and dentine MMPs. In this chapter, the effect of such addition on the interfacial physical properties of the adhesive systems was evaluated.

Optibond FL (Kerr, Orange, USA) "OB" is a three-step etch and rinse adhesive system with well reported physical interfacial properties in clinical and laboratory studies (Van Meerbeek et al., 2003). It is still considered as the "gold-standard" adhesive with the physical properties of other systems determined in comparison to it (Sarr et al., 2010). Prime&Bond NT (Dentsply, York, USA) "PB" is a water-free acetone based two-step etch and rinse adhesive system with enhanced primer penetration ability (Tay et al., 1998). The single-step dental adhesive system, G-Bond (GC, Tokyo, Japan) "GB", has a limited bond strength (Sarr et al., 2010; Eren et al., 2013) and acceptable clinical performance (Van Landuyt et al., 2008).

The acidic primer of these adhesive systems has the ability to activate different dentine MMPs (Chapter 2) (De Munck et al., 2009; De Munck et al., 2010; Mazzoni et al., 2013). This leads to the degradation and disorganization of unprotected collagen fibrils within the hybrid layer (Chaussain-Miller et al., 2006; Hannas et al., 2007). The use of an MMP inhibitor prior to the application of acidic primer was proven to enhance the mechanical properties and the sealing ability of different adhesive systems as discussed in Section 1.4.6.

The general chemical composition of different adhesive systems is already recognised in the literature. However, some chemical components and specific ratios between constituents are not always revealed by the manufacturers (Van Landuyt et al., 2007). The incorporation of any additional components, e.g. hydrophobic nano-gel particles (Moraes et al., 2012), can result in changes within the adhesive's chemical equilibrium. As a result, the overall stability and physical properties of the adhesive systems could be affected. This explains the limited studies that have tried to add MMP inhibitors, such as chlorhexidine, to these systems.

Micro-tensile bond strength testing has been used to evaluate adhesive bond strengths (De Munck et al., 2012). It provides versatility that could not be achieved using other bond strength testing methods (Section 1.4.5.2) (Armstrong et al., 2010).

Maximum sealing ability of dental adhesives is achieved through the presence of rich collagen network that provides micro- and nano-mechanical hybrid zone interlocking between the dentine and bonding agent (Aboushelib et al., 2008; Marshall et al., 2010). Micro-permeability assessments provide an evaluation of micro-porosity and pathways for water permeability within the hybrid layer, from pulp fluid (Griffiths et al., 1999; Sauro et al., 2008) (Section 1.4.5.2).

The aim of this study was to evaluate the effect of adding MMP inhibitors, GM6001 and BB94, to three commercial dental adhesives on the adhesives' physical properties. The null hypothesis investigated was that the addition of MMP inhibitors to each dental adhesive would not significantly affect the micro-tensile bond strength or the micro-permeability at a significance predetermined at $\alpha = 0.05$.

3.2 Materials and methods

3.2.1 Dentine bonding systems

The modified dental adhesives described in Section 2.2.1, were used in this study. The primers of Optibond FL "OB" (Kerr, Orange, USA), Prime&Bond NT "PB" (Dentsply, York, USA) and G-Bond "GB" (GC, Tokyo, Japan) were modified by the addition of the two MMP inhibitors, GM6001 (Millpore Ltd., Watford, UK) and BB94 (British Biotech Ltd., Oxford, UK) at a concentration of 5 μM. The same nine experimental groups were created (Table 2-2 and Table 3-1).

Table 3-1 The nine experimental groups created by the addition of the two inhibitors to each adhesive system.

Dental adhesive	Experimental group
OB	Control
	GM6001
	BB94
PB	Control
	GM6001
	BB94
GB	Control
	GM6001
	BB94

3.2.2 Micro-tensile bond strength (μTBS) measurement

Ninety extracted, sound human teeth were used in this study (Figure 3-1a) (obtained under the same ethical protocol described in Section 2.2). A flat, transversely-cut dentine surface was created on each tooth using a water-cooled circular saw diamond blade (Figure 3-1b). A smear layer was created using 600-grit SiC paper (Figure 3-1c). Each adhesive system, of the nine experimental groups, was applied on the moist dentine surface following the relevant manufacturers' instructions (Figure 3-1d). All teeth were restored with Filtek™ Supreme Ultra (3M ESPE, St. Paul, USA) resin composite restorative material applied using a flat plastic in two or three 2mm-thick increments (Figure 3-1e). Blue light source (470 nm, ~600 mW cm^{-2} with a 10 mm tip, Optilux VLC, Demetron Research Co., CT, USA) was used to activate the dental adhesives and each composite increment for 20 and 40 seconds respectively. Each sample was stored at 37°C for 24 hours to ensure complete polymerization and was then cut into 12 beams containing 1 mm^2 adhesive layers (Figure 3-1f). The beams obtained from five teeth in each of the nine experimental groups were tested immediately. Another 60 beams, obtained from different teeth, were tested after storage in distilled water at 37°C for 3 months (Figure 3-1g). Samples that failed during sample preparation were noted in each experimental group (pre-test failures).

Each beam was subjected to tensile load using a SMAC LAL300 linear actuator testing machine (SMAC Ltd., UK) with a crosshead speed of 1 mm/min (Figure 3-2). The force required to break the adhesive bond was recorded in MPa. Two-way ANOVA was used to compare the μTBS of all groups and the Sidak post hoc test was used to find the differences between any two groups in each adhesive system.

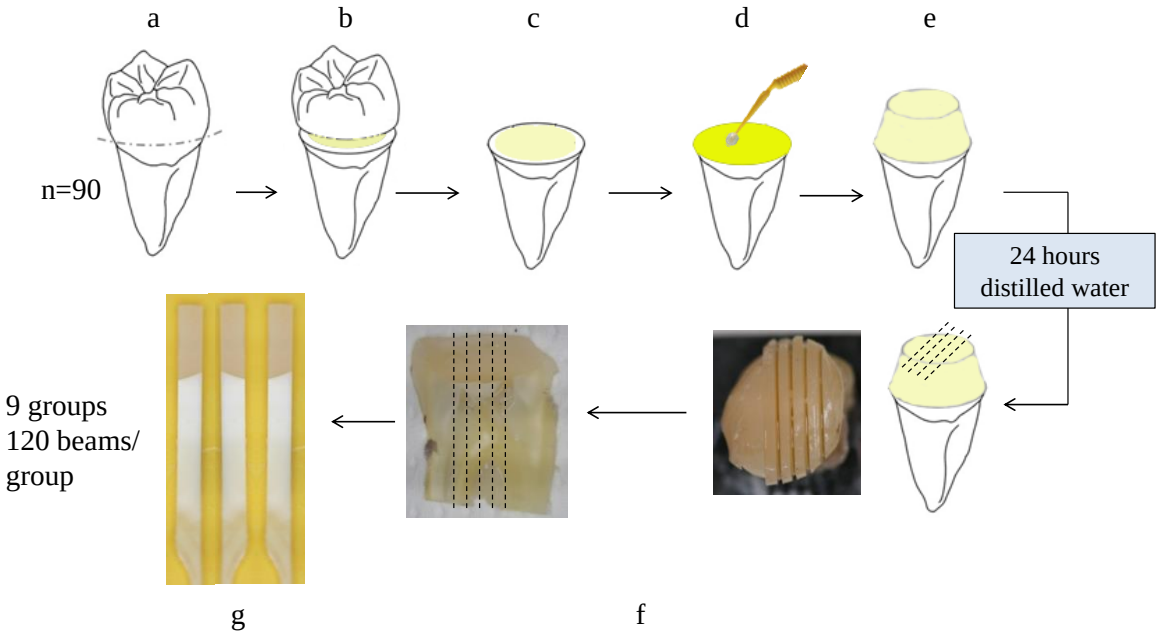

Figure 3-1 Sample preparation for micro-tensile bond strength testing. (a) Ninety teeth were included in this study; (b) the coronal third of each tooth was removed; (c) the exposed dentine surface was polished using 600 gritting SiC paper to create smear layer; (d) each adhesive system was applied following the relevant manufacturers' instructions; (e) all teeth were restored with Filtek™ Supreme Ultra (3M ESPE, St. Paul, USA) resin composite and kept for 24 hours in distilled water at 37°C; (f) each tooth was then sectioned into 12 beams; (g) 60 beams in each group were tested immediately and the other 60 beams were tested after 3-month aging.

Figure 3-2 Micro-tensile bond strength-testing jigs. Each beam was secured in place using cyanoacrylate adhesive (Zapit; Dental Ventures of America Inc., Corona, USA) and subjected to tensile load until failure of the adhesive bond. The force required to break the bond was recorded in MPa.

Following micro-tensile load testing, the failed beam interfaces were evaluated using stereo-microscopy (KYOWA; Optical CO Ltd., Japan), with magnification variable from 15-60x, to assess the mode and locus of tensile failure. The mode of failure was classified as a percentage of the total surface area of failed dentine exhibiting pure adhesive, cohesive or mixed failure modes.

3.2.3 Micro-permeability assessment

Twenty seven teeth were prepared as above (Section 3.2.2) and adhesive/resin composite were applied following the manufacturers' instructions in a standardised manner (Figure 3-3a). The crown segment of each tooth was obtained by removing the roots 1 mm beneath the cemento–enamel junction (CEJ) (Figure 3-3b). Pulp tissue was extirpated with small surgical tweezers without altering the predentine. The sample was inverted and an aqueous solution of Rhodamine B was introduced into the pulp chamber and was allowed to permeate for 3 hours under gravity (Figure 3-3c). The tooth was sliced vertically into three, 2 mm-thick slabs, (Figure 3-3d) each hand polished using 500, 800 and 1000 grit SiC papers and ultrasonicated between each paper grade, for 3 minutes. Using a tandem scanning confocal microscope (TSM; Noran Instruments, Middleton, WI, USA), slabs were examined using a 100 / 1.4 oil-immersion objective, 546 nm excitation and 600-630 nm emission filters. The degree of Rhodamine B penetration in five constant and pre-selected areas was recorded for each slab (Figure 3-3e).

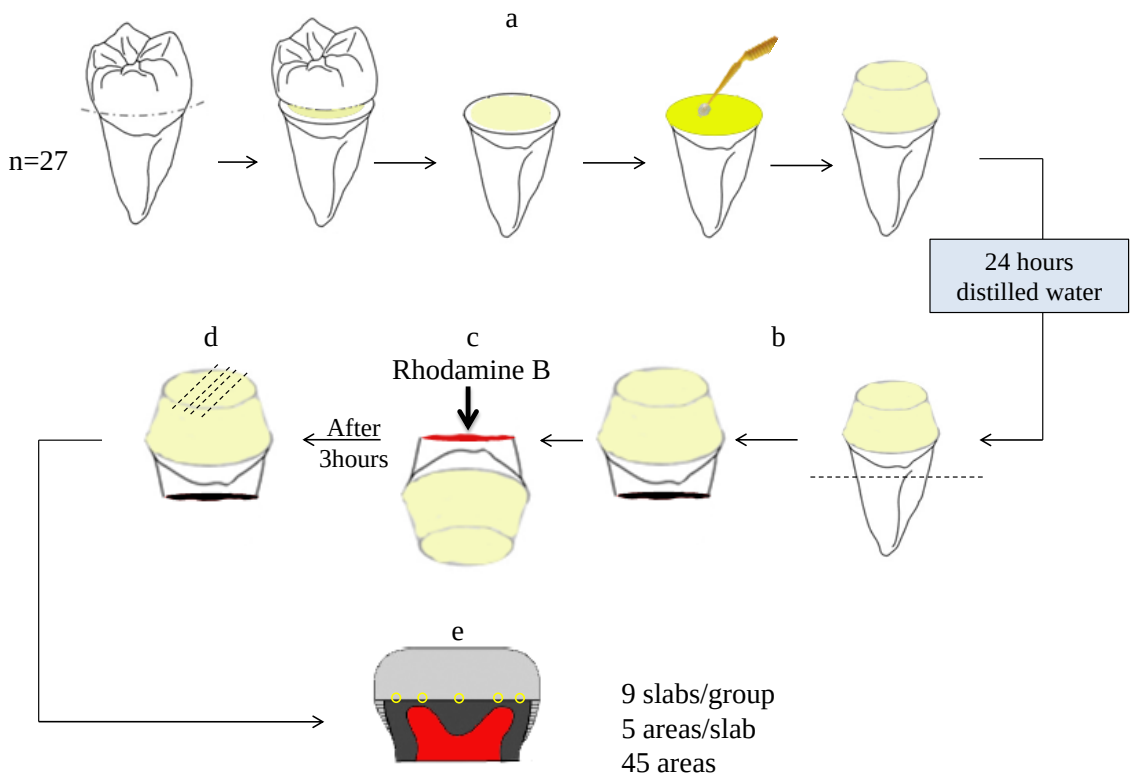

Figure 3-3 Sample preparation and the laboratory method for micro-permeability measurement. (a) Twenty seven teeth were used and the adhesives were applied with the same protocol described in Figure 3-1; (b) the root was removed at 1 mm beneath the cemento–enamel junction (CEJ); (c) each sample was inverted and an aqueous solution of Rhodamine B was introduced into the pulp chamber; (d) the tooth was then sliced vertically into three, 2mm-thick slabs; (e) the degree of Rhodamine B penetration in five constant and pre-selected areas was recorded in each slab using TSM.

A modified micro-permeability index reported by Sauro et al. (2008) was used to assess the degree of micro-permeability (Figure 3-4). Order logistic regression analysis was used to compare between the groups' scores for each adhesive system by taking into account the clustered analysis of the data.

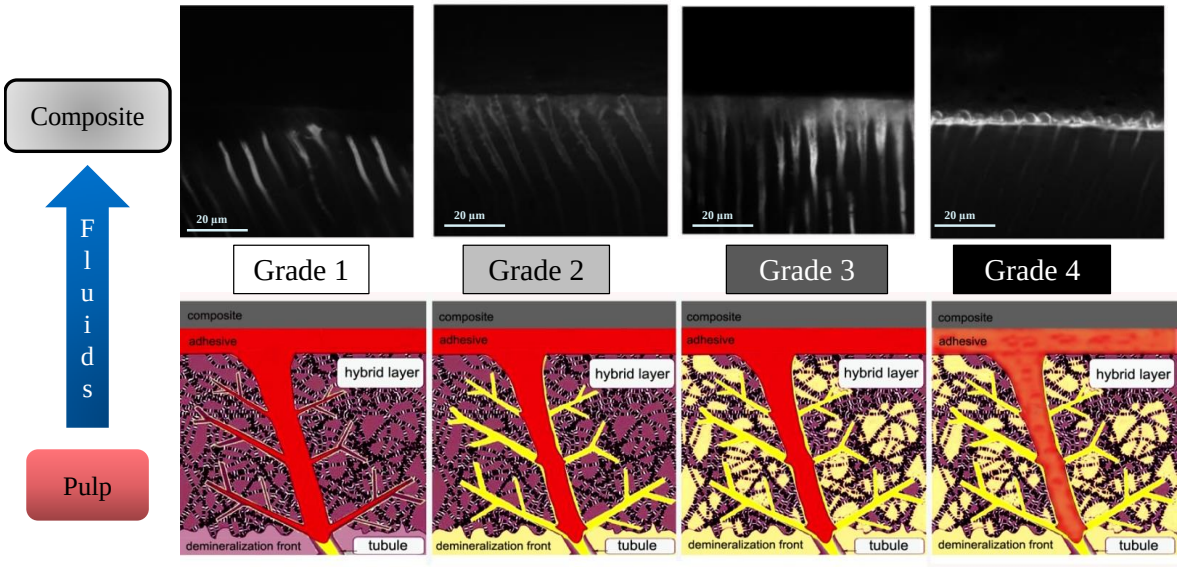

Figure 3-4 The modified micro-permeability index used to evaluate the micro-permeability of simulated pulp fluids (the arrow on the left) into the adhesive interface. Grade 1: completely intact hybrid layer with no dye reaching it; Grade 2: the dye reaches the base of the hybrid layer; Grade 3: the dye is infiltrated within the hybrid layer completely; Grade 4: the dye is reaching the adhesive layer.

3.3 Results

3.3.1 Micro-tensile bond strength (μTBS)

The results of the μTBS tests are summarised in Figure 3-5. The immediate μTBS for OB including inhibitors increased significantly ($p = 0.001$) when compared to its control. However, both BB94 and GM6001 groups showed significant reduction after 3-month storage.

No significant difference was found in the immediate or aged μTBS for all PB groups ($p = 0.39$), except for the aged GM6001 group which decreased significantly ($p = 0.001$).

For GB, the μTBS increased significantly ($p = 0.02$) with both inhibitors as compared to their control immediately. However no significant differences were found between the control and both MMP inhibitors groups following 3-month storage.

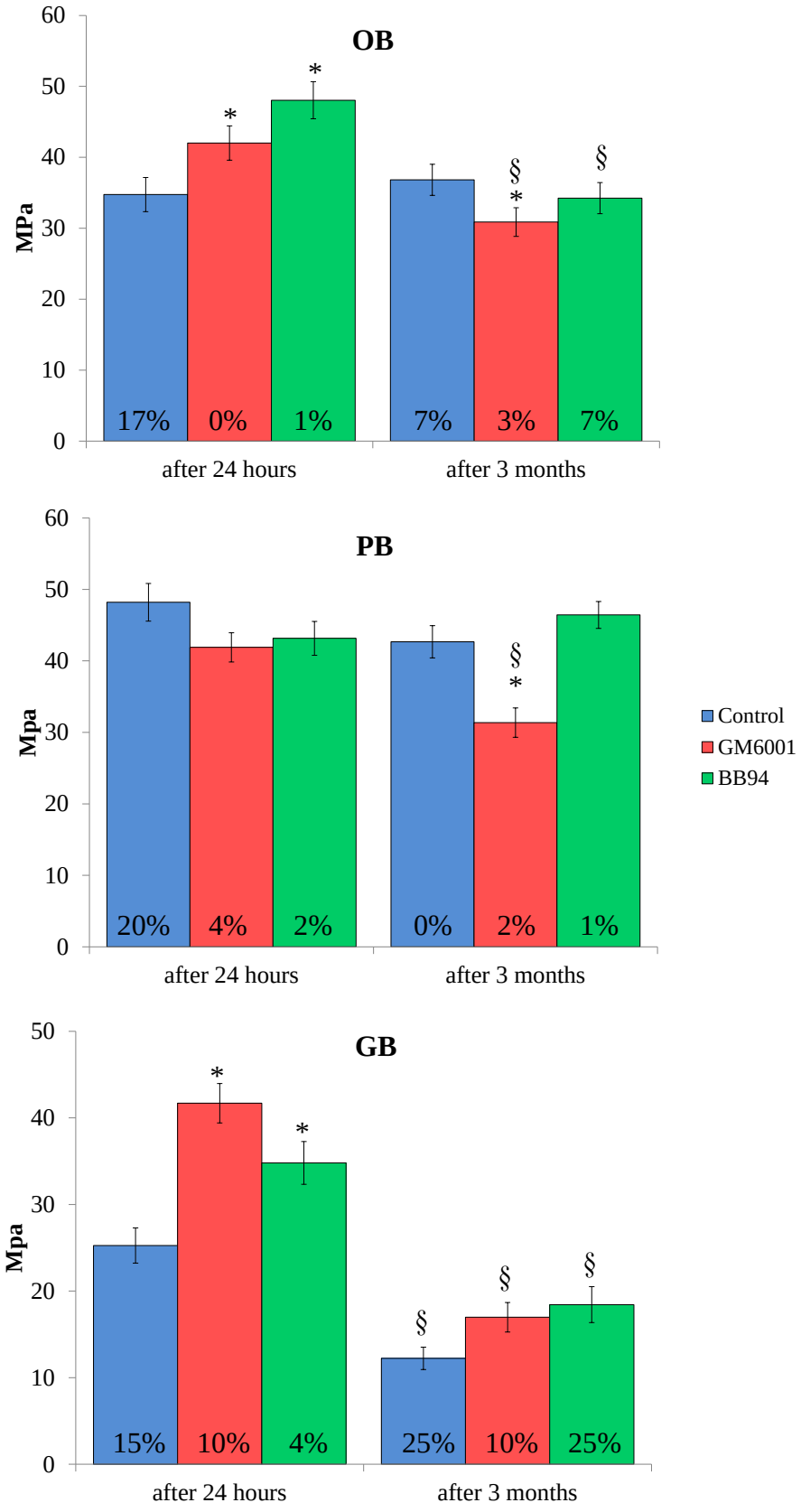

Figure 3-5 The mean µTBS results for OB, PB and GB with the standard error of the mean. The percentage below each bar represents the mean pre-test failure for that specific group; *significant when compared to the control at the same time; § significant difference after 3-month aging when compared to the same group initially.

The number of pre-test failures was less when both MMP inhibitors were added to all adhesives in the initial samples (Figure 3-5).

OB and PB resulted in more cohesive failures than GB (Figure 3-6). The cohesive failures in OB with GM6001 increased significantly after 3-month aging. This was the same for all PB groups with no significant differences between the groups. No significant differences were found in the mode of failure of GB.

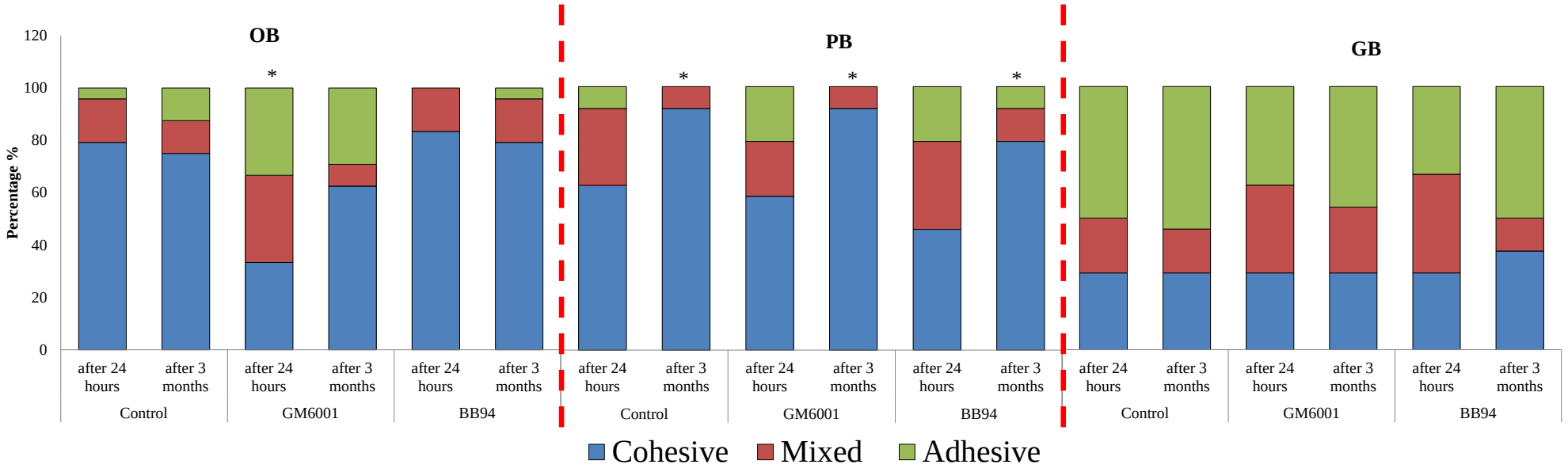

Figure 3-6 The failure mode for all experimental groups. Cohesive failure mode represents failures occurring mainly within dentine or resin composite. Adhesive type represents failures at the adhesive interface. The mixed failure designates a mixture of adhesive and cohesive failure within the same fractured surface; *significantly different when compared to other groups of the same adhesive system.

3.3.2 Micro-permeability assessment

The micro-permeability of OB (Figure 3-7a) did not change significantly (p = 0.79) after adding both MMP inhibitors. PB with MMP inhibitors (Figure 3-7b) exhibited significantly (p = 0.043) less dye in the hybrid layer than its equivalent control. Additionally, GB exhibited less dye reaching the adhesive layer when both MMP inhibitors were added (Figure 3-7c) (p = 0.01). Adding BB94 to PB resulted in a significant better sealing ability than adding GM6001 (p = 0.001). For GB, GM6001 had significant less dye reaching the adhesive layer when compared to BB94 (p = 0.02). Examples of the micro-permeability results for the three experimental groups created by OB, PB and GB adhesive systems are shown in Figure 3-8, Figure 3-9 and Figure 3-10 respectively.

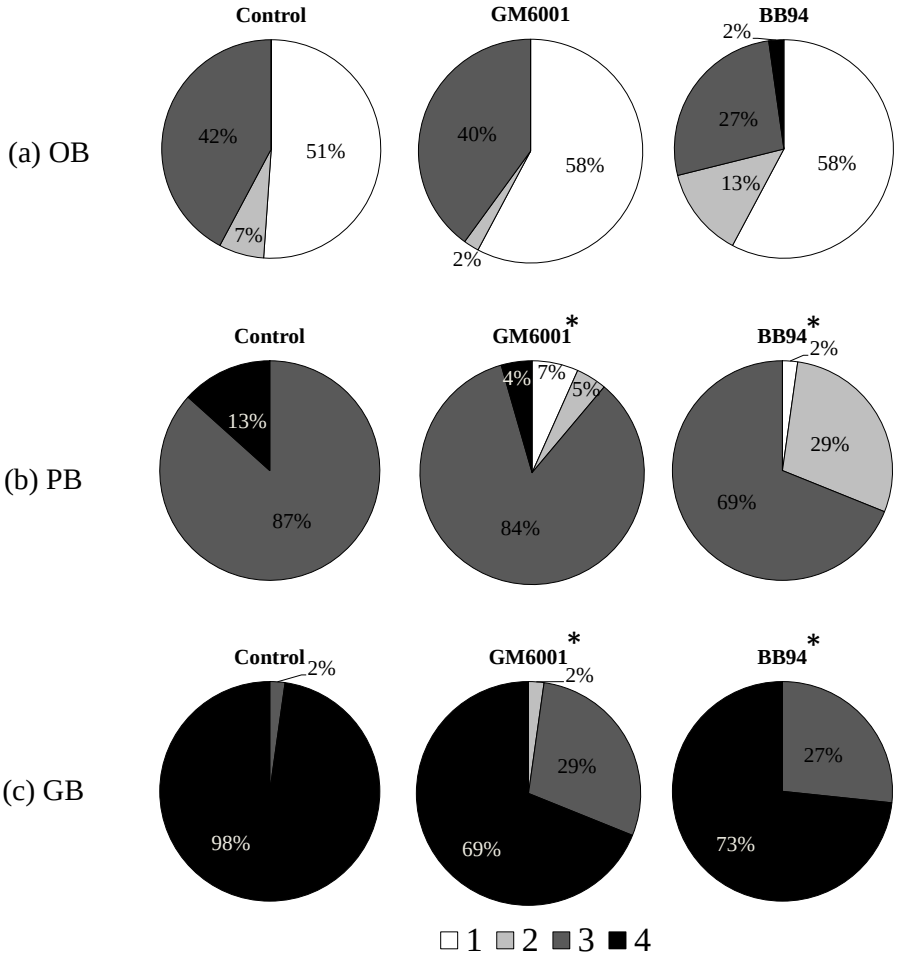

Figure 3-7 (a) Micro-permeability scores for OB with no change between the experimental and control groups; (b) PB had less dye reaching the hybrid layer (Grade 3) when both inhibitors were used; (c) GB with inhibitor had less dye in the adhesive (Grade 4); *Significantly different from the control.

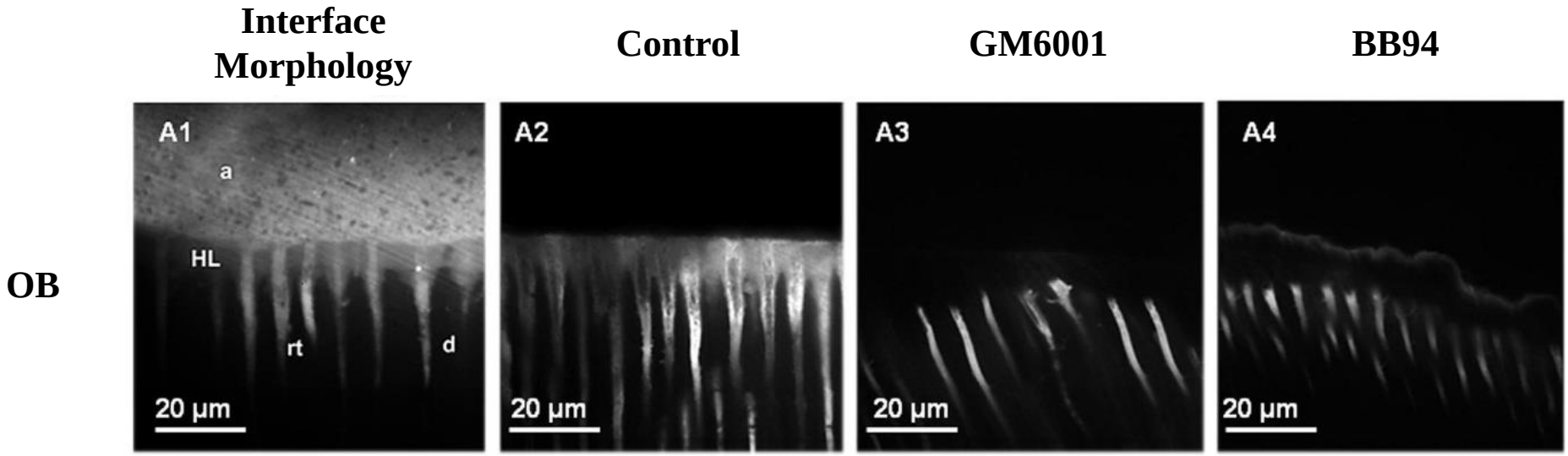

Figure 3-8 TSM images of the interface morphology and examples of the 3 experimental groups' micro-permeability results for OB adhesive system. (A1) TSM image captured in fluorescence mode (Rhodamine B excitation/emission), showing the interfacial characterization of the OB-bonded dentine specimens. It is possible to observe long resin tags (rt) and a 5-8 µm deep hybrid layer (HL) localized beneath a thick adhesive layer (a); d: dentine. The OB-bonded dentine showed dye penetration (micro-permeability) within the entire thickness of the HL (A2), while the micro-permeability of the resin-bonded interface created with the OB doped with GM6001 (A3) or BB94 (A4) was detected only inside the dentine tubules.

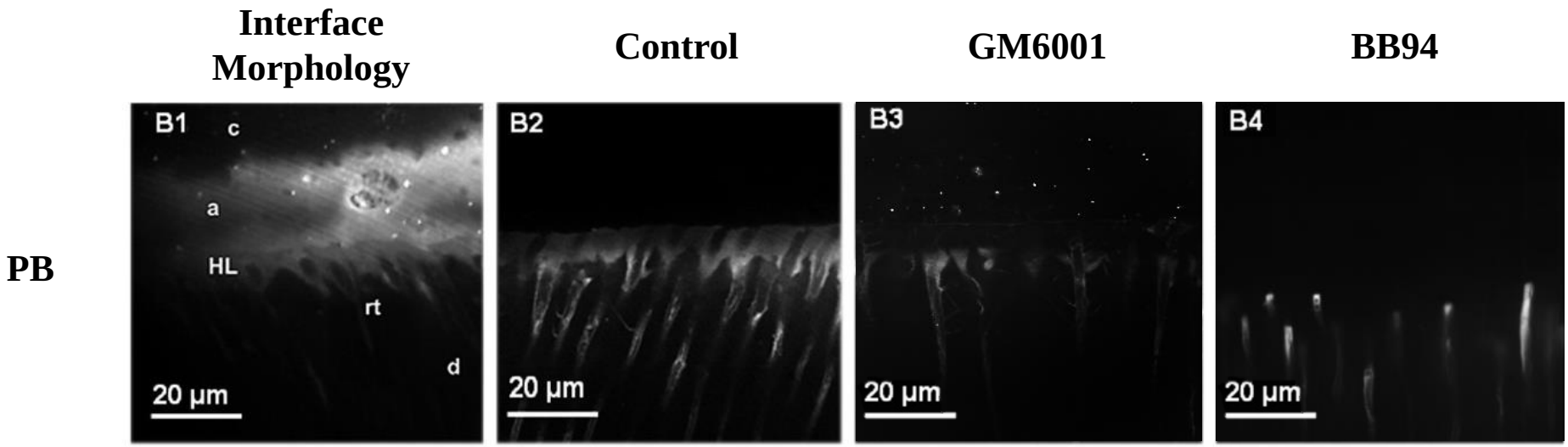

Figure 3-9 TSM images of the interface morphology and examples of the 3 experimental groups' micro-permeability results for PB adhesive system. (B1) The interfacial characterization of the PB-bonded dentine specimens, showing, in this case, a clear hybrid layer (HL) localized beneath a thick adhesive layer (a); c: resin composite; d: dentine. This type of interface showed micro-permeability within the entire thickness of the HL for the control group (B2). PB doped with GM6001 (B3) and BB94 (B4) had less dye reaching the hybrid layer.

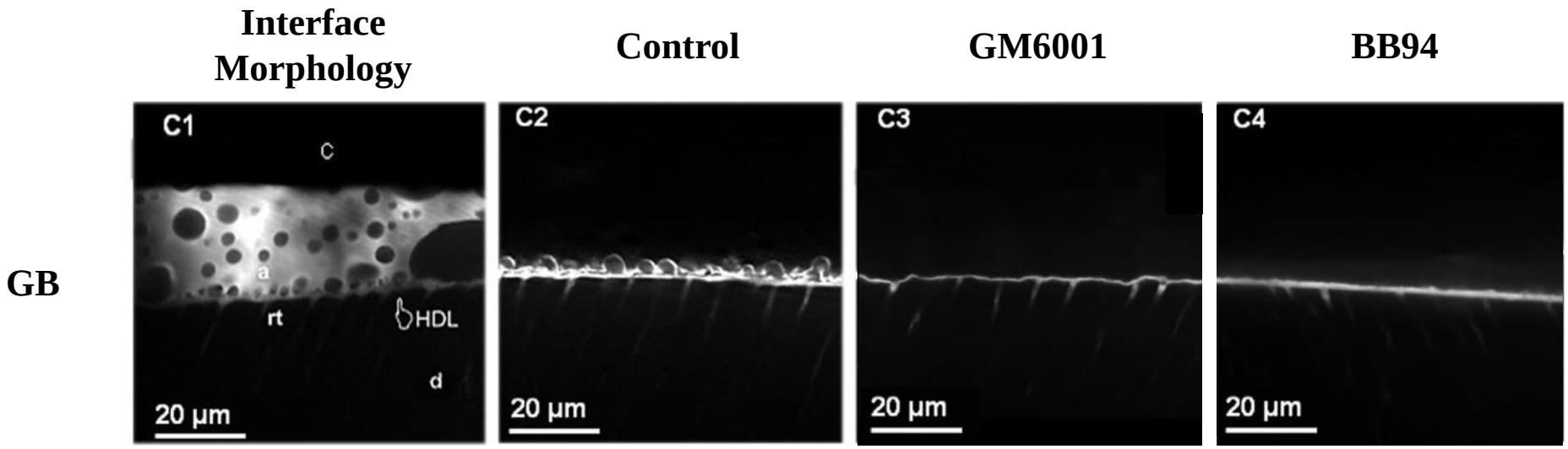

Figure 3-10 TSM images of the interface morphology and examples of the 3 experimental groups' micro-permeability results for GB adhesive system. (C1) A TSM image showing the interfacial characterization of the GB-bonded dentine specimens. It is possible to observe short resin tags (rt) and a 1-2 µm hybrid inter-diffusion layer (HDL) localized beneath a thick adhesive layer (a) characterized by the clear presence of phase separation; c: resin composite; d: dentine. This type of resin-bonded interface was affected by severe micro-permeability within both the hybrid inter-diffusion and part of the adhesive layer, created with GB only (C2). The incorporation of GM6001 (C3) and BB94 (C4) resulted in less dye reaching the adhesive layer.

3.4 Discussion

The null hypothesis was partially rejected as the micro-tensile bond strength changed immediately but not after aging. The micro-permeability of PB and GB adhesives was reduced following the addition of MMP inhibitors.

The micro-tensile bond strength of all adhesive systems including MMP inhibitors was not reduced in the present study when compared to their controls. The reduction in the μTBS for the aged PB with GM6001 could be related to the failure of the resin composite-adhesive interface rather than the failure of the adhesive itself, since 91.67% of the failures were located cohesively within the composite (Figure 3-6). The aged, modified OB showed a reduction in μTBS when compared to their initial data. However, their strength values (> 30 MPa) were no less than the controls and the acceptable reported values for OB (Scherrer et al., 2010). Interestingly, the present study showed that adding MMP inhibitors to a single-step adhesive system improved bond strength initially but not after 3-month ageing.

It was shown, previously, that bond degradation was reduced when chlorhexidine and MMP-2/MMP-9 specific inhibitors (SB-3CT) were used within the primer of etch and rinse adhesive systems (De Munck et al., 2009). However, these incorporated MMP inhibitors did not improve the self-etch adhesive systems.

Adding inhibitors to PB and GB improved the micro-permeability scores, i.e. the fluid permeation at the interface was reduced, when compared to controls. However, this was not observed with OB since it has a better sealing ability when compared to other adhesives and it has been used as a positive control for other adhesives (Griffiths et al., 1999; Sauro et al., 2008).

In contrast to the results of this study, Breschi et al. (2010b) found that pre-treating the etched dentine with GM6001, prior to the application of the two-step etch and rinse adhesive, reduced the bond degradation after 12 months but not immediately. This could be explained by more MMPs being blocked with the inhibiter applied directly as a primer. However, admixing GM6001 with dental adhesive resulted in an increase in the initial bond strength.

Different mechanisms could explain the increase in the initial bond strength (with minimal pre-test failures) and the reduction in the fluids permeating into the adhesive

interface. This could be due to the preservation of the delicate collagen matrix, the enzymatic chemical bond between MMPs and their inhibitors or due to a combination of both mechanisms resulting in improved micromechanical retention of the adhesive within the collagen matrix, suggesting an auxiliary bonding mechanism for these dentine adhesives. The quaternary ammonium compounds (QAMs) showed an electrostatic attraction within the active site of the MMP and render them inactive whilst preserving the collagen (Tezvergil-Mutluay et al., 2011b).

The incorporation of MMP inhibitors within dental adhesive systems may result in the enhancement of the micromechanical interlocking through the reaction between the MMPs and the inhibitor (Section 1.3.4.2). Being competitive towards the zinc ion active side, the inhibitor's functional group targets the dentine MMPs which are present around the collagen fibrils (Liu et al., 2011). As indirect evidence of this, the pre-treatment of the etched dentine with chlorhexidine disinfecting solution was found to reduce the solubility of the collagen fibrils as observed over time but not initially (Carrilho et al., 2007; Sadek et al., 2010). Additionally, no change in the immediate bond strength was found when GM6001 was applied separately (Breschi et al., 2010b).

The increase in immediate bond strength shown in our modified systems is unlikely to be due to preservation of collagen from MMP activity alone. Further investigations are required to elucidate mechanisms for inhibiting collagen matrix degradation and its preservation overtime. This is important not only for adhesive dentistry but also for finding therapeutic applications for restorative materials in caries prevention.

Section III Carious dentine

Chapter 4 Chemical analysis of carious dentine using micro-Raman spectroscopy.

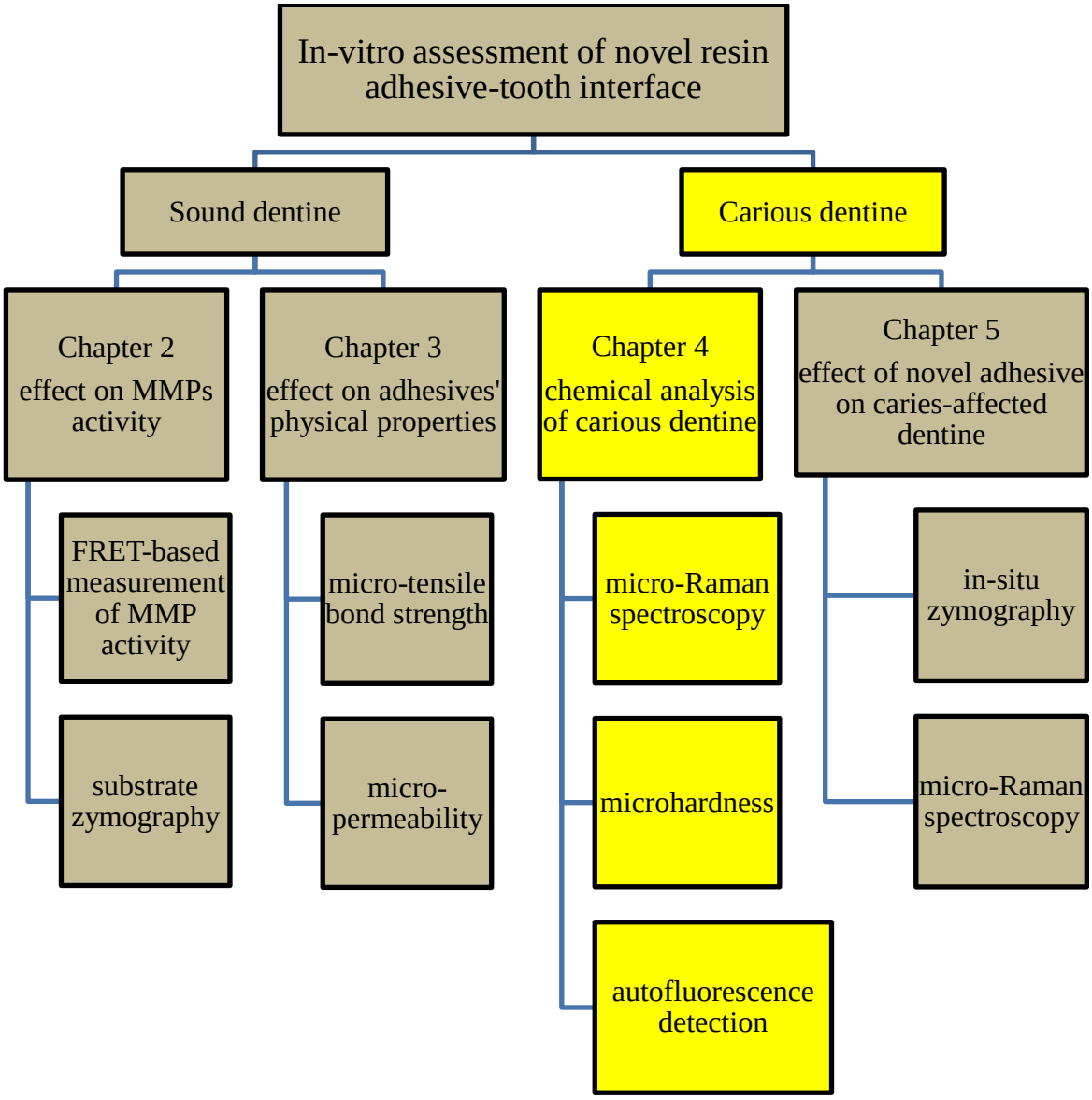

4.1 Introduction

Carious dentine is described clinically and histologically in terms of two altered zones, a superficial caries-infected and a deeper caries-affected layer (Section 1.2.3). The delineation between these zones is essential, both clinically and in laboratory investigations. The clinical excavation limited to the caries-infected dentine reduces the risk of unnecessary pulp exposure in deep cavities, excessive tissue destruction and maximizes the reparative potential of the dentine-pulp complex (Pugach et al., 2009). In the same way, the differentiation between the two carious zones is important during the in-vitro comparison and development of new minimally invasive operative caries excavation techniques (Banerjee et al., 2000a). Section 1.2.4 describes different techniques used to highlight the caries-infected dentine. However, these techniques do not show the biochemical changes in dentine that result from the caries process.

Raman spectroscopy detects the chemical content of tissues through their characteristic molecular vibrational energy signatures, or "fingerprints" (Wachsmann-Hogiu et al., 2009). The difference in energy between the incident and the inelastic scattered photons corresponds to the energy of the molecular vibration (Figure 4-1).

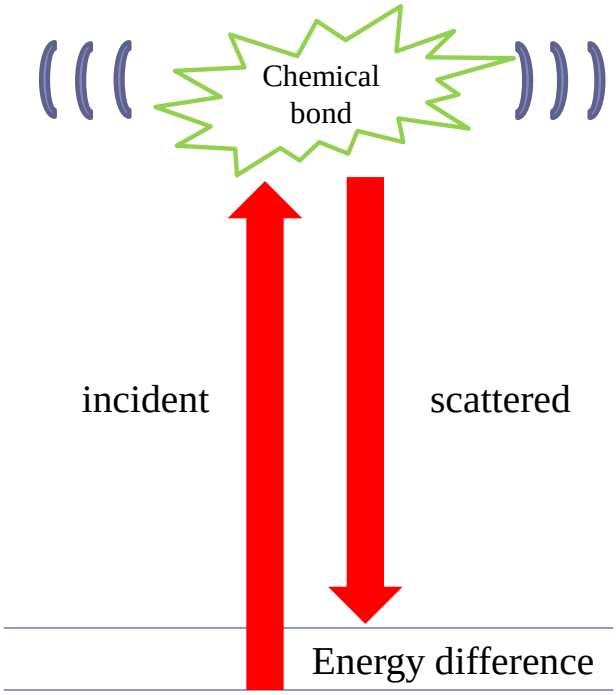

Figure 4-1 The molecular vibration energy, caused by an incident photon, calculated as the energy difference between the incident and scattered photons.

Detection of these scattered photons yields a spectrum of Raman peaks, each of which is characteristic of a specific molecular bond. Collectively, these peaks provide an intrinsic "molecular fingerprint" of the sample which is known as the Raman spectrum. The Raman spectrum in its entirety provides information about the identity, composition, structure and conformation of biological samples (Petry et al., 2003; Wachsmann-Hogiu et al., 2009). As an example, Figure 4-2 shows sound enamel and dentine Raman spectra with their characteristic peaks. The tentative assigned bands for these peaks are summarised in Table 4-1.

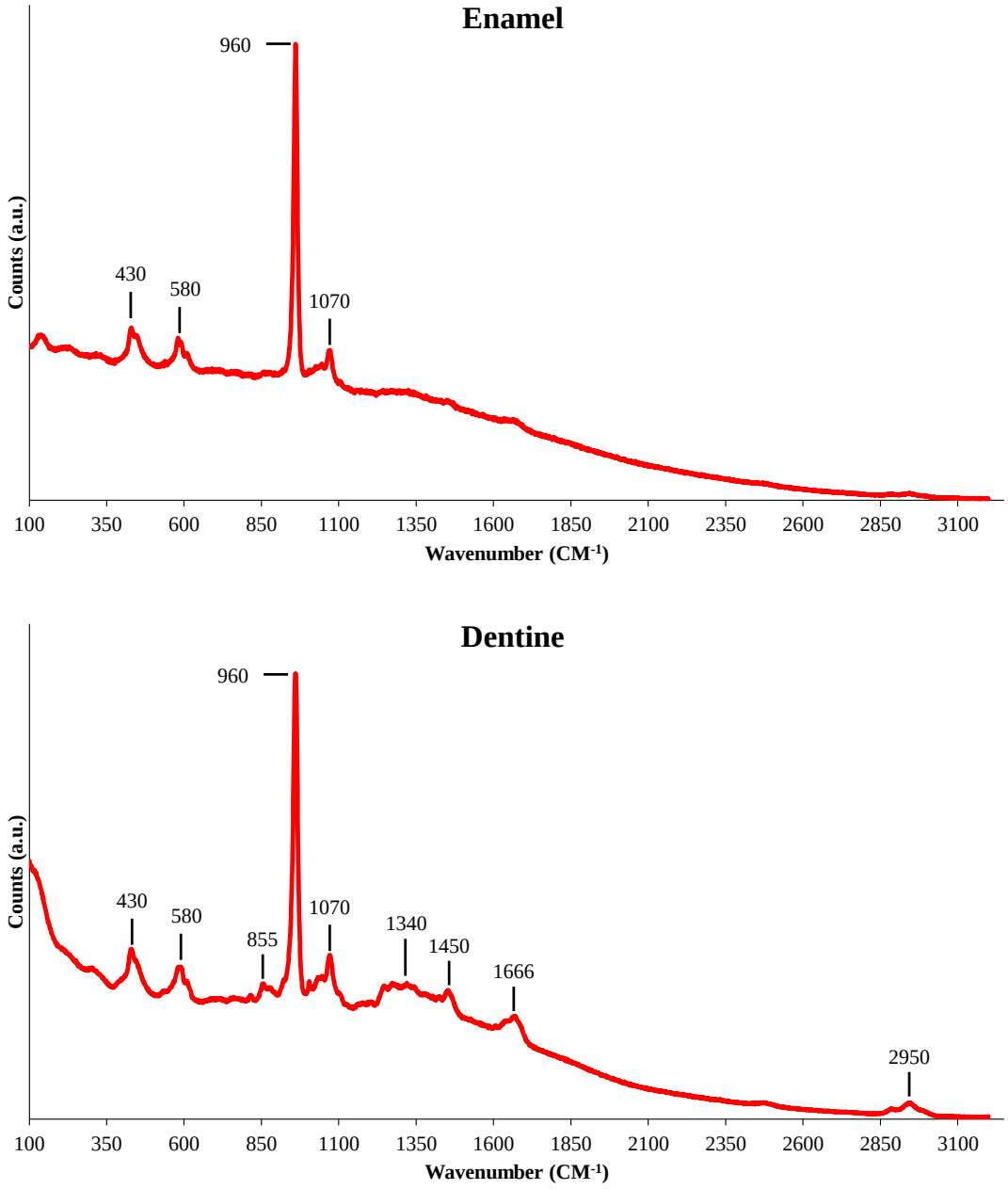

Figure 4-2 Raman spectra for sound enamel and dentine between 100-3100 cm^{-1} wavenumbers, the arrows represent the featured peaks. The tentative assigned bands for these peaks are summarised in Table 4-1.

Table 4-1 The common peaks and their corresponding tentative band assignments found in the Raman spectrum of enamel (Ko et al., 2005; Bulatov et al., 2008) and of dentine (Spencer et al., 2000) shown in Figure 4-2; the correlated histological component of each tentative band assignment is included; *v*: vibration mode.

Peak wavenumber (cm^{-1})	**The tentative band assignment**	**Correlated histological component**
430	v_2 PO_4^{3-}	Hydroxyapatite
580	v_4 PO_4^{3-}	Hydroxyapatite
855	C-C	Organic material
960	v_1 PO_4^{3-}	Hydroxyapatite
1070	v_1 CO_3	Hydroxyapatite
1340	amide III (C-N)	Protein
1450	CH_2, CH_3 deformation	Organic material
1666	amide I (C-O)	Protein
2950	C-H bending	Organic material

The advantages of using micro-Raman spectroscopic analysis include simple and non-destructive sample preparation, linear response to chemical concentrations and easier spectral and band analysis. Raman signals are emitted in the form of light scattering and can be observed from all directions, so by selecting independent axes for light excitation and detection the relatively weaker Raman signal is enhanced.

For the molecular detection and quantification of microscopic specimens, optical microscope can be incorporated with the Raman spectrometer (Wachsmann-Hogiu et al., 2009). Raman peaks are specific chemically and their signals can be detected from very small crystals (Tsuda and Arends, 1997). Additionally, micro-Raman spectrometers are able to probe samples under in-vivo conditions in order to aid the proper understanding of the cells and their activity (Baena and Lendl, 2004).

Conventionally, a point-by-point serial scanning mode is used to generate a micro-Raman intensity map of a sample surface, requiring very long acquisition times due to the low cross-section of Raman scattering. A faster StreamLine™ scanning technique has recently been developed (Renishaw Plc, Wotton-under-Edge, UK) to allow reduced acquisition times for large, artefact-free images. It uses line illumination optics with synchronized stage and CCD scanning technologies (Hedoux et al., 2011), making full use of the detector area and allowing parallel and continuous spectral acquisition. To date, the use of the StreamLine™ scanning technologies have not been reported in the dental literature.

The aim of this study was to delineate objectively the caries-infected, caries-affected and sound dentine zones by measuring the biochemical changes between them optically. The

high-resolution micro-Raman platform was validated by correlating the spectral results with the "gold-standard" microhardness and autofluorescence (AF) signals. The null hypotheses investigated were that the biochemical changes within different carious dentine zones would not be detected using StreamLine™ Raman scanning technologies and that there was no association between micro-Raman mapping, microhardness and the co-localised AF signals.

4.2 Materials and methods

Eight extracted human carious teeth were collected using an ethics protocol reviewed and approved by the East Central London Research Ethics Committee 1 (Reference 10/H0721/55). All teeth were stored in distilled water throughout the study. Each tooth was sectioned longitudinally through the lesions using a slow-speed (200 rpm) water-cooled diamond blade (Diamond wafering blade XL 12205, Benetec Ltd, London, UK) and one section containing a suitable coronal dentine lesion with surrounding healthy dentine was selected for analysis.

4.2.1 Clinical evaluation

Clinical microphotographs were obtained for each tooth using a stereo microscope (MEIJI Techno UK Ltd., UK) for the visual 'clinical' macroscopic evaluation of each lesion. The caries-infected, caries-affected and sound dentine areas were determined visually by three independent clinical experts depending on their histological appearance (Figure 4-3). The darker brown areas corresponded to caries-infected dentine, the paler brown/translucent areas to caries-affected dentine and the yellow-white areas to the sound dentine (Banerjee et al., 1999) (Section 1.2.4.1).

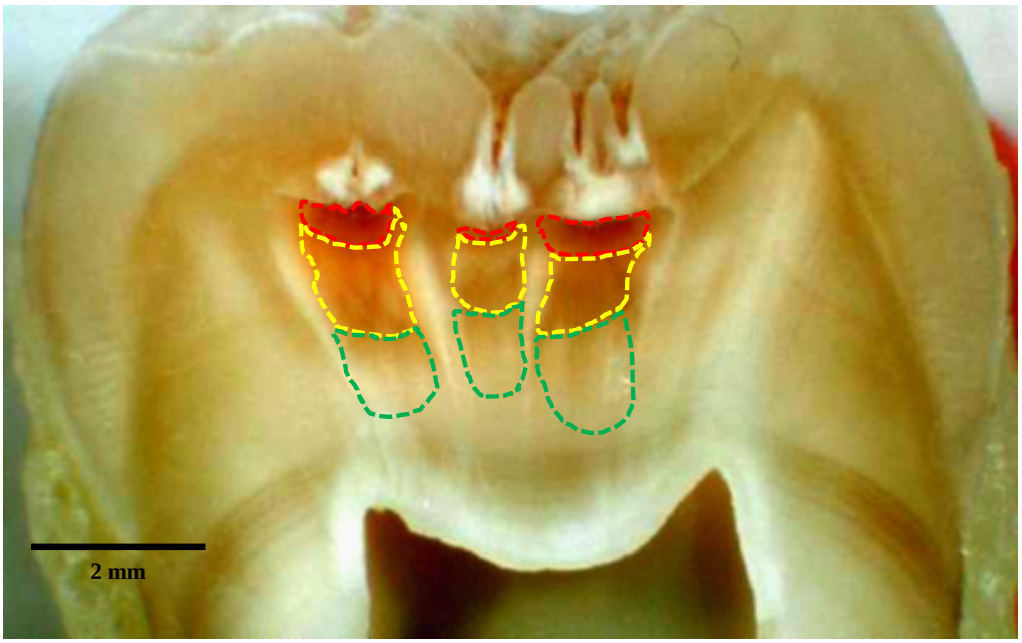

Figure 4-3 Clinical microphotograph for one of the teeth used in this study. The red dotted line represents the caries-infected dentine; the yellow dotted line represents the caries-affected dentine; the green dotted line represents the sound dentine.

4.2.2 Raman spectroscopy

A Renishaw "inVia" Raman microscope (Renishaw Plc, Wotton-under-Edge, UK) in StreamLine™ scanning mode was used in this study. Each tooth was examined using a 20 / 0.40 NA air objective and a montage image was created (Figure 4-4).

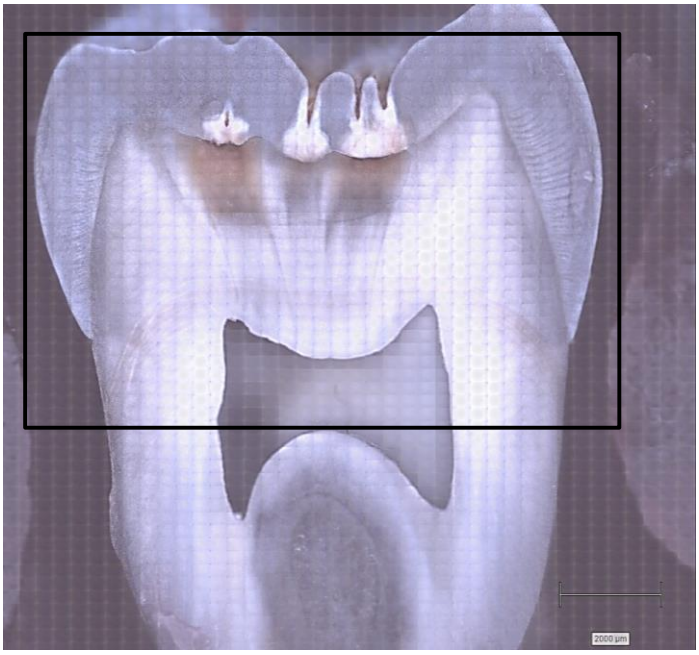

Figure 4-4 A montage image for the tooth in Figure 4-3 created with a Renishaw inVia Raman microscope. The rectangle represents the scanned area.

The entire sectioned surface of each tooth was scanned using a 785 nm diode laser (100 mW laser power) through the same objective while the Raman signal was acquired using a 600 lines/mm grating centred between 849 cm^{-1} and 1603 cm^{-1} and 2 seconds CCD exposure time. The spectral resolution was 8.55 cm^{-1}. For each tooth, around 400,000 spectra were recorded with an inter-spectrum distance of 80µm along the axis parallel to the enamel-dentine junction (EDJ) and 2.7 µm along the axis perpendicular to the EDJ. The scanning time was around 4 hours per tooth. Pearson-based cluster analysis of the dataset (over 3 million spectra) (Figure 4-5a) was performed using an in-house program designed to derive the most independent clusters. Firstly, k-mean cluster analysis was carried out using the Pearson Correlation Coefficient (PCC) to group similar spectra together (Figure 4-5b). The number of centroids is progressively increased until the average similarity coefficient reaches a maximum. Such an approach guarantees that subtle variations in the data set are recorded but leads to the "over-clusterisation" of the data (25 centroids). Secondly, the software uses a fitting-based optimisation routine to reduce this large centroid set to a smaller orthogonal set (five centroids) and the average spectrum for each centroid was calculated (Figure 4-5c). These small groups of components represent the minimum number of centroids which can accurately fit all the spectra within the entire data set. Finally, this five-component fitting base is used to fit all the spectra in the original data set (Figure 4-5d), leading to five grey-scale intensity maps representing the centroid contribution for each spectrum. The average percentage values for each centroid within the three different tissue types were independently obtained depending on the histological appearance.

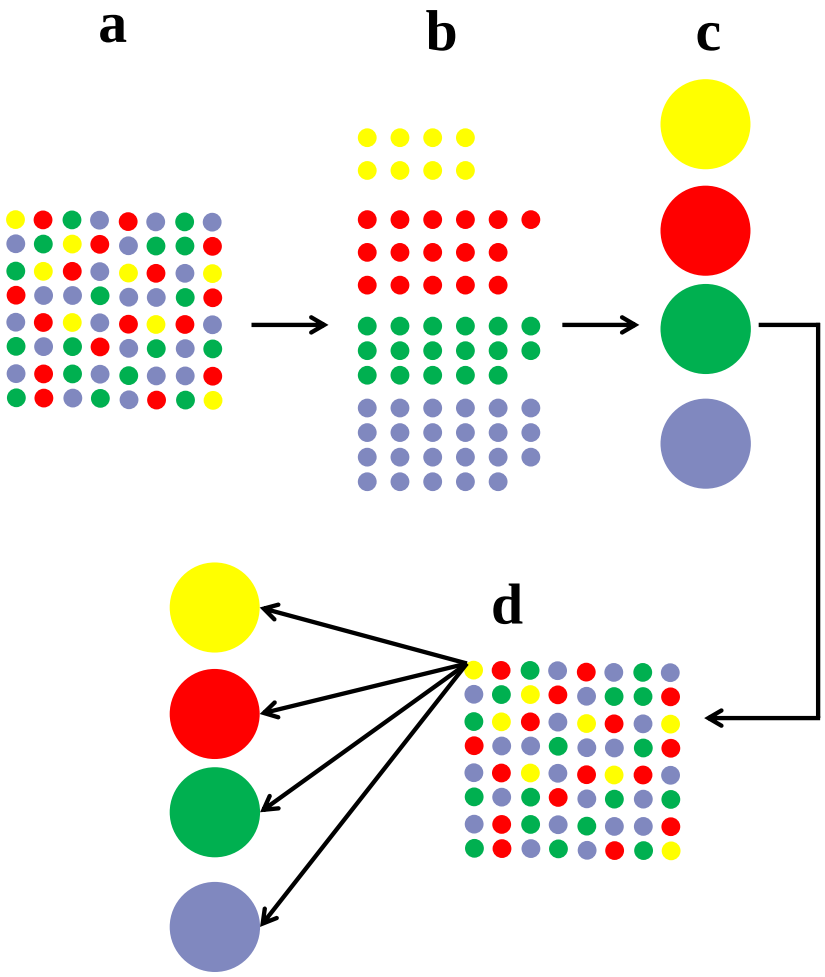

Figure 4-5 Schematic diagram explains the Pearson-based cluster analysis process. (a) The whole data set (over 3 million spectra) was loaded to the program. (b) Similar spectra were grouped together. (c) The number of centroids was reduced and the average spectrum for each group was calculated. (d) The component-fitting base is used to fit all the spectra in the original data set by finding the relation between each spectrum and the average spectrum of each centroid.

4.2.3 AF detection

The green AF signal from the carious teeth was mapped using confocal laser scanning microscopy (Leica TCS SP2, Leica Microsystems, Heidelberg GmbH, UK). The samples were illuminated with a 488 nm laser through a 10 / 0.40 NA oil immersion objective and the green autofluorescence emission recorded through a 510 - 580 nm bandpass filter (Figure 4-6).

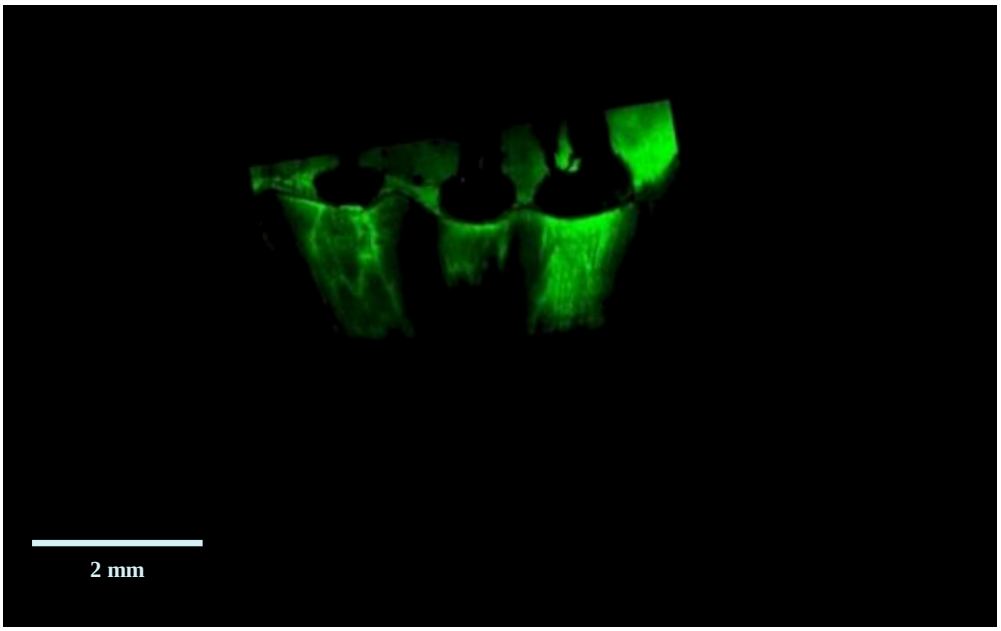

Figure 4-6 The blue-green AF signal for the tooth in Figure 4-3 mapped using CLSM.

4.2.4 Microhardness measurement

A Struers Duramin (Struers Ltd., Denmark) microhardness tester was used to obtain the Knoop microhardness (KHN) from a total of 233 areas across the eight carious teeth. Diamond-shaped indentations were produced using a 10 g load applied for 15 seconds. The indentations were evaluated using a 40 / 0.65 NA objective and the KHN was calculated using the manufacturer's software. A single indentation at each measurement site was made commencing approximately 100 µm from the lesion margin and progressing towards the pulp chamber, crossing the different histological layers of carious dentine. Four or five parallel indentation series were made through the lesion depending on its overall size. In all series, the long diagonal of each indentation was parallel to the EDJ and the distance between the indentation centres was 500 µm. The Knoop microhardness indentations were superimposed upon the macroscopic image for each tooth (Figure 4-7a and Figure 4-7b). The AF signature (Figure 4-7c) was similarly superimposed on this macroscopic image (Figure 4-7d).

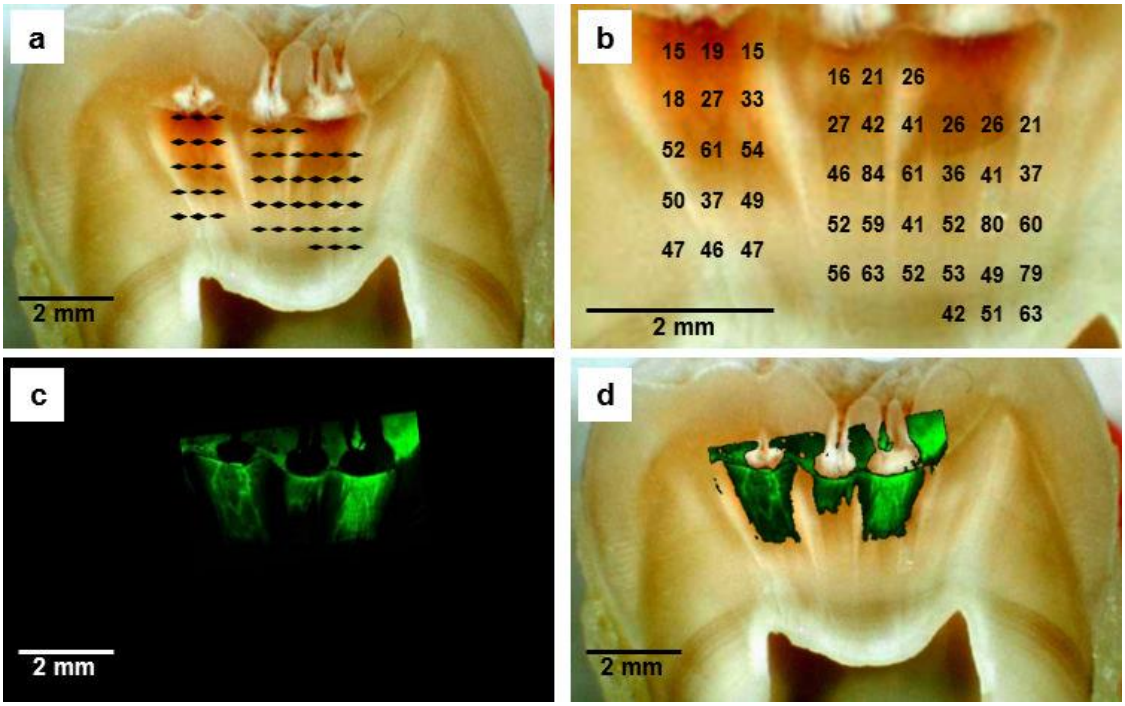

Figure 4-7 (a) The Knoop microhardness indentation areas of the tooth in Figure 4-3. (b) The KHN values. (c) The AF signal from the same tooth. (d) Superimposed image of the AF signal with the clinical microphotograph.

4.2.5 Statistical analysis

Using ImageJ software (Wayne Rasband, NIH, USA), the average green AF signal and the average cluster intensities were calculated for the corresponding KHN areas. These areas were divided into caries-infected, caries-affected and sound dentine layers based on their histological appearance and the relative contribution of each cluster was calculated for each zone. One way ANOVA was used to compare the differences in the KHN, the AF and the relative contribution of each cluster in the three layers. Tukey's test was used to detect the differences between any two layers. Collective sound dentine and sound enamel data obtained from all teeth was used as positive controls. To find the statistical association between the KHN, AF signal and the micro-Raman clusters, Pearson correlation coefficients were used.

4.3 Results

KHN and AF, current laboratory standards for carious dentine characterization, were used to verify the micro-Raman components. Cluster analysis derived five independent measurable spectral components which fitted accurately the entire spectral dataset. These clusters represented two Raman clusters, the mineral and protein content, and three

fluorescence clusters: porphyrin fluorescence (PF) from bacterial byproducts, infected dentine signal (IDS) and affected dentine signal (ADS) (Figure 4-8).

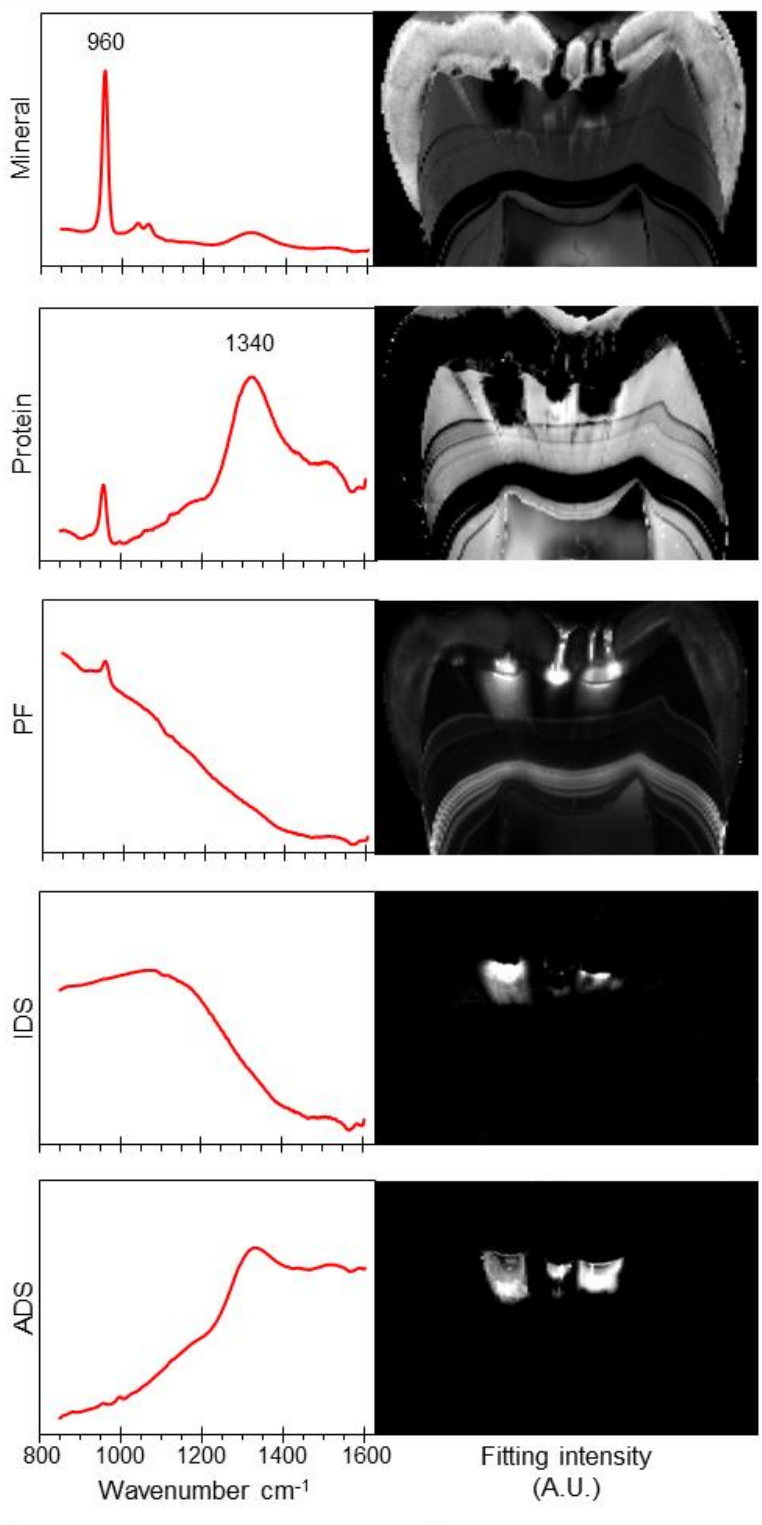

Figure 4-8 The five clusters obtained from the micro-Raman spectroscopy scanning of the tooth in Figure 4-3: mineral cluster represented by the phosphate (ν_1 PO_4^{3-}) peak at 960 cm^{-1}, protein content cluster represented by the amide III peak at 1340 cm^{-1}, PF (bacterial by-products) cluster with no reference peak, IDS cluster and finally the ADS cluster represented by the broad peak of amide III at 1340 cm^{-1}.

The mean KHN, AF and the micro-Raman clusters intensities of the caries-infected, caries-affected and sound dentine are summarised in Figure 4-9.

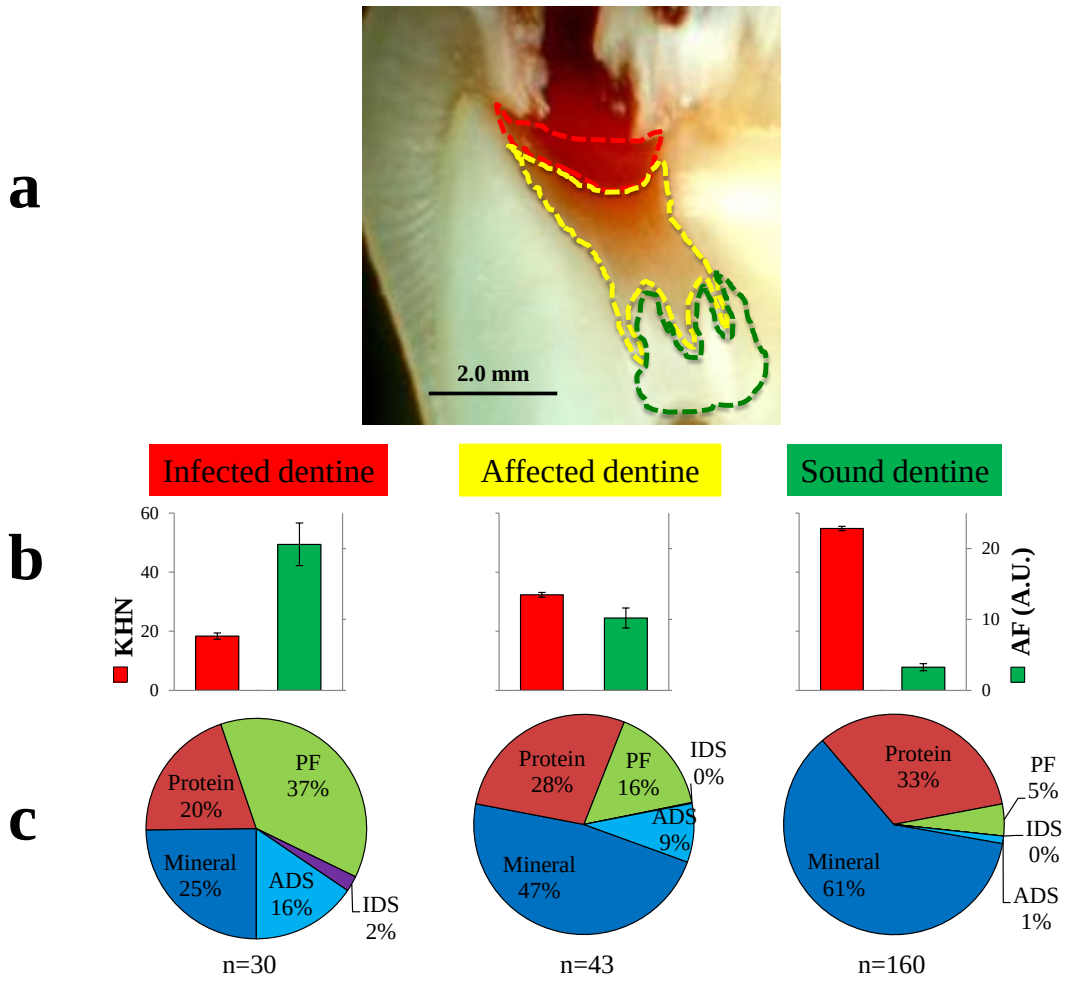

Figure 4-9 (a) The clinical delineation of the caries-infected (red dotted line), caries-affected (yellow dotted line) and sound dentine (green dotted line) layers. (b) The mean KHN and AF results for the three layers. The error bars represent the standard error of means. (c) The relative contribution of the mineral, protein, PF, IDS and ADS Raman and fluorescence clusters in the caries-infected, caries-affected and sound dentine.

The mineral content decreased significantly in the caries-infected dentine (24.8 % ± 5.7 (mean ± SEM)) with no statistically significant differences ($p = 0.06$) detected between the caries-affected (47.5 % ± 5.7) and sound dentine (61 % ± 2.7). There were no significant differences in the protein content of the three layers ($p = 0.10$). Regarding the PF component, significant differences ($P < 0.001$) were found between the caries-infected (37.4 % ± 5.9), caries-affected (15.8 % ± 3.9) and sound dentine (4.7 % ± 1.3). The IDS correlated with the caries-infected dentine (2.3 % ± 1.1). Contrarily, the ADS did not show significant differences between the caries-infected (15.5 % ± 4.8) and caries-

affected dentine layer (8.6 % ± 3.4) ($p = 0.15$). However, the sound dentine exhibited significantly less ADS (1.1 % ± 0.7).

Statistically significant objective delineation between the caries-infected, caries-affected and sound dentine was found using the KHN, the blue-green AF as well as in the changes detected in the PF cluster (Table 4-2).

Table 4-2 The 95 % CI (lower limit - upper limit) of the KHN, the AF and of the relative contribution of each Raman cluster in all detected clusters within different carious zones. Areas with the same colour are not significant ($p < 0.05$).

Area	**KHN**	**AF (A.U.)**	**Mineral (%)**	**Protein (%)**	**PF (%)**	**IDS (%)**	**ADS (%)**
Caries-infected dentine	16 – 21	14 – 27	13 – 36	10 – 30	25 – 50	0 – 5	6 – 25
Caries-affected dentine	31 – 34	7 – 13	36 – 59	17 – 39	8 – 24	0	2 – 16
Sound dentine	53 – 56	2 – 4	56 – 66	28 – 38	2 – 7	0	0 – 3

The Pearson Correlation results are summarised in Table 4-3. As the KHN increased, the AF signal as well as the PF, IDS and ADS components decreased significantly ($p < 0.05$) while the mineral component increased. However, the protein component was not correlated with the KHN, AF and IDS cluster but shows a significant negative relationship with the mineral component.

AF was significantly positively related to the PF, ADS and IDS clusters and negatively correlated to the mineral content. Similarly, the PF component significantly increased with the AF and IDS clusters, decreased with the mineral and protein content and did not correlate significantly with the ADS component. The IDS and ADS clusters behaved in a similar fashion with the other components but no significant correlation between IDS and protein, or ADS and PF could be found.

Table 4-3 Pearson correlation (r values) between KHN, AF, mineral cluster, protein cluster, PF cluster, IDS cluster and ADS cluster. The negative (r) values represent negative correlation. The correlations in shadowed areas are not statistically significant ($p > 0.05$).

	KHN	AF	Mineral	Protein	PF	IDS	ADS
KHN	1.00	-0.53	0.39	0.00	-0.38	-0.24	-0.27
AF	-0.53	1.00	-0.39	0.04	0.34	0.16	0.31
Mineral	0.39	-0.39	1.00	-0.61	-0.46	-0.19	-0.35
Protein	0.00	0.04	-0.61	1.00	-0.27	-0.13	-0.19
PF	-0.38	0.34	-0.46	-0.27	1.00	0.27	0.09
IDS	-0.24	0.16	-0.19	-0.13	0.27	1.00	0.16
ADS	-0.27	0.31	-0.35	-0.19	0.09	0.16	1.00

4.4 Discussion

The null hypotheses investigated in this study were rejected as the new scanning technique provided a detailed map of the biochemical changes in the different carious dentine zones. Also, a relationship was found between the KHN, AF and different micro-Raman clusters except the protein cluster.

Studies reporting the uses of micro-Raman spectrometry in dental research are limited, mainly due to the long acquisition times inherent to the Raman scattering process. In the current experiment setting, the scanning time was short when compared to the conventional method (around 4 hours per tooth). This was due to the parallelization of the StreamLine™ system.

Another cause for the limitation of the use of micro-Raman spectrometry technique is that most biological materials, including dental tissues, exhibit autofluorescence when irradiated by UV or visible laser light. As a consequence, the weaker Raman signals are generally masked resulting in a poor signal/noise ratio. This ratio can be enhanced by the removal of organic components by chemical means or by the use of a near-infrared laser instead of a visible laser (Tsuda and Arends, 1997).

Early enamel caries was detected using polarized Raman spectroscopy (Ko et al., 2006). A quantitative parameter, known as the depolarization ratio, was determined by calculating the intensity of the main phosphate peak from parallel- and cross-polarized Raman spectroscopic measurements, then dividing the cross-polarized value by the parallel-polarized value (Choo-Smith et al., 2008). This ratio showed high specificity and sensitivity in detection of enamel caries (Ko et al., 2008). However, the depolarized ratio

could not differentiate between the stained sound enamel and carious enamel (Huminicki et al., 2010).

The conventional point by point scanning technique has been used previously to evaluate chemical changes at the adhesive interface including the degree of monomer conversion and the interfacial nanoleakage (Spencer et al., 2000; Wang and Spencer, 2003; Wang et al., 2007; Santini and Miletic, 2008; Navarra et al., 2009b; Navarra et al., 2009a). Additionally, curve fitting was used in these studies to detect the changes in the main peaks' intensity in relation to a reference peak. Recently, principal component analysis (PCA) was shown to improve dramatically the signal-to-noise ratio of noisy spectra from large datasets (Hutchings et al., 2009) but became computationally impractical if the dataset was too large. However, due to the direct relationship between the solution of k-mean clustering and PCA (Ding and He, 2004), k-mean clustering offered the same level of analytical power of a large dataset but with vastly superior computational speed. The Pearson-based cluster analysis used in this study classified all scanned points into different independent clusters generated by averaging spectra similar to each other (Figure 4-5c). The advantage of this method is that it uses the raw original spectra without the need for background-correction. The large number of similar spectra used in this study permitted the creation of cluster spectra with excellent signal-to-noise ratios (Figure 4-8).

The large presence of sound enamel and dentine within the scanned teeth leads to the derivation of mineral and protein clusters. The difference between the cluster analysis method and the depolarization ratio calculation was that the entire components of the Raman spectrum were included rather than looking at a specific component, the phosphate peak. Additionally, such analysis allowed the detection of three different fluorescence clusters which are usually considered as a background and removed during other methods of calculation.

The labelling of the five clusters (Figure 4-8) was based upon the characteristic Raman peaks and the fluorescence signals found in them and on the histological location where each cluster was highly represented. The mineral cluster exhibits the characteristic phosphate (ν_1 PO_4^{3-}) peak at 960 cm^{-1}, the most intense Raman peak in dental hard tissue (Wang et al., 2007), and was primarily located in sound enamel where mineral is the primary content. The protein cluster had the broad amide III peak at 1340 cm^{-1} which is one of the chemical bonds found in protein structure and represented the organic content

(Overman and Thomas, 1999). Furthermore, due to the diversity of the organic material throughout the 8 teeth, the full width at half maximum (FWHM) of the amid III peak (101.9 cm^{-1}) is much broader than the width of the mineral phosphate peak (15.5 cm^{-1}). This cluster was found in the dentine structure but not in enamel. The PF cluster had no characteristic peak and was located mainly in the enamel and soft dentine lesions where cariogenic bacteria would be expected. Using an incident wavelength of 785 nm, only the very tail-end of the porphyrin fluorescence is excited, leading to a relatively modest signal when comparable to the emission obtained with a lower excitation wavelength. The PF spectrum found in this study was similar to the one reported by König et al. (1998) and Hibst et al. (2001). Interestingly, this fluorescence signal was clustered together with the fluorescence from the tetracycline bands in one of the samples due to the similarity in shape of the tail-end fluorescence emission spectra. No characteristic Raman peak could be found from the IDS cluster which was confined to the caries-infected dentine area. Finally, the ADS cluster, which may result from protein breakdown, had a slightly broadened amide III peak at 1340 cm^{-1} (FMHW is 113.7 cm^{-1} versus 101.9 cm^{-1} for sound dentine), and was located in dentine as opposed to enamel.

Comparing the relative fitting contribution of each of the five components across the map showed that sound dentine, the positive control, contained 61 % of the mineral clusters and 33 % of the protein clusters (Figure 4-9c). This result compared favourably with Linde and Goldberg (1993) who reported that the mineral and the organic phases in sound dentine accounted for about 50-60 % and 20-30 %, respectively (Section 1.1). To validate further the present analytical method, the mean cluster content of 40 different sound enamel areas, across the 8 teeth, was calculated and showed that enamel contains 95.5 % (SEM 2.0) mineral (Figure 4-10) which is similar to the reported percentage weight of its mineral content (Weatherell, 1975).

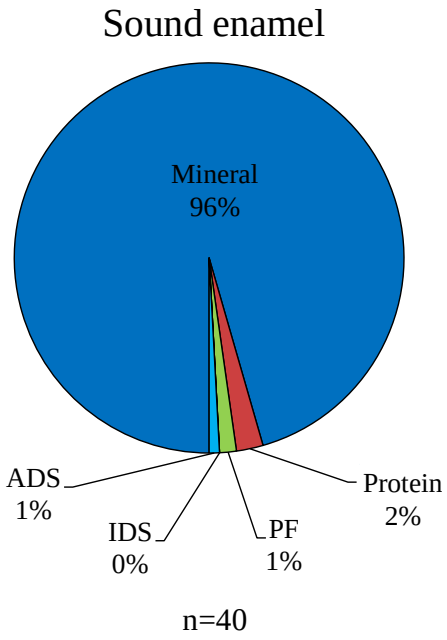

Figure 4-10 Sound enamel cluster content

The microhardness test is associated commonly with the relative mineral content of dental hard tissues and it is used routinely as a reference for their inherent physical properties, as it is not affected by the variability of dental samples (Bresciani et al., 2010; Kirsten et al., 2010) (Section 1.2.4.6). Using an Ultra-Micro-Indentation System (UMIS), Ca:P ratios of caries-affected dentine were found to correlate significantly with the microhardness values (Sakoolnamarka et al., 2005). Marshall et al. (2001) found that the elastic modulus and the hardness values of caries-affected and underlying sound dentine are not significantly different when examined using Atomic Force Microscopy (AFM) nano-indentation. However, other studies have shown that caries-affected dentine exhibits lower KHN values than that of sound dentine (Ogawa et al., 1983; Banerjee et al., 1999). In this study, KHN differed significantly between the caries-affected and sound dentine which is not seen in the micro-Raman mineral cluster. Histologically, the transparent zone, which is part of the affected histology, blends with the sound dentine with no clear delineation between the two. In addition, the mineral cluster indicated that the transparent zone has higher mineral content than adjacent sound dentine, due to mineral deposition leading to tubular sclerosis, which could explain the consistency of caries-affected and sound dentine mineral cluster contents and the 95 % CI overlap between the two layers (Table 4-2).

The protein cluster did not show any significant difference between caries-infected (20 % ± 4.8), caries-affected (28 % ± 5.3) and sound dentine (33.2 % ± 2.6) and it was not related to KHN or AF. However, a high negative correlation was found between the protein and mineral clusters. Additionally, the ADS was not significant between the caries-infected and caries-affected dentine. This could be explained by the fact that the degradation of the extracellular organic matrix in dentine caries occurs following the demineralisation of hydroxyapatite and part of this organic material can be still found within the demineralised dentine (Van Houte, 1994; Van Strijp et al., 2003). Using scanning electron microscopy, other organic content, including odontoblast processes, have been shown to extend from the underlying sound dentine to approach the deeper aspect of the caries-infected zone (Yamada et al., 1983). These proteinaceous structures and other proteins are thus grouped within the protein cluster.

The fluorescence signal detected in the spectral clusters was near-infrared in wavelength (excitation at 785 nm and emission at 841-898 nm) and has been used for caries diagnosis (Shigetani et al., 2003) (Section 1.2.4.4). Cluster analysis provides three broad fluorescence-like spectra: PF, ADS and IDS. The correlation between the PF and the IDS and the histological appearance suggested that both are emitted from bacterial byproducts. ADS was weakly related to IDS but not to PF which suggests that it has a different origin. The blue-green AF, emitted from the breakdown of structural proteins (Mcconnell et al., 2007) (Section 1.2.4.4), was related to ADS and both could therefore have the same origin. The AF was also related to PF which is explained by the presence of both fluorescent signals in the same area rather than having the same origin. Minimal PF (4.7 % ± 1.3) was found within sound dentine suggesting the presence of a small quantity of cariogenic bacteria which is unexpected in healthy tissue. However, Banerjee et al. (2002) reported the presence of bacterial counts of 0.34×10^6 per mg (SEM 0.05) within the same layer which are significant when compared to non-carious teeth.

This study includes the comparison of several objective caries diagnostic techniques to the subjective histological appearance. Previous studies have related the KHN and AF to the histological appearance of different carious zones (Banerjee et al., 1999; Banerjee et al., 2010a). The 95 % CI of the KHN (Table 4-2) of different areas are comparable with the results obtained in these studies (Section 1.2.4.6). Microhardness is a destructive test (Banerjee et al., 2010a) and each examined area cannot be tested twice. In this study, the KHN was obtained after the data from other methodologies were gathered and at least a 500 µm distance was maintained between each adjacent examined area. Only the areas

that represented the exact Knoop indentation sites were included for analysis although the micro-Raman spectroscopy included scans of more than 3 million points across the eight teeth.

The micro-Raman cluster mapping provided detailed microscopic data for large areas. The caries-infected dentine requiring clinical excavation can be delineated with the mineral (< 36 %), PF (> 25 %) and IDS (> 0.3 %) clusters (Table 4-2). The correlation between the KHN and AF with these micro-Raman clusters indicates that they could be used as caries-infected dentine objective microscopic markers.

Section II Carious dentine

Chapter 5 The effect of a modified adhesive on the caries-affected dentine.

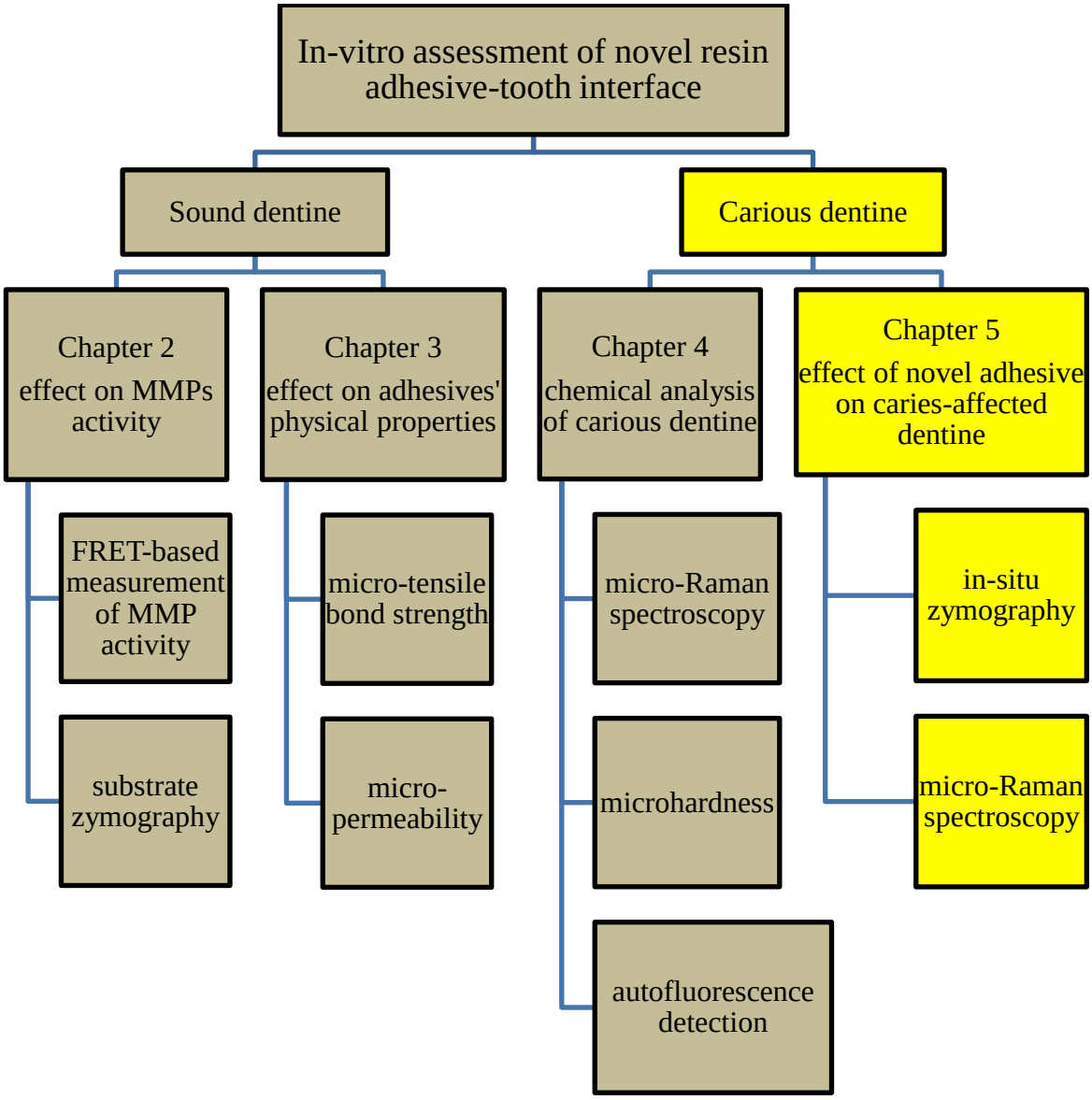

5.1 Introduction

Current minimally invasive, tooth preserving biological operative caries management techniques involve the excavation of the superficial caries-infected layer and preserving the deeper caries-affected dentine (Marshall et al., 1997; Banerjee and Watson, 2011). In most clinical scenarios, the caries-affected dentine can be considered a substrate to which an adhesive restoration may be sealed. More precisely, it is the outer layers of the caries-affected dentine, or the discoloured zone, which is involved in the hybridization process with dentine bonding agents. As described in Section 1.2.3.2, this zone is characterized by the presence of a dense, partially-exposed collagen matrix as a result of partial demineralisation and defibrillation of the unprotected collagen fibrils when compared to the underlying dentine. This allows easier diffusion of the dental adhesive and increased hybrid layer thickness (Haj-Ali et al., 2006; Erhardt et al., 2008). However, bonding to caries-affected dentine results in a reduction of the micro-tensile bond strength when compared to that of sound dentine (Nakajima et al., 2005; Joves et al., 2013).

An acidic environment within the discoloured zone results in the activation of various matrix metalloproteinases (MMPs) degrading the organic collagen matrix as the caries lesion progresses (Tjaderhane et al., 1998; Sulkala et al., 2001; Shimada et al., 2009) (Section 1.3.5). In addition, the use of acid-etch and/or acidic primer showed MMP activation within sound dentine (Chapter 2). This suggests that the caries-affected dentine-adhesive interface is subjected to additional MMP activity, when compared to sound dentine-adhesive interface, as a result of a combination of environments.

Several techniques had been used to detect MMPs within the caries lesion. Using substrate zymography, performed on excavated caries tissue, MMP-2, MMP-8 and MMP-9 have been identified (Tjaderhane et al., 1998). Shimada et al. (2009) found that the quantity of immunogold-labelled MMP-8 and MMP-9 was reduced in caries-affected dentine in comparison to sound dentine. However, there was no difference in MMP-2 quantity between the two tissues. In-situ zymography was used to detect MMP activity in carious dentine (Toledano et al., 2010) and to identify the sound dentine-adhesive interface MMP activity (Porto et al., 2009; Mazzoni et al., 2012). The MMP activity of the caries-affected dentine-adhesive interface was not detected previously. This might be due to the irregularity and variability of the hybrid layer formed which makes its use difficult as a controlled substrate for laboratory investigation (Haj-Ali et al., 2006; Komori et al., 2009).

Micro-Raman spectroscopy was used to detect the chemical changes at the sound dentine-adhesive interface (Chapter 4). Using the spectrum of selected points across the interface, Spencer et al. (2000) were able to detect and to quantify the chemical composition of the sound dentine-adhesive interface. It was concluded that due to the differences in the solvents and in the hydrophobicity, the relative resin content of two types of two-step etch and rinse adhesive systems were different. In addition, it was found that the hydrophilic component (HEMA) of the dental adhesive infiltrates the demineralised sound dentine more than the hydrophobic component (bis-GMA) (Wang and Spencer, 2003). Comparing the chemical changes within the caries-affected dentine-adhesive interface and the sound dentine-adhesive interface, Wang et al. (2007) found that the former had a greater demineralisation depth with a more complicated contents profile than the latter interface.

Micro-Raman spectroscopy was also used to measure the penetration depth and the degree of monomer conversion within sound dentine by identifying the dental adhesives' specific peaks and recognising the changes within them (Santini and Miletic, 2008; Navarra et al., 2009b; Navarra et al., 2009a; Shin et al., 2009). As shown in Chapter 4, the cluster analysis method had the ability to detect chemical changes of different carious dentine zones corresponding to their inherited characteristics.

The aims of this experiment were, firstly, to evaluate the effect of adding MMP inhibitor (BB94) to the primer of a three-step etch and rinse adhesive system on the caries-affected dentine MMP activity. Secondly, the effect of such inclusion on the chemical content of the caries-affected dentine-adhesive interface was assessed. The null hypotheses were that the addition of MMP inhibitor to the three-step etch and rinse adhesive system would not alter the caries-affected dentine MMP activity or the chemical content of the caries-affected dentine-adhesive interface at a significance predetermined at $\alpha = 0.05$.

5.2 Materials and methods

5.2.1 In-situ zymography

Three extracted human carious teeth were collected using an ethics protocol reviewed and approved by the East Central London Research Ethics Committee 1 (Reference 10/H0721/55). All teeth were stored in distilled water throughout the study. Caries-infected dentine was excavated selectively from all teeth with the aid of a chemo-

mechanical agent, Carisolv® gel (OraSolv AB, Gothenburg, Sweden) and its own hand instruments (Figure 5-1).

Figure 5-1 Carisolv® gel and the metal mace-tip instrument used to apply and agitate the gel to excavate chemo-mechanically the caries-infected dentine selectively.

The gel was applied and agitated as per manufacturer's instructions, using a proprietary abrasive metal mace-tip instrument (Figure 5-2a). Once the gel had become cloudy (Figure 5-2b), it was rinsed away and a second fresh mix of gel was applied and further agitated (Figure 5-2c). Excavation was deemed complete when the gel failed to become cloudy and the cavity was checked with a dental probe for a rubbery, scratchy and discoloured caries-affected dentine (Figure 5-2d). Each tooth was sectioned longitudinally through the caries-affected dentine (Figure 5-2e) using a slow-speed (200 rpm) water-cooled diamond blade (Diamond wafering blade XL 12205, Benetec Ltd, London, UK) into three 2mm-thick dentine slabs (Figure 5-2f).

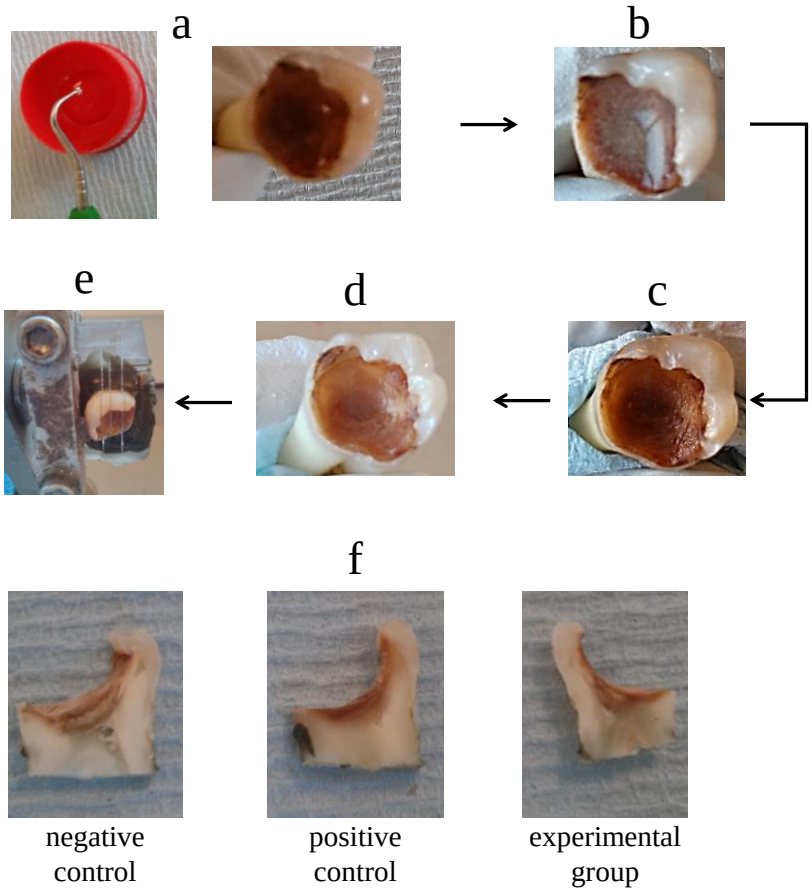

Figure 5-2 Clinical steps for the chemo-mechanical removal of caries-infected dentine using Carisolv®. (a) the abrasive metal mace-tip instrument was used to apply and agitate the gel. (b) the gel became cloudy after agitation indicating caries removal (c) the gel was rinsed and the tooth was checked using a dental probe for any remaining soft caries-infected dentine tissue. Further fresh mixes of gel were applied and agitated. (d) excavation was completed when the gel was not cloudy and the remaining dentine was scratchy and slightly sticky to a dental probe. (e) the tooth was sectioned longitudinally through the caries-affected dentine. (f) three 2mm-thick dentine slabs. Each slab was used in a different experimental group.

The caries-affected dentine in each slab was acid etched using 35% phosphoric acid for 15 seconds and then rinsed with water, air-dried gently and kept moist in order to remove excess water without drying the dentine.

Freshly made FITC-conjugated collagen was prepared by the addition of 1.0 ml of deionized water to DQ™ Collagen, Fluorescein Conjugate (D-12060, Molecular Probes, Eugene, USA) vials containing lyophilized substrate. Then, a diluted reaction buffer (150 mM NaCl, 50 mM $CaCl_2$, 50 mM Tris-HCl and 2 mM sodium azide, pH 7.6) was added to activate the solution. FITC-conjugated collagen was applied immediately on to the etched caries-affected dentine as MMP substrate.

The three slabs were then treated as follows:

- The first slab (negative control) was treated with Optibond FL "OB" (Kerr, Orange, USA) primer and then the bond was applied following the manufacturer instructions (group C)
- The second slab (positive control) was conditioned with 500 μM BB94 prior to the application of OB primer and bond (group B)
- The third slab (experimental group) was treated with OB primer that contained 5 μM BB94, prepared as described in Section 2.2.1, (group D). The bond was applied on the top of the conditioned caries-affected dentine

Rhodamine B powder was mixed with OB primer before its application in the three groups. All slabs were restored with Filtek™ Supreme Ultra (3M ESPE, St. Paul, USA) resin composite restorative material applied using a flat plastic in two or three 2mm-thick increments. A blue light source (470 nm, ~600 mW cm^{-2} with a 10 mm tip, Optilux VLC, Demetron Research Co., CT, USA) was used to photo-activate the dental adhesives and each resin composite increment for 20 and 40 seconds respectively. Each sample was stored at 37°C for 24 hours. Prior to examination, each slab was hand polished using 800, 1000 and 1200 grit SiC papers and ultrasonicated between each paper grade for 3 minutes. A Confocal Laser Scanning Microscope (CLSM; Leica TCS SP2, Leica Microsystems, Heidelberg GmbH, UK) was used to evaluate the dentine slabs through a 100 / 1.40 NA oil immersion objective. A FITC fluorescence signal was obtained by illuminating the samples with a 488 nm laser and the emission recorded through a 520-540 nm bandpass filter. Excitation by 568 nm laser and emission through a 600-630 nm filter were used to detect Rhodamine B fluorescence.

The presence of FITC signal within the hybrid layer of five reproducible, pre-selected areas, with 40 μm field width, was recorded in each slab. A total of 15 areas were included for each type of treatment group. The same slabs were stored in distilled water at 37°C and they were re-examined after two week using the same settings. The emission of FITC signal represented the MMP activity as a result of the breakdown of the FITC-conjugated collagen.

5.2.2 Caries-affected dentine-adhesive interface characterization

Another 5 extracted human carious teeth were used in this study. The caries-infected dentine tissue was removed using Carisolv® gel as described previously. Each tooth was

sectioned into three 2mm-thick dentine slabs using the same protocol described earlier in Section 5.2.1. The caries-affected dentine was acid etched using 35% phosphoric acid for 15 seconds, then rinsed and air-dried, but without over-drying. The three etched dentine slabs were treated as follows:

- The first slab (negative control) was treated with OB primer and then the bond applied following the manufacturer instructions (group C)
- The second slab (positive control) was conditioned with 500 µM BB94 prior to the application of OB primer and bond (group B)
- The third slab (experimental group) was treated with OB primer containing 5 µM BB94 (group D). The bond was applied on to the conditioned caries-affected dentine

All slabs were restored with Filtek™ Supreme Ultra (3M ESPE, St. Paul, USA) resin composite restorative material using a standardised protocol. Each sample was stored at 37°C for 24 hours. Prior to examination, the excess composite was removed manually by 1000 grit SiC paper.

Each slab was examined using a 20 / 0.40 NA air objective and a stitched montage image was created using a Renishaw "inVia" Raman microscope (Renishaw Plc, Wotton-under-Edge, UK). For each slab, two separate areas that contained resin composite, dental adhesive, hybrid layer, caries-affected dentine and sound dentine tissue were selected (Figure 5-3a). These areas were scanned with the StreamLine™ scanning mode using a 785 nm diode laser (100 mW laser power) through the 20 / 0.40 NA air objective while the Raman signal was acquired using a 600 lines/mm grating centred between 849 and 1603 cm^{-1} and 2 seconds CCD exposure time. The spectral resolution was 8.55 cm^{-1}.

Ten areas were scanned non-destructively for each treatment group immediately (time 1).The slabs were stored in distilled water at 37°C and were re-scanned after two weeks (time 2) and again after four weeks (time 3), using the same settings. Pearson-based cluster analysis of the dataset (over 1.8 million spectra) was performed using the same in-house program described in Section 4.2.2. Average line profiles for all clusters were also obtained across each sample starting from resin composite towards the sound dentine. The inclusion criteria for any scan to be included in the data analysis were to demonstrate the former component mainly at the beginning and the latter component at the end of the average line profile. Any scan failed to show any of these contents was excluded.

To determine the location of the hybrid layer, microphotography of the scanned area was used (Figure 5-3a). Firstly, the pixels parallel to the hybrid layer were averaged starting from the resin composite towards the sound dentine using ImageJ software (Wayne Rasband, NIH, USA) (Figure 5-3b). Then, the profile of the microphotograph was plotted using the same software (Figure 5-3c and Figure 5-4a).

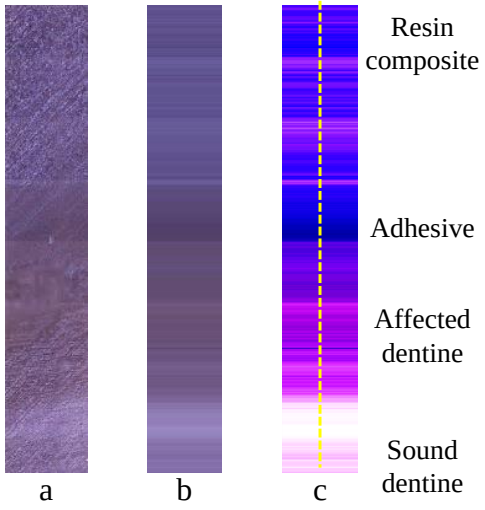

Figure 5-3 (a) Microphotograph of one scan containing resin composite, adhesive, caries-affected dentine and sound dentine. (b) The same scan with averaged pixels parallel to the hybrid layer. (c) An enhanced image for the averaged pixels to highlight the differences between the layers. The yellow dotted line represents where the intensity profile of the image was obtained.

Using the fact that the adhesive layer is not reflective and therefore has a low intensity profile, the hybrid layer was defined as the area adjacent to the adhesive layer. It was characterized by the sudden increase in the image intensity profile (histology) (Figure 5-4b). The image profile (histology) and the hybrid layer location were superimposed on the clusters' line profiles at the exact location (Figure 5-4c). The average cluster content within this area was calculated for all groups.

Two-way ANOVA and Tukey's post-hoc test were used to compare the differences in the relative contribution of each cluster between the three groups at the three different times.

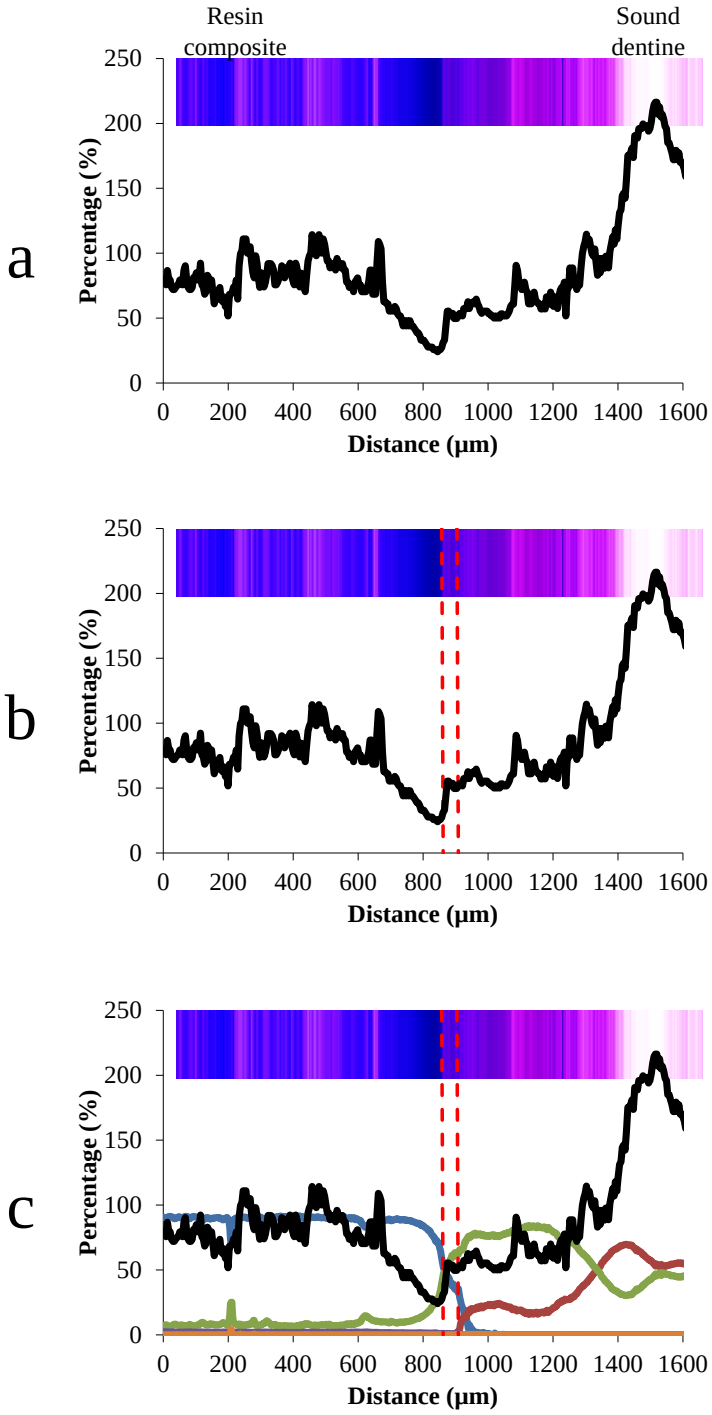

Figure 5-4 (a) Line profile of the microphotographic image (histology) in Figure 5-3. (b) Localization of the hybrid layer (between the two red dotted lines) on the histology profile. (c) The superimposition of the histology profile and the hybrid layer on the line profiles of all clusters.

5.3 Results

5.3.1 In-situ zymography

Using the dental adhesive without MMP inhibitor (group C) resulted in the breakdown of the FITC-conjugated collagen in all areas after 24 hours (Figure 5-5). For the B and D groups, only 6.7% and 20% of the areas expressed FITC fluorescence signal respectively. After two-week storage, only 53.3% of the control group areas showed FITC signal. Groups containing the MMP inhibitor had no FITC signal within the hybrid layer after aging. Examples of the examined area for the three groups are shown in Figure 5-6.

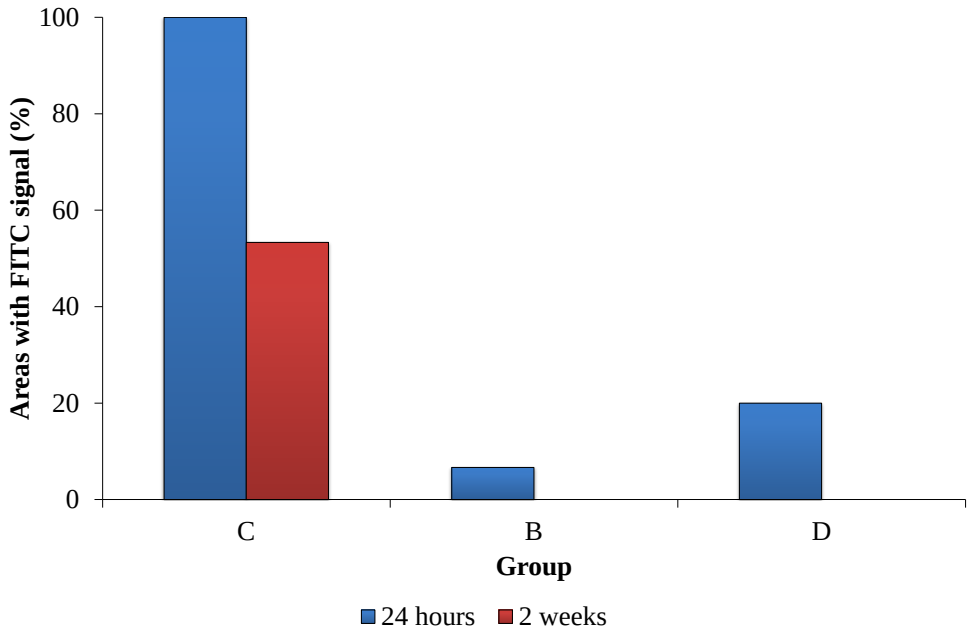

Figure 5-5 The percentage of areas that had FITC signal within the hybrid layer. All areas in the negative control (C) group expressed a FITC signal immediately as a result of FITC-conjugated collagen quenching by MMPs. However, approximately half of these areas continued to express the FITC signal after 2-week storage. Both groups with MMP inhibitor (B and D) had minimal MMP activity initially as fewer area expressed FITC signal. After 2-week aging, no FITC signal was detected in these two groups.

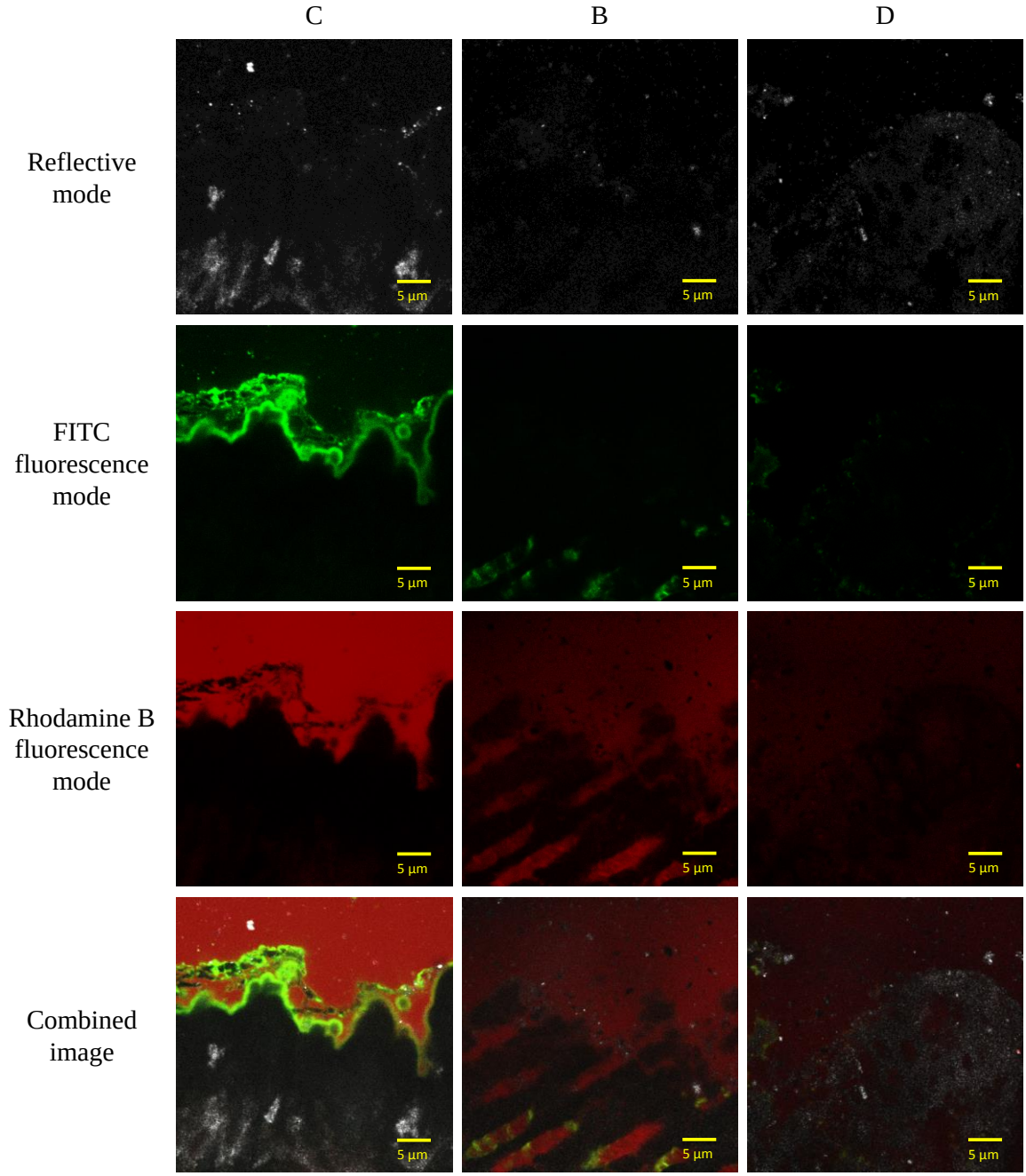

Figure 5-6 Example CLSM scans (100 / 1.40 NA oil immersion objective) for the in-situ zymography of the caries-affected dentine-adhesive interface. The scans of the three groups (C, B and D) were obtained from the same tooth and they were scanned immediately (after 24 hours). FITC fluorescence signal was expressed in the control group (C) but not in both groups with MMP inhibitor (B and D). The presence of such signal designates MMP activity that quenched the FITC-conjugated collagen. FITC fluorescence mode was obtained by illuminating the samples with a 488 nm laser and the emission recorded through a 520-540 nm bandpass filter. Rhodamine B fluorescence mode was acquired by exciting the samples with a 568 nm laser and a 600-630 nm filter was used for the fluorescence emission. The combined images represent the superimposition of the reflective and both fluorescence modes.

5.3.2 Caries-affected dentin-adhesive interface characterization

The cluster analysis of the 90 sample scans resulted in two Raman clusters and four fluorescence clusters defined (Figure 5-7). Resin Raman cluster had characteristic peaks at 1115, 1190 and 1450 cm^{-1} (Figure 5-7a). The phosphate peak at 960 cm^{-1} and the amide I peak at 1450 cm^{-1} defined the sound dentine Raman cluster (Figure 5-7b). The four fluorescence clusters were porphyrin fluorescence (Figure 5-7c), resin fluorescence (Figure 5-7d), and two bacterial growth fluorescence clusters (Figure 5-7e and f). The latter three clusters appeared over time (time 2 and 3) but not in the immediate analysis (time 1).

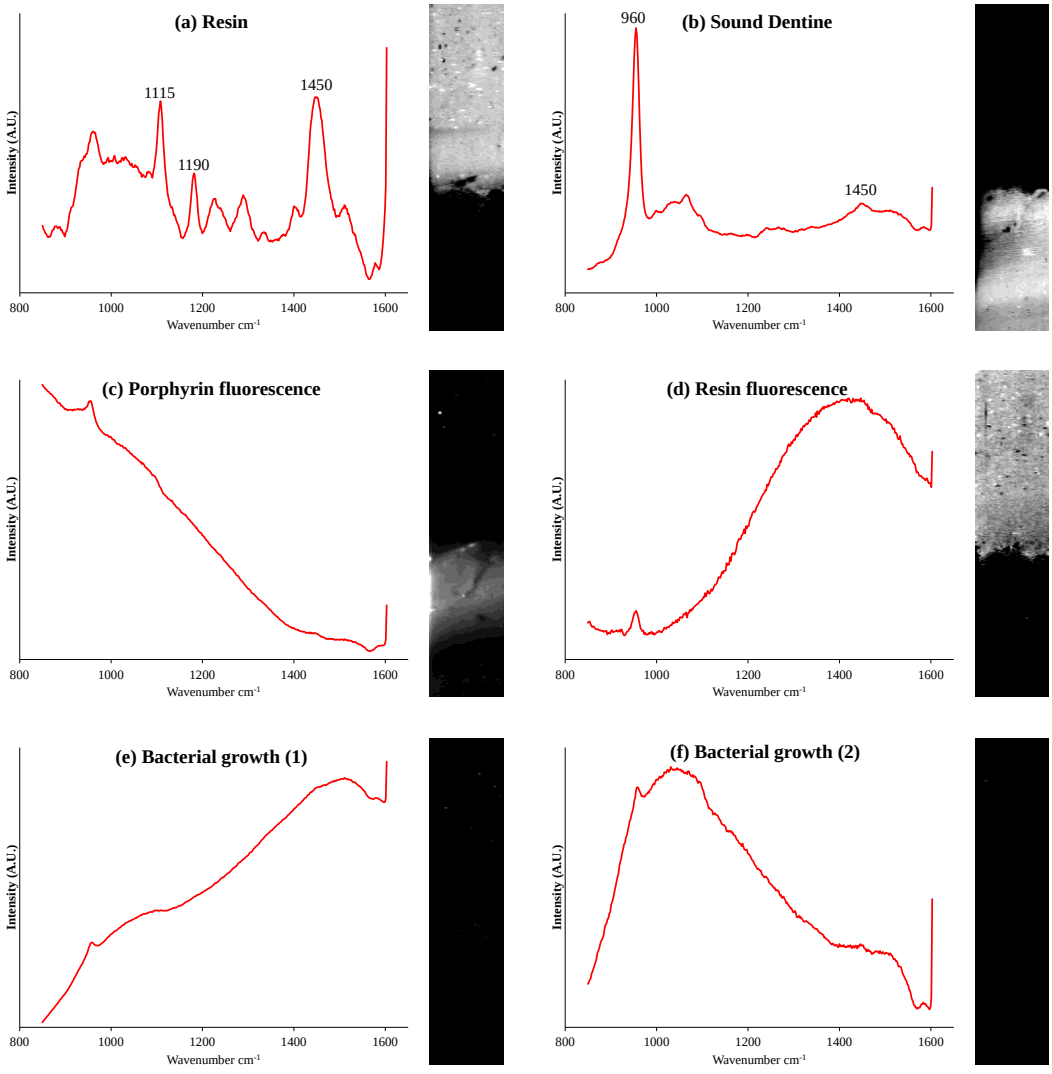

Figure 5-7 The Raman spectra of the six clusters obtained from the analysis of the 90 scans. An example for the locations where each cluster was highly present is also shown on the spectrum side. (a) the resin Raman cluster with its characteristic peaks at 1115, 1190 and 1450 cm^{-1}; (b) sound dentine Raman cluster with phosphate peak at 960 cm^{-1} and the amide peak at 1450 cm^{-1} (c) porphyrin fluorescence cluster; (d) resin fluorescence cluster; (e) and (f) are two independent bacterial growth fluorescence clusters.

The line profile of all clusters' relative contribution was plotted along with intensity profile of the microphotograph (histology) of all scans. Examples of these profiles for each experimental group scanned immediately, after 2 weeks and after 4 weeks of aging are shown in Figure 5-8, Figure 5-9 and Figure 5-10 respectively. Only 61 scans fulfilled the inclusion criteria. The number of scans that are included in each experimental group at different time intervals are summarised in Table 5-1. Examples for the line profile of included and excluded scans are shown in Figure 5-11.

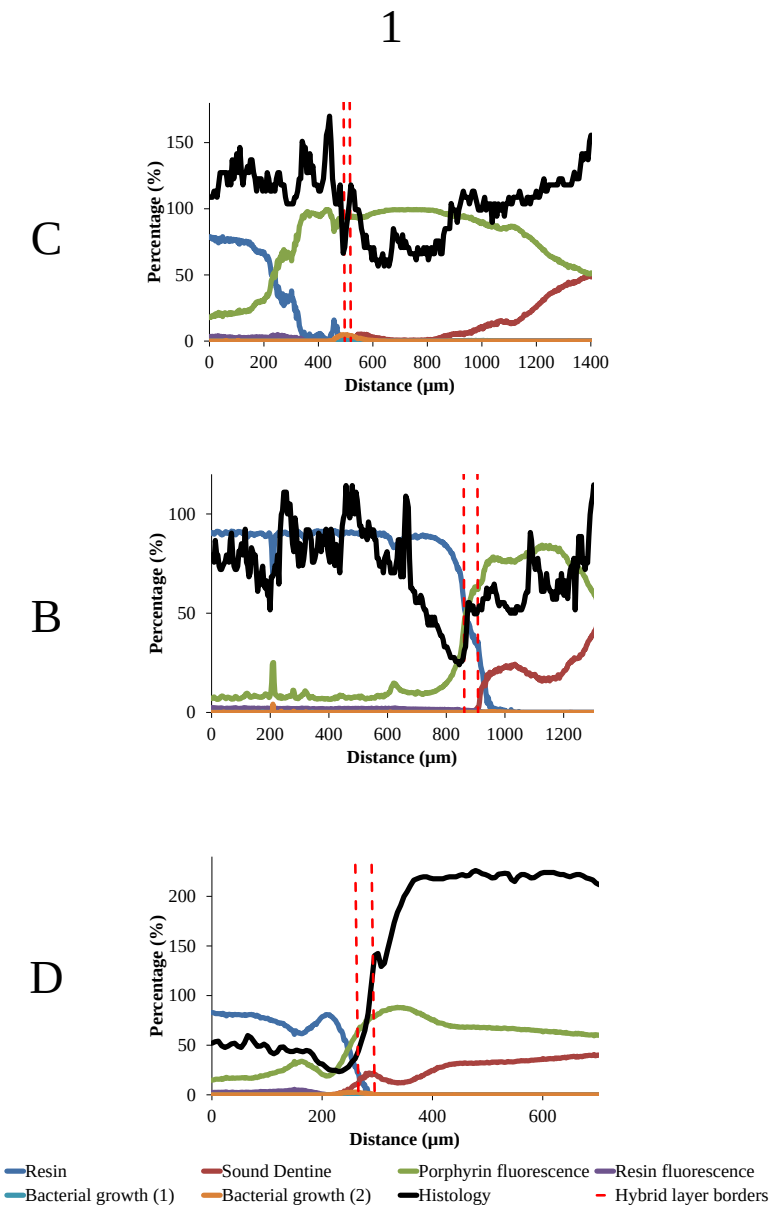

Figure 5-8 Examples of the line profile for the three experimental groups C, B and D scanned immediately (time 1). The intensity image profile of the scanned area (histology) was also included in the graph to determine the position of the hybrid layer (red dotted line). The relative contribution of all clusters within this layer was calculated for each group. The percentage of resin cluster was increased in B and D groups in comparison to C group.

2

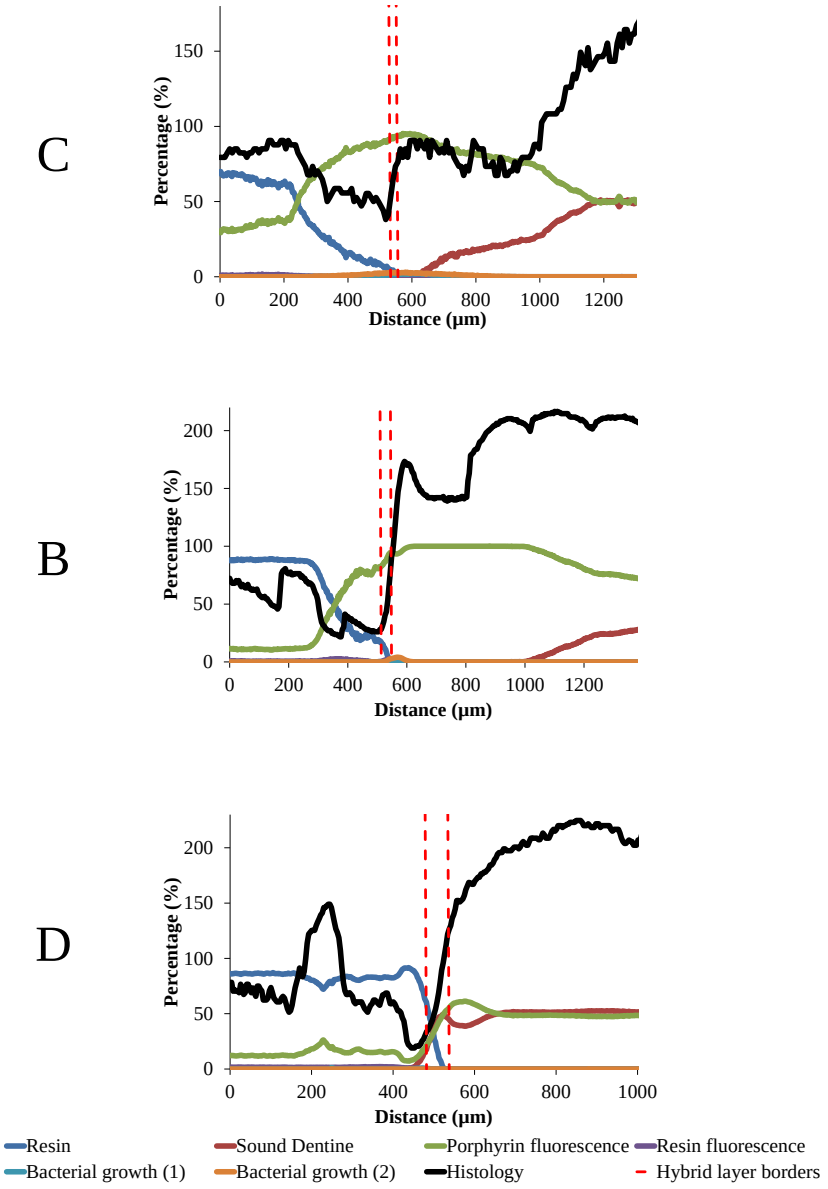

Figure 5-9 Examples of the line profile for the three experimental groups C, B and D scanned after 2 weeks of aging (time 2). The intensity image profile of the scanned area (histology) was also included in the graph to determine the position of the hybrid layer (red dotted line).

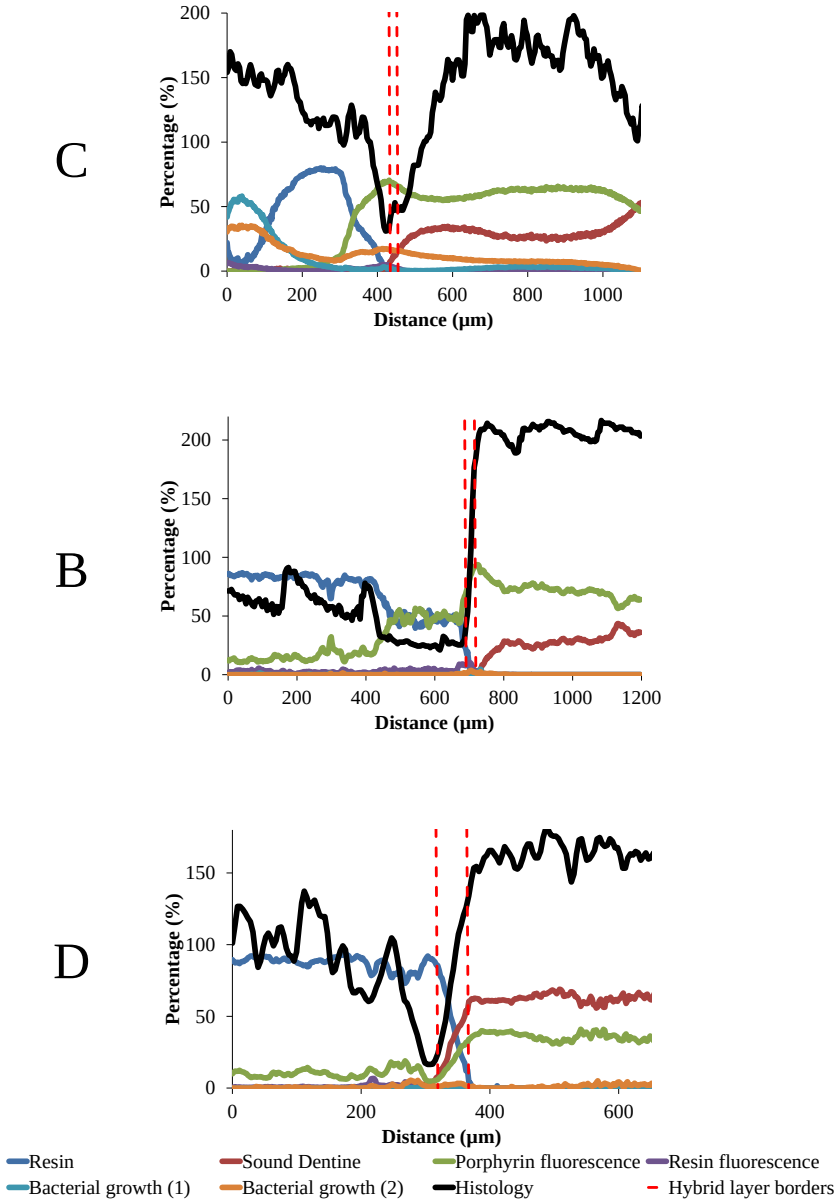

Figure 5-10 Examples of the line profile for the three experimental groups C, B and D scanned after 4 weeks of aging (time 3). The intensity image profile of the scanned area (histology) was also included in the graph to determine the position of the hybrid layer (red dotted line).

Table 5-1 The number of scans included in each group after excluding the scans that did not fit the inclusion criteria.

Group	**Time**		
	1	**2**	**3**
C	7	10	5
B	8	6	6
D	5	7	7

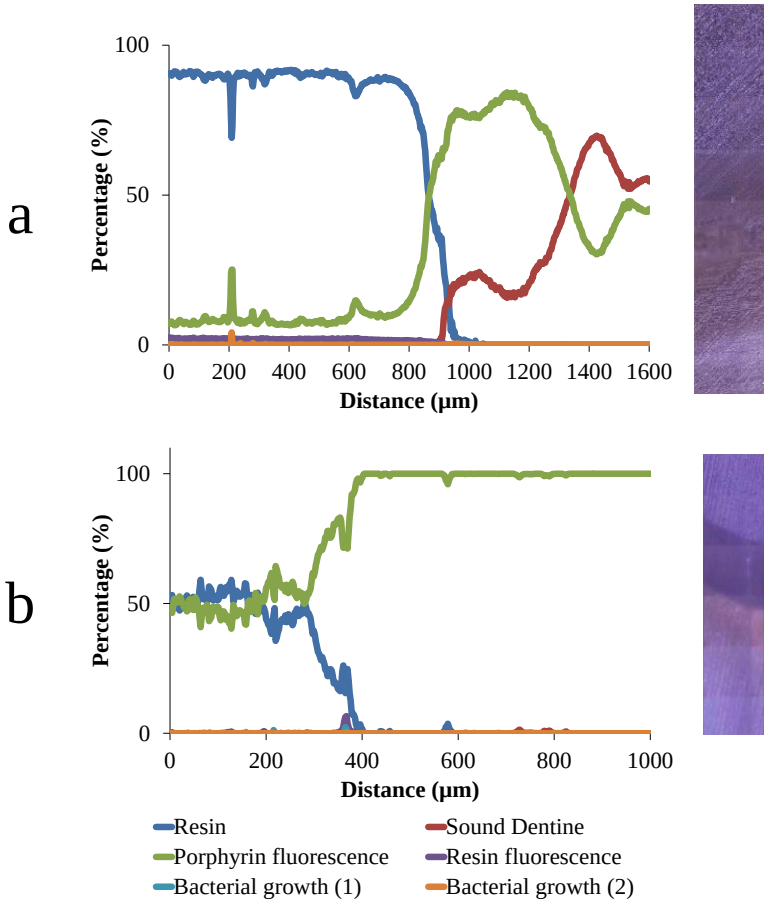

Figure 5-11 The profiles of one of the included and one of the excluded scans with their microphotographic appearance; (a) the included scans profile started with approximately 90% resin cluster in the resin composite area and then dropped as the scan move towards the sound dentine tissue. The sound dentine cluster (the other control) started near the caries-affected dentine-adhesive interface and then kept increasing till the end of the scanned area. (b) One of the excluded scans that shows around 50% resin at the resin composite area and no sound dentine cluster was detected.

Within the hybrid layer, no statistically significant differences were detected between the resin cluster content of the control groups immediately (mean ± SEM) (1.6% ± 0.4) (Figure 5-12 C1), after two weeks (1.5% ± 0.4) (p = 0.98) (Figure 5-12 C2) or after four-week aging (1.4% ± 0.4) (p = 0.97) (Figure 5-12 C3). However, the positive control group (B) had a significantly greater resin cluster immediately (32.9% ± 5.1) (Figure 5-12 B1) when compared to both aging intervals (17.4% ± 3.7 (p = 0.001) and 16.7% ± 4.3 (p = 0.003) respectively) (Figure 5-12 B2 and B3). The same was observed with the experimental group (D) which had 32.8% ± 3.9 resin cluster immediately (Figure 5-12 D1), 23.9% ± 3.9 after 2 weeks (Figure 5-12 D2) and 20.8% ± 2.7 after 4 weeks

(Figure 5-12 D3). Groups with BB94 (B and D) had significantly ($p < 0.001$) more resin cluster content within the hybrid layer than the control (C) (Figure 5-12) with no significant difference between the D and B groups ($p = 0.30$).

The sound dentine cluster contents were not different significantly ($p = 0.34$) between all groups at all-time intervals.

The control group had significantly ($p < 0.01$) more porphyrin fluorescence immediately (93% ± 1.6) (Figure 5-12 C1) when compared to B (62.3% ± 7.2) (Figure 5-12 B1) and D (61.9% ± 1.4) (Figure 5-12 D1) groups.

Resin fluorescence and bacterial growth (1) clusters were minimal and no significant differences ($p = 0.99$ and $p = 0.24$ respectively) were detected across all groups (Figure 5-12). However, the bacterial growth (2) cluster had increased significantly in the control group ($p < 0.001$) after four-week aging and reached 10% ± 1.7 (Figure 5-12 C3).

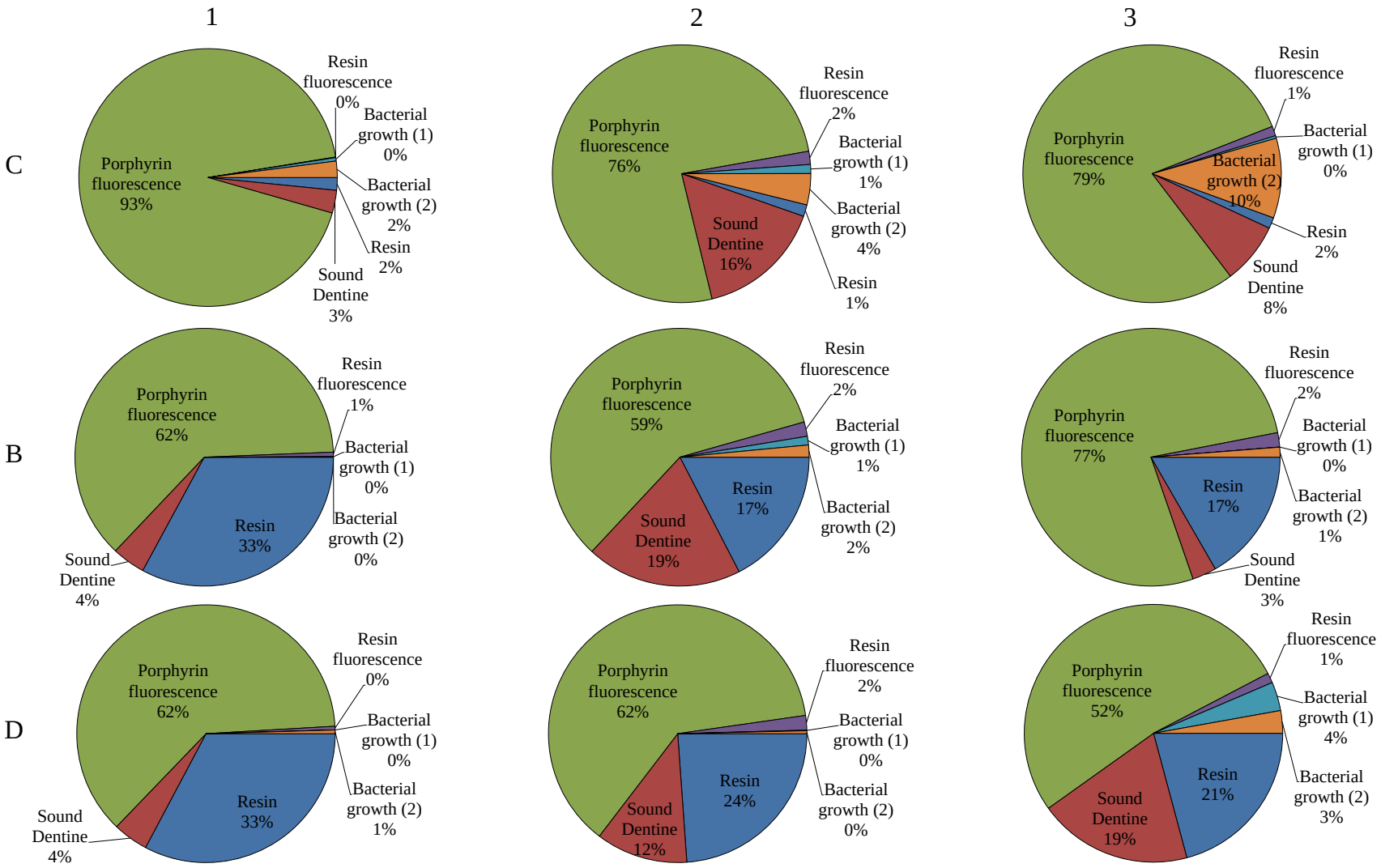
1
2
3
C
B
D
Porphyrin fluorescence 93%
Resin fluorescence 0%
Bacterial growth (1) 0%
Bacterial growth (2) 2%
Resin 2%
Sound Dentine 3%
Porphyrin fluorescence 76%
Resin fluorescence 2%
Bacterial growth (1) 1%
Bacterial growth (2) 4%
Resin 1%
Sound Dentine 16%
Porphyrin fluorescence 79%
Resin fluorescence 1%
Bacterial growth (1) 0%
Bacterial growth (2) 10%
Resin 2%
Sound Dentine 8%
Porphyrin fluorescence 62%
Resin fluorescence 1%
Bacterial growth (1) 0%
Bacterial growth (2) 0%
Resin 33%
Sound Dentine 4%
Porphyrin fluorescence 59%
Resin fluorescence 2%
Bacterial growth (1) 1%
Bacterial growth (2) 2%
Resin 17%
Sound Dentine 19%
Porphyrin fluorescence 77%
Resin fluorescence 2%
Bacterial growth (1) 0%
Bacterial growth (2) 1%
Resin 17%
Sound Dentine 3%
Porphyrin fluorescence 62%
Resin fluorescence 0%
Bacterial growth (1) 0%
Bacterial growth (2) 1%
Resin 33%
Sound Dentine 4%
Porphyrin fluorescence 62%
Resin fluorescence 2%
Bacterial growth (1) 0%
Bacterial growth (2) 0%
Resin 24%
Sound Dentine 12%
Porphyrin fluorescence 52%
Resin fluorescence 1%
Bacterial growth (1) 4%
Bacterial growth (2) 3%
Resin 21%
Sound Dentine 19%

Figure 5-12 The mean cluster content of the hybrid layer formed by each experimental group at different time intervals (1, 2 and 3). Using BB94 as a primer (B) or incorporating it with the dental adhesive's primer (D) resulted in a significant increase in the resin content within the hybrid layer when compared to the control group (C).

5.4 Discussion

The null hypotheses were rejected as the addition of MMP inhibitor (BB94) to the three-step etch and rinse adhesive system (OB) resulted in an inhibition of MMP activity within the caries-affected dentine. It also modified the chemical content of the caries-affected dentine-adhesive interface.

In the current study, caries-infected dentine was excavated chemo-mechanically using the Carisolv® system. The technique was preferred over the conventional rotary method as it has been shown to excavate more selectively the unrepairable collagen fibrils in the caries-infected dentine, whilst leaving the repairable tissue. The chemical agent in the Carisolv® system is composed of two solutions that are mixed prior to application in a methylcellulose gel preparation (Sakoolnamarka et al., 2005; Lozano-Chourio et al., 2006). Sodium hypochlorite (NaOCl), at a concentration of 0.5%, is used in the first solution. The second solution contains three amino acids (leucine, lysine, glutamic acid), sodium hydroxide (NaOH) and sodium chloride (NaCl) in purified water (Beeley et al., 2000; Morrow et al., 2000). During mixing of the two solutions, the amino acids bind chlorine and form chloramines (pH 11), which reduce the aggressiveness of sodium hypochlorite on the healthy collagen (Hannig, 1999; Tonami et al., 2003). Furthermore, these chloramines react with the unprotected collagen fibrils of the caries-infected dentine and convert the hydroxyproline into pyrrole-2-carboxylic acid, which is known as the "chlorinating" effect (Kronman et al., 1977). This acid induces the destruction of the denaturalized collagen fibres (Ericson et al., 1999). The specially designed instruments used with Carisolv® gel, enhance the selective mechanical removal of the caries-infected tissue through its sharp edges and blunt cutting angles (Banerjee et al., 2000b; Morrow et al., 2000). Compared to bur excavation and sonic abrasion, the chemo-mechanical excavation of dental caries using Carisolv® gel was found to be very effected in removing the carious lesion in relation to its autofluorescence signature *in vitro* (Banerjee et al., 2000b) and *in vivo* (Ericson et al., 1999). The Knoop microhardness of the remaining tissue was similar when both hand and chemo-mechanical caries excavation techniques were used (Fluckiger et al., 2005).

In-situ zymography was used to detect the ability of the modified adhesive to inhibit MMPs within caries-affected dentine. The technique was chosen because it provides the localization of MMP activity within the tissue without the need for their extraction (Snoek-Van Beurden and Von Den Hoff, 2005; Kupai et al., 2010). The MMP activity was represented by the breakdown of the FITC-conjugated collagen and the emission of FITC signal.

Previously, in-situ zymography was performed by the application of the FITC-conjugated collagen on the surface of the already bonded resin composite-dentine slabs (Porto et al., 2009; Mazzoni et al., 2012). In the present study, the FITC-conjugated collagen was applied directly on the etched dentine prior to the application of MMP inhibitor and the bonding agent. Such a procedure brought the MMPs substrate close to the proteases within the caries-affected dentine, after their activation, immediately without bonding interference. In addition, it allowed better evaluation of MMP activity in deeper structures, by the use of confocal microscopy, rather than purely examining the surface, which could be affected by the environment.

Labelling of OB primer with Rhodamine B allowed better characterization of the interfacial morphology especially in areas where FITC signal could not be detected (Figure 5-6). The technique of double labelling was possible through the application of the FITC-conjugated collagen on the etched dentine rather than the surface of the already bonded samples.

Generally, the resulting data showed that the use of OB adhesive with BB94 resulted in MMP inhibition. Although B group samples had fewer areas with FITC signal in comparison to the D group, quantification of the fluorescence signal detected using this technique is limited and considered as one of its limitations (Mungall and Pollitt, 2001; Yan and Blomme, 2003). The two-week aged samples showed a decrease in the FITC signal for the control group. This could be explained by the fade/quenching of the fluorophore rather than the reduction in MMP activity per se, which is another limitation for the in-situ zymography (Kupai et al., 2010).

The main chemical constituents of the bonded resin composite-affected dentine slabs were grouped into six different clusters (Figure 5-7). As reported in Chapter 4, these clusters were identified based on the characteristic Raman peaks and on the histological location where each cluster was most represented. In addition, the time when each cluster appeared was also considered in the identification.

The resin Raman cluster had characteristic peaks at 1115, 1190 and 1450 cm^{-1} (Figure 5-7a) which represent the phenyl (C-O-C), gem-dimethyl (CH_3-C-CH_3) and CH_2, CH_3 deformation (C=C) respectively (Spencer et al., 2000; Wang and Spencer, 2003). Previous studies had assigned the 1190 cm^{-1} peak for the hydrophobic part (bis-GMA) and the 1450 cm^{-1} peak to both the hydrophobic and hydrophilic (HEMA) monomers (Wang and Spencer, 2003; Wang et al., 2007; Shin et al., 2009; Zou et al., 2010). In these studies, the ratio between the intensity of each assigned peak to the intensity of the reference amide I (collagen) peak at 1666 cm^{-1} was used to determine the infiltration of each component into the demineralised substrate. The use of such a technique is relevant when the collagen peak is constant across the interface, as found in the demineralised sound dentine. However, the use of collagen structure as a reference to detect the adhesive chemical changes within the caries-affected dentine is more challenging as the collagen varies across the interface and irregular composition resulted (Wang et al., 2007).

In the current study, the resin Raman cluster, containing the 1190 cm^{-1} peak, was maximally represented in the resin composite area in both the histological appearance and in the cluster line profile. Generally, the hydrophilic part of the dental adhesive could not be detected separately as it shares its peaks with the hydrophobic monomer and/or the dentine substrate. Detection of the cross-linked polymers within the hybrid layer is more important than the functional monomers as they provide the mechanical strength for bonding agents (Section 1.4.3).

The sound dentine cluster represented a combination of the mineral and protein content clusters found in Chapter 4. Labelling of this cluster was different from the two clusters as it contains both the phosphate ($\nu 1$ PO_4^{3-}) and the amide peaks at 960 and 1450 cm^{-1} respectively (Figure 5-7b). The sound dentine cluster tended to increase towards the histological sound dentine tissue away from the hybrid layer.

The porphyrin fluorescence cluster (Figure 5-7c) was the same as the one reported in Chapter 4. A resin fluorescence cluster (Figure 5-7d) appeared mainly within the resin composite area while the bacterial growth (1) fluorescence (Figure 5-7e) and bacterial growth (2) fluorescence (Figure 5-7f) clusters had no characteristic histological location. Additionally, these three fluorescence clusters had no characteristic peak and they appeared only after aging. Detecting such content is essential to rule out the effect of bacterial growth on the dentine samples as a result of their storage. The other

fluorescence clusters reported in Chapter 4, IDS and ADS, were not detected in this study. This is explained by the chemo-mechanical removal of the tissues that they represent, as the agents are capable of removing the broken down collagen fibrils. In addition, the hybridization between the resin and the caries-affected dentine could change or mask these fluorescence signals.

The choice of the scanned area to be perpendicular to the hybrid layer allowed plotting of the line profile for each cluster and then plotting of their relative contributions. However, this was not possible in all scans as the caries-affected dentine was irregular and different even within the same carious lesion. The resin and sound dentine clusters were considered as controls that should be present in all scans and they should not change in all groups. Scans that had one of these clusters absent, as a result of tissue irregularity or technical problems within the scanner (Figure 5-11b), were excluded. However, at least 5 different scanned areas were included in the analysis for each group at different times (Table 5-1).

The localization of the hybrid layer was based on the histological appearance of its start and its penetration depth. Different attempts had been made to locate the layer objectively on the line profile plotting. However, due to variances in the resin penetration within the caries-affected dentine, the hybrid layer localization was not apparent. The hybrid layer is described as the interaction zone between the dental adhesive and the dentine structure that is noticed microscopically on histological samples (Nakabayashi et al., 1982) (Section 1.4.1). Thus, microphotographs were used to localise it. The hybrid layers in all scans included in the data analysis, comprised a mixture of the resin Raman cluster and sound dentine cluster (Figure 5-8, Figure 5-9 and Figure 5-10) which is comparable to the results of previous micro-Raman studies (Wang and Spencer, 2003; Wang et al., 2007; Shin et al., 2009).

The use of BB94 as a primer prior to dental adhesive application or incorporating it within the adhesive system resulted in the existence of a more hydrophobic resin within the hybrid layer. This could be explained by the preservation of the unprotected collagen matrix as a consequence of blocking the caries-affected dentine MMP activity. Thus, more collagen substrate is penetrated by dental adhesive. As indirect evidence, the porphyrin fluorescence cluster content, which is found within the caries-affected dentine tissue, was reduced overtime when the MMP inhibitor was excluded. This finding suggests the partial loss of the caries-affected dentine. In addition, such tissue loss allowed more bacteria to grow in the hybrid layer of the control group aged for four

weeks. Using the MMP inhibitor resulted in the preservation of the caries-affected dentine tissue as neither the porphyrin fluorescence cluster or the bacterial growth (2) cluster contents changed overtime.

As discussed in Sections 1.3.4.2 and 3.4, a competitive mechanism of action was found between the BB94 and the MMP active-site zinc ion. As a result, most of the MMPs found in the caries-affected dentine were inhibited immediately. This was shown clearly by the in-situ zymography. Such a competitive mechanism brings the adhesive primer closely to the collagen matrix and enhances the dental adhesive wettability, which could be another explanation of the presence of more resin within the hybrid layer.

In conclusion, bonding the modified adhesive to caries-affected dentine resulted in the inhibition of MMP activity together with the presence of more hydrophobic adhesive component, within the hybrid layer, which was kept over time.

Chapter 6 General summary

The overall aim of this study was to test the effect of adding MMP inhibitors to contemporary dental adhesive systems on both sound and caries-affected dentine. It was thought that such an addition could interfere with the inhibitor's ability to block MMP activity as they were diluted to a 5 μM concentration. Furthermore, the MMP inhibitor addition could have made the physical properties of the resulting modified adhesives inferior to contemporary adhesives as a result of phase separation of the chemical components.

Prior to testing the modified adhesives on dentine MMPs, their ability to inhibit recombinant MMP-1 and MMP-2, at the chosen concentration, was tested *in vitro*. The two recombinant MMPs represented the collagenase and gelatinase groups respectively, which are the major MMPs groups found within dentine (Table 1-6). Substrate zymography was used to detect the inhibitory effect of modified adhesives on MMPs found within pulverised sound dentine tissue. For the effect on the MMPs situated within the caries-affected dentine, in-situ zymography was chosen. The technique provided the localization of MMP activity at the caries-affected dentine-adhesive interface without the need of excising the tissue. Similar MMP groups were found in the sound and caries-affected dentine structures. However, MMPs originating either from gingival crevicular fluid (GCF) or salivary gland secretions (Section 1.3.3.1) were also present within the carious dentine as a result of its exposure to the oral environment. Hence, the distribution of MMPs within caries-affected dentine was expected to be inconsistent when compared to sound dentine.

The modified adhesives exhibited high initial MMP inhibition regardless of the tissue type that contained them or their origin. This is important clinically as the preservation of the demineralised dentine collagen matrix allows better micro- and nano-mechanical interlocking between the dentine and the bonding agent. In addition, the presence of a dense collagen matrix enhances the adhesive wettability and reduces the amount of free uncured monomer. Thus, adequate sealing of cavity margins may be achieved and the longevity of the adhesive restoration enhanced.

To assess the physical properties of the modified adhesives, the widely acceptable micro-tensile bond strength testing was used initially and after aging for samples bonded to sound dentine. Bonding to caries-affected dentine revealed a reduction in the micro-

tensile bond strength of contemporary adhesives due to the substrate tissues' structural changes. The variability of the caries-affected dentine histology could interfere with the bond strength results, as more pre-test failures were expected, and proper strength assessment for the modified adhesive bonded to such structures could not be achieved.

Micro-Raman spectroscopy was used as an alternative technique to assess the caries-affected dentine adhesive interface. However, the use of this technique on carious tissue has not been widely demonstrated before. Thus verification of the technique on carious dentine was undertaken before using it for the chemical evaluation of the caries-affected dentine adhesive interface. Results revealed that micro-Raman spectroscopy provided an objective delineation of caries-infected, caries-affected and sound dentine. It also correlated with the microhardness and the autofluorescence of these tissues. Although the technique had been used widely *in vitro*, only a few studies had reported the possibility of using Raman spectroscopy technology clinically, in particular to aid in cancer diagnosis. Haka et al. (2006) had demonstrated that an optical fibre probe attached to a Raman spectroscope had the ability to analyse the margins of malignant lesions during partial mastectomy breast surgery with an overall accuracy of 93% when compared to pathological diagnosis. The development of such technology for clinical use in dentistry might be possible in the future for the objective detection and diagnosis of dental caries as shown by the current in-vitro study.

Although micro-Raman spectroscopy techniques had been used previously to assess the sound dentine-adhesive interface, proper interpretation of the data has not been reported. Detecting the changes within a specific chemical component rather than assessing the whole tissue chemical contents have been used to obtain limited results. Therefore, in this study, a faster data acquiring technique together with cluster analysis methods were used to define the chemical components of the caries-affected dentine adhesive interface.

The modified adhesives had an initial increase in the micro-tensile bond strength with a reduced micro-permeability. In addition, more hydrophobic resin was found within the caries-affected dentine hybrid layer using micro-Raman spectroscopy. This means that the use of MMP inhibitors appeared to enhance the monomer conversion, within the dentine-adhesive interface, reduced the water sorption and prevented the leaching of uncured monomer. Such properties enhance the clinical performance of adhesive systems as suggested by clinical data (Peumans et al., 2007; Van Meerbeek et al., 2010).

The micro-tensile bond strength results for the 3-month aged samples suggested that the effect of MMP inhibitors reduced with time. However, the chemical content of the caries-affected dentine hybrid layer was maintained after one month. This could be explained by the relatively larger exposed surface area of the micro-tensile samples compared to the micro-Raman samples allowing more content diffusion into the storage medium. In addition, the aging time for the two sets of samples was different as the former were aged for three months while the latter were aged for one month. In general, micro-tensile bond strength sample preparation subjected the dentine-adhesive interface to more stress, which made it deteriorate faster during aging (Armstrong et al., 2010).

As discussed in Sections 3.4 and 5.4, the enhanced properties of the dental adhesives could have resulted from (1) the preservation of the delicate collagen matrix, (2) the enzymatic chemical bond between MMPs and their inhibitors or (3) due to a combination of both mechanisms, suggesting an auxiliary bonding mechanism for these adhesives. The MMP inhibitors used in this study were dissolved in methanol as a 500 µM stock. The addition of more solvent to the dental adhesive could enhance its wettability and the resultant bond strength. However, such an effect was diminished as only 1% of the stock was incorporated within the dental adhesive systems. In addition, not all modified adhesive systems had enhanced micro-tensile bond strength initially.

In conclusion, the addition of MMP inhibitors to contemporary dental adhesive systems resulted in modified adhesives that had an enhanced dentine-adhesive interface with inhibited MMP activity. These results were maintained when the modified adhesives were bonded to both sound and caries-affected dentine.

Chapter 7 Suggestions for future work

Future work must involve:

1. Understanding the mechanisms by which the MMP inhibitors, within the dental adhesives, improved the adhesive-dentine interface. This could be achieved by assessing the hypothesised mechanisms as follows:
    a. Evaluation of the quality of the exposed collagen matrix following its exposure to adhesives with and without the inhibitors. Advanced imaging techniques, such as multi-photon microscopy and second harmonic generation detection, could be considered for this evaluation.
    b. Assessment of the interaction between the MMPs and their inhibitors within the dentine-adhesive interface using histochemical staining.
2. Incorporating other advanced MMP inhibitors with dental adhesives and examining their effect on the adhesive-dentine interface.
3. The identification of the specific MMPs that are involved in the caries process and the designing of synthetic specific inhibitors capable of blocking their action.
4. Developing the micro-Raman spectroscopy technique to make it useful for clinical caries assessment.

Appendix

List of publications in international peer-reviewed journals:

- Almahdy, A., Downey, F. C., Sauro, S., Cook, R. J., Sherriff, M., Richards, D., Watson, T. F., Banerjee, A. & Festy, F. (2012). Microbiochemical analysis of carious dentine using raman and fluorescence spectroscopy. Caries Res, 46, 432-40.

- Almahdy, A., Koller, G., Sauro, S., Bartsch, J. W., Sherriff, M., Watson, T. F. & Banerjee, A. (2012). Effects of MMP inhibitors incorporated within dental adhesives. J Dent Res, 91, 605-11.

List of abstracts submitted to national and international conferences

- Chemical Analysis of Carious Teeth Using Raman Spectroscopy (Poster Presentation), Biophotonics Meeting, KCL, London, UK, 8th June 2010.

- Chemical analysis of carious dentinal tissue using micro-Raman spectroscopy (Poster Presentation), IADR 89th general session, San Diego, California, USA 16th -19th March 2011.

- Raman Analysis meeting, (Oral presentation), KCL, London, UK, 30th March 2011.

- Chemical analysis of carious dentinal tissue using micro-Raman (Oral presentation), KCL, London, UK, 1st April 2011.

- Chemical analysis of carious dentinal tissue using micro-Raman spectroscopy (Oral presentation), The Annual Dental Institute Postgraduate Research Day, KCL, London, UK, 13th April 2011.

- In-vitro characterization of the physico/chemo-mechanical properties of novel resin-based adhesives and tooth tissue (Oral presentation), KCL, London, UK, 3rd June 2011.

- The Effect of MMP Inhibitors on Dental Adhesive Systems (Oral presentation) KCL, London, UK, 9th September 2011.

- The Effect of MMP Inhibitors on Dental Adhesive Systems (Oral presentation), BSODR 2011, Sheffield, UK, 12th -15th September 2011.

- Micro-Raman spectroscopy analysis of carious dentine (Poster Presentation), Frontiers in BioImaging, Manchester, UK 20th -21st September 2011.

- Micro-Raman spectroscopy analysis of carious dentine (Poster Presentation), ConsEuro Meeting, Istanbul, Turkey 13th-15th October 2011.

- The effect of MMP inhibitors incorporated within dental adhesives (Oral presentation), The Annual Dental Institute Postgraduate Research Day, KCL, London, UK, 3rd April 2012.

- Biochemical analysis of carious dentine using Raman spectroscopy (Oral presentation), IADR/PER Congress 2012, Helsinki, Finland 12th -15th September 2012.

Scientific awards:

- Best Poster for the "Operative Dentistry" category in ConsEuro Meeting, Istanbul, Turkey 13th-15th October 2011.

- Excellency award from the Royal embassy of Saudi Arabia, 31st March 2013.

References

Aboushelib, M. N., Matinlinna, J. P., Salameh, Z. & Ounsi, H. 2008. Innovations in bonding to zirconia-based materials: Part I. *Dent Mater,* 24**,** 1268-72.

Al-Ahmad, A., Wunder, A., Auschill, T. M., Follo, M., Braun, G., Hellwig, E. & Arweiler, N. B. 2007. The in vivo dynamics of Streptococcus spp., Actinomyces naeslundii, Fusobacterium nucleatum and Veillonella spp. in dental plaque biofilm as analysed by five-colour multiplex fluorescence in situ hybridization. *Journal of Medical Microbiology,* 56**,** 681-687.

Al-Khateeb, S., Forsberg, C. M., De Josselin De Jong, E. & Angmar-Mansson, B. 1998. A longitudinal laser fluorescence study of white spot lesions in orthodontic patients. *American Journal of Orthodontics and Dentofacial Orthopedics,* 113**,** 595-602.

Alleman, D. S. & Magne, P. 2012. A systematic approach to deep caries removal end points: the peripheral seal concept in adhesive dentistry. *Quintessence Int,* 43**,** 197-208.

Amaral, F. L., Colucci, V., Palma-Dibb, R. G. & Corona, S. A. 2007. Assessment of in vitro methods used to promote adhesive interface degradation: a critical review. *J Esthet Restor Dent,* 19**,** 340-53; discussion 354.

Angker, L., Nockolds, C., Swain, M. V. & Kilpatrick, N. 2004. Correlating the mechanical properties to the mineral content of carious dentine - a comparative study using an ultra-micro indentation system (UMIS) and SEM-BSE signals. *Archives of Oral Biology,* 49**,** 369-378.

Angmar-Mansson, B. & Ten Bosch, J. J. 1987. Optical methods for the detection and quantification of caries. *Adv Dent Res,* 1**,** 14-20.

Ansari, G., Beeley, J. A., Reid, J. S. & Foye, R. H. 1999. Caries detector dyes—an in vitro assessment of some new compounds. *Journal of Oral Rehabilitation,* 26**,** 453-8.

Arends, J. & Christoffersen, J. 1986. The nature of early caries lesions in enamel. *J Dent Res,* 65**,** 2-11.

Armstrong, S., Geraldeli, S., Maia, R., Raposo, L. H. A., Soares, C. J. & Yamagawa, J. 2010. Adhesion to tooth structure: A critical review of "micro" bond strength test methods. *Dental Materials,* 26**,** e50-e62.

Armstrong, S. R., Vargas, M. A., Chung, I., Pashley, D. H., Campbell, J. A., Laffoon, J. E. & Qian, F. 2004. Resin-dentin interfacial ultrastructure and microtensile dentin bond strength after five-year water storage. *Oper Dent,* 29**,** 705-12.

Armstrong, W. G. 1963. Fluorescence Characteristics of Sound and Carious Human Dentine Preparations. *Archives of Oral Biology,* 8**,** 79-90.

Arnold, W. H., Konopka, S., Kriwalsky, M. S. & Gaengler, P. 2003. Morphological analysis and chemical content of natural dentin carious lesion zones. *Ann Anat,* 185**,** 419-24.

Bader, J. D., Shugars, D. A. & Bonito, A. J. 2001. Systematic reviews of selected dental caries diagnostic and management methods. *Journal of Dental Education,* 65**,** 960-8.

Baena, J. R. & Lendl, B. 2004. Raman spectroscopy in chemical bioanalysis. *Current Opinion in Chemical Biology,* 8**,** 534-539.

Bainton, D. F. 1981. The Discovery of Lysosomes. *Journal of Cell Biology,* 91**,** S66-S76.

Baker, A. H., Edwards, D. R. & Murphy, G. 2002. Metalloproteinase inhibitors: biological actions and therapeutic opportunities. *J Cell Sci,* 115**,** 3719-27.

Banerjee, A. & Boyde, A. 1998. Autofluorescence and mineral content of carious dentine: scanning optical and backscattered electron microscopic studies. *Caries Research,* 32**,** 219-26.

Banerjee, A. 1999. *Applications of scanning microscopy in the assessment of dentine caries and methods for its removal.* PhD, University of London.

Banerjee, A., Sherriff, M., Kidd, E. A. & Watson, T. F. 1999. A confocal microscopic study relating the autofluorescence of carious dentine to its microhardness. *Br Dent J,* 187**,** 206-10.

Banerjee, A., Watson, T. F. & Kidd, E. A. 2000a. Dentine caries: take it or leave it? *Dent Update,* 27**,** 272-6.

Banerjee, A., Kidd, E. A. & Watson, T. F. 2000b. In vitro evaluation of five alternative methods of carious dentine excavation. *Caries Res,* 34**,** 144-50.

Banerjee, A., Yasseri, M. & Munson, M. 2002. A method for the detection and quantification of bacteria in human carious dentine using fluorescent in situ hybridisation. *Journal of Dentistry,* 30**,** 359-363.

Banerjee, A., Cook, R., Kellow, S., Shah, K., Festy, F., Sherriff, M. & Watson, T. 2010a. A confocal micro-endoscopic investigation of the relationship between the microhardness of carious dentine and its autofluorescence. *Eur J Oral Sci,* 118**,** 75-9.

Banerjee, A., Kellow, S., Mannocci, F., Cook, R. J. & Watson, T. F. 2010b. An in vitro evaluation of microtensile bond strengths of two adhesive bonding agents to residual dentine after caries removal using three excavation techniques. *Journal of Dentistry,* 38**,** 480-489.

Banerjee, A. & Watson, T. F. 2011. *Pickard's Manual of Operative Dentistry,* Oxford, Oxford University Press.

Bedini, R., Manzon, L., Fratto, G. & Pecci, R. 2010. Microhardness and morphological changes induced by Nd:Yag laser on dental enamel: an in vitro study. *Annali dell Istituto Superiore di Sanita,* 46**,** 168-72.

Beeley, J. A., Yip, H. K. & Stevenson, A. G. 2000. Chemochemical caries removal: a review of the techniques and latest developments. *Br Dent J,* 188**,** 427-30.

Begue-Kirn, C., Krebsbach, P. H., Bartlett, J. D. & Butler, W. T. 1998. Dentin sialoprotein, dentin phosphoprotein, enamelysin and ameloblastin: tooth-specific molecules that are distinctively expressed during murine dental differentiation. *Eur J Oral Sci,* 106**,** 963-70.

Bellahcene, A., Castronovo, V., Ogbureke, K. U., Fisher, L. W. & Fedarko, N. S. 2008. Small integrin-binding ligand N-linked glycoproteins (SIBLINGs): multifunctional proteins in cancer. *Nat Rev Cancer,* 8**,** 212-26.

Benedict, H. C. 1928. A Note on the Fluorescence of Teeth in Ultra-Violet Rays. *Science,* 67**,** 442.

Bernick, S., Warren, O. & Baker, R. F. 1954. Electron microscopy of carious dentin. *J Dent Res,* 33**,** 20-6.

Bildt, M. M., Bloemen, M., Kuijpers-Jagtman, A. M. & Von Den Hoff, J. W. 2009. Matrix metalloproteinase inhibitors reduce collagen gel contraction and alpha-smooth muscle actin expression by periodontal ligament cells. *Journal of Periodontal Research,* 44**,** 266-74.

Birkedal-Hansen, H., Moore, W. G., Bodden, M. K., Windsor, L. J., Birkedal-Hansen, B., Decarlo, A. & Engler, J. A. 1993. Matrix metalloproteinases: a review. *Crit Rev Oral Biol Med,* 4**,** 197-250.

Birkedal-Hansen, H. 1993. Role of matrix metalloproteinases in human periodontal diseases. *J Periodontol,* 64**,** 474-84.

Birkedal-Hansen, H. 1995. Proteolytic remodeling of extracellular matrix. *Current Opinion in Cell Biology,* 7**,** 728-735.

Bjørndal, L. & Thylstrup, A. 1995. A structural analysis of approximal enamel caries lesions and subjacent dentin reactions. *Eur J Oral Sci,* 103**,** 25-31.

Bjørndal, L., Darvann, T. & Lussi, A. 1999. A computerized analysis of the relation between the occlusal enamel caries lesion and the demineralized dentin. *Eur J Oral Sci,* 107**,** 176-82.

Blavier, L., Henriet, P., Imren, S. & Declerck, Y. A. 1999. Tissue inhibitors of matrix metalloproteinases in cancer. *Ann N Y Acad Sci,* 878**,** 108-19.

Borisova, E., Uzunov, T. & Avramov, L. 2006. Laser-induced autofluorescence study of caries model in vitro. *Lasers Med Sci,* 21**,** 34-41.

Boskey, A., Spevak, L., Tan, M., Doty, S. B. & Butler, W. T. 2000. Dentin sialoprotein (DSP) has limited effects on in vitro apatite formation and growth. *Calcif Tissue Int,* 67**,** 472-8.

Boskey, A. L., Maresca, M., Doty, S., Sabsay, B. & Veis, A. 1990. Concentration-dependent effects of dentin phosphophoryn in the regulation of in vitro hydroxyapatite formation and growth. *Bone and Mineral,* 11**,** 55-65.

Boskey, A. L., Spevak, L., Paschalis, E., Doty, S. B. & Mckee, M. D. 2002. Osteopontin deficiency increases mineral content and mineral crystallinity in mouse bone. *Calcif Tissue Int,* 71**,** 145-54.

Bourboulia, D. & Stetler-Stevenson, W. G. 2010. Matrix metalloproteinases (MMPs) and tissue inhibitors of metalloproteinases (TIMPs): Positive and negative regulators in tumor cell adhesion. *Seminars in Cancer Biology,* 20**,** 161-8.

Bowen, R. L. 1965. Adhesive bonding of various materials to hard tooth tissues. II. Bonding to dentin promoted by a surface-active comonomer. *J Dent Res,* 44**,** 895-902.

Braga, M. M., Morais, C. C., Nakama, R. C. S., Leamari, V. M., Siqueira, W. L. & Mendes, F. M. 2009. In vitro performance of methods of approximal caries detection in primary molars. *Oral Surgery Oral Medicine Oral Pathology Oral Radiology and Endodontology,* 108**,** E35-E41.

Braga, R. R., Meira, J. B. C., Boaro, L. C. C. & Xavier, T. A. 2010. Adhesion to tooth structure: A critical review of "macro" test methods. *Dental Materials,* 26**,** e38-e49.

Breschi, L., Mazzoni, A., Ruggeri, A., Cadenaro, M., Di Lenarda, R. & De Stefano Dorigo, E. 2008. Dental adhesion review: aging and stability of the bonded interface. *Dent Mater,* 24**,** 90-101.

Breschi, L., Mazzoni, A., Nato, F., Carrilho, M., Visintini, E., Tjäderhane, L., Ruggeri Jr, A., Tay, F. R., Dorigo, E. D. S. & Pashley, D. H. 2010a. Chlorhexidine stabilizes the adhesive interface: A 2-year in vitro study. *Dental Materials,* 26**,** 320-325.

Breschi, L., Martin, P., Mazzoni, A., Nato, F., Carrilho, M., Tjäderhane, L., Visintini, E., Cadenaro, M., Tay, F. R., Dorigo, E. D. S. & Pashley, D. H. 2010b. Use of a specific MMP-inhibitor (galardin) for preservation of hybrid layer. *Dental Materials,* 26**,** 571-578.

Bresciani, E., Wagner, W. C., Navarro, M. F., Dickens, S. H. & Peters, M. C. 2010. In vivo dentin microhardness beneath a calcium-phosphate cement. *J Dent Res,* 89**,** 836-41.

Bulatov, V., Feller, L., Yasman, Y. & Schechter, I. 2008. Dental enamel caries (early) diagnosis and mapping by laser Raman Spectral Imaging. *Instrumentation Science & Technology,* 36**,** 235-244.

Buonocore, M., Wileman, W. & Brudevold, F. 1956. A report on a resin composition capable of bonding to human dentin surfaces. *J Dent Res,* 35**,** 846-51.

Buonocore, M. G. 1955. A simple method of increasing the adhesion of acrylic filling materials to enamel surfaces. *J Dent Res,* 34**,** 849-53.

Butler, W. T. 1984. Dentin collagen: chemical structure and role in mineralization. *In:* Linde, A. (ed.) *Dentin and Dentinogensis.* volume II Boca Raton, Florida, chapter 8, pp 37-53.

Butler, W. T., Bhown, M., Brunn, J. C., D'souza, R. N., Farach-Carson, M. C., Happonen, R. P., Schrohenloher, R. E., Seyer, J. M., Somerman, M. J., Foster, R. A. & Et Al. 1992. Isolation, characterization and immunolocalization of a 53-kDal dentin sialoprotein (DSP). *Matrix,* 12**,** 343-51.

Butler, W. T. 1995. Dentin matrix proteins and dentinogenesis. *Connective Tissue Research,* 32**,** 381-387.

Butler, W. T. & Ritchie, H. 1995. The nature and functional significance of dentin extracellular matrix proteins. *Int J Dev Biol,* 39**,** 169-79.

Camarda, A. J., Butler, W. T., Finkelman, R. D. & Nanci, A. 1987. Immunocytochemical localization of gamma-carboxyglutamic acid-containing proteins (osteocalcin) in rat bone and dentin. *Calcif Tissue Int,* 40**,** 349-55.

Carrilho, M. R., Carvalho, R. M., De Goes, M. F., Di Hipolito, V., Geraldeli, S., Tay, F. R., Pashley, D. H. & Tjaderhane, L. 2007. Chlorhexidine preserves dentin bond in vitro. *J Dent Res,* 86**,** 90-4.

Carrilho, M. R., Tay, F. R., Donnelly, A. M., Agee, K. A., Tjaderhane, L., Mazzoni, A., Breschi, L., Foulger, S. & Pashley, D. H. 2009. Host-derived loss of dentin matrix stiffness associated with solubilization of collagen. *J Biomed Mater Res B Appl Biomater,* 90**,** 373-80.

Carvalho, R. V., Ogliari, F. A., De Souza, A. P., Silva, A. F., Petzhold, C. L., Line, S. R., Piva, E. & Etges, A. 2009. 2-hydroxyethyl methacrylate as an inhibitor of matrix metalloproteinase-2. *Eur J Oral Sci,* 117**,** 64-7.

Castelhano, A. L., Billedeau, R., Dewdney, N., Donnelly, S., Horne, S., Kurz, L. J., Liak, T. J., Martin, R., Uppington, R., Yuan, Z. Y. & Krantz, A. 1995. Novel Indolactam-Based Inhibitors of Matrix Metalloproteinases. *Bioorganic & Medicinal Chemistry Letters,* 5**,** 1415-1420.

Cawston, T. 1998. Matrix metalloproteinases and TIMPs: properties and implications for the rheumatic diseases. *Molecular Medicine Today,* 4**,** 130-7.

Chai, Z., Li, F., Fang, M., Wang, Y., Ma, S., Xiao, Y., Huang, L. & Chen, J. 2011. The bonding property and cytotoxicity of a dental adhesive incorporating a new antibacterial monomer. *Journal of Oral Rehabilitation,* 38**,** 849-56.

Chaussain-Miller, C., Fioretti, F., Goldberg, M. & Menashi, S. 2006. The role of matrix metalloproteinases (MMPs) in human caries. *J Dent Res,* 85**,** 22-32.

Choo-Smith, L. P., Dong, C. C., Cleghorn, B. & Hewko, M. 2008. Shedding new light on early caries detection. *J Can Dent Assoc,* 74**,** 913-8.

Chun, Y. H., Yamakoshi, Y., Kim, J. W., Iwata, T., Hu, J. C. & Simmer, J. P. 2006. Porcine SPARC: isolation from dentin, cDNA sequence, and computer model. *Eur J Oral Sci,* 114 Suppl 1**,** 78-85; discussion 93-5, 379-80.

Clark, R. D., Smith, J. G., Jr. & Davidson, E. A. 1965. Hexosamine and acid glycosaminoglycans in human teeth. *Biochimica et Biophysica Acta,* 101**,** 267-72.

Coussens, L. M., Fingleton, B. & Matrisian, L. M. 2002. Matrix metalloproteinase inhibitors and cancer: trials and tribulations. *Science,* 295**,** 2387-92.

D'alpino, P. H., Pereira, J. C., Svizero, N. R., Rueggeberg, F. A. & Pashley, D. H. 2006. Use of fluorescent compounds in assessing bonded resin-based restorations: a literature review. *J Dent,* 34**,** 623-34.

D'souza, R. N., Bachman, T., Baumgardner, K. R., Butler, W. T. & Litz, M. 1995. Characterization of cellular responses involved in reparative dentinogenesis in rat molars. *J Dent Res,* 74**,** 702-9.

Dacosta, T. & Gibbons, R. J. 1968. Hydrolysis of levan by human plaque streptococci. *Arch Oral Biol,* 13**,** 609-17.

Daculsi, G., Legeros, R. Z., Jean, A. & Kerebel, B. 1987. Possible physico-chemical processes in human dentin caries. *J Dent Res,* 66**,** 1356-9.

Darling, A. I. 1961. The selective attack of caries on the dental enamel. *Annals of the Royal College of Surgeons of England,* 29**,** 354-69.

Dawes, C. 2003. What is the critical pH and why does a tooth dissolve in acid? *Journal / Canadian Dental Association. Journal de l Association Dentaire Canadienne,* 69**,** 722-4.

De Josselin De Jong, E., Sundstrom, F., Westerling, H., Tranaeus, S., Ten Bosch, J. J. & Angmar-Mansson, B. 1995. A new method for in vivo quantification of changes in initial enamel caries with laser fluorescence. *Caries Res,* 29**,** 2-7.

De Munck, J., Van Landuyt, K., Peumans, M., Poitevin, A., Lambrechts, P., Braem, M. & Van Meerbeek, B. 2005. A critical review of the durability of adhesion to tooth tissue: methods and results. *J Dent Res,* 84**,** 118-32.

De Munck, J., Van Den Steen, P. E., Mine, A., Van Landuyt, K. L., Poitevin, A., Opdenakker, G. & Van Meerbeek, B. 2009. Inhibition of enzymatic degradation of adhesive-dentin interfaces. *J Dent Res,* 88**,** 1101-6.

De Munck, J., Mine, A., Van Den Steen, P. E., Van Landuyt, K. L., Poitevin, A., Opdenakker, G. & Van Meerbeek, B. 2010. Enzymatic degradation of adhesive–dentin interfaces produced by mild self-etch adhesives. *European Journal Of Oral Sciences,* 118**,** 494-501.

De Munck, J., Mine, A., Poitevin, A., Van Ende, A., Cardoso, M. V., Van Landuyt, K. L., Peumans, M. & Van Meerbeek, B. 2012. Meta-analytical review of parameters involved in dentin bonding. *J Dent Res,* 91**,** 351-7.

Ding, C. & He, X. F. 2004. Cluster structure of K-means clustering via principal component analysis. *Advances in Knowledge Discovery and Data Mining, Proceedings,* 3056**,** 414-418.

Dorman, G., Cseh, S., Hajdu, I., Barna, L., Konya, D., Kupai, K., Kovacs, L. & Ferdinandy, P. 2010. Matrix metalloproteinase inhibitors: a critical appraisal of design principles and proposed therapeutic utility. *Drugs,* 70**,** 949-64.

Dundar, M., Ozcan, M., Comlekoglu, M. E. & Sen, B. H. 2011. Nanoleakage inhibition within hybrid layer using new protective chemicals and their effect on adhesion. *J Dent Res,* 90**,** 93-8.

Dung, S. Z., Gregory, R. L., Li, Y. & Stookey, G. K. 1995. Effect of lactic acid and proteolytic enzymes on the release of organic matrix components from human root dentin. *Caries Res,* 29**,** 483-9.

Duve, C. 1975. Exploring cells with a centrifuge. *Science,* 189**,** 186-94.

Dymock, D., Weightman, A. J., Scully, C. & Wade, W. G. 1996. Molecular analysis of microflora associated with dentoalveolar abscesses. *Journal of Clinical Microbiology,* 34**,** 537-42.

Ehrmann, R. L. & Gey, G. O. 1956. The growth of cells on a transparent gel of reconstituted rat-tail collagen. *Journal of the National Cancer Institute,* 16**,** 1375-403.

Eick, J. D., Gwinnett, A. J., Pashley, D. H. & Robinson, S. J. 1997. Current concepts on adhesion to dentin. *Crit Rev Oral Biol Med,* 8**,** 306-35.

El Zohairy, A. A., Saber, M. H., Abdalla, A. I. & Feilzer, A. J. 2010. Efficacy of microtensile versus microshear bond testing for evaluation of bond strength of dental adhesive systems to enamel. *Dental Materials,* 26**,** 848-854.

Embery, G., Hall, R., Waddington, R., Septier, D. & Goldberg, M. 2001. Proteoglycans in dentinogenesis. *Crit Rev Oral Biol Med,* 12**,** 331-49.

Eren, D., Bektas, O. O. & Siso, S. H. 2013. Three different adhesive systems; three different bond strength test methods. *Acta Odontol Scand*.

Erhardt, M. C., Toledano, M., Osorio, R. & Pimenta, L. A. 2008. Histomorphologic characterization and bond strength evaluation of caries-affected dentin/resin interfaces: effects of long-term water exposure. *Dent Mater,* 24**,** 786-98.

Ericson, D., Zimmerman, M., Raber, H., Gotrick, B., Bornstein, R. & Thorell, J. 1999. Clinical evaluation of efficacy and safety of a new method for chemo-mechanical removal of caries. A multi-centre study. *Caries Res,* 33**,** 171-7.

Fanchon, S., Bourd, K., Septier, D., Everts, V., Beertsen, W., Menashi, S. & Goldberg, M. 2004. Involvement of matrix metalloproteinases in the onset of dentin mineralization. *European Journal Of Oral Sciences,* 112**,** 171-176.

Fanjul-Fernández, M., Folgueras, A. R., Cabrera, S. & López-Otín, C. 2010. Matrix metalloproteinases: Evolution, gene regulation and functional analysis in mouse models. *Biochimica et Biophysica Acta (BBA) - Molecular Cell Research,* 1803**,** 3-19.

Fejerskov, O. & Kidd, E. a. M. 2008. *Dental caries : the disease and its clinical management,* Oxford, Wiley-Blackwell.

Fluckiger, L., Waltimo, T., Stich, H. & Lussi, A. 2005. Comparison of chemomechanical caries removal using Carisolv or conventional hand excavation in deciduous teeth in vitro. *J Dent,* 33**,** 87-90.

Fusayama, T., Okuse, K. & Hosoda, H. 1966. Relationship between Hardness Discoloration and Microbial Invasion in Carious Dentin. *Journal of Dental Research,* 45**,** 1033-46.

Fusayama, T. & Terachima, S. 1972. Differentiation of two layers of carious dentin by staining. *J Dent Res,* 51**,** 866.

Fusayama, T., Nakamura, M., Kurosaki, N. & Iwaku, M. 1979. Non-pressure adhesion of a new adhesive restorative resin. *J Dent Res,* 58**,** 1364-70.

Fusayama, T. 1979. Two layers of carious dentin; diagnosis and treatment. *Oper Dent,* 4**,** 63-70.

Fusayama, T. 1990. Posterior adhesive composite resin: a historic review. *Journal of Prosthetic Dentistry,* 64**,** 534-8.

Galis, Z. S., Sukhova, G. K. & Libby, P. 1995. Microscopic localization of active proteases by in situ zymography: detection of matrix metalloproteinase activity in vascular tissue. *FASEB J,* 9**,** 974-80.

Gendron, R., Grenier, D., Sorsa, T. & Mayrand, D. 1999. Inhibition of the activities of matrix metalloproteinases 2, 8, and 9 by chlorhexidine. *Clin Diagn Lab Immunol,* 6**,** 437-9.

George, J., Teear, M. L., Norey, C. G. & Burns, D. D. 2003. Evaluation of an imaging platform during the development of a FRET protease assay. *J Biomol Screen,* 8**,** 72-80.

Gianetto, R. & Duve, C. D. 1955. Tissue Fractionation Studies .4. Comparative Study of the Binding of Acid Phosphatase, Beta-Glucuronidase and Cathepsin by Rat-Liver Particles. *Biochemical Journal,* 59**,** 433-438.

Goldberg, M. & Takagi, M. 1993. Dentine proteoglycans: composition, ultrastructure and functions. *Histochemical Journal,* 25**,** 781-806.

Goldberg, M., Kulkarni, A. B., Young, M. & Boskey, A. 2011. Dentin: structure, composition and mineralization. *Frontiers in Bioscience,* 3**,** 711-35.

Goldberg, M. 2011. Pulp healing and regeneration: more questions than answers. *Adv Dent Res,* 23**,** 270-4.

Golub, L. M., Lee, H. M., Ryan, M. E., Giannobile, W. V., Payne, J. & Sorsa, T. 1998. Tetracyclines inhibit connective tissue breakdown by multiple non-antimicrobial mechanisms. *Adv Dent Res,* 12**,** 12-26.

Golub, L. M. 2011. Introduction and background. *Pharmacological Research,* 63**,** 99-101.

Gomis-Ruth, F. X., Maskos, K., Betz, M., Bergner, A., Huber, R., Suzuki, K., Yoshida, N., Nagase, H., Brew, K., Bourenkov, G. P., Bartunik, H. & Bode, W. 1997. Mechanism of inhibition of the human matrix metalloproteinase stromelysin-1 by TIMP-1. *Nature,* 389**,** 77-81.

Granstrom, G. & Linde, A. 1976. A comparison of ATP-degrading enzyme activities in rat incisor odontoblasts. *Journal of Histochemistry and Cytochemistry,* 24**,** 1026-32.

Green, D. J. & Banerjee, A. 2011. Contemporary adhesive bonding: bridging the gap between research and clinical practice. *Dent Update,* 38**,** 439-40, 443-6, 449-50.

Griffiths, B. M., Watson, T. F. & Sherriff, M. 1999. The influence of dentine bonding systems and their handling characteristics on the morphology and micropermeability of the dentine adhesive interface. *Journal of Dentistry,* 27**,** 63-71.

Grobelny, D., Poncz, L. & Galardy, R. E. 1992. Inhibition of human skin fibroblast collagenase, thermolysin, and Pseudomonas aeruginosa elastase by peptide hydroxamic acids. *Biochemistry,* 31**,** 7152-4.

Gross, J. & Lapiere, C. M. 1962. Collagenolytic activity in amphibian tissues: a tissue culture assay. *Proceedings of the National Academy of Sciences of the United States of America,* 48**,** 1014-22.

Gustafson, G. 1957. The Histopathology of Caries of Human Dental Enamel with special reference to the division of the carious lesion into zones. *Acta Odontologica Scandinavica,* 15**,** 13-55.

Haj-Ali, R., Walker, M., Williams, K., Wang, Y. & Spencer, P. 2006. Histomorphologic characterization of noncarious and caries-affected dentin/adhesive interfaces. *Journal of Prosthodontics,* 15**,** 82-8.

Haka, A. S., Volynskaya, Z., Gardecki, J. A., Nazemi, J., Lyons, J., Hicks, D., Fitzmaurice, M., Dasari, R. R., Crowe, J. P. & Feld, M. S. 2006. In vivo margin assessment during partial mastectomy breast surgery using raman spectroscopy. *Cancer Research,* 66**,** 3317-22.

Hall, R., Septier, D., Embery, G. & Goldberg, M. 1999. Stromelysin-1 (MMP-3) in forming enamel and predentine in rat incisor-coordinated distribution with proteoglycans suggests a functional role. *Histochemical Journal,* 31**,** 761-70.

Han, L., Okamoto, A., Fukushima, M. & Okiji, T. 2006. Evaluation of a new fluoride-releasing one-step adhesive. *Dent Mater J,* 25**,** 509-15.

Hannas, A. R., Pereira, J. C., Granjeiro, J. M. & Tjaderhane, L. 2007. The role of matrix metalloproteinases in the oral environment. *Acta Odontol Scand,* 65**,** 1-13.

Hannig, M. 1999. Effect of Carisolv solution on sound, demineralized and denatured dentin--an ultrastructural investigation. *Clin Oral Investig,* 3**,** 155-9.

Hartles, R. L. & Leaver, A. G. 1953. The fluorescence of teeth under ultraviolet irradiation. *Biochem J,* 54**,** 632-8.

Hashimoto, M., Ohno, H., Sano, H., Kaga, M. & Oguchi, H. 2003a. In vitro degradation of resin-dentin bonds analyzed by microtensile bond test, scanning and transmission electron microscopy. *Biomaterials,* 24**,** 3795-3803.

Hashimoto, M., Tay, F. R., Ohno, H., Sano, H., Kaga, M., Yiu, C., Kumagai, H., Kudou, Y., Kubota, M. & Oguchi, H. 2003b. SEM and TEM analysis of water degradation of human dentinal collagen. *J Biomed Mater Res B Appl Biomater,* 66**,** 287-98.

Hashimoto, M., Ito, S., Tay, F. R., Svizero, N. R., Sano, H., Kaga, M. & Pashley, D. H. 2004. Fluid movement across the resin-dentin interface during and after bonding. *J Dent Res,* 83**,** 843-8.

Hedoux, A., Guinet, Y. & Descamps, M. 2011. The contribution of Raman spectroscopy to the analysis of phase transformations in pharmaceutical compounds. *International Journal of Pharmaceutics,* 417**,** 17-31.

Heikinheimo, K. & Salo, T. 1995. Expression of basement membrane type IV collagen and type IV collagenases (MMP-2 and MMP-9) in human fetal teeth. *J Dent Res,* 74**,** 1226-34.

Heussen, C. & Dowdle, E. B. 1980. Electrophoretic Analysis of Plasminogen Activators in Polyacrylamide Gels Containing Sodium Dodecyl-Sulfate and Copolymerized Substrates. *Analytical Biochemistry,* 102**,** 196-202.

Hibst, R., Paulus, R. & Lussi, A. 2001. Detection of Occlusal Caries by Laser Fluorescence: Basic and Clinical Investigations. *Medical Laser Application,* 16**,** 205-213.

Hjerpe, A., Antonopoulos, C. A., Engfeldt, B. & Wikstrom, B. 1983. Analysis of dentine glycosaminoglycans using high-performance liquid chromatography. *Calcif Tissue Int,* 35**,** 496-501.

Holmen, L., Thylstrup, A., Ogaard, B. & Kragh, F. 1985a. A polarized light microscopic study of progressive stages of enamel caries in vivo. *Caries Res,* 19**,** 348-54.

Holmen, L., Thylstrup, A., Ogaard, B. & Kragh, F. 1985b. A scanning electron microscopic study of progressive stages of enamel caries in vivo. *Caries Res,* 19**,** 355-67.

Hoshino, E. 1985. Predominant obligate anaerobes in human carious dentin. *J Dent Res,* 64**,** 1195-8.

Huminicki, A., Dong, C., Cleghorn, B., Sowa, M., Hewko, M. & Choo-Smith, L. P. 2010. Determining the effect of calculus, hypocalcification, and stain on using optical coherence tomography and polarized Raman spectroscopy for detecting white spot lesions. *International journal of dentistry,* 2010**,** 879252.

Hutchings, J., Kendall, C., Smith, B., Shepherd, N., Barr, H. & Stone, N. 2009. The potential for histological screening using a combination of rapid Raman mapping and principal component analysis. *Journal of Biophotonics,* 2**,** 91-103.

Huth, K. C., Neuhaus, K. W., Gygax, M., Bucher, K., Crispin, A., Paschos, E., Hickel, R. & Lussi, A. 2008. Clinical performance of a new laser fluorescence device for detection of occlusal caries lesions in permanent molars. *J Dent,* 36**,** 1033-40.

Imazato, S., Russell, R. R. & Mccabe, J. F. 1995. Antibacterial activity of MDPB polymer incorporated in dental resin. *J Dent,* 23**,** 177-81.

Ishiguro, K., Yamashita, K., Nakagaki, H., Iwata, K. & Hayakawa, T. 1994. Identification of tissue inhibitor of metalloproteinases-1 (TIMP-1) in human teeth and its distribution in cementum and dentine. *Archives of Oral Biology,* 39**,** 345-349.

Ismail, A. I. 1997. Clinical diagnosis of precavitated carious lesions. *Community Dent Oral Epidemiol,* 25**,** 13-23.

Ismail, A. I. 2004. Visual and visuo-tactile detection of dental caries. *J Dent Res,* 83 Spec No C**,** C56-66.

Iwami, Y., Hayashi, N., Yamamoto, H., Hayashi, M., Takeshige, F. & Ebisu, S. 2007. Evaluating the objectivity of caries removal with a caries detector dye using color evaluation and PCR. *Journal of Dentistry,* 35**,** 749-754.

Iwami, Y., Hayashi, N., Takeshige, F. & Ebisu, S. 2008. Relationship between the color of carious dentin with varying lesion activity, and bacterial detection. *J Dent,* 36**,** 143-51.

Iwami, Y., Yamamoto, H., Hayashi, M. & Ebisu, S. 2011. Relationship between laser fluorescence and bacterial invasion in arrested dentinal carious lesions. *Lasers Med Sci,* 26**,** 439-44.

Iyer, R. P., Patterson, N. L., Fields, G. B. & Lindsey, M. L. 2012. The history of matrix metalloproteinases: milestones, myths, and misperceptions. *Am J Physiol Heart Circ Physiol,* 303**,** H919-30.

Jones, I. L. & Leaver, A. G. 1974. Glycosaminoglycans of human dentine. *Calcified Tissue Research,* 16**,** 37-44.

Jones, S. J. & Boyde, A. 1984. Ultrastructure of dentin and dentinogenesis. *In:* Linde, A. (ed.) *Dentin and Dentinogensis.* volume I Boca Raton, Florida, chapter 4, pp 81-134.

Joves, G. J., Inoue, G., Nakashima, S., Sadr, A., Nikaido, T. & Tagami, J. 2013. Mineral density, morphology and bond strength of natural versus artificial caries-affected dentin. *Dent Mater J,* 32**,** 138-43.

Kaipatur, N. R., Murshed, M. & Mckee, M. D. 2008. Matrix Gla protein inhibition of tooth mineralization. *J Dent Res,* 87**,** 839-44.

Kanca, J., 3rd 1992. Improving bond strength through acid etching of dentin and bonding to wet dentin surfaces. *J Am Dent Assoc,* 123**,** 35-43.

Karlsson, L. 2010. Caries Detection Methods Based on Changes in Optical Properties between Healthy and Carious Tissue. *Int J Dent,* 2010**,** 270729.

Kawasaki, K. & Featherstone, J. D. 1997. Effects of collagenase on root demineralization. *J Dent Res,* 76**,** 588-95.

Kidd, E. A., Joyston-Bechal, S. & Beighton, D. 1993a. Microbiological validation of assessments of caries activity during cavity preparation. *Caries Res,* 27**,** 402-8.

Kidd, E. A., Joyston-Bechal, S. & Beighton, D. 1993b. The use of a caries detector dye during cavity preparation: a microbiological assessment. *Br Dent J,* 174**,** 245-8.

Kidd, E. A., Ricketts, D. N. & Beighton, D. 1996. Criteria for caries removal at the enamel-dentine junction: a clinical and microbiological study. *Br Dent J,* 180**,** 287-91.

Kidd, E. A. 2004. How 'clean' must a cavity be before restoration? *Caries Res,* 38**,** 305-13.

Kidd, E. A. & Fejerskov, O. 2004. What constitutes dental caries? Histopathology of carious enamel and dentin related to the action of cariogenic biofilms. *J Dent Res,* 83 Spec No C**,** C35-8.

Kim, J., Uchiyama, T., Carrilho, M., Agee, K. A., Mazzoni, A., Breschi, L., Carvalho, R. M., Tjäderhane, L., Looney, S., Wimmer, C., Tezvergil-Mutluay, A., Tay, F. R. & Pashley, D. H. 2010a. Chlorhexidine binding to mineralized versus demineralized dentin powder. *Dental Materials,* 26**,** 771-778.

Kim, Y. K., Gu, L. S., Bryan, T. E., Kim, J. R., Chen, L., Liu, Y., Yoon, J. C., Breschi, L., Pashley, D. H. & Tay, F. R. 2010b. Mineralisation of reconstituted collagen using polyvinylphosphonic acid/polyacrylic acid templating matrix protein analogues in the presence of calcium, phosphate and hydroxyl ions. *Biomaterials,* 31**,** 6618-27.

Kirsten, G. A., Takahashi, M. K., Rached, R. N., Giannini, M. & Souza, E. M. 2010. Microhardness of dentin underneath fluoride-releasing adhesive systems subjected to cariogenic challenge and fluoride therapy. *Journal of Dentistry,* 38**,** 460-468.

Kleiner, D. E. & Stetler-Stevenson, W. G. 1994. Quantitative zymography: detection of picogram quantities of gelatinases. *Analytical Biochemistry,* 218**,** 325-9.

Kleter, G. A. 1998. Discoloration of dental carious lesions (a review). *Arch Oral Biol,* 43**,** 629-32.

Kleter, G. A., Damen, J. J., Buijs, M. J. & Ten Cate, J. M. 1998. Modification of amino acid residues in carious dentin matrix. *J Dent Res,* 77**,** 488-95.

Knight, C. G., Willenbrock, F. & Murphy, G. 1992. A novel coumarin-labelled peptide for sensitive continuous assays of the matrix metalloproteinases. *FEBS Letters,* 296**,** 263-6.

Knobloch, L. A., Gailey, D., Azer, S., Johnston, W. M., Clelland, N. & Kerby, R. E. 2007. Bond strengths of one- and two-step self-etch adhesive systems. *Journal of Prosthetic Dentistry,* 97**,** 216-22.

Ko, A. C., Choo-Smith, L. P., Hewko, M., Leonardi, L., Sowa, M. G., Dong, C. C., Williams, P. & Cleghorn, B. 2005. Ex vivo detection and characterization of early dental caries by optical coherence tomography and Raman spectroscopy. *J Biomed Opt,* 10**,** 031118.

Ko, A. C., Choo-Smith, L. P., Hewko, M., Sowa, M. G., Dong, C. C. & Cleghorn, B. 2006. Detection of early dental caries using polarized Raman spectroscopy. *Optics express,* 14**,** 203-15.

Ko, A. C. T., Hewko, M., Sowa, M. G., Dong, C. C. S., Cleghorn, B. & Choo-Smith, L. P. 2008. Early dental caries detection using a fibre-optic coupled polarization-resolved Raman spectroscopic system. *Optics express,* 16**,** 6274-6284.

Koh, S. H., Powers, J. M., Bebermeyer, R. D. & Li, D. 2001. Tensile bond strengths of fourth- and fifth-generation dentin adhesives with packable resin composites. *J Esthet Restor Dent,* 13**,** 379-86.

Komori, P. C., Pashley, D. H., Tjaderhane, L., Breschi, L., Mazzoni, A., De Goes, M. F., Wang, L. & Carrilho, M. R. 2009. Effect of 2% chlorhexidine digluconate on the bond strength to normal versus caries-affected dentin. *Oper Dent,* 34**,** 157-65.

König, K., Hibst, R., Meyer, H., Flemming, G. & Schneckenburger, H. 1993. Laser-Induced Autofluorescence of Carious Regions of Human Teeth and Caries-Involved Bacteria. *Proceedings of Dental Applications of Lasers,* 2080**,** 170-180.

König, K. & Schneckenburger, H. 1994. Laser-induced autofluorescence for medical diagnosis. *Journal of Fluorescence,* 4**,** 17-40.

König, K., Flemming, G. & Hibst, R. 1998. Laser-induced autofluorescence spectroscopy of dental caries. *Cell Mol Biol (Noisy-le-grand),* 44**,** 1293-300.

König, K., Schneckenburger, H. & Hibst, R. 1999. Time-gated in vivo autofluorescence imaging of dental caries. *Cell Mol Biol (Noisy-le-grand),* 45**,** 233-9.

Kramer, I. R. & Lee, K. W. 1960. The demonstration of glycerophosphoric acid dimethacrylate in dentin and filling material following the use of a cavity sealer. *J Dent Res,* 39**,** 1003-8.

Kramer, I. R. H. & Mclean, J. W. 1952. Alterations in the staining reactions of dentine resulting from a constituent of a new self polymerizing resin. *British dental journal,* 92**,** 150-153.

Kronman, J. H., Goldman, M., Habib, C. M. & Mengel, L. 1977. Electron microscopic evaluation of altered collagen structure induced by N-monochloroglycine (GK-101). *J Dent Res,* 56**,** 1539-45.

Kuboki, Y., Ohgushi, K. & Fusayama, T. 1977. Collagen biochemistry of the two layers of carious dentin. *J Dent Res,* 56**,** 1233-7.

Kugel, G. & Ferrari, M. 2000. The science of bonding: from first to sixth generation. *J Am Dent Assoc,* 131 Suppl**,** 20S-25S.

Kupai, K., Szucs, G., Cseh, S., Hajdu, I., Csonka, C., Csont, T. & Ferdinandy, P. 2010. Matrix metalloproteinase activity assays: Importance of zymography. *J Pharmacol Toxicol Methods,* 61**,** 205-9.

Leber, T. M. & Balkwill, F. R. 1997. Zymography: a single-step staining method for quantitation of proteolytic activity on substrate gels. *Analytical Biochemistry,* 249**,** 24-8.

Leloup, G., D'hoore, W., Bouter, D., Degrange, M. & Vreven, J. 2001. Meta-analytical review of factors involved in dentin adherence. *J Dent Res,* 80**,** 1605-14.

Lennon, A. M., Buchalla, W., Brune, L., Zimmermann, O., Gross, U. & Attin, T. 2006. The ability of selected oral microorganisms to emit red fluorescence. *Caries Res,* 40**,** 2-5.

Lester, K. S. & Boyde, A. 1968. Some Preliminary Observations on Caries (Remineralization) Crystals in Enamel and Dentine by Surface Electron Microscopy. *Virchows Archiv Abteilung a Pathologische Anatomie,* 344**,** 196-212.

Linde, A., Bhown, M. & Butler, W. T. 1980. Noncollagenous proteins of dentin. A re-examination of proteins from rat incisor dentin utilizing techniques to avoid artifacts. *J Biol Chem,* 255**,** 5931-42.

Linde, A., Bhown, M., Cothran, W. C., Hoglund, A. & Butler, W. T. 1982. Evidence for several gamma-carboxyglutamic acid-containing proteins in dentin. *Biochimica et Biophysica Acta,* 704**,** 235-9.

Linde, A. 1984. Noncollagenous proteins and proteoglycans in dentinogenesis. *In:* Linde, A. (ed.) *Dentin and Dentinogensis.* volume II Boca Raton, Florida, chapter 9, pp 55-92.

Linde, A. & Goldberg, M. 1993. Dentinogenesis. *Crit Rev Oral Biol Med,* 4**,** 679-728.

Linsenmayer, T. F., Gibney, E., Igoe, F., Gordon, M. K., Fitch, J. M., Fessler, L. I. & Birk, D. E. 1993. Type V collagen: molecular structure and fibrillar organization of the chicken alpha 1(V) NH2-terminal domain, a putative regulator of corneal fibrillogenesis. *Journal of Cell Biology,* 121**,** 1181-9.

Liu, Y., Tjaderhane, L., Breschi, L., Mazzoni, A., Li, N., Mao, J., Pashley, D. H. & Tay, F. R. 2011. Limitations in bonding to dentin and experimental strategies to prevent bond degradation. *Journal of Dental Research,* 90**,** 953-68.

Loesche, W. J. & Syed, S. A. 1973. The predominant cultivable flora of carious plaque and carious dentine. *Caries Res,* 7**,** 201-16.

Lozano-Chourio, M. A., Zambrano, O., Gonzalez, H. & Quero, M. 2006. Clinical randomized controlled trial of chemomechanical caries removal (Carisolv). *International Journal of Paediatric Dentistry,* 16**,** 161-7.

Lu, Y., Ye, L., Yu, S., Zhang, S., Xie, Y., Mckee, M. D., Li, Y. C., Kong, J., Eick, J. D., Dallas, S. L. & Feng, J. Q. 2007. Rescue of odontogenesis in Dmp1-deficient mice by

targeted re-expression of DMP1 reveals roles for DMP1 in early odontogenesis and dentin apposition in vivo. *Developmental Biology,* 303**,** 191-201.

Luo, G., Ducy, P., Mckee, M. D., Pinero, G. J., Loyer, E., Behringer, R. R. & Karsenty, G. 1997. Spontaneous calcification of arteries and cartilage in mice lacking matrix GLA protein. *Nature,* 386**,** 78-81.

Lussi, A., Francescut, P., Achermann, F., Reich, E., Hotz, P. & Megert, B. 2000. The use of the DIAGNOdent during cavity preparation. 47th ORCA Congress, 2000 Alghero, Sardinia. Caries Research, 327-328.

Lussi, A., Megert, B., Longbottom, C., Reich, E. & Francescut, P. 2001. Clinical performance of a laser fluorescence device for detection of occlusal caries lesions. *European Journal Of Oral Sciences,* 109**,** 14-19.

Lussi, A., Hibst, R. & Paulus, R. 2004. DIAGNOdent: an optical method for caries detection. *J Dent Res,* 83 Spec No C**,** C80-3.

Macdougall, M., Simmons, D., Luan, X., Nydegger, J., Feng, J. & Gu, T. T. 1997. Dentin phosphoprotein and dentin sialoprotein are cleavage products expressed from a single transcript coded by a gene on human chromosome 4. Dentin phosphoprotein DNA sequence determination. *J Biol Chem,* 272**,** 835-42.

Makela, M., Salo, T., Uitto, V. J. & Larjava, H. 1994. Matrix metalloproteinases (MMP-2 and MMP-9) of the oral cavity: cellular origin and relationship to periodontal status. *J Dent Res,* 73**,** 1397-406.

Manji, F., Fejerskov, O., Nagelkerke, N. J. & Baelum, V. 1991. A random effects model for some epidemiological features of dental caries. *Community Dent Oral Epidemiol,* 19**,** 324-8.

Markowitz, K. & Rosenblum, M. A. 2010. The effect of cationic polymer treatment on dye staining and on the adhesion of charged particles to dentin. *Arch Oral Biol,* 55**,** 60-7.

Marquis, R. E. 1995. Oxygen metabolism, oxidative stress and acid-base physiology of dental plaque biofilms. *Journal of Industrial Microbiology and Biotechnology,* 15**,** 198-207.

Marshall, G. W., Marshall, S. J., Kinney, J. H. & Balooch, M. 1997. The dentin substrate: structure and properties related to bonding. *Journal of Dentistry,* 25**,** 441-458.

Marshall, G. W., Habelitz, S., Gallagher, R., Balooch, M., Balooch, G. & Marshall, S. J. 2001. Nanomechanical properties of hydrated carious human dentin. *J Dent Res,* 80**,** 1768-71.

Marshall, S. J., Bayne, S. C., Baier, R., Tomsia, A. P. & Marshall, G. W. 2010. A review of adhesion science. *Dental Materials,* 26**,** e11-e16.

Martin-De Las Heras, S., Valenzuela, A. & Overall, C. M. 2000. The matrix metalloproteinase gelatinase A in human dentine. *Archives of Oral Biology,* 45**,** 757-765.

Martins, V. L., Caley, M. & O'toole, E. A. 2012. Matrix metalloproteinases and epidermal wound repair. *Cell and Tissue Research,* 351**,** 255-268.

Mazzoni, A., Mannello, F., Tay, F. R., Tonti, G. A., Papa, S., Mazzotti, G., Di Lenarda, R., Pashley, D. H. & Breschi, L. 2007. Zymographic analysis and characterization of MMP-2 and -9 forms in human sound dentin. *J Dent Res,* 86**,** 436-40.

Mazzoni, A., Carrilho, M., Papa, V., Tjäderhane, L., Gobbi, P., Nucci, C., Di Lenarda, R., Mazzotti, G., Tay, F. R., Pashley, D. H. & Breschi, L. 2011. MMP-2 assay within the hybrid layer created by a two-step etch-and-rinse adhesive: Biochemical and immunohistochemical analysis. *Journal of Dentistry,* 39**,** 470-477.

Mazzoni, A., Nascimento, F. D., Carrilho, M., Tersariol, I., Papa, V., Tjaderhane, L., Di Lenarda, R., Tay, F. R., Pashley, D. H. & Breschi, L. 2012. MMP activity in the hybrid layer detected with in situ zymography. *J Dent Res,* 91**,** 467-72.

Mazzoni, A., Scaffa, P., Carrilho, M., Tjaderhane, L., Di Lenarda, R., Polimeni, A., Tezvergil-Mutluay, A., Tay, F. R., Pashley, D. H. & Breschi, L. 2013. Effects of etch-and-rinse and self-etch adhesives on dentin MMP-2 and MMP-9. *J Dent Res,* 92**,** 82-6.

Mccomb, D. 2005. Conservative Operative Management Strategies. *Dental Clinics of North America,* 49**,** 847-865.

Mcconnell, G., Girkin, J. M., Ameer-Beg, S. M., Barber, P. R., Vojnovic, B., Ng, T., Banerjee, A., Watson, T. F. & Cook, R. J. 2007. Time-correlated single-photon counting fluorescence lifetime confocal imaging of decayed and sound dental structures with a white-light supercontinuum source. *Journal of Microscopy,* 225**,** 126-36.

Mcknight, D. A., Simmer, J. P., Hart, P. S., Hart, T. C. & Fisher, L. W. 2008. Overlapping DSPP mutations cause dentin dysplasia and dentinogenesis imperfecta. *J Dent Res,* 87**,** 1108-11.

Mclean, J. W. 1999. The pioneers of enamel and dentin bonding. *J Adhes Dent,* 1**,** 185-7.

Melcher, A. H. & Chan, J. 1981. Phagocytosis and digestion of collagen by gingival fibroblasts in vivo: a study of serial sections. *Journal of Ultrastructure Research,* 77**,** 1-36.

Mendes, F. M., Hissadomi, M. & Imparato, J. C. 2004. Effects of drying time and the presence of plaque on the in vitro performance of laser fluorescence in occlusal caries of primary teeth. *Caries Res,* 38**,** 104-8.

Michaud, D. 1998. Gel electrophoresis of proteolytic enzymes. *Analytica Chimica Acta,* 372**,** 173-185.

Milan, A. M., Sugars, R. V., Embery, G. & Waddington, R. J. 2005. Modulation of collagen fibrillogenesis by dentinal proteoglycans. *Calcif Tissue Int,* 76**,** 127-35.

Milan, A. M., Sugars, R. V., Embery, G. & Waddington, R. J. 2006. Adsorption and interactions of dentine phosphoprotein with hydroxyapatite and collagen. *European Journal Of Oral Sciences,* 114**,** 223-231.

Mjör, I. A. 1984. The morphology of dentin and dentinogenesis. *In:* Linde, A. (ed.) *Dentin and Dentinogensis.* volume I Boca Raton, Florida, chapter 1, pp 1-18.

Moraes, R. R., Garcia, J. W., Wilson, N. D., Lewis, S. H., Barros, M. D., Yang, B., Pfeifer, C. S. & Stansbury, J. W. 2012. Improved dental adhesive formulations based on reactive nanogel additives. *J Dent Res,* 91**,** 179-84.

Morrow, L. A., Hassall, D. C., Watts, D. C. & Wilson, N. H. 2000. A chemomechanical method for caries removal. *Dent Update,* 27**,** 398-401.

Moss, M. L. & Rasmussen, F. H. 2007. Fluorescent substrates for the proteinases ADAM17, ADAM10, ADAM8, and ADAM12 useful for high-throughput inhibitor screening. *Analytical Biochemistry,* 366**,** 144-148.

Moszner, N., Salz, U. & Zimmermann, J. 2005. Chemical aspects of self-etching enamel-dentin adhesives: a systematic review. *Dental materials : official publication of the Academy of Dental Materials,* 21**,** 895-910.

Moszner, N., Fischer, U. K., Angermann, J. & Rheinberger, V. 2008. A partially aromatic urethane dimethacrylate as a new substitute for Bis-GMA in restorative composites. *Dent Mater,* 24**,** 694-9.

Moter, A. & Gobel, U. B. 2000. Fluorescence in situ hybridization (FISH) for direct visualization of microorganisms. *Journal of Microbiological Methods,* 41**,** 85-112.

Mungall, B. A. & Pollitt, C. C. 2001. In situ zymography: topographical considerations. *J Biochem Biophys Methods,* 47**,** 169-76.

Munksgaard, E. C., Butler, W. T. & Richardson, W. S., 3rd 1977. Phosphoprotein from dentin. New approaches to achieve and assess purity. *Preparative Biochemistry,* 7**,** 321-31.

Munson, M. A., Banerjee, A., Watson, T. F. & Wade, W. G. 2004. Molecular analysis of the microflora associated with dental caries. *Journal of Clinical Microbiology,* 42**,** 3023-3029.

Murphy, G. & Nagase, H. 2008. Progress in matrix metalloproteinase research. *Molecular Aspects of Medicine,* 29**,** 290-308.

Nagase, H., Visse, R. & Murphy, G. 2006. Structure and function of matrix metalloproteinases and TIMPs. *Cardiovasc Res,* 69**,** 562-73.

Nakabayashi, N., Kojima, K. & Masuhara, E. 1982. The promotion of adhesion by the infiltration of monomers into tooth substrates. *Journal of Biomedical Materials Research,* 16**,** 265-73.

Nakajima, M., Kitasako, Y., Okuda, M., Foxton, R. M. & Tagami, J. 2005. Elemental distributions and microtensile bond strength of the adhesive interface to normal and caries-affected dentin. *J Biomed Mater Res B Appl Biomater,* 72**,** 268-75.

Navarra, C. O., Cadenaro, M., Codan, B., Mazzoni, A., Sergo, V., De Stefano Dorigo, E. & Breschi, L. 2009a. Degree of conversion and interfacial nanoleakage expression of three one-step self-etch adhesives. *Eur J Oral Sci,* 117**,** 463-9.

Navarra, C. O., Cadenaro, M., Armstrong, S. R., Jessop, J., Antoniolli, F., Sergo, V., Di Lenarda, R. & Breschi, L. 2009b. Degree of conversion of Filtek Silorane Adhesive System and Clearfil SE Bond within the hybrid and adhesive layer: an in situ Raman analysis. *Dent Mater,* 25**,** 1178-85.

Nikiforuk, G. & Fraser, D. 1979. Etiology of Enamel Hypoplasia and Interglobular Dentin: The Roles of Hypocalcemia and Hypophosphatemia. *Metabolic Bone Disease and Related Research,* 2**,** 17-23.

Nishitani, Y., Yoshiyama, M., Wadgaonkar, B., Breschi, L., Mannello, F., Mazzoni, A., Carvalho, R. M., Tjaderhane, L., Tay, F. R. & Pashley, D. H. 2006. Activation of gelatinolytic/collagenolytic activity in dentin by self-etching adhesives. *Eur J Oral Sci,* 114**,** 160-6.

Nishiyama, N., Suzuki, K., Takahashi, K. & Nemoto, K. 2004. The pKa effects of the carboxylic acid in N-methacryloyl-omega-amino acid on the demineralization and bond strengths to the teeth. *Biomaterials,* 25**,** 5441-7.

Nordstrom, H., Gossas, T., Hamalainen, M., Kallblad, P., Nystrom, S., Wallberg, H. & Danielson, U. H. 2008. Identification of MMP-12 inhibitors by using biosensor-based screening of a fragment library. *Journal of Medicinal Chemistry,* 51**,** 3449-59.

Ogawa, K., Yamashita, Y., Ichijo, T. & Fusayama, T. 1983. The ultrastructure and hardness of the transparent layer of human carious dentin. *J Dent Res,* 62**,** 7-10.

Orgel, J. P., Irving, T. C., Miller, A. & Wess, T. J. 2006. Microfibrillar structure of type I collagen in situ. *Proceedings of the National Academy of Sciences of the United States of America,* 103**,** 9001-5.

Orimo, H. 2010. The mechanism of mineralization and the role of alkaline phosphatase in health and disease. *J Nihon Med Sch,* 77**,** 4-12.

Osorio, R., Yamauti, M., Osorio, E., Ruiz-Requena, M. E., Pashley, D., Tay, F. & Toledano, M. 2011. Effect of dentin etching and chlorhexidine application on metalloproteinase-mediated collagen degradation. *European Journal Of Oral Sciences,* 119**,** 79-85.

Overall, C. M. & Lopez-Otin, C. 2002. Strategies for MMP inhibition in cancer: innovations for the post-trial era. *Nat Rev Cancer,* 2**,** 657-72.

Overman, S. A. & Thomas, G. J., Jr. 1999. Raman markers of nonaromatic side chains in an alpha-helix assembly: Ala, Asp, Glu, Gly, Ile, Leu, Lys, Ser, and Val residues of phage fd subunits. *Biochemistry,* 38**,** 4018-27.

Page-Mccaw, A., Ewald, A. J. & Werb, Z. 2007. Matrix metalloproteinases and the regulation of tissue remodelling. *Nat Rev Mol Cell Biol,* 8**,** 221-33.

Palosaari, H., Wahlgren, J., Larmas, M., Ronka, H., Sorsa, T., Salo, T. & Tjaderhane, L. 2000. The expression of MMP-8 in human odontoblasts and dental pulp cells is down-regulated by TGF-beta1. *J Dent Res,* 79**,** 77-84.

Palosaari, H., Ding, Y., Larmas, M., Sorsa, T., Bartlett, J. D., Salo, T. & Tjaderhane, L. 2002. Regulation and interactions of MT1-MMP and MMP-20 in human odontoblasts and pulp tissue in vitro. *J Dent Res,* 81**,** 354-9.

Palosaari, H., Pennington, C. J., Larmas, M., Edwards, D. R., Tjäderhane, L. & Salo, T. 2003. Expression profile of matrix metalloproteinases (MMPs) and tissue inhibitors of

MMPs in mature human odontoblasts and pulp tissue. *European Journal Of Oral Sciences,* 111**,** 117-127.

Pashley, D. H. 1991. Clinical correlations of dentin structure and function. *The Journal of Prosthetic Dentistry,* 66**,** 777-781.

Pashley, D. H., Agee, K. A., Nakajima, M., Tay, F. R., Carvalho, R. M., Terada, R. S., Harmon, F. J., Lee, W. K. & Rueggeberg, F. A. 2001. Solvent-induced dimensional changes in EDTA-demineralized dentin matrix. *Journal of Biomedical Materials Research,* 56**,** 273-81.

Pashley, D. H., Tay, F. R., Yiu, C., Hashimoto, M., Breschi, L., Carvalho, R. M. & Ito, S. 2004. Collagen degradation by host-derived enzymes during aging. *J Dent Res,* 83**,** 216-21.

Pashley, D. H., Tay, F. R., Carvalho, R. M., Rueggeberg, F. A., Agee, K. A., Carrilho, M., Donnelly, A. & Garcia-Godoy, F. 2007. From dry bonding to water-wet bonding to ethanol-wet bonding. A review of the interactions between dentin matrix and solvated resins using a macromodel of the hybrid layer. *Am J Dent,* 20**,** 7-20.

Pashley, D. H., Tay, F. R. & Imazato, S. 2011a. How to increase the durability of resin-dentin bonds. *Compend Contin Educ Dent,* 32**,** 60-4, 66.

Pashley, D. H., Tay, F. R., Breschi, L., Tjäderhane, L., Carvalho, R. M., Carrilho, M. & Tezvergil-Mutluay, A. 2011b. State of the art etch-and-rinse adhesives. *Dental Materials,* 27**,** 1-16.

Patel, P. 2001. Soundbites. *Nature Genetics,* 27**,** 129-30.

Perdigão, J. 2007. New developments in dental adhesion. *Dent Clin North Am,* 51**,** 333-57, viii.

Perdigão, J. 2010. Dentin bonding-Variables related to the clinical situation and the substrate treatment. *Dental Materials,* 26**,** e24-e37.

Pernak, J., Rogoza, J. & Mirska, I. 2001. Synthesis and antimicrobial activities of new pyridinium and benzimidazolium chlorides. *Eur J Med Chem,* 36**,** 313-20.

Petruska, J. A. & Hodge, A. J. 1964. A Subunit Model for the Tropocollagen Macromolecule. *Proceedings of the National Academy of Sciences of the United States of America,* 51**,** 871-6.

Petry, R., Schmitt, M. & Popp, J. 2003. Raman Spectroscopy - A Prospective Tool in the Life Sciences. *ChemPhysChem,* 4**,** 14-30.

Peumans, M., Kanumilli, P., De Munck, J., Van Landuyt, K., Lambrechts, P. & Van Meerbeek, B. 2005. Clinical effectiveness of contemporary adhesives: a systematic review of current clinical trials. *Dent Mater,* 21**,** 864-81.

Peumans, M., De Munck, J., Van Landuyt, K., Lambrechts, P. & Van Meerbeek, B. 2007. Five-year clinical effectiveness of a two-step self-etching adhesive. *J Adhes Dent,* 9**,** 7-10.

Pitts, N. B. & Wefel, J. S. 2009. Remineralization/desensitization: what is known? What is the future? *Adv Dent Res,* 21**,** 83-6.

Porter, S., Clark, I. M., Kevorkian, L. & Edwards, D. R. 2005. The ADAMTS metalloproteinases. *Biochem J,* 386**,** 15-27.

Porto, I. M., Rocha, L. B., Rossi, M. A. & Gerlach, R. F. 2009. In situ zymography and immunolabeling in fixed and decalcified craniofacial tissues. *Journal of Histochemistry and Cytochemistry,* 57**,** 615-22.

Posner, A. S. & Tannenbaum, P. J. 1984. The mineral phase of dentin. *In:* Linde, A. (ed.) *Dentin and Dentinogensis.* volume II Boca Raton, Florida, chapter 7, pp 17-36.

Pretty, I. A. 2006. Caries detection and diagnosis: novel technologies. *J Dent,* 34**,** 727-39.

Pugach, M. K., Strother, J., Darling, C. L., Fried, D., Gansky, S. A., Marshall, S. J. & Marshall, G. W. 2009. Dentin caries zones: mineral, structure, and properties. *J Dent Res,* 88**,** 71-6.

Qin, C., Cook, R. G., Orkiszewski, R. S. & Butler, W. T. 2001. Identification and characterization of the carboxyl-terminal region of rat dentin sialoprotein. *J Biol Chem,* 276**,** 904-9.

Qin, C., Baba, O. & Butler, W. T. 2004. Post-translational modifications of sibling proteins and their roles in osteogenesis and dentinogenesis. *Crit Rev Oral Biol Med,* 15**,** 126-36.

Qin, C., D'souza, R. & Feng, J. Q. 2007. Dentin matrix protein 1 (DMP1): new and important roles for biomineralization and phosphate homeostasis. *J Dent Res,* 86**,** 1134-41.

Rahemtulla, F., Prince, C. W. & Butler, W. T. 1984. Isolation and partial characterization of proteoglycans from rat incisors. *Biochem J,* 218**,** 877-85.

Ramos-Fernandez, M., Bellolio, M. F. & Stead, L. G. 2011. Matrix Metalloproteinase-9 as a Marker for Acute Ischemic Stroke: A Systematic Review. *Journal of Stroke & Cerebrovascular Diseases,* 20**,** 47-54.

Rasmussen, H. S. & Mccann, P. P. 1997. Matrix Metalloproteinase Inhibition as a Novel Anticancer Strategy: A Review with Special Focus on Batimastat and Marimastat. *Pharmacology & Therapeutics,* 75**,** 69-75.

Revenko, I., Sommer, F., Minh, D. T., Garrone, R. & Franc, J. M. 1994. Atomic force microscopy study of the collagen fibre structure. *Biologie Cellulaire,* 80**,** 67-9.

Reynolds, J. J. 1970. Degradation processes in bone and cartilage. *Calcified Tissue Research***,** Suppl:52-6.

Ribeiro Figueiredo, A. C., Kurachi, C. & Bagnato, V. S. 2005. Comparison of fluorescence detection of carious dentin for different excitation wavelengths. *Caries Res,* 39**,** 393-6.

Robinson, C., Shore, R. C., Brookes, S. J., Strafford, S., Wood, S. R. & Kirkham, J. 2000. The chemistry of enamel caries. *Crit Rev Oral Biol Med,* 11**,** 481-95.

Romberg, R. W., Werness, P. G., Riggs, B. L. & Mann, K. G. 1986. Inhibition of hydroxyapatite crystal growth by bone-specific and other calcium-binding proteins. *Biochemistry,* 25**,** 1176-80.

Sadek, F. T., Braga, R. R., Muench, A., Liu, Y., Pashley, D. H. & Tay, F. R. 2010. Ethanol wet-bonding challenges current anti-degradation strategy. *Journal of Dental Research,* 89**,** 1499-504.

Sakoolnamarka, R., Burrow, M. F., Swain, M. & Tyas, M. J. 2005. Microhardness and Ca:P ratio of carious and Carisolv treated caries-affected dentine using an ultra-micro-indentation system and energy dispersive analysis of x-rays--a pilot study. *Aust Dent J,* 50**,** 246-50.

Salz, U., Mucke, A., Zimmermann, J., Tay, F. R. & Pashley, D. H. 2006. pKa value and buffering capacity of acidic monomers commonly used in self-etching primers. *J Adhes Dent,* 8**,** 143-50.

Sano, H., Ciucchi, B., Matthews, W. G. & Pashley, D. H. 1994. Tensile properties of mineralized and demineralized human and bovine dentin. *J Dent Res,* 73**,** 1205-11.

Santini, A. & Miletic, V. 2008. Quantitative micro-Raman assessment of dentine demineralization, adhesive penetration, and degree of conversion of three dentine bonding systems. *European Journal Of Oral Sciences,* 116**,** 177-183.

Santos, F. P., Malaquias, P., Luque-Martinez, I. V., Muñoz, M. A., Grande, R. S., Reis, A. & Loguercio, A. D. 2013. Evaluation of Benzalkonium Chloride-containing Acid on the Durability of Resin-Dentin Interfaces. *IADR General Session.* Seattle, Washington, USA.

Sapadin, A. N. & Fleischmajer, R. 2006. Tetracyclines: Nonantibiotic properties and their clinical implications. *Journal of the American Academy of Dermatology,* 54**,** 258-265.

Sarr, M., Kane, A. W., Vreven, J., Mine, A., Van Landuyt, K. L., Peumans, M., Lambrechts, P., Van Meerbeek, B. & De Munck, J. 2010. Microtensile bond strength and interfacial characterization of 11 contemporary adhesives bonded to bur-cut dentin. *Oper Dent,* 35**,** 94-104.

Sauro, S., Pashley, D. H., Mannocci, F., Tay, F. R., Pilecki, P., Sherriff, M. & Watson, T. F. 2008. Micropermeability of current self-etching and etch-and-rinse adhesives bonded to deep dentine: a comparison study using a double-staining/confocal microscopy technique. *European Journal Of Oral Sciences,* 116**,** 184-193.

Scherczinger, C. A., Ladd, C., Bourke, M. T., Adamowicz, M. S., Johannes, P. M., Scherczinger, R., Beesley, T. & Lee, H. C. 1999. A systematic analysis of PCR contamination. *Journal of Forensic Sciences,* 44**,** 1042-5.

Scherrer, S. S., Cesar, P. F. & Swain, M. V. 2010. Direct comparison of the bond strength results of the different test methods: a critical literature review. *Dent Mater,* 26**,** e78-93.

Selwitz, R. H., Ismail, A. I. & Pitts, N. B. 2007. Dental caries. *Lancet,* 369**,** 51-9.

Senger, D. R., Wirth, D. F. & Hynes, R. O. 1979. Transformed mammalian cells secrete specific proteins and phosphoproteins. *Cell,* 16**,** 885-93.

Seow, W. K. 2003. Diagnosis and management of unusual dental abscesses in children. *Australian Dental Journal,* 48**,** 156-168.

Shigetani, Y., Okamoto, A., Abu-Bakr, N., Tanabe, K., Kondo, S. & Iwaku, M. 2003. Caries diagnosis using a laser fluorescence system--observation of autofluorescence of dental caries. *Dent Mater J,* 22**,** 56-65.

Shimada, Y., Ichinose, S., Sadr, A., Burrow, M. F. & Tagami, J. 2009. Localization of matrix metalloproteinases (MMPs-2, 8, 9 and 20) in normal and carious dentine. *Aust Dent J,* 54**,** 347-54.

Shin, T. P., Yao, X., Huenergardt, R., Walker, M. P. & Wang, Y. 2009. Morphological and chemical characterization of bonding hydrophobic adhesive to dentin using ethanol wet bonding technique. *Dent Mater,* 25**,** 1050-7.

Sideridou, I., Tserki, V. & Papanastasiou, G. 2002. Effect of chemical structure on degree of conversion in light-cured dimethacrylate-based dental resins. *Biomaterials,* 23**,** 1819-29.

Smith, A. J., Scheven, B. A., Takahashi, Y., Ferracane, J. L., Shelton, R. M. & Cooper, P. R. 2012. Dentine as a bioactive extracellular matrix. *Archives of Oral Biology,* 57**,** 109-121.

Snoek-Van Beurden, P. A. & Von Den Hoff, J. W. 2005. Zymographic techniques for the analysis of matrix metalloproteinases and their inhibitors. *Biotechniques,* 38**,** 73-83.

Söderholm, K. J. 2007. Dental adhesives .... how it all started and later evolved. *J Adhes Dent,* 9 Suppl 2**,** 227-30.

Soeno, K., Taira, Y., Matsumura, H. & Atsuta, M. 2001. Effect of desensitizers on bond strength of adhesive luting agents to dentin. *Journal of Oral Rehabilitation,* 28**,** 1122-8.

Somogyi, E., Petersson, U., Sugars, R. V., Hultenby, K. & Wendel, M. 2004. Nucleobindin--a Ca2+-binding protein present in the cells and mineralized tissues of the tooth. *Calcif Tissue Int,* 74**,** 366-76.

Sone, S., Nakamura, M., Maruya, Y., Takahashi, I., Mizoguchi, I., Mayanagi, H. & Sasano, Y. 2005. Expression of versican and ADAMTS during rat tooth eruption. *J Mol Histol,* 36**,** 281-8.

Sorsa, T., Tjäderhane, L. & Salo, T. 2004. Matrix metalloproteinases (MMPs) in oral diseases. *Oral Diseases,* 10**,** 311-318.

Spencer, P., Wang, Y., Walker, M. P., Wieliczka, D. M. & Swafford, J. R. 2000. Interfacial chemistry of the dentin/adhesive bond. *J Dent Res,* 79**,** 1458-63.

Stack, M. S. & Gray, R. D. 1989. Comparison of vertebrate collagenase and gelatinase using a new fluorogenic substrate peptide. *J Biol Chem,* 264**,** 4277-81.

Stangel, I., Ellis, T. H. & Sacher, E. 2007. Adhesion to tooth structure mediated by contemporary bonding systems. *Dent Clin North Am,* 51**,** 677-94, vii.

Steinman, R. R. 1960. Possible role of bacterial hyaluronidase in incipient carious lesions. *J Dent Res,* 39**,** 150-2.

Stookey, G. K. 2005. Quantitative Light Fluorescence: A Technology for Early Monitoring of the Caries Process. *Dental Clinics of North America,* 49**,** 753-770.

Sulkala, M., Wahlgren, J., Larmas, M., Sorsa, T., Teronen, O., Salo, T. & Tjaderhane, L. 2001. The effects of MMP inhibitors on human salivary MMP activity and caries progression in rats. *J Dent Res,* 80**,** 1545-9.

Sulkala, M., Larmas, M., Sorsa, T., Salo, T. & Tjaderhane, L. 2002. The localization of matrix metalloproteinase-20 (MMP-20, enamelysin) in mature human teeth. *J Dent Res,* 81**,** 603-7.

Sulkala, M., Tervahartiala, T., Sorsa, T., Larmas, M., Salo, T. & Tjäderhane, L. 2007. Matrix metalloproteinase-8 (MMP-8) is the major collagenase in human dentin. *Archives of Oral Biology,* 52**,** 121-127.

Suppa, P., Breschi, L., Ruggeri, A., Mazzotti, G., Prati, C., Chersoni, S., Lenarda, R. D., Pashley, D. H. & Tay, F. R. 2005. Nanoleakage within the hybrid layer: A correlative FEISEM/TEM investigation. *Journal of Biomedical Materials Research Part B: Applied Biomaterials,* 73B**,** 7-14.

Suzuki, S., Sreenath, T., Haruyama, N., Honeycutt, C., Terse, A., Cho, A., Kohler, T., Müller, R., Goldberg, M. & Kulkarni, A. B. 2009. Dentin sialoprotein and dentin phosphoprotein have distinct roles in dentin mineralization. *Matrix Biology,* 28**,** 221-229.

Tang, B. L. 2001. ADAMTS: a novel family of extracellular matrix proteases. *International Journal of Biochemistry and Cell Biology,* 33**,** 33-44.

Tay, F. R., Gwinnett, A. J., Pang, K. M. & Wei, S. H. 1996. Resin permeation into acid-conditioned, moist, and dry dentin: a paradigm using water-free adhesive primers. *J Dent Res,* 75**,** 1034-44.

Tay, F. R., Gwinnett, J. A. & Wei, S. H. 1998. Relation between water content in acetone/alcohol-based primer and interfacial ultrastructure. *J Dent,* 26**,** 147-56.

Tay, F. R. & Pashley, D. H. 2001. Aggressiveness of contemporary self-etching systems. I: Depth of penetration beyond dentin smear layers. *Dent Mater,* 17**,** 296-308.

Tay, F. R., Pashley, D. H., Loushine, R. J., Weller, R. N., Monticelli, F. & Osorio, R. 2006. Self-Etching Adhesives Increase Collagenolytic Activity in Radicular Dentin. *Journal of Endodontics,* 32**,** 862-868.

Tay, F. R. & Pashley, D. H. 2008. Guided tissue remineralisation of partially demineralised human dentine. *Biomaterials,* 29**,** 1127-37.

Ten Cate, J. M. & Featherstone, J. D. B. 1991. Mechanistic Aspects of the Interactions between Fluoride and Dental Enamel. *Critical Reviews in Oral Biology and Medicine,* 2**,** 283-296.

Ten Cate, J. M. 1999. Current concepts on the theories of the mechanism of action of fluoride. *Acta Odontologica Scandinavica,* 57**,** 325-329.

Termine, J. D., Kleinman, H. K., Whitson, S. W., Conn, K. M., Mcgarvey, M. L. & Martin, G. R. 1981. Osteonectin, a bone-specific protein linking mineral to collagen. *Cell,* 26**,** 99-105.

Tezvergil-Mutluay, A., Agee, K. A., Hoshika, T., Tay, F. R. & Pashley, D. H. 2010. The inhibitory effect of polyvinylphosphonic acid on functional matrix metalloproteinase activities in human demineralized dentin. *Acta Biomater,* 6**,** 4136-42.

Tezvergil-Mutluay, A., Mutluay, M. M., Gu, L.-S., Zhang, K., Agee, K. A., Carvalho, R. M., Manso, A., Carrilho, M., Tay, F. R., Breschi, L., Suh, B.-I. & Pashley, D. H. 2011a. The anti-MMP activity of benzalkonium chloride. *Journal of Dentistry,* 39**,** 57-64.

Tezvergil-Mutluay, A., Agee, K. A., Uchiyama, T., Imazato, S., Mutluay, M. M., Cadenaro, M., Breschi, L., Nishitani, Y., Tay, F. R. & Pashley, D. H. 2011b. The inhibitory effects of quaternary ammonium methacrylates on soluble and matrix-bound MMPs. *J Dent Res,* 90**,** 535-40.

Tjaderhane, L., Larjava, H., Sorsa, T., Uitto, V. J., Larmas, M. & Salo, T. 1998. The activation and function of host matrix metalloproteinases in dentin matrix breakdown in caries lesions. *J Dent Res,* 77**,** 1622-9.

Toledano, M., Nieto-Aguilar, R., Osorio, R., Campos, A., Osorio, E., Tay, F. R. & Alaminos, M. 2010. Differential expression of matrix metalloproteinase-2 in human coronal and radicular sound and carious dentine. *J Dent,* 38**,** 635-40.

Tonami, K., Araki, K., Mataki, S. & Kurosaki, N. 2003. Effects of chloramines and sodium hypochlorite on carious dentin. *Journal of Medical and Dental Sciences,* 50**,** 139-46.

Trask, B. J. 1991. Fluorescence in situ hybridization: applications in cytogenetics and gene mapping. *Trends in Genetics,* 7**,** 149-54.

Tsuda, H. & Arends, J. 1997. Raman spectroscopy in dental research: a short review of recent studies. *Adv Dent Res,* 11**,** 539-47.

Turk, B., Dolenc, I., Lenarcic, B., Krizaj, I., Turk, V., Bieth, J. G. & Bjork, I. 1999. Acidic pH as a physiological regulator of human cathepsin L activity. *European Journal of Biochemistry,* 259**,** 926-932.

Twetman, S., Axelsson, S., Dahlen, G., Espelid, I., Mejare, I., Norlund, A. & Tranaeus, S. 2012. Adjunct methods for caries detection: A systematic review of literature. *Acta Odontol Scand.*

Uitto, V.-J., Overall, C. M. & Mcculloch, C. 2003. Proteolytic host cell enzymes in gingival crevice fluid. *Periodontology 2000,* 31**,** 77-104.

Van Der Rest, M. & Garrone, R. 1990. Collagens as multidomain proteins. *Biochimie,* 72**,** 473-84.

Van Der Rest, M. & Garrone, R. 1991. Collagen family of proteins. *FASEB Journal,* 5**,** 2814-23.

Van Der Veen, M. H. & Ten Bosch, J. J. 1996. The influence of mineral loss on the auto-fluorescent behaviour of in vitro demineralised dentine. *Caries Res,* 30**,** 93-9.

Van Houte, J. 1994. Role of micro-organisms in caries etiology. *J Dent Res,* 73**,** 672-81.

Van Landuyt, K. L., De Munck, J., Snauwaert, J., Coutinho, E., Poitevin, A., Yoshida, Y., Inoue, S., Peumans, M., Suzuki, K., Lambrechts, P. & Van Meerbeek, B. 2005. Monomer-solvent phase separation in one-step self-etch adhesives. *J Dent Res,* 84**,** 183-8.

Van Landuyt, K. L., Snauwaert, J., De Munck, J., Peumans, M., Yoshida, Y., Poitevin, A., Coutinho, E., Suzuki, K., Lambrechts, P. & Van Meerbeek, B. 2007. Systematic review of the chemical composition of contemporary dental adhesives. *Biomaterials,* 28**,** 3757-85.

Van Landuyt, K. L., Peumans, M., Fieuws, S., De Munck, J., Cardoso, M. V., Ermis, R. B., Lambrechts, P. & Van Meerbeek, B. 2008. A randomized controlled clinical trial of a HEMA-free all-in-one adhesive in non-carious cervical lesions at 1 year. *J Dent,* 36**,** 847-55.

Van Meerbeek, B., Inokoshi, S., Braem, M., Lambrechts, P. & Vanherle, G. 1992. Morphological aspects of the resin-dentin interdiffusion zone with different dentin adhesive systems. *J Dent Res,* 71**,** 1530-40.

Van Meerbeek, B., Perdigão, J., Lambrechts, P. & Vanherle, G. 1998. The clinical performance of adhesives. *Journal of Dentistry,* 26**,** 1-20.

Van Meerbeek, B., De Munck, J., Yoshida, Y., Inoue, S., Vargas, M., Vijay, P., Van Landuyt, K., Lambrechts, P. & Vanherle, G. 2003. Buonocore memorial lecture. Adhesion to enamel and dentin: current status and future challenges. *Oper Dent,* 28**,** 215-35.

Van Meerbeek, B., Peumans, M., Poitevin, A., Mine, A., Van Ende, A., Neves, A. & De Munck, J. 2010. Relationship between bond-strength tests and clinical outcomes. *Dent Mater,* 26**,** e100-21.

Van Meerbeek, B., Yoshihara, K., Yoshida, Y., Mine, A., De Munck, J. & Van Landuyt, K. L. 2011. State of the art of self-etch adhesives. *Dent Mater,* 27**,** 17-28.

Van Strijp, A. J., Jansen, D. C., Degroot, J., Ten Cate, J. M. & Everts, V. 2003. Host-derived proteinases and degradation of dentine collagen in situ. *Caries Res,* 37**,** 58-65.

Vanuspong, W., Eisenburger, M. & Addy, M. 2002. Cervical tooth wear and sensitivity: erosion, softening and rehardening of dentine; effects of pH, time and ultrasonication. *Journal of Clinical Periodontology,* 29**,** 351-7.

Verma, R. P. & Hansch, C. 2007. Matrix metalloproteinases (MMPs): Chemical-biological functions and (Q)SARs. *Bioorganic and Medicinal Chemistry,* 15**,** 2223-2268.

Vicente, A. & Bravo, L. A. 2008. Influence of an etchant and a desensitizer containing benzalkonium chloride on shear bond strength of brackets. *J Adhes Dent,* 10**,** 205-9.

Visse, R. & Nagase, H. 2003. Matrix metalloproteinases and tissue inhibitors of metalloproteinases: structure, function, and biochemistry. *Circ Res,* 92**,** 827-39.

Vu, T. H. & Werb, Z. 2000. Matrix metalloproteinases: effectors of development and normal physiology. *Genes and Development,* 14**,** 2123-33.

Wachsmann-Hogiu, S., Weeks, T. & Huser, T. 2009. Chemical analysis in vivo and in vitro by Raman spectroscopy--from single cells to humans. *Current Opinion in Biotechnology,* 20**,** 63-73.

Waddington, R. J., Hall, R. C., Embery, G. & Lloyd, D. M. 2003. Changing profiles of proteoglycans in the transition of predentine to dentine. *Matrix Biology,* 22**,** 153-61.

Wade, W. 2002. Unculturable bacteria - the uncharacterized organisms that cause oral infections. *Journal of the Royal Society of Medicine,* 95**,** 81-83.

Wang, Y. & Spencer, P. 2003. Hybridization efficiency of the adhesive/dentin interface with wet bonding. *J Dent Res,* 82**,** 141-5.

Wang, Y., Spencer, P. & Walker, M. P. 2007. Chemical profile of adhesive/caries-affected dentin interfaces using Raman microspectroscopy. *J Biomed Mater Res A,* 81**,** 279-86.

Watanabe, I. & Nakabayashi, N. 1993. Bonding durability of photocured phenyl-P in TEGDMA to smear layer-retained bovine dentin. *Quintessence Int,* 24**,** 335-42.

Watanabe, N. & Ikeda, U. 2004. Matrix metalloproteinases and atherosclerosis. *Curr Atheroscler Rep,* 6**,** 112-20.

Watson, T. F. 1989. A confocal optical microscope study of the morphology of the tooth/restoration interface using Scotchbond 2 dentin adhesive. *J Dent Res,* 68**,** 1124-31.

Watson, T. F., Cook, R. J., Festy, F., Pilecki, P. & Sauro, S. 2008. Optical imaging techniques for dental biomaterials interfaces. *In:* Curtis, R. V. & Watson, T. F. (eds.) *Dental biomaterials : imaging, testing and modelling.* Cambridge, chapter 2, pp 37-57.

Weatherell, J. A., Robinson, C. & Hallsworth, A. S. 1974. Variations in the chemical composition of human enamel. *J Dent Res,* 53**,** 180-92.

Weatherell, J. A. 1975. Composition of dental enamel. *British Medical Bulletin,* 31**,** 115-9.

Wennström, J. L., Newman, H. N., Macneill, S. R., Killoy, W. J., Griffiths, G. S., Gillam, D. G., Krok, L., Needleman, I. G., Weiss, G. & Garrett, S. 2001. Utilisation of locally delivered doxycycline in non-surgical treatment of chronic periodontitis. *Journal Of Clinical Periodontology,* 28**,** 753-761.

Whittaker, M., Floyd, C. D., Brown, P. & Gearing, A. J. H. 1999. Design and Therapeutic Application of Matrix Metalloproteinase Inhibitors. *Chemical Reviews,* 99**,** 2735-2776.

Williamson, R. A., Marston, F. A., Angal, S., Koklitis, P., Panico, M., Morris, H. R., Carne, A. F., Smith, B. J., Harris, T. J. & Freedman, R. B. 1990. Disulphide bond assignment in human tissue inhibitor of metalloproteinases (TIMP). *Biochem J,* 268**,** 267-74.

Wilson, M. J., Weightman, A. J. & Wade, W. G. 1997. Applications of molecular ecology in the characterization of uncultured microorganisms associated with human disease. *Reviews in Medical Microbiology,* 8**,** 91-102.

Woessner, J. F., Jr. 1962. Catabolism of collagen and non-collagen protein in the rat uterus during post-partum involution. *Biochem J,* 83**,** 304-14.

Wojtowicz-Praga, S. M., Dickson, R. B. & Hawkins, M. J. 1997. Matrix metalloproteinase inhibitors. *Invest New Drugs,* 15**,** 61-75.

Xiao, Y. H., Ma, S., Chen, J. H., Chai, Z. G., Li, F. & Wang, Y. J. 2009. Antibacterial activity and bonding ability of an adhesive incorporating an antibacterial monomer DMAE-CB. *J Biomed Mater Res B Appl Biomater,* 90**,** 813-7.

Yamada, T., Nakamura, K., Iwaku, M. & Fusayama, T. 1983. The extent of the odontoblast process in normal and carious human dentin. *J Dent Res,* 62**,** 798-802.

Yamakoshi, Y., Hu, J. C., Fukae, M., Zhang, H. & Simmer, J. P. 2005. Dentin glycoprotein: the protein in the middle of the dentin sialophosphoprotein chimera. *J Biol Chem,* 280**,** 17472-9.

Yan, C. & Boyd, D. D. 2007. Regulation of matrix metalloproteinase gene expression. *Journal of Cellular Physiology,* 211**,** 19-26.

Yan, S. J. & Blomme, E. A. 2003. In situ zymography: a molecular pathology technique to localize endogenous protease activity in tissue sections. *Veterinary Pathology,* 40**,** 227-36.

Yonemoto, K., Eguro, T., Maeda, T. & Tanaka, H. 2006. Application of DIAGNOdent® as a guide for removing carious dentin with Er:YAG laser. *Journal of Dentistry,* 34**,** 269-276.

Yoshida, Y., Nagakane, K., Fukuda, R., Nakayama, Y., Okazaki, M., Shintani, H., Inoue, S., Tagawa, Y., Suzuki, K., De Munck, J. & Van Meerbeek, B. 2004. Comparative study on adhesive performance of functional monomers. *J Dent Res,* 83**,** 454-8.

Zandoná, A. F., Santiago, E., Eckert, G., Fontana, M., Ando, M. & Zero, D. T. 2010. Use of ICDAS Combined with Quantitative Light-Induced Fluorescence as a Caries Detection Method. *Caries Research,* 44**,** 317-322.

Zheng, X., Pan, H., Wang, Z. & Chen, H. 2011. Real-time enzymatic degradation of human dentin collagen fibrils exposed to exogenous collagenase: an AFM study in situ. *Journal of Microscopy,* 241**,** 162-70.

Zhou, J., Tan, J., Chen, L., Li, D. & Tan, Y. 2009. The incorporation of chlorhexidine in a two-step self-etching adhesive preserves dentin bond in vitro. *J Dent,* 37**,** 807-12.

Zhou, J., Tan, J., Yang, X., Xu, X., Li, D. & Chen, L. 2011. MMP-inhibitory effect of chlorhexidine applied in a self-etching adhesive. *The journal of adhesive dentistry,* 13**,** 111-5.

Zou, Y. A., Armstrong, S. R. & Jessop, J. L. P. 2010. Quantitative analysis of adhesive resin in the hybrid layer using Raman spectroscopy. *Journal of Biomedical Materials Research Part A,* 94A**,** 288-297.

Zsolt, R. & Krasimir, K. 2011. Matrix metalloproteinases at key junctions in the pathomechanism of stroke. *Central European Journal of Biology,* 6**,** 471-485.